REVISION STATUS SHEET

Document Title: Control Building and Firewater Service Complex Seismic Structure-Soil-Structure Interaction Analysis Report

Revision #: 3 **Type:** Engineering Report – Design

Safety Related Classification Code: N/A **MPL No.:** A25-5110, U63-5110, U73-5110

"|" Vertical Sidebar Denotes Change

Rev #	DOORS BL	Change Number	MM/DD/YYYY	Preparing Organization	Issue / Release Status	Verification Status
0	N/A	ECO-0015270	05/26/2015	GEH	Issued for Use-Design	Verified
1	N/A	ECO-0015977	05/29/2015	GEH	Issued for Use-Design	Verified
2	N/A	ECO-0016783	06/30/2015	GEH	Issued for Use-Design	Verified
3	N/A	ECO-0017433	07/24/2015	GEH	Issued for Use-Design	Verified

MADE BY	APPROVALS	AUTH. DATE
Luben Todorovski GEH	Tanya B. Kirby GEH	05/26/2015

REVISION CHART (CONT)

Rev #	DOORS BL	Change Number	MM/DD/YYYY	Preparing Organization	Issue / Release Status	Verification Status

RECORD OF REVISION

Rev #	Description
0	Initial issue
1	Revised to correct editorial errors
2	Incorporate comments on Rev.1
3	Incorporate comments on Rev.2

TABLE OF CONTENTS

LIST OF TABLES

LIST OF FIGURES

LIST OF ACRONYMS

ARS	Acceleration Response Spectra
BE	Best Estimate
CB	Control Building
CPSD	Cumulative Power Spectral Density
DCD	Design Control Document
EW	East-West
FFT	Fast Fourier Transformation
FIRS	Foundation Input Response Spectra
FPE	Fire Pump Enclosure
FWS	Firewater Storage Tanks
FWSC	Firewater Service Complex
ISRS	In-Structure Response Spectra
LB	Lower Bound
LMSM	Lumped Mass-Stick Model
MSM	Modified Subtraction Method
NA3	North Anna Unit 3
NS	North-South
OBE	Operating Basis Earthquake
PSD	Power Spectral Density
SDOF	Single Degree of Freedom
SRP	Standard Review Plan
SRSS	Square Root of the Sum of the Squares
SSE	Safe Shutdown Earthquake
SSI	Soil-Structure Interaction
SSSI	Structure-Soil-Structure Interaction
UB	Upper Bound

1. INTRODUCTION AND PURPOSE

This report presents the North Anna Unit 3 (NA3) site-specific evaluations of the effects of structure-soil-structure interaction (SSSI) between the ESBWR Firewater Service Complex (FWSC) and the adjacent Control Building (CB). The evaluations follow a methodology consistent with the one used in the ESBWR standard design control document (DCD) to determine:

- The SSSI effects of the FWSC on the CB seismic response based on results of site-specific SSSI analyses of the CB-FWSC combined model
- The SSSI effects of the CB on the FWSC seismic response based on results of site-specific SSSI analyses of the FWSC-CB combined model

The site-specific SSSI analyses are performed using the Modified Subtraction Method (MSM) and the SASSI2010 computer program. The combined SSSI models are developed from the standard design SASSI structural models described in Section 4.3 coupled with site-specific strain compatible dynamic subsurface properties. The combined models representing the dynamic properties of the CB and FWSC structures also include near-field subgrade elements providing an explicit representation of the subgrade conditions existing between the FWSC and the CB. The near-field solid elements model the concrete fill and structural fill backfilled into the gap between the buildings. The concrete fill is backfilled up to the top of the Zone III rock elevation, and the structural fill is backfilled above the Zone III rock elevation up to the finished ground level grade.

The site-specific SSSI effects of the FWSC on the CB seismic response are evaluated using the results of the SSSI analyses of the CB-FWSC combined model for the full column subgrade profiles representing strain-compatible dynamic soil/rock properties at the CB location. The SSSI analyses are performed on full column profiles to accurately capture the effects of concrete fill placed below the FWSC foundation on the CB seismic response. To account for the effects of the potential variability in the properties of the soil and rock, the CB-FWSC SSSI analyses are performed for the two bounding subgrade stiffness conditions using the upper bound (UB) and lower bound (LB) CB full column profiles and corresponding in-layer input motions defined by the CB soil-structure interaction (SSI) design spectra applied at the bottom of the CB foundation. Section 3 describes the subgrade dynamic properties and input motions used for the CB-FWSC SSSI analysis that are identical to those used for the SSI analysis of the CB standalone model. The use of identical inputs enables the SSSI effect of the FWSC on the CB seismic response to be directly evaluated by comparing the results obtained from the SSSI analyses of the CB-FWSC combined model with the results of the SSI analyses of the CB standalone model.

The site-specific SSSI effects of the FWSC on the CB site-specific seismic design basis are evaluated by comparing the site-specific CB-FWSC SSSI analysis results with the corresponding CB site-specific seismic design basis structural loads and in-structure response spectra (ISRS) that are developed as envelope of the results of the SSI analyses of the CB

standalone models. Comparisons are also made with the corresponding seismic loads and ISRS used for the standard design of the CB that are documented in Reference 2-j.

The site-specific SSSI effects of the CB on the FWSC seismic response are evaluated using the results of the SSSI analyses of the FWSC-CB combined model for the subgrade profiles representing strain-compatible dynamic soil/rock properties at the FWSC location. Section 3 describes the subgrade dynamic properties and the input motions used for the site-specific FWSC-CB SSSI analyses that are identical to those used for the site-specific FWSC standalone model SSI analyses. The only difference between the FWSC-CB combined model and the FWSC standalone model is that the structural fill placed in the gap between the two buildings and around the concrete fill below the FWSC foundation is explicitly included in the FWSC-CB combined model and is neglected in the FWSC standalone model. The inclusion of the structural fill in the combined model is intended to address the effects of the structural fill on the FWSC seismic response, in particular the structural fill placed between the two buildings. The consideration of the site conditions at the FWSC location enables the SSSI effect of the CB on the FWSC seismic response to be directly evaluated by comparing the results obtained from the SSSI analyses of the FWSC-CB combined model with the results of the SSI analyses of the FWSC standalone model.

The SSSI effects of the CB on the FWSC site-specific seismic design basis are evaluated by comparing the site-specific FWSC-CB SSSI analysis results with the corresponding FWSC enveloping seismic load demands and site-specific ISRS developed as envelope of the results of the SSI analyses of the FWSC standalone model. Comparisons are also made with the corresponding structural seismic loads and ISRS used for the standard design of the FWSC that are documented in Reference 2-l.

The results of these SSSI evaluations show that the site-specific design based solely on responses obtained from the SSI analysis of the standalone FWSC model do not envelope the SSSI effects of the CB on the FWSC seismic response. Therefore, in Reference 2-k, the FWSC seismic responses obtained from the site-specific SSSI analyses of the FWSC-CB combined model presented in this report are used together with the responses obtained from the standalone FWSC model SSI analyses to develop the bases for the site-specific design and evaluation of the NA3 FWSC.

In order to fully capture the effects of the variability of the soil and rock properties and of different elevations of input control motion of the FWSC site-specific seismic design, the SSSI analyses of the FWSC-CB combined model are performed for the same set of inputs as the ones used for the SSI analysis of the FWSC standalone model in Reference 2-k. The following SSSI analyses cases are performed on the FWSC-CB combined model with Operating Basis Earthquakes (OBE) damping values to obtain the SSSI responses needed for the development of the FWSC site-specific design ISRS in Reference 2-k:

- LB, best estimate (BE), and UB full column profiles using the surface outcrop input motion compatible with the FWSC foundation input response spectra (FIRS) that governs the FWSC ISRS at lower frequencies.

- LB, BE, and UB full column profiles using the corresponding in-column input motion compatible to the SSI design spectra at the bottom of the concrete fill placed below the FWSC foundation that governs the FWSC ISRS at high frequencies.

The following SSSI analysis cases are performed on the FWSC-CB combined model with SSE damping values to obtain the SSSI responses that are used in Reference 2-k for the development of the site-specific seismic load demands on the FWSC:

- LB, BE, and UB full column profiles using the corresponding in-column input motion compatible to the SSI design spectra at the bottom of the concrete fill placed below the FWSC foundation that governs the FWSC maximum SSI site-specific seismic load demand as discussed in Section 6.2.

1.1 Limitations on Use

This report is issued without limitation.

2. REFERENCES

a. TODI WG3-3-A25-TDI-0005, "North Anna 3 Power Block Excavation/Backfill Drawings, Concrete Backfill Properties & Plot Plan", Revision 5
b. TODI WG3-3-A25-TDI-0006, "North Anna 3 Best Estimate Elevation of Top of Zone III Rock and Top of Zone III-IV Rock for RB/FB, CB and FWSC Structures", Revision 0
c. TODI WG3-A25-TDI-S-0004, "North Anna 3 RB/FB, CB & FWSC SSI Analyses EPRI 2013 GMPE Based Inputs", Revision 0
d. TODI WG3-A25-TDI-S-0005, "North Anna 3 RB/FB, CB & FWSC Distances from Adjacent Structures & Sheet Piling", Revision 0
e. TODI WG3-A25-TDI-S-0006, "North Anna 3 RB/FB, CB & FWSC Outcrop SSI Design Motion Time-Histories", Revision 0
f. 105E3908, "ESBWR Nuclear Island General Arrangement Drawing", Revision 5
g. 105E4483, "ESBWR FWSC General Arrangement Drawing", Revision 1
h. 26A6642AL, "ESBWR Design Control Document Tier 2 Chapter 3 Appendices 3A – 3F", Revision 10
i. 26A6642AN, "ESBWR Design Control Document Tier 2 Chapter 3 Appendices 3G – 3L", Revision 10
j. 26A6648, "ESBWR Seismic Analysis of Control Building", Revision 4
k. WG3-U63-ERD-S-0001, "Firewater Service Complex Seismic Analysis Report", Revision 0
l. 26A7419, "ESBWR Seismic Analysis of Firewater Service Complex", Revision 1
m. 26A6654, "ESBWR Stability Analysis of Control Building", Revision 4
n. USNRC, "Interim Staff Guidance on Ensuring Hazard-Consistent Seismic Input for Site Response and Soil Structure Interaction Analyses", DC/COL-ISG-017 (NRC ADAMS Accession Number ML092230543)
o. USNRC, Regulatory Guide 1.60: "Design Response Spectra for Seismic Design of Nuclear Power Plants", Revision 2, July 2014

p. USNRC, NUREG-0800, "Standard Review Plan for the Review of Safety Analysis Reports for Nuclear Power Plants – LWR Edition", Revision 4
q. SRP 3.7.1, "Seismic Design Parameters", Revision 3, March 2007
r. SER-DMN-011, "Benchmarking of SASSI2010 MSM Results from NA3 Site-Specific SSI Analysis", Revision 0
s. USNRC, Regulatory Guide 1.61: "Damping Values for Seismic Design of Nuclear Power Plants", Revision 1, March 2007
t. S/VTR-SAS, "Validation Test Report for SASSI2010 Version 1", Revision G
u. Ostadan, F. and Deng, N., "SASSI2010 Version 1.0 User's Manual", May 2012
v. USNRC, "Interim Staff Guidance on Seismic Issues Associated with High Frequency Ground Motion in Design Certification and Combined License Applications", DC/COL-ISG-01 (NRC ADAMS Accession Number ML081400293)
w. WG3-U71-ERD-S-0001, "North Anna 3 Reactor/Fuel Building Complex Seismic Analysis Report", Revision 0
x. 26A7420, "ESBWR Firewater Service Complex Structural Design Report", Revision 2
y. DBR-0009791, "Soil-Structure Interaction Absolute Acceleration Transfer Functions With Respect to Outcrop Motion and Design Motion Power Spectral Densities For RB/FB SSI, CB SSI, FWSC SSI, CB-FWSC SSSI, and CB-RB/FB SSSI Analyses ", Revison 4

3. SITE-SPECIFIC INPUT

3.1 Site-Specific Subsurface Properties

The site-specific evaluation of the SSSI effect of the FWSC on the CB seismic response is based on the results of the SSSI analyses of the CB-FWSC combined model performed for the LB and UB full column profiles representing the lower and upper bound dynamic properties of the in-situ materials at the CB location. These SSSI analyses use subgrade properties that are compatible to the strains generated by the site-specific design ground motion for the CB. The site-specific strain compatible dynamic properties of the in-situ rock and saprolite subgrade materials are assigned to the far-field SASSI SITE models and the excavated volume elements of SASSI HOUSE models. Reference 2-c provides the strain compatible dynamic properties of the far-field site-specific in-situ subgrade materials used as input for the CB-FWSC SSSI analyses that are listed in Tables 3.1-1 and 3.1-2.

The CB-FWSC combined model also includes the structural and concrete fill materials placed around the CB exterior walls and concrete fill placed below the CB and FWSC basemats. The dynamic properties of these fill materials are assigned to the near-field solid elements in the SASSI HOUSE models. The structural fill dynamic properties are compatible with the strains generated by the design ground motion. The dynamic properties used for the concrete fill are independent of strain, reflecting the linear elastic behavior of the concrete under the small design-earthquake-induced strains. Reference 2-c provides the dynamic properties of the structural and concrete fill materials that are listed in Tables 3.1-6 and 3.1-7. Table 3.1-11 presents the average strain-compatible shear wave velocities ($V_{s\text{-}ave}$) and shear

column frequencies (f_{sc}) of the concrete fill, structural fill, and in-situ materials describing the overall dynamic properties of the materials around the CB.

The site-specific analyses of the FWSC are developed in Reference 2-k based on the results of the SSI analyses of the FWSC standalone model and the SSSI analyses of the FWSC-CB combined model for BE, LB, and UB subgrade profiles representing the BE, LB, and UB dynamic properties of the subgrade material at the FWSC location that are compatible with the strains generated by the site-specific design ground motion. The site-specific strain compatible dynamic properties of the in-situ rock and saprolite subgrade materials are assigned to the far-field SASSI SITE models and the excavated volume elements of the SASSI HOUSE models. Reference 2-c provides the strain compatible dynamic properties of the far-field site-specific in-situ subgrade materials used as input for the FWSC-CB SSSI analysis that are listed in Tables 3.1-3, 3.1-4, and 3.1-5.

The FWSC-CB SSSI analysis also considers the dynamic properties for the structural and concrete fill materials placed around the CB exterior walls and concrete fill placed below the CB and FWSC basemats. These dynamic properties are assigned to the near-field solid elements in the SASSI HOUSE models. The structural fill dynamic properties are compatible with the strains generated by the site-specific design ground motion. The dynamic properties used for the concrete fill are independent of strain, reflecting the linear elastic behavior of the concrete under the small earthquake-induced strains. Reference 2-c provides the dynamic properties of the structural fill and concrete fill materials that are listed in Tables 3.1-8, 3.1-9, and 3.1-10. Table 3.1-12 presents the average strain-compatible shear wave velocities ($V_{s\text{-}ave}$) and shear column frequencies (f_{sc}) of the backfill and in-situ materials describing the overall dynamic properties of subgrade around the concrete fill supporting the FWSC location.

The P-wave velocity of the saprolite and structural fill material located below the ground water level is set equal to or close to, but not less than, that of the water to capture the effect of ground water on P-wave velocity of the saturated soil unless the Poisson's ratio value that relates the S and P wave velocities becomes too high. A maximum value of 0.48 is used for the Poisson's ratio of the subgrade materials in order to ensure the numerical stability of the analysis results.

3.2 Site-Specific Input Motion

Reference 2-c provides the two sets of statistically independent ground motion time histories used as the input control motion in the three orthogonal directions for the SSSI analyses of the CB-FWSC combined model for the LB and UB full column profiles. These ground motion time histories represent the in-column free-field motion at the CB foundation bottom elevation. These time histories have their time-history response spectra compatible with the SSI design spectra representing the envelope of the CB FIRS and the broadband spectra specified in RG 1.60 (Reference 2-o) anchored at 0.1 g. The in-column ground motion time histories used for the CB-FWSC SSSI analysis are checked using the NEI method as required by ISG-017 (Reference 2-n).

Reference 2-c provides the following four sets of statistically independent ground motion time histories used as the input control motion in the three orthogonal directions for the SSSI analyses of the FWSC-CB combined model:

i. Surface outcrop motion acceleration time histories for the analysis of the FWSC compatible with the FWSC FIRS defining the design ground motion at the bottom of FWSC basemat EL 282 ft NAVD88.

ii. In-column motion acceleration time histories for the analysis of the FWSC LB, BE, and UB profiles compatible with the SSI design spectra defining the FWSC ground motion at the bottom of the concrete fill EL 220 ft NAVD88.

The duration of the time histories is 29.98 seconds and the time step is 0.005 seconds.

Figure 3.2-1 presents the 5 percent damped acceleration response spectra (ARS), the power spectral density (PSD), and the cumulative power spectral density (CPSD) of the input acceleration time histories used for the CB-FWSC SSSI analyses illustrating the energy content of the input motion at different frequencies. Figures 3.2-2, 3.2-3, and 3.2-4 present the 5 percent damped ARS, PSD, and CPSD of the input acceleration time histories used for the FWSC-CB analyses of the LB, BE, and UB subgrade profiles, respectively. The presented PSDs are computed based on the strong motion portion of the time record of which the duration is defined by the time interval required for the Arias intensities to increase from 5 percent to 75 percent. Frequency averaging intervals of ±20 percent are applied in compliance with Standard Review Plan (SRP) 3.7.1 (Reference 2-q).

4. STRUCTURE-SOIL-STRUCTURE INTERACTION ANALYSIS

4.1 Analysis Method

The SSSI analyses of the CB-FWSC and FWSC-CB combined models are performed using the SASSI2010 computer program with the MSM where only selected nodes of the excavated volume are specified as interaction nodes. Reference 2-r provides the benchmarking evaluations of the accuracy of the MSM solutions for the NA3 site-specific application. The SASSI2010 computer program uses finite elements with complex moduli for modeling the dynamic properties of the structure, foundation, backfill, and the excavated volume. It provides the solution for the seismic response of the structure-subgrade interaction system based on the frequency domain complex response method. The lumped mass-beam models described in DCD Section 3A.5.1 (Reference 2-h) are coupled with the finite element soil model of the subgrade with the site-specific strain compatible dynamic properties. The model details are described in Section 4.3. Structural responses in terms of accelerations, relative displacements, ARS, member forces, and moments are computed directly from the SASSI2010 computer program results.

The SSSI analyses are performed separately for each one of the three directional components of input ground motion. The maximum co-directional seismic forces, moments, and accelerations for each of the three ground motion time history components are combined using the Square Root of the Sum of the Squares (SRSS) method. The co-directional

soil/rock reactions are combined using the algebraic or absolute sum method in the time domain for sliding, soil bearing evaluations, calculation of lateral soil pressures and base reactions. The absolute sum method is a conservative approach that provides enveloping responses for algebraic sum of all possible combination of the input directions.

The co-directional ISRS are combined using the SRSS method. The ISRS are developed for responses at the edges of the building by taking into account coupling effects between vertical and rocking, and between lateral and torsional motions. The procedure used for the development of the ISRS is the same as that used for the development of the ISRS from the site-specific SSI analyses of the CB and FWSC standalone models.

The SSSI effects are evaluated based on the responses obtained from the CB-FWSC and FWSC-CB combined models with full (uncracked concrete) stiffness properties and OBE structural damping values. The FWSC-CB combined model with full (uncracked concrete) stiffness properties and OBE structural damping values is also used to calculate the ARS used for the development of the FWSC site-specific design ISRS in accordance with RG 1.61 (Reference 2-s). The FWSC-CB combined model with Safe Shutdown Earthquake (SSE) structural damping values and full (uncracked concrete) stiffness properties is used for the development of the site-specific structural load demands on the FWSC structures and the calculation of base reaction time histories for the FWSC foundation uplift and stability evaluations. Per Section C.1.2 of R.G. 1.61 (Reference 2-s), the use of SSE damping values for the development of structural loads is adequate because the stresses obtained from the models with SSE damping values will remain lower than the stress limits considered by the applicable structural design codes. The use of SSE damping values for the foundation uplift and stability evaluations are also adequate because these analyses also consider limiting conditions that are associated with a high dissipation of energy in the SSSI dynamic system.

4.2 Structure-Soil-Structure Interaction Analysis Cases

Table 4.2-1 presents the two analysis cases considered for site-specific evaluation of the SSSI effects of the FWSC on the CB seismic response. Table 4.2-2 presents the nine analysis cases performed to include the SSSI effects of the CB on the FWSC seismic response in the FWSC site-specific design basis.

The frequency step and Fast Fourier Transformation (FFT) number used for the SSSI analysis are 0.0244 Hz and 8192, respectively. Table 4.2-3 provides a list of frequencies used for each of the SSSI analyses performed for the CB-FWSC and FWSC-CB combined models. As described in Subsection 5.1, acceleration transfer function results obtained from each analysis case are inspected to ensure that the selected frequencies of analysis provide numerically accurate results.

Values of cut-off frequencies of analysis are used that are equal to or lower than the passing frequency of the SSI model (the highest frequency of seismic waves that can be transmitted through the SSI model). The SSSI analyses of the CB-FWSC combined model that are performed for the two bounding subgrade stiffness conditions, use cut-off frequencies of analysis that are identical to those used for the corresponding SSI analyses. This ensures that

the energy content of the input motion captured by the SSSI analyses and the reference SSI analyses is the same and does not affect the SSSI evaluations. The analyses of the CB-FWSC combined model and the CB standalone model for the LB full column profile are performed using a cut-off frequency of 34 Hz. The analyses of the CB-FWSC combined model and the CB standalone model for the UB full column profile are performed using a cut-off frequency of 70 Hz.

The SSSI analyses of the FWSC-CB combined model are performed for the same set of input subgrade properties and ground motion time histories as the ones used for the SSI analyses of the FWSC standalone model. This ensures that the results of the FWSC-CB analyses that are used to develop the FWSC site-specific design basis completely capture the effects of the subgrade properties variations. The cut-off-frequencies used for the SSSI analyses of the FWSC-CB combined model ensure that these analyses provide site-specific design ISRS that, per the guidelines of ISG-01 (Reference 2-v), are adequate for the design and qualification of components and equipment in the FWSC for frequencies up to 50 Hz. The cut-off frequency used for the FWSC-CB SSSI analysis of the UB subgrade profile is 70 Hz; identical to the cut-off frequency used for the corresponding SSI analyses of the FWSC standalone model for the UB soil profile. As shown in Table 4.2-2, the analyses of the UB profiles capture virtually all (≈ 99%) of the input motion energy.

The FWSC-CB SSSI analyses of the BE and LB profiles use cut-off frequencies of 47 Hz and 30 Hz, respectively, and can capture at least 72% of the input motion energy. These cut-off frequencies are slightly lower than the cut-off frequencies of 36 Hz and 55 Hz used for the corresponding SSI analyses of the FWSC standalone model for the LB and BE soil profiles.

Results of the FWSC-CB SSSI analyses presented in Section 6 show that the FWSC-CB SSSI analyses of the UB subgrade profile with deep control motion at EL 220 ft, NAVD88 govern the responses of the FWSC at high frequencies. The comparison of the 5% damped ISRS results obtained from the FWSC-CB analyses of LB, BE and UB subgrade profiles show that the FWSC-CB SSSI analyses of BE profiles provide bounding ISRS amplitudes for frequencies below 30 Hz that is 17 Hz less than the cut-off frequency of analyses used for these analyses. The FWSC-CB SSSI analyses of LB subgrade profiles bound the ISRS results for frequencies below 24 Hz that is 6 Hz less than the cut-off frequency of analyses used for these analyses.

4.3 Analysis Models

The standalone CB and FWSC seismic models used for the site-specific SSSI analyses shown in Figures 4.3-1 and 4.3-2 are based on the three-dimensional lumped mass-stick models (LMSMs) that were used for the standard design seismic response analysis, which considers shear, bending, torsion, and axial deformations. These two models are designated in DCD Table 3A.6-1 (Reference 2-h) as the base models CL-2 and FL-2. For the site-specific SSSI analyses, additional rigid outriggers are installed at each floor elevation to facilitate calculation of ISRS and displacements at floor edges.

Two structural models are developed for the site-specific SSSI analyses between CB and FWSC performed for the full column subgrade profiles. Figures 4.3-3 and 4.3-4 show the conceptual configurations of the fully embedded CB-FWSC and FWSC-CB combined models, respectively. For each combined model, ground surface level, soil properties, and input motions from design input for each building are considered separately. Specifically, in the CB-FWSC combined model, the CB soil properties are used and the control point of input motions are specified at the bottom of CB basemat. While in the FWSC-CB combined model, the FWSC soil properties are used and the control point of input motions are defined at the bottom of FWSC basemat and bottom of the concrete fill.

The combined models use near-field solid elements to represent the actual site conditions between the CB and FWSC and include the concrete and structural fill materials placed around the CB exterior walls and concrete fill placed below the CB and FWSC. The lateral extent of backfill at the three sides of CB and FWSC is taken to be one-half of the fill width between buildings or the width of the excavation on the side without adjacent buildings, whichever is smaller. The fill width on the side without adjacent buildings could be based on the dimensions to the inside face of sheet piling as described in (Reference 2-d). The minimum values of the lateral extent of fill materials around the CB and FWSC are listed in Tables 4.3-1 and 4.3-2, respectively.

Figures 4.3-5 through 4.3-7 present the CB-FWSC combined model used for evaluation of SSSI effects of FWSC on the CB seismic response. Figures 4.3-8 through 4.3-10 present the FWSC-CB combined model used for evaluation of SSSI effects of CB on the FWSC seismic response. The model axes in the horizontal X-direction and Y-direction represent the north-south (NS) direction and the east-west (EW) direction of the NA3 site, respectively. Plant north for NA3 is oriented 23.54 degrees east of true north (Reference 2-a). The Z axis represents the vertical direction. Based on the CB and FWSC layout, the combined models are assumed symmetrical about the YZ-plane along the building's centerline in the EW direction.

The CB below-grade exterior walls and the CB and FWSC foundation basemats are modeled using plate elements similar to the standalone CB and FWSC SASSI models used for standard design SSI analyses. However, because the soil medium between the finished ground level grade or Zone III rock and the foundation basemat are modeled in the site-specific SSSI analysis, the vertical spacing of the CB wall nodes is adjusted for a closer match with the site-specific subsurface layers. The mesh sizes of the plate elements are also adjusted to satisfy the SASSI2010 computer program user's manual (Reference 2-u) requirement for mesh size that limits the size of the elements to not more than 20 percent of the shortest length of the shear wave that can pass through the soil model. In the CB-FWSC combined model, the FWSC is modeled embedded along the thickness of its basemat to match the same plant grade level as the CB. While in the FWSC-CB combined model, the FWSC basemat embedment is neglected matching the configuration of the FWSC standalone model SSI analysis. Massless shell elements with thickness set as a quarter of the CB basemat width are used in the CB-FWSC and FWSC-CB combined models along the thickness of the CB basemat between EL -7.4 to -10.4 m to model the rigid connections

between the exterior walls and the basemat. In the CB-FWSC combined model, shell elements with thickness set as a quarter of the FWSC basemat width are also used along the thickness of the FWSC basemat between EL 4.5 m to 2.15 m to connect the basemat shell elements with the FWSC lumped-mass stick models at plant grade EL 4.5 m..

The SSSI analyses use combined models with full (uncracked) concrete stiffness properties and OBE damping values for the reinforced concrete structures. Additional cases are performed for the FWSC-CB combined model having full (uncracked) concrete stiffness properties and SSE damping values assigned to all of the CB and FWSC structural members. The responses obtained from the FWSC-CB combined model with SSE damping values are used for the development of site-specific load demands on the FWSC structures and the base reaction time histories for the foundation uplift, and stability evaluations.

The mesh size of the excavated volume elements is refined enough to ensure that per SASSI2010 computer program criteria, the maximum element size in all three directions does not exceed 20 percent of the shear wave length of the excavated soil at the highest (cut-off) frequency of analysis. The backfill surrounding the buildings is included in the structural models and is modeled using 3-D solid elements with mesh that is consistent with the mesh of the plate elements of the basemat and exterior walls. A refined mesh is required for the top layers of softer in-situ soil and structural fill located above the Zone III rock in the SSSI analysis in order to capture sufficient energy of the design input motion. To ensure the overall model size do not exceed the program limitations, the soil medium and concrete fill below the Zone III rock level are modeled with coarser mesh. In the transitional layers non-uniform irregular elements are used, namely, triangular shell elements, prism, tetrahedral, and pyramid solid elements. The passing frequencies and cut-off frequencies used for the CB-FWSC and FWSC-CB SSSI analyses are shown in Tables 4.2-1 and 4.2-2, respectively. The passing frequencies are calculated on the basis of both the maximum horizontal and vertical dimensions of the excavated volume and backfill mesh. The tables show that the model maximum passing frequencies for all subsurface profiles are no smaller than the cut-off frequency of analysis. The SSSI analyses of UB subgrade profiles capture up to 99 percent of the input motion energy. The SSSI analysis of LB subgrade profiles can capture more than 70 percent of the input motion energy.

The maximum aspect ratios of the regular 3-D thin shell elements in the CB-FWSC and FWSC-CB combined models are 1:2.7 and 1:1.6, respectively. The maximum aspect ratios of the regular 3-D solid brick elements in the CB-FWSC and FWSC-CB combined models are 1:2.9 and 1:3.5, respectively. As described in Reference 2-t, the accuracy of the SASSI2010 computer program has been verified and validated for models with a maximum aspect ratio of 1:4 for both the 3-D thin shell and 3-D solid brick finite elements. Additionally, the accuracy of using non-uniform irregular elements is also demonstrated for the CB standalone model SSI analysis by a comparative study.

The site profiles used for the site-specific CB-FWSC SSSI analysis are presented in Tables 4.3-3 and 4.3-4 for the model. Tables 4.3-5 through 4.3-7 represent the site profiles used for the FWSC-CB SSSI analyses. The maximum value of soil Poisson's ratio considered in the site models is 0.48 which is within the range to which the accuracy of the SASSI2010

computer program has been verified and validated (Reference 2-t). The shear and compression wave velocities, unit weights, and damping ratios of the profiles used for the SSSI analysis are identical to those provided in the strain iterated soil profiles listed in Tables 3.1-1 through 3.1-10 developed from the results of the site response analysis. Some of the layers in these site response analysis profiles are subdivided so the site models used for site-specific SSSI analyses can meet the passing frequency requirements. A graphical comparison between the adjusted soil profiles of shear wave velocities, compression wave velocities, and damping ratios used in the SSSI analyses and the corresponding strain iterated soil profiles from the site response analyses are provided in Figures 4.3-11 and 4.3-12. As shown, there are no differences between the SSSI analyses soil profiles and the site response soil profiles except for the CB-FWSC combined model soil profile in which the soil properties are averaged around EL -6.17 m in order to reduce the overall model size.

The CB-FWSC and FWSC-CB combined models, respectively, include 27 and 29 layers on top of a half-space. The top of the half-space in the SSSI models is established at standard design elevation -146.5 m. Consistent with SASSI2010 user's manual (Reference 2-u) recommendations, the half-space simulation consists of an additional ten layers with viscous dashpots added at the base of the site finite element model to account for the dissipation of energy at the model lower boundary. The half-space model has a thickness of 1.5 Vs/f, where Vs is the shear wave velocity of the half-space and f is the frequency of the analysis. The total depth of the site model used for SSSI analyses is more than 220 m, which is close to or exceeds two times the footprint dimension of the analyzed structures. The footprint of the CB is 30.3 m x 23.8 m. The footprint of the FWSC is 52.0 m x 20.0 m.

The excavated volume models are shown in Figures 4.3-7 and 4.3-10 for the CB-FWSC and FWSC-CB combined models, respectively. The selection of the interaction nodes is based on the conclusions of the NA3 site-specific MSM benchmarking report (Reference 2-r). In addition to the nodes at the sides, top, and bottom surfaces of the excavated volumes of the CB and FWSC, nodes at vertical plane between CB and FWSC, nodes at vertical plane between the CB and FWSC, nodes at two horizontal planes within the excavated volumes are added as interaction nodes for both models.

As indicated in Figures 4.3-5 and 4.3-8, the CB stick model is connected to the basemat and side walls at floor EL -7.4 m, -2.0 m, and 4.5 m by a set of rigid beams. The FWSC stick model is connected to the basemat using rigid beams along the footprint of walls of the Firewater Storage Tanks (FWS) and the Fire Pump Enclosure (FPE). In the CB-FWSC combined model, the FWSC stick is also connected to the side of the basemat at EL 4.5 m by rigid beams.

In the CB-FWSC combined model, 3-D spring elements are established at the CB exterior wall/backfill interfaces and concrete fill under the CB basemat as shown in Figure 4.3-6. 3-D spring elements are also established at the interfaces around the FWSC basemat with the backfill and concrete fill. In the FWSC-CB combined model, 3-D spring elements are established at the interfaces around the CB exterior walls and basemat with the backfill and concrete fill as shown in Figure 4.3-9. 3-D spring elements are also established at the interfaces around the concrete fill under the FWSC basemat. These spring elements are

assigned global stiffness properties high enough to ensure they do not affect the dynamic properties of the analyzed SSI system but also low enough to not cause numerical instability. The interface spring elements provide spring force results that serve as input for calculation of the site-specific wall lateral pressure and foundation bearing pressure demands. The spring forces results also serve as input for calculation of seismic driving forces for the site-specific stability evaluations.

5. EVALUATION OF FWSC SSSI EFFECTS ON CB SEIMIC RESPONSE

This section presents the results of the evaluation of site-specific SSSI effects of the FWSC on the CB seismic response. The evaluation is based on the comparison of the results of the site-specific SSSI analyses of the CB-FWSC combined model listed in Table 4.2-1 for the response of the CB with the corresponding results obtained from the site-specific SSI analysis of the standalone CB model for the LB and UB full column profiles. Plots of the calculated and interpolated acceleration transfer function results for the responses of the CB are used to demonstrate the accuracy of the interpolated results from the SSSI analyses of the two bounding subgrade stiffness cases. The SSSI effects of the FWSC on the CB seismic response are evaluated by comparing the results for outcrop motion transfer functions, maximum accelerations, maximum member forces, maximum lateral pressures on below grade exterior walls, and ISRS.

The SSSI effects of FWSC on the CB site-specific seismic design basis are evaluated by comparing the site-specific CB-FWSC SSSI analysis results with the corresponding CB site-specific seismic design basis structural loads and ISRS that are developed as envelope of the results of the SSI analyses of the CB standalone models. Comparisons are also made with the corresponding seismic loads and ISRS used for the standard design of the CB that are documented in Reference 2-j to further evaluate the significance of the site-specific SSSI effects.

5.1 Acceleration Transfer Function Results

Appendix B presents plots of the amplitudes of the acceleration transfer functions obtained directly from the SASSI2010 computer program analyses, which are transfer functions relative to the in-layer seismic input motion, for the responses at the following key locations within the CB:

Location	Node Number	SASSI Model Node Number
CB Top	6	500
CB Basemat	2	410

The amplitudes of the acceleration transfer functions are presented from the analyses of the full column LB and UB soil profiles. Each figure presented in Appendix B includes three plots presenting the CB responses in the three orthogonal directions due to the three earthquake components. The computed values of the transfer functions in these plots are depicted with dots. The interpolated values of the transfer functions are depicted by solid lines.

As expected, the acceleration transfer functions for the horizontal response of CB are characterized with large peaks at frequencies that are close to the embedment shear column frequencies listed in Table 3.1-11 and at frequencies where dips occur in the response spectra of the input in-layer acceleration time histories presented in Figure 3.2-1. Therefore, these large peaks in the acceleration transfer functions that represent the response amplifications relative to the in-column input motion are not reflected in the acceleration response spectra results.

The plots generally have no numerical anomalies in the interpolated transfer functions (e.g., sharp narrow spikes) that can potentially impact the accuracy of the frequency domain SSSI analyses results. The isolated sharp peak in a few cases does not affect the accuracy of the corresponding responses.

The large peaks at soil column frequencies are not present in the transfer functions representing the structural responses relative to the input outcrop motion making them a better indicator of structural response. These outcrop transfer functions are calculated in the following three steps:

1. FFT are performed on the time histories of in-layer and outcrop ground motion at the CB basemat bottom elevation obtained from Reference 2-e.
2. The ratio between the in-layer and outcrop motion Fourier spectra yields transfer functions representing the transformation of the CB in-layer motion into an outcrop motion.
3. The product of the complex in-layer/outcrop transfer functions calculated in step 2 and the SASSI2010 calculated complex transfer functions of the structural response relative to the in-column motion provide the transfer functions for structural response relative to the outcrop motion.

Figure 5.1-1 presents amplitudes of the transfer functions representing the transformation of the corresponding in-layer motion time histories used as input for the CB-FWSC SSSI analysis of the LB and UB full column profiles into the horizontal and vertical design outcrop motion time histories. The first valleys in the horizontal full column motion in-layer/outcrop transfer functions occur at frequencies close to the rock embedment shear column frequencies listed in Table 3.1-11.

Figure 5.1-2 presents the outcrop transfer functions amplitude for the co-directional responses of the CB top (Node 6) in the NS (X), EW (Y), and vertical (Z) directions obtained from the analyses of LB and UB full column profiles. Figure 5.1-3 presents the outcrop transfer functions amplitudes for the rotational accelerations that are representative of the torsional and the rocking response along the EW (Y) direction at the top of CB basemat (Node 2) due to NS (X) and vertical (Z) components of the input motion, respectively. The plots compare the results from the site-specific SSSI analyses of the CB-FWSC combined model presented by solid lines with the results from the site-specific SSI analyses of the CB standalone model presented with dashed lines. Comparisons are shown for the outcrop transfer function results obtained from the analyses of LB and UB full column profiles to illustrate the effects of the subgrade stiffness on the SSSI responses. The plots also show the

outcrop motion design spectra for the partial column and full column with solid and dashed lines, respectively.

The comparisons in Figure 5.1-2 show that the SSSI effect can amplify the horizontal response of CB without any significant shifts in the peak responses frequencies. The SSSI effects of the FWSC on the CB vertical response are very small. The comparisons in Figure 5.1-3 of the outcrop motion transfer function results indicate that the SSSI effect amplifies the torsional and rocking response of the CB basemat. The comparisons in Figures 5.1-2 and 5.1-3 of the outcrop function results obtained from the SSSI and SSI analyses of the UB profile show that the SSSI amplifications of the CB peak responses occur at frequencies where the energy of the full column motion is significantly smaller than that of the partial column motion.

5.2 SSSI Effects of FWSC on CB Maximum Responses

Figure 5.2-1 presents comparisons of the results for maximum absolute accelerations at CB mass locations from the site-specific SSSI analyses of CB-FWSC combined model with the corresponding results from the site-specific SSI analyses of the CB standalone model for the LB and UB full column profiles. Table 5.2-1 shows the comparison of the results from the SSSI analyses of the CB-FWSC combined model and the SSI analyses of the CB standalone model for maximum accelerations of the Single Degree of Freedom (SDOF) oscillators representing the out-of-plane vibrations of the CB flexible slabs. Figure 5.2-2 presents the comparisons of the results for maximum shear forces and torsion from the SSSI analyses of the CB-FWSC combined model with the corresponding results from the SSI analyses of the CB standalone model for the LB and UB full column profiles. The figures show the results from the CB-FWSC SSSI analyses with red dashed lines. The results obtained from the SSI analyses of the CB standalone model are shown with green solid lines.

The comparisons in Figures 5.2-1 and 5.2-2 show that the SSSI induced rocking of CB along the centerline of CB-FWSC combined model can amplify the CB maximum accelerations and shear forces in the EW (Y) direction. The SSSI with FWSC has very small effect on the CB response in the NS and vertical direction. The effects of SSSI on the rocking of CB are more pronounced for the softer LB subgrade profile and are small for the stiffer UB subgrade. On the other hand, as shown in Figure 5.2-2, the SSSI analyses of the UB full column profile indicate that the SSSI with the FWSC can amplify the CB torsional response. The comparisons in Table 5.2-1 show in that the SSSI effects on the maximum vertical accelerations of the CB flexible slabs are small. The SSSI with FWSC can either slightly amplify or reduce the maximum accelerations of the CB slabs oscillators.

5.3 SSSI Effects of FWSC on Dynamic Lateral Pressures on CB Below-Grade Walls

As discussed in Section 4.3, spring elements between “double nodes” are installed on the CB wall interfaces with surrounding subgrade to calculate the lateral seismic pressures on the CB below-grade walls. The calculations of dynamic lateral pressures are performed in the following steps:

1. The time histories of the spring forces are extracted from each SASSI run for each contact spring element.
2. The absolute value of the spring force magnitudes obtained from the analyses of the three orthogonal input earthquake motion components are combined absolutely in the time domain.
3. The maximum lateral forces normal to the wall plane are obtained at all contact spring elements.
4. The absolute values of the maximum lateral forces for all spring elements at the same elevations are summed up to obtain the total maximum lateral forces at the respective elevations for the three CB below-grade exterior walls separately.
5. The total maximum lateral forces are divided by the tributary area for each node group at the same elevation to obtain the soil pressure distribution for the three exterior walls.

Figures 5.3-1 and 5.3-2 present the SASSI calculated dynamic lateral pressures on the CB below-grade walls located at column lines C1 and C5. Figures 5.3-3 and 5.3-4 present the dynamic lateral pressures on the CB below-grade walls located at column lines CA and CD, respectively. The figures compare the dynamic lateral pressures obtained from the site-specific SSSI analyses of the CB-FWSC combined model that are presented with solid red curves with the corresponding dynamic lateral pressures obtained from the site-specific SSI analyses of the CB standalone model that are presented with green lines. Comparisons are presented of the results obtained from the analyses of the LB and UB full column profiles. The figures show that the dynamic lateral pressures are generally lower except for wall at column row CA where the SSSI pressure is significantly higher. The SSSI wall pressure, however, is bounded by the enveloping SSI analysis wall pressures.

5.4 SSSI Effects of FWSC on CB ISRS

Figures 5.4-1 through 5.4-3 present a comparison of the results from the site-specific SSSI analyses of the CB-FWSC combined model and the site-specific SSI analyses of the CB standalone model for 5% damped ISRS for response in the NS, EW, and vertical direction, respectively. ISRS are presented for the CB response at the two key locations within the CB listed in Section 5.1. The following is the procedure used for the development of the floor ISRS:

1. For each of the four outrigger locations (ne, nw, se, sw) at particular floor elevations, three components (X, Y, and Z) of the ARS due to input motion in three directions (X, Y, and Z) are calculated by the SASSI2010 MOTION module to obtain a total of 36 ARS results:

$$\text{Outrigger}^{(ne)} \rightarrow (f_{XX}^{(ne)}, f_{XY}^{(ne)}, f_{XZ}^{(ne)}, f_{YX}^{(ne)}, f_{YY}^{(ne)}, f_{YZ}^{(ne)}, f_{ZX}^{(ne)}, f_{ZY}^{(ne)}, f_{ZZ}^{(ne)})$$

$$\text{Outrigger}^{(nw)} \rightarrow (f_{XX}^{(nw)}, f_{XY}^{(nw)}, f_{XZ}^{(nw)}, f_{YX}^{(nw)}, f_{YY}^{(nw)}, f_{YZ}^{(nw)}, f_{ZX}^{(nw)}, f_{ZY}^{(nw)}, f_{ZZ}^{(nw)})$$

$$\text{Outrigger}^{(se)} \rightarrow (f_{XX}^{(se)}, f_{XY}^{(se)}, f_{XZ}^{(se)}, f_{YX}^{(se)}, f_{YY}^{(se)}, f_{YZ}^{(se)}, f_{ZX}^{(se)}, f_{ZY}^{(se)}, f_{ZZ}^{(se)})$$

$$\text{Outrigger}^{(sw)} \rightarrow (f_{XX}^{(sw)}, f_{XY}^{(sw)}, f_{XZ}^{(sw)}, f_{YX}^{(sw)}, f_{YY}^{(sw)}, f_{YZ}^{(sw)}, f_{ZX}^{(sw)}, f_{ZY}^{(sw)}, f_{ZZ}^{(sw)})$$

where f_{ij} represents ARS for response in j-direction due to earthquake in i-direction.

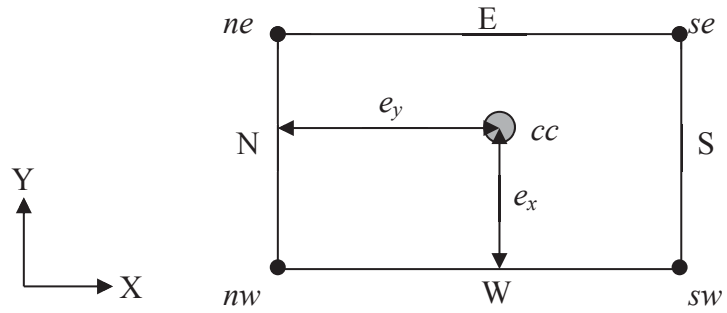

The spectra for the nodal responses due to the three input motion components in the X, Y, and Z directions are combined using the SRSS method to obtain a total of 12 ARS of the response of each of the four outrigger nodes (ne, nw, se, sw) in three orthogonal directions (X, Y, and Z):

$$f_X^{(ne)} = \sqrt{f_{XX}^{(ne)2} + f_{YX}^{(ne)2} + f_{ZX}^{(ne)2}} \quad , \quad f_Y^{(ne)} = \sqrt{f_{XY}^{(ne)2} + f_{YY}^{(ne)2} + f_{ZY}^{(ne)2}}$$

$$f_Z^{(ne)} = \sqrt{f_{XZ}^{(ne)2} + f_{YZ}^{(ne)2} + f_{ZZ}^{(ne)2}}$$

$$f_X^{(nw)} = \sqrt{f_{XX}^{(nw)2} + f_{YX}^{(nw)2} + f_{ZX}^{(nw)2}} \quad , \quad f_Y^{(nw)} = \sqrt{f_{XY}^{(nw)2} + f_{YY}^{(nw)2} + f_{ZY}^{(nw)2}}$$

$$f_Z^{(nw)} = \sqrt{f_{XZ}^{(nw)2} + f_{YZ}^{(nw)2} + f_{ZZ}^{(nw)2}}$$

$$f_X^{(se)} = \sqrt{f_{XX}^{(se)2} + f_{YX}^{(se)2} + f_{ZX}^{(se)2}} \quad , \quad f_Y^{(se)} = \sqrt{f_{XY}^{(se)2} + f_{YY}^{(se)2} + f_{ZY}^{(se)2}}$$

$$f_Z^{(se)} = \sqrt{f_{XZ}^{(se)2} + f_{YZ}^{(se)2} + f_{ZZ}^{(se)2}}$$

$$f_X^{(sw)} = \sqrt{f_{XX}^{(sw)2} + f_{YX}^{(sw)2} + f_{ZX}^{(sw)2}} \quad , \quad f_Y^{(sw)} = \sqrt{f_{XY}^{(sw)2} + f_{YY}^{(sw)2} + f_{ZY}^{(sw)2}}$$

$$f_Z^{(sw)} = \sqrt{f_{XZ}^{(sw)2} + f_{YZ}^{(sw)2} + f_{ZZ}^{(sw)2}}$$

2. The ARS calculated for each outrigger location are enveloped to obtain the three ARS for the floor response in three orthogonal directions (X, Y, and Z):

$$F_X = max(f_X^{(ne)}, f_X^{(nw)}, f_X^{(se)}, f_X^{(sw)})$$

$$F_Y = max(f_Y^{(ne)}, f_Y^{(nw)}, f_Y^{(se)}, f_Y^{(sw)})$$

$$F_Z = max(f_Z^{(ne)}, f_Z^{(nw)}, f_Z^{(se)}, f_Z^{(sw)})$$

The comparison of the ISRS results in Figures 5.4-1 through 5.4-3 show that the SSSI with the FWSC can amplify the peaks of the horizontal CB ISRS. The results obtained from the analyses of the LB full column profile show SSSI amplifications of the ISRS peaks at frequencies between 7 and 15 Hz. The amplifications of the ISRS peaks obtained from the analyses of the UB full column profile occur at frequencies above 10 Hz. Peak amplifications can also be observed in the vertical ISRS around 30 Hz for the LB subgrade and 50 Hz for the UB subgrade. The amplifications of ISRS peaks are consistent with the observations

made from the comparisons of the outcrop motion transfer function results discussed in Section 5.1.

5.5 SSSI Effects of FWSC on Site-Specific Load Demands on CB Structure

The seismic structural loads representative of the site-specific seismic demands on the CB structure are developed following the methodology used to develop the standard design enveloping maximum structural loads presented in Reference 2-j. The horizontal load demands on the CB reinforced concrete structure are developed from the diagrams of the maximum enveloping shear forces and maximum enveloping torsional moments obtained as the envelope of the member force results from the analyses of the six subgrade profiles. The vertical site-specific seismic load demands on the CB structure are developed from the diagrams of the maximum enveloping vertical floor mass accelerations obtained as the envelope of the maximum acceleration results from the analyses of the six subgrade profiles. The maximum enveloping bending moments are also used for the structural evaluation of the CB to account for the effects of floor rocking on the wall axial forces. The results for maximum enveloping vertical accelerations of the SDOF oscillator mass are used to develop the local out-of-plane load demands on the CB flexible slabs.

The SSSI effects of the FWSC on the site-specific seismic load demands on the CB structure are evaluated based on the diagrams of the maximum vertical accelerations, member shear forces and moments obtained as the envelope of the results from the site-specific SSSI analyses of CB-FWSC combined model for the LB and UB full column profiles. Figures 5.5-1 and 5.5-2 compare the envelopes of the SSSI results with the corresponding diagrams of enveloping site-specific maximum horizontal and vertical load demands obtained as envelopes of the results of site-specific SSI analysis of the CB standalone model for:

i. LB, BE, and UB partial column profiles
ii. LB, BE, and UB full column profiles

The figures present the envelope of the SSSI results with solid red lines and the NA3 enveloping seismic demands from the CB site-specific SSI analyses with solid green lines. Figures 5.5-1 and 5.5-2 also provide, with dashed blue lines, the diagrams of the horizontal and vertical seismic loads used for the standard design of the CB reinforced concrete structures.

Table 5.5-1 compares the envelope of the site-specific SSSI analyses results for maximum accelerations at the CB floor mass locations with the corresponding NA3 enveloping maximum accelerations obtained from the SSI analyses of the CB standalone model and the standard design enveloping maximum accelerations. Table 5.2-1 presents comparisons of the envelope of the SSSI analyses results for the maximum acceleration of the slab SDOF oscillators with corresponding NA3 SSI enveloping and standard design values. The comparisons of the envelope of the site-specific SSSI analyses results for maximum member forces and moments with the corresponding standard design and NA3 SSI enveloping values is presented in Table 5.5-2. Figures 5.3-1 through 5.3-4 compare the site-specific SSSI

analyses results for dynamic lateral pressures with the corresponding NA3 enveloping dynamic pressures obtained from the SSI analyses of the CB standalone model.

The comparisons show that the site-specific enveloping load demands on the CB structure obtained as the envelope of the results of the SSI analyses of fully and partially embedded standalone models envelope the SSSI effects of the FWSC on the CB seismic response. The only exception is the torsional demands on the CB that is induced by the eccentricity of the FWSC with respect to NS axis. The calculations in Table 5.5-3 demonstrate that the additional torsion-induced shear is well enveloped by the enveloping shear load demands obtained from the site-specific SSI analyses of CB standalone model.

The NA3 CB structural loads presented in this section are based on the models with full concrete stiffness (uncracked) and OBE damping values in both SSI and SSSI analyses.

5.6 SSSI Effects of FWSC on CB Site-Specific Design ISRS

Figures 5.4-1 through 5.4-3 provide a comparison of the 5% damped ISRS obtained from the site-specific SSSI analyses of the CB-FWSC combined model with the corresponding 5% damped NA3 site-specific design and standard design ISRS shown with thick blue and black lines, respectively. The NA3 site-specific design ISRS that are broadened by $\pm$15% and valley filled, represent the envelope of the ISRS results from the site-specific SSI analyses of CB standalone model and serve as the basis for the site-specific design and qualification of CB equipment and components. The comparisons show that NA3 site-specific design ISRS envelope the results of the site-specific SSSI analyses of the CB-FWSC combined model. The only exceedance (approximately 10%) is in Figure 5.4-3 at cut-off frequency of 50 Hz.

6. EVALUATION OF SSSI EFFECTS OF CB ON FWSC SEISMIC RESPONSE

This section presents the results of the site-specific evaluation of the SSSI effects of the CB on the FWSC seismic response. The evaluation is based on the comparison of the results of the site-specific SSSI analyses of the FWSC-CB combined model listed in Table 4.2-2 for the response of the FWSC with the corresponding results obtained from the site-specific SSI analysis of the standalone FWSC model for all profiles with the control motion applied both at EL 282 ft. and 220 ft. NAVD88. Plots of the calculated and interpolated acceleration transfer function results for the responses of the FWSC are used to demonstrate the accuracy of the interpolated results from the FWSC-CB SSSI analyses.

The SSSI effects of the CB on the FWSC seismic response are evaluated based on the results of the site-specific SSSI analyses of the FWSC-CB combined model with the full (uncracked concrete) stiffness properties and OBE damping values (analysis cases FC1 through FC6 in Table 4.2-2). To evaluate the effect of SSSI of the CB on the FWSC seismic response for different subgrade conditions and locations of the input motion, comparisons are made of the FWSC-CB SSSI analyses results for outcrop motion transfer functions, maximum accelerations, maximum member forces, and ISRS with the corresponding results from the SSI analyses of the FWSC standalone model with the full (uncracked concrete) stiffness properties and OBE damping values.

The SSSI effects of the CB on the FWSC site-specific seismic design basis are evaluated by comparing the results of the site-specific FWSC-CB SSSI analyses with the corresponding site-specific and standard design FWSC seismic design envelopes. The impact of the SSSI effects on the site-specific seismic load demands on the FWSC structures is assessed based on the results of the SSSI analyses of the FWSC-CB combined model with the full (uncracked concrete) stiffness properties and SSE damping values (analysis cases FC7, FC8, and FC9 in Table 4.2-2). The effects of SSSI on the site-specific design of the equipment and components within the FWSC are evaluated based on the ISRS results obtained from the SSSI analyses of the FWSC-CB combined model with the full (uncracked concrete) stiffness properties and OBE damping values (analysis cases FC1 through FC6 in Table 4.2-2).

6.1 Acceleration Transfer Function Results

Appendix C presents plots of the amplitudes of the acceleration transfer functions obtained directly from the SASSI2010 computer program analyses for the responses at the following key locations within the FWSC:

Location	Node Number	SASSI Model Node Number
FWS Wall Top	9	209
FWS Base	1	201
FPE Top	405	405
FPE Base	404	404

The amplitudes of the acceleration transfer functions are presented from the analyses of the LB, BE, and UB soil profiles with the control motion applied at the bottom of the FWSC basemat at EL 282 ft, NAVD88 and at the top of Zone III/IV rock (bottom of the concrete fill below the FWSC foundation) at nominal EL 220 ft, NAVD88. Each figure includes three plots presenting the FWSC responses in the three orthogonal directions due to the three earthquake components. The SASSI computed values of the transfer functions in these plots are depicted with dots. The interpolated values of the transfer functions are depicted by solid lines.

As expected, the acceleration transfer function results for the horizontal response of the FWSC obtained from the analysis with deep control motion input at EL 220 ft, NAVD88 are characterized with large peaks at frequencies that are close to the embedment shear column frequencies listed in Table 3.1-12 and at frequencies where dips occur in the response spectra of the input in-layer acceleration time histories presented in Figures 3.2-2 through 3.2-4. Therefore, these large peaks in the acceleration transfer functions that represent the response amplifications relative to the in-column input motion are not reflected in the acceleration response spectra results.

The plots generally show no numerical anomalies (e.g., sharp narrow spikes) in the interpolated transfer functions that can potentially impact the accuracy of the SSSI analyses results. The isolated sharp peak found in a few cases does not affect the accuracy of the corresponding responses.

Figures 6.1-1 through 6.1-3 present comparisons of the acceleration transfer function results for the response at the FWS and FPE structures relative to the input outcrop motion at the surface of the LB, BE, and UB subgrade profiles located at EL 282 ft, NAVD88 (bottom of basemat) that are obtained from the SSSI analysis of the FWSC-CB combined model and the SSI analyses of the FWSC standalone model. Figures 6.1-1 and 6.1-2, respectively, present the transfer functions for the co-directional responses of the FWS and FPE in the direction of the applied input motion. The comparisons shown in these figures indicate that the SSSI effects can amplify the FWS and FPE responses at peak frequencies with small shifts of the peak responses to higher frequencies. The transfer function results show that the most affected response by the SSSI effects is the EW response of the FWS structure.

Figure 6.1-3 presents the comparisons of the transfer functions for the cross-directional responses of the FWS structure. The transfer functions for the FWS response in the EW (Y) direction due to the NS (X) component of the earthquake show that the CB SSSI effects amplify the FWSC torsional response. The transfer functions for the FWS response in the EW direction due to the vertical (Z) component of the earthquake indicate SSSI amplifications of the FWSC rocking response in the EW direction.

6.2 SSSI Effects of CB on FWSC Maximum Responses

Figures 6.2-1 through 6.2-3 present comparisons of the maximum accelerations at the FWS mass locations obtained from the SSSI analyses of the FWSC-CB combined model and the SSI analyses of the FWSC standalone model for the LB, BE, and UB subgrade profiles, respectively. Figures 6.2-4 through 6.2-6 present comparisons of the maximum accelerations at the FPE mass locations obtained from the FWSC-CB SSSI analyses and the FWSC standalone SSI analyses for the LB, BE, and UB subgrade profiles, respectively. Figures 6.2-7 through 6.2-12 compare the FWSC-CB SSSI analyses and the FWSC standalone SSI analyses results for the shear forces and torsions of the stick members of the FWS and FPE LMSMs. The figures show the results from the FWSC-CB SSSI analyses with red dashed lines. The results obtained from the SSI analyses of the FWSC standalone model are shown with green solid lines.

Table 6.2-1 compares the results from the SSSI analyses of the FWSC-CB combined model and the SSI analyses of the FWSC standalone model for maximum accelerations of the SDOF oscillators representing the out-of-plane vibrations of the FWS roof and the hydrodynamic response of the water in the FWS tank.

These comparisons of the maximum responses presented in this section are based on the results obtained from the SSSI and SSI analyses of the FWSC-CB combined model and FWSC standalone model with full (uncracked concrete) stiffness properties and OBE damping values.

The comparisons show that the SSSI effects of the CB can amplify the maximum responses of the FWSC, in particular the responses of the FWS structure. The highest overall amplifications of the maximum accelerations and member shear forces are observed in the plots of Figures 6.2-1, 6.2-4, and 6.2-7 comparing the results from the analyses of the LB

subgrade profile with motion applied at the bottom of the FWSC basemat at EL 282 ft, NAVD88. This indicates that the SSSI effects are most pronounced for the softer subgrade conditions and input motions with low frequency energy content. The SSSI effects can amplify the maximum responses of the FWS by as much as 20% in the horizontal direction and 25% in the vertical direction. The comparisons of the maximum acceleration results in Table 6.2-1 also show that the SSSI with the CB can also amplify, by 34%, the response of the SDOF oscillator representing the out-of-plane acceleration of the FWSC roof.

The comparisons in Figures 6.2-7 through 6.2-9 show that the SSSI effects of the CB also affects the torsional response of the FWS. The SSSI-induced amplifications of the FWSC torsional moments are as much as 100% and can be observed in the results obtained from the analyses of LB, BE, and UB profiles.

The comparisons of the maximum accelerations in Figures 6.2-4 through 6.2-6 and the comparisons of the maximum shear forces and torsions in Figures 6.2-10 through 6.2-12 indicate that the SSSI between the CB and FWSC has small effect on the response of the FPE structure.

6.3 SSSI Effects of CB on FWSC ISRS

Figures 6.3-1 through 6.3-12 present a comparison of the results from the site-specific SSSI analyses of the FWSC-CB combined model and the site-specific SSI analyses of the FWSC standalone model for 5% damped ISRS for the NS, EW, and vertical response of the FWSC at the same key locations as the ones listed in Section 6.1. The ISRS are developed following the procedure described in Section 5.3 using the results of the SSSI and SSI analyses of the FWSC-CB combined model and FWSC standalone model, respectively, with full (uncracked concrete) stiffness properties and OBE damping values.

The comparisons of the ISRS results in Figures 6.3-1 through 6.3-12 show that the SSSI with the CB affects the FWSC response in the EW direction along the centerline of the FWSC and CB and in the vertical direction. The SSSI effects are manifested by amplifications of the peaks in the ISRS for the FWS response in the EW direction for a frequency range from 9 Hz for the LB subgrade stiffness to 30 Hz for the UB subgrade stiffness. The SSSI-induced amplifications of the vertical ISRS peaks are smaller and occur at frequencies above 20 Hz depending on the stiffness of the subgrade. The CB SSSI effects on the FWSC ISRS in the NS direction are relatively minor.

6.4 SSSI Effects of CB on Site-Specific Load Demands on FWSC Structures

The seismic structural loads representative of the site-specific seismic demands on the FWSC structures are developed following the methodology used to develop the standard design enveloping maximum structural loads presented in Reference 2-l. The horizontal load demands on the FWSC structures are developed from the diagrams of the maximum enveloping shear forces and maximum enveloping torsional moments. The vertical site-specific seismic load demands on the FWSC structures are developed from the diagrams of the maximum enveloping vertical floor mass accelerations and the maximum enveloping bending moments that account for the effects of floor rocking on the wall axial forces. The

results for maximum enveloping vertical acceleration of the FWSC SDOF oscillator mass are used to develop the local out-of-plane load on the FWS roof. The site-specific load demands on the FWSC structures are obtained from the results of the seismic response analyses performed on models representing full (uncracked) stiffness properties of the concrete structural members in conjunction with SSE damping values. Per Section C.1.2 of R.G. 1.61 (Reference 2-s), the use of SSE damping values for the development of structural loads is adequate because the stresses obtained from the models with SSE damping values will remain lower than the stress limits considered by the applicable structural design codes.

The effects of different subgrade conditions and input control motion locations on the FWSC site-specific seismic loads are evaluated first based on the results of the SSSI analyses of the FWSC-CB combined model with full stiffness properties and OBE damping values (analysis cases FC1 to FC6 in Table 4.4-2). Figures 6.4-1 and 6.4-2 provide comparisons of the diagrams of the horizontal and vertical loads on the FWS structure obtained from the results of the analyses of the LB, BE, and UB subgrade profiles with input motions specified at EL 282 ft, NAVD88 (bottom of basemat) and EL 220 ft, NAVD88 (bottom of concrete fill). The diagrams of the site-specific horizontal and vertical loads on the FPE structure obtained from the FWSC-CB SSSI analyses cases FC1 to FC6 are presented in Figures 6.4-3 and 6.4-4, respectively. The comparisons of the results from the different FWSC-CB SSSI analysis cases show that the analysis of the UB subgrade profiles with the deep input control motion at EL 220 ft, NAVD88 (analysis case FC6) yield bounding results for the seismic loads. The only exception is the FWS torsion presented in Figure 6.4-1 which is bounded by the results obtained from the FWSC-CB SSSI analysis of the BE subgrade profile with deep input control motion (analysis case FC5).

Since the SSSI analyses with deep input control motion at EL 220 ft, NAVD88 yield bounding results, the SSSI effects of the CB on the site-specific seismic load demands on the FWSC structures are evaluated based on the diagrams of the maximum vertical accelerations, member shear forces and moments obtained as the envelope of the results from the site-specific SSSI analyses of the FWSC-CB combined model with SSE damping values and the deep input control motion for the LB, BE, and UB full column profiles (analysis cases FC7, FC8, and FC9). Figures 6.4-5 through 6.4-8 compare these SSSI envelopes with the site-specific SSI enveloping maximum horizontal and vertical load demands obtained as envelopes of the results of the corresponding SSI analysis of the FWSC standalone model with full (uncracked concrete) stiffness properties, and SSE damping values for the LB, BE, and UB profiles with deep input motion at EL 220 ft, NAVD88. The figures present the envelope of the SSSI results with dashed red lines and the NA3 enveloping seismic demands from the FWSC site-specific SSI analyses with solid green lines. Diagrams of the horizontal and vertical seismic loads used for the standard design of the FWSC reinforced concrete structures are also provided in Figures 6.4-5 through 6.4-8 with dashed blue lines.

The comparisons in Figure 6.4-5 show that the SSSI with the CB amplifies the horizontal loads on the FWS structure. These SSSI amplifications result in small exceedances of the site-specific shear load demands with respect to the loads used for the standard design of the FWS structure. Similar to the results of the CB-FWSC SSSI evaluation presented in Section

5, the SSSI-induced amplifications of the FWS torsion are much bigger resulting in site-specific demands that are four times the torsion load considered in the standard design. The comparisons in Figure 6.4-6 show that the site-specific CB SSSI effects on the FWS vertical loads are small. Figures 6.4-7 and 6.4-8 also show that site-specific CB SSSI effects on the site-specific load demands on the FPE structure are small and that the small SSSI-induced exceedances in FPE loads are enveloped by the standard design loads.

Table 6.4-1 compares the maximum equivalent vertical accelerations representing the out-of-plane load on the FWS roof slab obtained from the results of the site-specific SSSI and SSI analyses of the FWSC-CB combined model and FWSC standalone model, respectively, with full stiffness properties and SSE damping values. The out-of-plane loads are computed based on the results for the maximum vertical accelerations of the FWS roof SDOF oscillator mass and the FWS roof lumped mass following the methodology described in Appendix D of the site-specific RB/FB seismic analysis report (Reference 2-w). These site-specific out-of-plane load demands are also compared to the FWS roof out-of-plane seismic load used for the standard design of the FWSC structures in Reference 2-x. The comparisons show that the SSSI effects on the FWS roof out-of-plane loads are not significant and enveloped by the corresponding load used for the standard design of the FWSC structures.

6.5 SSSI Effects of CB on FWSC Site-Specific Design ISRS

Figures 6.3-1 through 6.3-12 provide comparison of the 5% damped ISRS obtained from the site-specific SSSI analyses of the FWSC-CB combined model with full stiffness properties and OBE damping values with the corresponding 5% damped NA3 SSI enveloping ISRS and standard design ISRS shown with thick blue and black lines, respectively. The NA3 SSI enveloping ISRS represent the $\pm$15% broadened and valley filled envelope of the ISRS obtained from the site-specific SSI analyses of the FWSC standalone model with full stiffness properties and OBE damping values for the LB, BE, and UB profiles and input control motions located at EL of 282 ft, NAVD88 and EL 220 ft, NAVD88. The comparisons show that there are peaks in the ISRS obtained from the FWSC-CB SSSI analyses that exceed the NA3 site-specific SSI enveloping ISRS. Significant, greater than 10%, exceedances in the ISRS can be observed for:

- The EW response of the FWS roof between frequencies of 12 and 18 Hz
- The vertical response of the FWS roof and basemat between frequencies of 30 and 40 Hz
- The vertical response of the FPE roof between frequencies of 35 and 50 Hz
- The vertical response of the FPE basemat between frequencies of 30 and 50 Hz

Figures 6.3-6 and 6.3-12 show that the ISRS for the vertical response of the FWSC basemat also exceed the corresponding standard design ISRS.

7. CONCLUSIONS

The results of the evaluations presented in this report show that, in general, the SSSI between the CB and the FWSC have small effects on the site-specific seismic responses of these two structures.

The site-specific design of the CB envelops the SSSI effects of the FWSC on the CB seismic response. The CB site-specific design is based on the envelope of the results obtained from the SSI analyses of the CB standalone models representing two bounding embedment conditions:

- Partially embedded in Zone III rock that neglects the effects of the structural fill and in-situ saprolite on the seismic response of the CB
- Fully embedded that includes the effects of the structural fill and in-situ saprolite on the seismic response of the CB

The consideration of these two bounding embedment conditions provides a site-specific design basis that envelopes the amplification of the CB seismic response due to SSSI with the nearby FWSC.

The site-specific seismic response analyses of the FWSC consider that the FWSC is essentially a surface founded structure that is supported by a block of concrete fill embedded in the in-situ saprolite and Zone III rock. The SSI analyses of the FWSC standalone model consider LB, BE, and UB subgrade properties and two input control motions specified at the bottom of the FWSC foundation at EL 282 ft, NAVD88 and at the bottom of the concrete fill at EL 220 ft, NAVD88. The results of the evaluations of the SSSI effects between CB and FWSC presented in this report show that the responses obtained from these SSI analyses do not envelope all possible SSSI-induced amplifications of the FWSC response. The results obtained from the FWSC-CB SSSI analyses presented in this report will be used to develop the FWSC site-specific design basis that will envelop amplifications of the FWSC response that are due to the SSSI with the CB.

Table 3.1-1 LB In-Situ Subsurface Properties at CB Location

Layer #	Thickness (m)	Top-Depth (m)	Unit Weight (t/m^3)	V_s (m/s)	V_p (m/s)	Damping (%)
1	0.76	0.00	2.00	180	365	4.83
2	0.76	0.76	2.00	180	365	4.83
3	0.76	1.52	2.00	186	782	7.42
4	0.76	2.29	2.00	186	949	7.42
5	0.76	3.05	2.00	186	949	7.42
6	0.76	3.81	2.00	186	949	7.42
7	0.76	4.57	2.08	302	1463	6.53
8	0.76	5.33	2.08	302	1463	6.53
9	0.76	6.10	2.08	302	1463	6.53
10	0.76	6.86	2.08	302	1463	6.53
11	0.76	7.62	2.32	471	1463	1.06
12	0.76	8.38	2.32	471	1463	1.06
13	0.76	9.14	2.32	471	1463	1.06
14	0.76	9.91	2.32	471	1463	1.06
15	0.76	10.67	2.32	561	1715	1.14
16	0.76	11.43	2.32	561	1715	1.14
17	0.76	12.19	2.32	561	1715	1.14
18	0.76	12.95	2.32	561	1715	1.14
19	0.76	13.72	2.32	561	1715	1.14
20	0.46	14.48	2.32	561	1715	1.14
21	1.07	14.94	2.32	561	1715	1.14
22	0.76	16.00	2.32	561	1715	1.14
23	0.76	16.76	2.32	662	2022	0.96
24	0.76	17.53	2.32	662	2022	0.96
25	0.76	18.29	2.32	662	2022	0.96
26	0.76	19.05	2.32	662	2022	0.96
27	0.30	19.81	2.61	1613	3450	1.82
28	0.91	20.12	2.61	1613	3450	1.82
29	0.91	21.03	2.61	1613	3450	1.82
30	0.91	21.95	2.61	1613	3450	1.82
31	0.91	22.86	2.61	1738	3488	1.82
32	0.61	23.77	2.61	1738	3488	1.82
33	1.52	24.38	2.61	1738	3488	1.82
34	1.52	25.91	2.61	1738	3488	1.82
35	1.52	27.43	2.61	1738	3488	1.82
36	1.52	28.96	2.61	1977	3767	1.82
37	1.52	30.48	2.61	1977	3767	1.82
38	1.52	32.00	2.63	2154	3897	1.82
39	1.52	33.53	2.63	2154	3897	1.82
40	1.52	35.05	2.63	2051	3909	1.82
41	1.52	36.58	2.63	2051	3909	1.82
42	1.52	38.10	2.63	2155	4031	1.82
43	1.52	39.62	2.63	2155	4031	1.82
44	1.52	41.15	2.63	2195	3855	1.82
45	1.52	42.67	2.63	2195	3855	1.82
46	1.52	44.20	2.63	2324	4205	1.82
47	1.52	45.72	2.63	2324	4205	1.82
48	1.52	47.24	2.63	2289	4282	1.82
49	1.52	48.77	2.63	2289	4282	1.82
50		50.29	2.63	2290	3915	1.82

Table 3.1-2 UB In-Situ Subsurface Properties at CB Location

Layer #	Thickness (m)	Top-Depth (m)	Unit Weight (t/m^3)	V_s (m/s)	V_p (m/s)	Damping (%)
1	0.76	0.00	2.00	394	800	1.60
2	0.76	0.76	2.00	394	800	1.60
3	0.76	1.52	2.00	506	2126	2.08
4	0.76	2.29	2.00	506	2126	2.08
5	0.76	3.05	2.00	506	2126	2.08
6	0.76	3.81	2.00	506	2126	2.08
7	0.76	4.57	2.08	621	2608	2.19
8	0.76	5.33	2.08	621	2608	2.19
9	0.76	6.10	2.08	621	2608	2.19
10	0.76	6.86	2.08	621	2608	2.19
11	0.76	7.62	2.32	808	2469	0.36
12	0.76	8.38	2.32	808	2469	0.36
13	0.76	9.14	2.32	808	2469	0.36
14	0.76	9.91	2.32	808	2469	0.36
15	0.76	10.67	2.32	1014	3098	0.35
16	0.76	11.43	2.32	1014	3098	0.35
17	0.76	12.19	2.32	1014	3098	0.35
18	0.76	12.95	2.32	1014	3098	0.35
19	0.76	13.72	2.32	1014	3098	0.35
20	0.46	14.48	2.32	1014	3098	0.35
21	1.07	14.94	2.32	1014	3098	0.35
22	0.76	16.00	2.32	1014	3098	0.35
23	0.76	16.76	2.32	993	3034	0.29
24	0.76	17.53	2.32	993	3034	0.29
25	0.76	18.29	2.32	993	3034	0.29
26	0.76	19.05	2.32	993	3034	0.29
27	0.30	19.81	2.61	2420	5174	0.55
28	0.91	20.12	2.61	2420	5174	0.55
29	0.91	21.03	2.61	2420	5174	0.55
30	0.91	21.95	2.61	2420	5174	0.55
31	0.91	22.86	2.61	2607	5233	0.55
32	0.61	23.77	2.61	2607	5233	0.55
33	1.52	24.38	2.61	2607	5233	0.55
34	1.52	25.91	2.61	2607	5233	0.55
35	1.52	27.43	2.61	2607	5233	0.55
36	1.52	28.96	2.61	2965	5650	0.55
37	1.52	30.48	2.61	2965	5650	0.55
38	1.52	32.00	2.63	3231	5845	0.55
39	1.52	33.53	2.63	3231	5845	0.55
40	1.52	35.05	2.63	3077	5863	0.55
41	1.52	36.58	2.63	3077	5863	0.55
42	1.52	38.10	2.63	3232	6047	0.55
43	1.52	39.62	2.63	3232	6047	0.55
44	1.52	41.15	2.63	3293	5783	0.55
45	1.52	42.67	2.63	3293	5783	0.55
46	1.52	44.20	2.63	3487	6308	0.55
47	1.52	45.72	2.63	3487	6308	0.55
48	1.52	47.24	2.63	3434	6424	0.55
49	1.52	48.77	2.63	3434	6424	0.55
50		50.29	2.63	3434	5872	0.55

Table 3.1-3 LB In-Situ Subsurface Properties at FWSC Location

Layer #	Thickness (m)	Top-Depth (m)	Unit Weight (t/m^3)	V_s (m/s)	V_p (m/s)	Damping (%)
1	0.91	0.00	2.00	147	750	6.63
2	0.91	0.91	2.00	147	750	6.63
3	0.91	1.83	2.00	147	750	6.63
4	0.91	2.74	2.00	147	750	6.63
5	0.91	3.66	2.00	184	940	8.25
6	0.91	4.57	2.00	184	940	8.25
7	0.91	5.49	2.00	184	940	8.25
8	1.22	6.40	2.00	184	940	8.25
9	1.22	7.62	2.00	184	940	8.25
10	1.22	8.84	2.08	310	1463	6.08
11	0.91	10.06	2.08	436	1463	4.37
12	0.61	10.97	2.08	436	1463	4.37
13	1.22	11.58	2.32	581	1775	1.14
14	1.22	12.80	2.32	581	1775	1.14
15	1.22	14.02	2.32	581	1775	1.14
16	1.22	15.24	2.32	581	1775	1.14
17	1.22	16.46	2.32	655	2002	0.94
18	1.22	17.68	2.32	655	2002	0.94
19	0.91	18.90	2.61	1464	3130	1.82
20	0.91	19.81	2.61	1464	3130	1.82
21	0.91	20.73	2.61	1738	3488	1.82
22	1.22	21.64	2.61	1738	3488	1.82
23	1.22	22.86	2.61	1738	3488	1.82
24	0.91	24.08	2.63	1977	3767	1.82
25	1.22	24.99	2.63	1977	3767	1.82
26	1.22	26.21	2.63	1977	3767	1.82
27	0.91	27.43	2.63	2154	3897	1.82
28	1.22	28.35	2.63	2154	3897	1.82
29	1.22	29.57	2.63	2154	3897	1.82
30	0.91	30.78	2.63	2051	3909	1.82
31	1.22	31.70	2.63	2051	3909	1.82
32	1.22	32.92	2.63	2051	3909	1.82
33	0.91	34.14	2.63	2155	4031	1.82
34	1.22	35.05	2.63	2155	4031	1.82
35	1.22	36.27	2.63	2155	4031	1.82
36	0.91	37.49	2.63	2195	3855	1.82
37	1.22	38.40	2.63	2195	3855	1.82
38	1.22	39.62	2.63	2195	3855	1.82
39	0.91	40.84	2.63	2324	4205	1.82
40	1.22	41.76	2.63	2324	4205	1.82
41	1.22	42.98	2.63	2324	4205	1.82
42	0.91	44.20	2.63	2289	4282	1.82
43	1.22	45.11	2.63	2289	4282	1.82
44	1.22	46.33	2.63	2289	4282	1.82
45		47.55	2.63	2290	3915	1.82

Table 3.1-4 BE In-Situ Subsurface Properties at FWSC Location

Layer #	Thickness (m)	Top-Depth (m)	Unit Weight (t/m^3)	V_s (m/s)	V_p (m/s)	Damping (%)
1	0.91	0.00	2.00	226	1153	4.18
2	0.91	0.91	2.00	226	1153	4.18
3	0.91	1.83	2.00	226	1153	4.18
4	0.91	2.74	2.00	226	1153	4.18
5	0.91	3.66	2.00	298	1463	5.00
6	0.91	4.57	2.00	298	1463	5.00
7	0.91	5.49	2.00	298	1463	5.00
8	1.22	6.40	2.00	298	1463	5.00
9	1.22	7.62	2.00	298	1463	5.00
10	1.22	8.84	2.08	432	1814	3.97
11	0.91	10.06	2.08	596	1821	2.89
12	0.61	10.97	2.08	596	1821	2.89
13	1.22	11.58	2.32	763	2331	0.64
14	1.22	12.80	2.32	763	2331	0.64
15	1.22	14.02	2.32	763	2331	0.64
16	1.22	15.24	2.32	763	2331	0.64
17	1.22	16.46	2.32	821	2508	0.53
18	1.22	17.68	2.32	821	2508	0.53
19	0.91	18.90	2.61	1976	4225	1.00
20	0.91	19.81	2.61	1976	4225	1.00
21	0.91	20.73	2.61	2128	4273	1.00
22	1.22	21.64	2.61	2128	4273	1.00
23	1.22	22.86	2.61	2128	4273	1.00
24	0.91	24.08	2.63	2421	4613	1.00
25	1.22	24.99	2.63	2421	4613	1.00
26	1.22	26.21	2.63	2421	4613	1.00
27	0.91	27.43	2.63	2638	4772	1.00
28	1.22	28.35	2.63	2638	4772	1.00
29	1.22	29.57	2.63	2638	4772	1.00
30	0.91	30.78	2.63	2512	4787	1.00
31	1.22	31.70	2.63	2512	4787	1.00
32	1.22	32.92	2.63	2512	4787	1.00
33	0.91	34.14	2.63	2639	4937	1.00
34	1.22	35.05	2.63	2639	4937	1.00
35	1.22	36.27	2.63	2639	4937	1.00
36	0.91	37.49	2.63	2689	4722	1.00
37	1.22	38.40	2.63	2689	4722	1.00
38	1.22	39.62	2.63	2689	4722	1.00
39	0.91	40.84	2.63	2847	5150	1.00
40	1.22	41.76	2.63	2847	5150	1.00
41	1.22	42.98	2.63	2847	5150	1.00
42	0.91	44.20	2.63	2804	5245	1.00
43	1.22	45.11	2.63	2804	5245	1.00
44	1.22	46.33	2.63	2804	5245	1.00
45		47.55	2.63	2804	4794	1.00

Table 3.1-5 UB In-Situ Subsurface Properties at FWSC Location

Layer #	Thickness (m)	Top-Depth (m)	Unit Weight (t/m^3)	V_s (m/s)	V_p (m/s)	Damping (%)
1	0.91	0.00	2.00	348	1463	2.64
2	0.91	0.91	2.00	348	1463	2.64
3	0.91	1.83	2.00	348	1463	2.64
4	0.91	2.74	2.00	348	1463	2.64
5	0.91	3.66	2.00	483	2030	3.03
6	0.91	4.57	2.00	483	2030	3.03
7	0.91	5.49	2.00	483	2030	3.03
8	1.22	6.40	2.00	483	2030	3.03
9	1.22	7.62	2.00	483	2030	3.03
10	1.22	8.84	2.08	600	2524	2.60
11	0.91	10.06	2.08	814	2488	1.92
12	0.61	10.97	2.08	814	2488	1.92
13	1.22	11.58	2.32	1002	3060	0.36
14	1.22	12.80	2.32	1002	3060	0.36
15	1.22	14.02	2.32	1002	3060	0.36
16	1.22	15.24	2.32	1002	3060	0.36
17	1.22	16.46	2.32	1028	3141	0.30
18	1.22	17.68	2.32	1028	3141	0.30
19	0.91	18.90	2.61	2667	5703	0.55
20	0.91	19.81	2.61	2667	5703	0.55
21	0.91	20.73	2.61	2607	5233	0.55
22	1.22	21.64	2.61	2607	5233	0.55
23	1.22	22.86	2.61	2607	5233	0.55
24	0.91	24.08	2.63	2965	5650	0.55
25	1.22	24.99	2.63	2965	5650	0.55
26	1.22	26.21	2.63	2965	5650	0.55
27	0.91	27.43	2.63	3231	5845	0.55
28	1.22	28.35	2.63	3231	5845	0.55
29	1.22	29.57	2.63	3231	5845	0.55
30	0.91	30.78	2.63	3077	5863	0.55
31	1.22	31.70	2.63	3077	5863	0.55
32	1.22	32.92	2.63	3077	5863	0.55
33	0.91	34.14	2.63	3232	6047	0.55
34	1.22	35.05	2.63	3232	6047	0.55
35	1.22	36.27	2.63	3232	6047	0.55
36	0.91	37.49	2.63	3293	5783	0.55
37	1.22	38.40	2.63	3293	5783	0.55
38	1.22	39.62	2.63	3293	5783	0.55
39	0.91	40.84	2.63	3487	6308	0.55
40	1.22	41.76	2.63	3487	6308	0.55
41	1.22	42.98	2.63	3487	6308	0.55
42	0.91	44.20	2.63	3434	6424	0.55
43	1.22	45.11	2.63	3434	6424	0.55
44	1.22	46.33	2.63	3434	6424	0.55
45		47.55	2.63	3434	5872	0.55

Table 3.1-6 LB Properties of Structural and Concrete Fill at CB Location

Layer #	Thickness (m)	Top-Depth (m)	Unit Weight (t/m^3)	V_s (m/s)	V_p (m/s)	Damping (%)
1	0.76	0.00	2.08	134	251	4.98
2	0.76	0.76	2.08	134	251	4.98
3	0.76	1.52	2.08	148	277	7.17
4	0.76	2.29	2.08	148	755	7.17
5	0.76	3.05	2.08	146	742	8.38
6	0.76	3.81	2.08	146	742	8.38
7	0.76	4.57	2.08	150	764	9.11
8	0.76	5.33	2.08	150	764	9.11
9	0.76	6.10	2.08	157	800	8.93
10	0.76	6.86	2.08	157	800	8.93
Concrete Fill		7.62	2.32	1829	2850	1.80

Table 3.1-7 UB Properties of Structural and Concrete Fill at CB Location

Layer #	Thickness (m)	Top-Depth (m)	Unit Weight (t/m^3)	V_s (m/s)	V_p (m/s)	Damping (%)
1	0.76	0.00	2.08	292	546	1.98
2	0.76	0.76	2.08	292	546	1.98
3	0.76	1.52	2.08	350	655	2.72
4	0.76	2.29	2.08	350	1463	2.72
5	0.76	3.05	2.08	360	1463	3.24
6	0.76	3.81	2.08	360	1463	3.24
7	0.76	4.57	2.08	358	1463	3.84
8	0.76	5.33	2.08	358	1463	3.84
9	0.76	6.10	2.08	391	1463	3.60
10	0.76	6.86	2.08	391	1463	3.60
Concrete Fill		7.62	2.32	2438	3800	0.55

Table 3.1-8 LB Properties of Structural and Concrete Fill at FWSC Location

Layer #	Thickness (m)	Top-Depth (m)	Unit Weight (t/m^3)	V_s (m/s)	V_p (m/s)	Damping (%)
1	1.00	0.00	2.08	146	744	7.33
2	0.915	1.00	2.08	150	763	7.50
3	0.915	1.92	2.08	153	782	7.85
4	0.915	2.83	2.08	155	788	8.29
5	0.915	3.75	2.08	160	818	8.02
6	0.915	4.66	2.08	155	790	8.50
7	0.915	5.58	2.08	158	805	8.54
8	1.22	6.49	2.08	158	809	8.87
9	1.22	7.71	2.08	157	799	9.19
10	1.22	8.93	2.08	168	856	8.74
11	0.91	10.15	2.08	162	825	9.35
12	0.61	11.06	2.08	162	825	9.35
Concrete Fill		11.67	2.32	1829	2850	1.82

Table 3.1-9 BE Properties of Structural and Concrete Fill at FWSC Location

Layer #	Thickness (m)	Top-Depth (m)	Unit Weight (t/m^3)	V_s (m/s)	V_p (m/s)	Damping (%)
1	1.00	0.00	2.08	227	1158	4.74
2	0.915	1.00	2.08	231	1180	4.83
3	0.915	1.92	2.08	239	1219	4.97
4	0.915	2.83	2.08	239	1216	5.33
5	0.915	3.75	2.08	258	1314	5.17
6	0.915	4.66	2.08	253	1291	5.47
7	0.915	5.58	2.08	253	1291	5.65
8	1.22	6.49	2.08	260	1325	5.67
9	1.22	7.71	2.08	258	1318	5.96
10	1.22	8.93	2.08	272	1389	5.75
11	0.91	10.15	2.08	271	1383	5.95
12	0.61	11.06	2.08	271	1383	5.95
Concrete Fill		11.67	2.32	2134	3325	1.00

Table 3.1-10 UB Properties of Structural and Concrete Fill at FWSC Location

Layer #	Thickness (m)	Top-Depth (m)	Unit Weight (t/m^3)	V_s (m/s)	V_p (m/s)	Damping (%)
1	1.00	0.00	2.08	354	1463	3.06
2	0.915	1.00	2.08	358	1463	3.11
3	0.915	1.92	2.08	373	1463	3.15
4	0.915	2.83	2.08	368	1463	3.42
5	0.915	3.75	2.08	414	1463	3.33
6	0.915	4.66	2.08	413	1463	3.52
7	0.915	5.58	2.08	406	1463	3.74
8	1.22	6.49	2.08	426	1463	3.63
9	1.22	7.71	2.08	427	1463	3.87
10	1.22	8.93	2.08	442	1463	3.78
11	0.91	10.15	2.08	455	1463	3.79
12	0.61	11.06	2.08	455	1463	3.79
Concrete Fill		11.67	2.32	2438	3800	0.55

Table 3.1-11 Average Strain-Compatible Shear Wave Velocities and Shear Column Frequencies of the Fill and In-Situ Materials at CB Location

Soil Case	Concrete Fill/ Zone III Rock Embedment					Structural Fill/ Saprolite Embedment				
	Depth	Backfill		In-Situ		Depth	Backfill		In-Situ	
		$V_{s\text{-}ave}$	f_{sc}	$V_{s\text{-}ave}$	f_{sc}		$V_{s\text{-}ave}$	f_{sc}	$V_{s\text{-}ave}$	f_{sc}
	m	m/s	Hz	m/s	Hz	m	m/s	Hz	m/s	Hz
LB	7.3	1829	62.8	520	17.8	7.6	147	4.8	218	7.2
UB		2438	83.7	917	31.4		347	11.4	515	16.9

Table 3.1-12 Average Strain-Compatible Shear Wave Velocities and Shear Column Frequencies of the Fill and In-Situ Materials around concrete fill below FWSC Foundation

Soil Case	Zone III Rock			Structural Fill/ Saprolite					Full Column				
	Depth	$V_{s\text{-}ave}$	f_{sc}	Depth	Backfill		In-Situ		Depth	Backfill		In-Situ	
					$V_{s\text{-}ave}$	f_{sc}	$V_{s\text{-}ave}$	f_{sc}		$V_{s\text{-}ave}$	f_{sc}	$V_{s\text{-}ave}$	f_{sc}
	m	m/s	Hz	m	m/s	Hz	m/s	Hz	m	m/s	Hz	m/s	Hz
LB	7.3	604	20.6	11.7	157	3.4	191	4.1	19.0	242	3.2	259	3.4
BE		781	26.7		252	5.4	297	6.4		382	5.0	390	5.1
UB		1011	34.5		405	8.7	459	9.8		597	7.9	582	7.7

Table 4.2-1 CB-FWSC Site-Specific SSSI Analysis Cases, Passing, and Cut-off Frequencies

Case No.	Subgrade Profile		Method	Control Motion El.	Passing Freq.	Cut-off Freq.	Captured Motion Energy		
					(Hz)	(Hz)	X (NS)	Y (EW)	Z (Vert.)
CF1	Full Column	LB	MSM	241 ft	34	34	83%	82%	86%
CF2		UB			74	70	99%	99%	99%

Table 4.2-2 FWSC-CB Site-Specific SSSI Analysis Cases, Passing and Cut-off Frequencies

(a) FWSC-CB Combined Model with OBE Damping

Case No.	Subgrade Profile	Method	Control Motion El.	Passing Freq.	Cut-off Freq.	Captured Motion Energy		
				(Hz)	(Hz)	X (NS)	Y (EW)	Z (Vert.)
FC1	LB	MSM	282 ft	30	30	84%	81%	75%
FC2	BE			47	47	98%	97%	95%
FC3	UB			72	70	99%	99%	99%
FC4	LB		220 ft	30	30	80%	72%	72%
FC5	BE			47	47	98%	96%	95%
FC6	UB			72	70	99%	99%	99%

(b) FWSC-CB Combined Model with SSE Damping

Case No.	Subgrade Profile	Method	Control Motion El.	Passing Freq.	Cut-off Freq.	Captured Motion Energy		
				(Hz)	(Hz)	X (NS)	Y (EW)	Z (Vert.)
FC7	LB	MSM	220 ft	30	30	80%	72%	72%
FC8	BE			47	47	98%	96%	95%
FC9	UB			72	70	99%	99%	99%

Table 4.2-3 List of Frequencies for SSSI Analyses

Frequency No.	Frequency (Hz)				
	CB-FWSC SSSI Analysis		FWSC-CB SSSI Analysis		
	LB	UB	LB	BE	UB
1	0.0244	0.0244	0.0244	0.0244	0.0244
41	1.0010	1.0010	1.0010	1.0010	1.0010
82	2.0020	2.0020	2.0020	2.0020	2.0020
123	3.0029	3.0029	3.0029	3.0029	3.0029
164	4.0039	4.0039	4.0039	4.0039	4.0039
205	5.0049	5.0049	5.0049	5.0049	5.0049
246	6.0059	6.0059	6.0059	6.0059	6.0059
287	7.0068	7.0068	7.0068	7.0068	7.0068
328	8.0078	8.0078	8.0078	8.0078	8.0078
369	9.0088	9.0088	9.0088	9.0088	9.0088
410	10.0098	10.0098	10.0098	10.0098	10.0098
451	11.0107	11.0107	11.0107	11.0107	11.0107
492	12.0117	12.0117	12.0117	12.0117	12.0117
532	12.9883	12.9883	12.9883	12.9883	12.9883
573	13.9893	13.9893	13.9893	13.9893	13.9893
614	14.9902	14.9902	14.9902	14.9902	14.9902
655	15.9912	15.9912	15.9912	15.9912	15.9912
696	16.9922	16.9922	16.9922	16.9922	16.9922
737	17.9932	17.9932	17.9932	17.9932	17.9932
778	18.9941	18.9941	18.9941	18.9941	18.9941
819	19.9951	19.9951	19.9951	19.9951	19.9951
860	20.9961	20.9961	20.9961	20.9961	20.9961
901	21.9971	21.9971	21.9971	21.9971	21.9971
942	22.9980	22.9980	22.9980	22.9980	22.9980
983	23.9990	23.9990	23.9990	23.9990	23.9990
1024	25.0000	25.0000	25.0000	25.0000	25.0000
1065	26.0010	26.0010	26.0010	26.0010	26.0010
1106	27.0020	27.0020	27.0020	27.0020	27.0020
1147	28.0029	28.0029	28.0029	28.0029	28.0029
1188	29.0039	29.0039	29.0039	29.0039	29.0039
1229	30.0049	30.0049	30.0049	30.0049	30.0049
1270	31.0059	31.0059		31.0059	31.0059
1311	32.0068	32.0068		32.0068	32.0068
1352	33.0078	33.0078		33.0078	33.0078
1393	34.0088	34.0088		34.0088	34.0088
1434		35.0098		35.0098	35.0098
1475		36.0107		36.0107	36.0107
1516		37.0117		37.0117	37.0117
1557		38.0127		38.0127	38.0127
1598		39.0137		39.0137	39.0137
1639		40.0146		40.0146	40.0146
1680		41.0156		41.0156	41.0156
1721		42.0166		42.0166	42.0166
1762		43.0176		43.0176	43.0176
1803		44.0186		44.0186	44.0186
1844		45.0195		45.0195	45.0195
1885		46.0205		46.0205	46.0205
1926		47.0215		47.0215	47.0215

Table 4.2-3 List of Frequencies for SSSI Analyses (Continued)

Frequency No.	Frequency (Hz)				
	CB-FWSC SSSI Analysis		FWSC-CB SSSI Analysis		
	LB	UB	LB	BE	UB
1966		47.9980			47.9980
2007		48.9990			48.9990
2048		50.0000			50.0000
2089		51.0010			51.0010
2130		52.0020			52.0020
2171		53.0029			53.0029
2212		54.0039			54.0039
2253		55.0049			55.0049
2294		56.0059			56.0059
2335		57.0068			57.0068
2376		58.0078			58.0078
2417		59.0088			59.0088
2458		60.0098			60.0098
2499		61.0107			61.0107
2540		62.0117			62.0117
2581		63.0127			63.0127
2622		64.0137			64.0137
2663		65.0146			65.0146
2703		65.9912			65.9912
2744		66.9922			66.9922
2785		67.9932			67.9932
2826		68.9941			68.9941
2867		69.9951			69.9951

Table 4.3-1 Lateral Extent of Structural Fill around CB

North	3730 mm (12.24 ft)	Minimum distance to inside face of Sheet Piling adjacent to CB
South	3730 mm (12.24 ft)	One-half the distance between CB and Service Building (SB) 0.5 x 7460 mm (24.48 ft)
East	6020 mm (19.75 ft)	One-half the distance between CB and FWSC 0.5 x 12040 mm (39.5 ft)
West	6975 mm (22.88 ft)	One-half the distance between CB and RB/FB 0.5 x 13950 mm (45.77 ft)
Minimum Distance	3730 mm (12.24 ft)	CB lateral extent of backfill

Table 4.3-2 Lateral Extent of Structural Fill around FWSC

North	5990 mm (19.65 ft)	Minimum distance to inside face of Sheet Piling adjacent to FWSC
South	5990 mm (19.65 ft)	Minimum distance to inside face of Sheet Piling adjacent to FWSC
East	5990 mm (19.65 ft)	Minimum distance to inside face of Sheet Piling adjacent to FWSC
West	6020 mm (19.75 ft)	One-half the distance between FWSC and CB 0.5 x 12040 mm (39.5 ft)
Minimum Distance	5990 mm (19.65 ft)	FWSC lateral extent of backfill

Table 4.3-3 Subsurface Properties for CB-FWSC SSSI Analysis of LB Profile

	EL	Soil						Backfill					
		Unit Weight	Vs	Vp	Damping	Highest Frequency	Poisson's	Unit Weight	Vs	Vp	Damping	Highest Frequency	Poisson's
	[m]	[t/m^3]	[m/sec]	[m/sec]	[%]	[Hz]	ratio	[t/m^3]	[m/sec]	[m/sec]	[%]	[Hz]	ratio
	4.50	2.00	180	365	4.83	36.2	0.339	2.08	134	251	4.98	33.7	0.301
	3.74												
	3.74	2.00	180	365	4.83	36.2	0.339	2.08	134	251	4.98	33.7	0.301
	2.98												
①	2.98	2.00	186	793	7.42	37.5	0.471	2.08	148	291	7.17	35.6	0.326
	2.15												
	2.15	2.00	186	949	7.42	37.5	0.480	2.08	148	755	7.17	37.3	0.480
	1.45												
	1.45	2.00	186	949	7.42	37.5	0.480	2.08	146	742	8.38	36.8	0.480
	0.69												
	0.69	2.00	186	949	7.42	37.5	0.480	2.08	146	742	8.38	36.8	0.480
	-0.07												
	-0.07	2.08	302	1463	6.53	60.8	0.478	2.08	150	764	9.11	37.8	0.480
	-0.72												
	-0.72	2.08	302	1463	6.53	60.8	0.478	2.08	150	764	9.11	37.8	0.480
	-1.37												
②	-1.37	2.08	302	1463	6.53	60.8	0.478	2.08	154	786	9.00	38.8	0.480
	-2.00												
	-2.00	2.08	302	1463	6.53	60.8	0.478	2.08	157	800	8.93	39.5	0.480
	-2.56												
	-2.56	2.08	302	1463	6.53	60.8	0.478	2.08	157	800	8.93	39.5	0.480
	-3.12												
	-3.12	2.32	471	1463	1.06	44.0	0.442	2.32	1829	2850	1.80	170.9	0.150
	-5.26												
③	-5.26	2.32	519	1598	1.11	48.5	0.441	2.32	1829	2850	1.80	170.9	0.150
	-7.40												
	-7.40	2.32	561	1715	1.14	56.1	0.440	2.32	1829	2850	1.80	182.9	0.150
	-8.90												
	-8.90	2.32	561	1715	1.14	56.1	0.440	2.32	1829	2850	1.80	182.9	0.150
	-10.40												
	-10.40	2.32	561	1715	1.14	56.1	0.440	2.32	1829	2850	1.80	182.9	0.150
	-12.26												
	-12.26	2.32	662	2022	0.96	66.2	0.440	2.32	1829	2850	1.80	182.9	0.150
	-13.785												
	-13.785	2.32	662	2022	0.96	66.2	0.440	2.32	1829	2850	1.80	182.9	0.150
	-15.31												
	-15.31	2.61	1613	3450	1.82	105.7	0.360						
	-18.36												
	-18.36	2.61	1738	3488	1.82	56.9	0.335						
	-24.46												
	-24.46	2.61	1977	3767	1.82	130.0	0.310						
	-27.50												
	-27.50	2.63	2154	3897	1.82	141.2	0.280						
	-30.55												
	-30.55	2.63	2051	3909	1.82	134.4	0.310						
	-33.60												
	-33.60	2.63	2155	4031	1.82	141.3	0.300						
	-36.65												
	-36.65	2.63	2195	3855	1.82	143.9	0.260						
	-39.70												
	-39.70	2.63	2324	4205	1.82	152.8	0.280						
	-42.74												
	-42.74	2.63	2289	4282	1.82	150.0	0.300						
	-45.79												
	-45.79	2.63	2290	3915	1.82		0.240						
	-												

Note: The soil properties of the adjusted layer, shown in the red box, are evaluated from the original properties shown below.

Table 4.3-3 Subsurface Properties for CB-FWSC SSSI Analysis of LB Profile (Continued)

Original data

	EL	Soil						Backfill					
	[m]	Unit Weight [t/m^3]	Vs [m/sec]	Vp [m/sec]	Damping [%]	Highest Frequency [Hz]	Poisson's ratio	Unit Weight [t/m^3]	Vs [m/sec]	Vp [m/sec]	Damping [%]	Highest Frequency [Hz]	Poisson's ratio
①	2.980	2.00	186	782	7.42		0.470	2.08	148	277	7.17		0.300
	2.215												
	2.215	2.00	186	949	7.42		0.480	2.08	148	755	7.17		0.480
	2.150												
②	-1.370	2.08	302	1463	6.53		0.478	2.08	150	764	9.11		0.480
	-1.600												
	-1.600	2.08	302	1463	6.53		0.478	2.08	157	800	8.93		0.480
	-2.000												
③	-5.260	2.32	471	1463	1.06		0.442	2.32	1829	2850	1.80		0.150
	-6.170												
	-6.170	2.32	561	1715	1.14		0.440	2.32	1829	2850	1.80		0.150
	-7.400												

Vs and Vp are determined using the equivalent wave travel time procedure.
Example ③: 519=(7.40-5.26)/(0.91/471+1.23/561)
Damping ratio is determined using the thickness weighted average procedure.
Example ③: 1.11=(1.06x(6.17-5.26)+1.14x(7.40-6.17))/(0.91+1.23)

Table 4.3-4 Subsurface Properties for CB-FWSC SSSI Analysis of UB Profile

	EL	Soil						Backfill					
		Unit Weight	Vs	Vp	Damping	Highest Frequency	Poisson's	Unit Weight	Vs	Vp	Damping	Highest Frequency	Poisson's
	[m]	[t/m^3]	[m/sec]	[m/sec]	[%]	[Hz]	ratio	[t/m^3]	[m/sec]	[m/sec]	[%]	[Hz]	ratio
	4.50	2.00	394	800	1.60	79.4	0.340	2.08	292	546	1.98	73.6	0.300
	3.74												
	3.74	2.00	394	800	1.60	79.4	0.340	2.08	292	546	1.98	73.6	0.300
	2.98												
①	2.98	2.00	506	2126	2.08	102.0	0.470	2.08	350	685	2.72	84.3	0.323
	2.15												
	2.15	2.00	506	2126	2.08	102.0	0.470	2.08	350	1463	2.72	88.2	0.470
	1.45												
	1.45	2.00	506	2126	2.08	102.0	0.470	2.08	360	1463	3.24	90.7	0.468
	0.69												
	0.69	2.00	506	2126	2.08	102.0	0.470	2.08	360	1463	3.24	90.7	0.468
	-0.07												
	-0.07	2.08	621	2608	2.19	125.2	0.470	2.08	358	1463	3.84	90.2	0.468
	-0.72												
	-0.72	2.08	621	2608	2.19	125.2	0.470	2.08	358	1463	3.84	90.2	0.468
	-1.37												
②	-1.37	2.08	621	2608	2.19	125.2	0.470	2.08	378	1463	3.69	95.3	0.464
	-2.00												
	-2.00	2.08	621	2608	2.19	125.2	0.470	2.08	391	1463	3.60	98.6	0.462
	-2.56												
	-2.56	2.08	621	2608	2.19	125.2	0.470	2.08	391	1463	3.60	98.6	0.462
	-3.12												
	-3.12	2.32	808	2469	0.36	75.5	0.440	2.32	2438	3800	0.55	227.8	0.150
	-5.26												
③	-5.26	2.32	915	2795	0.35	85.5	0.440	2.32	2438	3800	0.55	227.8	0.150
	-7.40												
	-7.40	2.32	1014	3098	0.35	101.4	0.440	2.32	2438	3800	0.55	243.8	0.150
	-8.90												
	-8.90	2.32	1014	3098	0.35	101.4	0.440	2.32	2438	3800	0.55	243.8	0.150
	-10.40												
	-10.40	2.32	1014	3098	0.35	101.4	0.440	2.32	2438	3800	0.55	243.8	0.150
	-12.26												
	-12.26	2.32	993	3034	0.29	99.3	0.440	2.32	2438	3800	0.55	243.8	0.150
	-13.785												
	-13.785	2.32	993	3034	0.29	99.3	0.440	2.32	2438	3800	0.55	243.8	0.150
	-15.31												
	-15.31	2.61	2420	5174	0.55	158.6	0.360						
	-18.36												
	-18.36	2.61	2607	5233	0.55	85.4	0.335						
	-24.46												
	-24.46	2.61	2965	5650	0.55	195.0	0.310						
	-27.50												
	-27.50	2.63	3231	5845	0.55	211.8	0.280						
	-30.55												
	-30.55	2.63	3077	5863	0.55	201.7	0.310						
	-33.60												
	-33.60	2.63	3232	6047	0.55	211.9	0.300						
	-36.65												
	-36.65	2.63	3293	5783	0.55	215.9	0.260						
	-39.70												
	-39.70	2.63	3487	6308	0.55	229.4	0.280						
	-42.74												
	-42.74	2.63	3434	6424	0.55	225.1	0.300						
	-45.79												
	-45.79	2.63	3434	5872	0.55		0.240						
	-												

Note: The soil properties of the adjusted layer, shown in the red box, are evaluated from the original properties shown below.

Table 4.3-4 Subsurface Properties for CB-FWSC SSSI Analysis of UB Profile (Continued)

Original data

	EL	Soil						Backfill					
		Unit Weight	Vs	Vp	Damping	Highest Frequency	Poisson's	Unit Weight	Vs	Vp	Damping	Highest Frequency	Poisson's
	[m]	[t/m^3]	[m/sec]	[m/sec]	[%]	[Hz]	ratio	[t/m^3]	[m/sec]	[m/sec]	[%]	[Hz]	ratio
①	2.980	2.00	506	2126	2.08		0.470	2.08	350	655	2.72		0.300
	2.215												
	2.215	2.00	506	2126	2.08		0.470	2.08	350	1463	2.72		0.470
	2.150												
②	-1.370	2.08	621	2608	2.19		0.470	2.08	358	1463	3.84		0.468
	-1.600												
	-1.600	2.08	621	2608	2.19		0.470	2.08	391	1463	3.60		0.462
	-2.000												
③	-5.260	2.32	808	2469	0.36		0.440	2.32	2438	3800	0.55		0.150
	-6.170												
	-6.170	2.32	1014	3098	0.35		0.440	2.32	2438	3800	0.55		0.150
	-7.400												

Vs and Vp are determined using the equivalent wave travel time procedure.
Example ③: 915=(7.40-5.26)/(0.91/808+1.23/1014)
Damping ratio is determined using the thickness weighted average procedure.
Example ③: 0.35=(0.36x(6.17-5.26)+0.35x(7.40-6.17))/(0.91+1.23)

Table 4.3-5 Subsurface Properties for FWSC-CB SSSI Analysis of LB Profile

	EL	Soil						Backfill					
		Unit Weight [t/m^3]	Vs [m/sec]	Vp [m/sec]	Damping [%]	Highest Frequency [Hz]	Poisson's ratio	Unit Weight [t/m^3]	Vs [m/sec]	Vp [m/sec]	Damping [%]	Highest Frequency [Hz]	Poisson's ratio
	[m]												
	2.15	2.00	147	750	6.63	30.3	0.480	2.08	146	744	7.33	36.5	0.480
	1.45												
①	1.45	2.00	147	750	6.63	30.3	0.480	2.08	148	755	7.43	37.0	0.480
	0.75												
②	0.75	2.00	147	750	6.63	30.3	0.480	2.08	151	769	7.61	37.7	0.480
	0.00												
	0.00	2.00	147	750	6.63	30.3	0.480	2.08	153	782	7.85	38.2	0.480
	-0.68												
	-0.68	2.00	147	750	6.63	30.3	0.480	2.08	155	788	8.29	38.7	0.480
	-1.40												
③	-1.40	2.00	170	867	7.71	35.0	0.480	2.08	158	808	8.11	39.5	0.480
	-2.00												
	-2.00	2.00	184	940	8.25	37.9	0.480	2.08	160	818	8.02	40.0	0.480
	-2.51												
	-2.51	2.00	184	940	8.25	37.9	0.480	2.08	155	790	8.50	38.7	0.480
	-3.17												
④	-3.17	2.00	184	940	8.25	37.9	0.480	2.08	157	801	8.53	34.8	0.480
	-4.07												
⑤	-4.07	2.00	184	940	8.25	37.9	0.480	2.08	158	808	8.77	35.1	0.480
	-4.97												
⑥	-4.97	2.00	184	940	8.25	37.9	0.480	2.08	158	806	8.98	35.1	0.480
	-5.87												
	-5.87	2.00	184	940	8.25	37.9	0.480	2.08	157	799	9.19	34.5	0.480
	-6.78												
	-6.78	2.08	310	1463	6.08	63.9	0.476	2.08	168	856	8.74	42.0	0.480
	-7.40												
	-7.40	2.08	310	1463	6.08	63.9	0.476	2.08	168	856	8.74	42.0	0.480
	-8.00												
	-8.00	2.08	436	1463	4.37	89.8	0.451	2.08	162	825	9.35	40.5	0.480
	-8.70												
	-8.70	2.08	436	1463	4.37	89.8	0.451	2.08	162	825	9.35	39.5	0.480
	-9.52												
	-9.52	2.32	581	1775	1.14	42.2	0.440	2.32	1829	2850	1.82	415.6	0.150
	-10.40												
	-10.40	2.32	581	1775	1.14	42.2	0.440	2.32	1829	2850	1.82	182.9	0.150
	-12.40												
	-12.40	2.32	581	1775	1.14	42.2	0.440	2.32	1829	2850	1.82	182.9	0.150
	-14.40												
	-14.40	2.32	655	2002	0.94	47.6	0.440	2.32	1829	2850	1.82	149.9	0.150
	-16.84												
	-16.84	2.61	1464	3130	1.82	106.4	0.360						
	-18.67												
	-18.67	2.61	1738	3488	1.82	103.7	0.335						
	-22.02												
	-22.02	2.63	1977	3767	1.82	118.0	0.310						
	-25.37												
	-25.37	2.63	2154	3897	1.82	128.5	0.280						
	-28.72												
	-28.72	2.63	2051	3909	1.82	122.0	0.310						
	-32.08												
	-32.08	2.63	2155	4031	1.82	128.6	0.300						
	-35.43												
	-35.43	2.63	2195	3855	1.82	131.0	0.260						
	-38.78												
	-38.78	2.63	2324	4205	1.82	138.3	0.280						
	-42.14												
	-42.14	2.63	2289	4282	1.82	136.6	0.300						
	-45.49												
	-45.49	2.63	2290	3915	1.82	-	0.240						
	-												

Note: The soil properties of the adjusted layer, shown in the red box, are evaluated from the original properties shown below.

Table 4.3-5 Subsurface Properties for FWSC-CB SSSI Analysis of LB Profile (Continued)

Original data

	EL	Soil						Backfill					
		Unit Weight	Vs	Vp	Damping	Highest Frequency	Poisson's	Unit Weight	Vs	Vp	Damping	Highest Frequency	Poisson's
	[m]	[t/m^3]	[m/sec]	[m/sec]	[%]	[Hz]	ratio	[t/m^3]	[m/sec]	[m/sec]	[%]	[Hz]	ratio
①	1.450	2.00	147	750	6.63		0.480	2.08	146	744	7.33		0.480
	1.150												
	1.150	2.00	147	750	6.63		0.480	2.08	150	763	7.50		0.480
	0.750												
②	0.750	2.00	147	750	6.63		0.480	2.08	150	763	7.50		0.480
	0.230												
	0.230	2.00	147	750	6.63		0.480	2.08	153	782	7.85		0.480
	0.000												
③	-1.400	2.00	147	750	6.63		0.480	2.08	155	788	8.29		0.480
	-1.600												
	-1.600	2.00	184	940	8.25		0.480	2.08	160	818	8.02		0.480
	-2.000												
④	-3.170	2.00	184	940	8.25		0.480	2.08	155	790	8.50		0.480
	-3.430												
	-3.430	2.00	184	940	8.25		0.480	2.08	158	805	8.54		0.480
	-4.070												
⑤	-4.070	2.00	184	940	8.25		0.480	2.08	158	805	8.54		0.480
	-4.340												
	-4.340	2.00	184	940	8.25		0.480	2.08	158	809	8.87		0.480
	-4.970												
⑥	-4.970	2.00	184	940	8.25		0.480	2.08	158	809	8.87		0.480
	-5.560												
	-5.560	2.00	184	940	8.25		0.480	2.08	157	799	9.19		0.480
	-5.870												

Vs and Vp are determined using the equivalent wave travel time procedure.

Example ③: 170=(2.00-1.40)/(0.20/147+0.40/184)

Damping ratio is determined using the thickness weighted average procedure.

Example ③: 7.71=(6.63x(1.60-1.40)+8.25x(2.00-1.60))/(0.20+0.40)

Table 4.3-6 Subsurface Properties for FWSC-CB SSSI Analysis of UB Profile

	EL	Soil						Backfill					
		Unit Weight	Vs	Vp	Damping	Highest Frequency	Poisson's	Unit Weight	Vs	Vp	Damping	Highest Frequency	Poisson's
	[m]	[t/m^3]	[m/sec]	[m/sec]	[%]	[Hz]	ratio	[t/m^3]	[m/sec]	[m/sec]	[%]	[Hz]	ratio
	2.15	2.00	348	1463	2.64	71.7	0.470	2.08	354	1463	3.06	88.5	0.469
	1.45												
①	1.45	2.00	348	1463	2.64	71.7	0.470	2.08	356	1463	3.09	89.0	0.469
	0.75												
②	0.75	2.00	348	1463	2.64	71.7	0.470	2.08	362	1463	3.12	90.5	0.467
	0.00												
	0.00	2.00	348	1463	2.64	71.7	0.470	2.08	373	1463	3.15	93.2	0.465
	-0.68												
	-0.68	2.00	348	1463	2.64	71.7	0.470	2.08	368	1463	3.42	92.0	0.466
	-1.40												
③	-1.40	2.00	428	1798	2.90	88.2	0.470	2.08	397	1463	3.36	99.2	0.460
	-2.00												
	-2.00	2.00	483	2030	3.03	99.5	0.470	2.08	414	1463	3.33	103.5	0.456
	-2.51												
	-2.51	2.00	483	2030	3.03	99.5	0.470	2.08	413	1463	3.52	103.2	0.457
	-3.17												
④	-3.17	2.00	483	2030	3.03	99.5	0.470	2.08	408	1463	3.68	90.6	0.458
	-4.07												
⑤	-4.07	2.00	483	2030	3.03	99.5	0.470	2.08	420	1463	3.66	93.3	0.455
	-4.97												
⑥	-4.97	2.00	483	2030	3.03	99.5	0.470	2.08	426	1463	3.71	94.6	0.454
	-5.87												
	-5.87	2.00	483	2030	3.03	99.5	0.470	2.08	427	1463	3.87	93.8	0.453
	-6.78												
	-6.78	2.08	600	2524	2.60	123.7	0.470	2.08	442	1463	3.78	110.5	0.450
	-7.40												
	-7.40	2.08	600	2524	2.60	123.7	0.470	2.08	442	1463	3.78	110.5	0.450
	-8.00												
	-8.00	2.08	814	2488	1.92	167.8	0.440	2.08	455	1463	3.79	113.7	0.446
	-8.70												
	-8.70	2.08	814	2488	1.92	167.8	0.440	2.08	455	1463	3.79	110.9	0.446
	-9.52												
	-9.52	2.32	1002	3060	0.36	72.8	0.440	2.32	2438	3800	0.55	554.0	0.150
	-10.40												
	-10.40	2.32	1002	3060	0.36	72.8	0.440	2.32	2438	3800	0.55	243.8	0.150
	-12.40												
	-12.40	2.32	1002	3060	0.36	72.8	0.440	2.32	2438	3800	0.55	243.8	0.150
	-14.40												
	-14.40	2.32	1028	3141	0.30	74.7	0.440	2.32	2438	3800	0.55	199.8	0.150
	-16.84												
	-16.84	2.61	2667	5703	0.55	193.9	0.360						
	-18.67												
	-18.67	2.61	2607	5233	0.55	155.6	0.335						
	-22.02												
	-22.02	2.63	2965	5650	0.55	177.0	0.310						
	-25.37												
	-25.37	2.63	3231	5845	0.55	192.8	0.280						
	-28.72												
	-28.72	2.63	3077	5863	0.55	183.1	0.310						
	-32.08												
	-32.08	2.63	3232	6047	0.55	192.9	0.300						
	-35.43												
	-35.43	2.63	3293	5783	0.55	196.5	0.260						
	-38.78												
	-38.78	2.63	3487	6308	0.55	207.5	0.280						
	-42.14												
	-42.14	2.63	3434	6424	0.55	205.0	0.300						
	-45.49												
	-45.49	2.63	3434	5872	0.55	-	0.240						
	-												

Note: The soil properties of the adjusted layer, shown in the red box, are evaluated from the original properties shown below.

Table 4.3-6 Subsurface Properties for FWSC-CB SSSI Analysis of UB Profile (Continued)

Original data

	EL	Soil						Backfill					
		Unit Weight	Vs	Vp	Damping	Highest Frequency	Poisson's	Unit Weight	Vs	Vp	Damping	Highest Frequency	Poisson's
	[m]	[t/m^3]	[m/sec]	[m/sec]	[%]	[Hz]	ratio	[t/m^3]	[m/sec]	[m/sec]	[%]	[Hz]	ratio
①	1.450	2.00	348	1463	2.64		0.470	2.08	354	1463	3.06		0.469
	1.150												
	1.150	2.00	348	1463	2.64		0.470	2.08	358	1463	3.11		0.468
	0.750												
②	0.750	2.00	348	1463	2.64		0.470	2.08	358	1463	3.11		0.468
	0.230												
	0.230	2.00	348	1463	2.64		0.470	2.08	373	1463	3.15		0.465
	0.000												
③	-1.400	2.00	348	1463	2.64		0.470	2.08	368	1463	3.42		0.466
	-1.600												
	-1.600	2.00	483	2030	3.03		0.470	2.08	414	1463	3.33		0.456
	-2.000												
④	-3.170	2.00	483	2030	3.03		0.470	2.08	413	1463	3.52		0.457
	-3.430												
	-3.430	2.00	483	2030	3.03		0.470	2.08	406	1463	3.74		0.458
	-4.070												
⑤	-4.070	2.00	483	2030	3.03		0.470	2.08	406	1463	3.74		0.458
	-4.340												
	-4.340	2.00	483	2030	3.03		0.470	2.08	426	1463	3.63		0.454
	-4.970												
⑥	-4.970	2.00	483	2030	3.03		0.470	2.08	426	1463	3.63		0.454
	-5.560												
	-5.560	2.00	483	2030	3.03		0.470	2.08	427	1463	3.87		0.453
	-5.870												

Vs and Vp are determined using the equivalent wave travel time procedure.

Example ③: 428=(2.00-1.40)/(0.20/348+0.40/483)

Damping ratio is determined using the thickness weighted average procedure.

Example ③: 2.90=(2.64x(1.60-1.40)+3.03x(2.00-1.60))/(0.20+0.40)

Table 4.3-7 Subsurface Properties for FWSC-CB SSSI Analysis of BE Profile

	EL	Soil						Backfill					
		Unit Weight	Vs	Vp	Damping	Highest Frequency	Poisson's	Unit Weight	Vs	Vp	Damping	Highest Frequency	Poisson's
	[m]	[t/m^3]	[m/sec]	[m/sec]	[%]	[Hz]	ratio	[t/m^3]	[m/sec]	[m/sec]	[%]	[Hz]	ratio
	2.15	2.00	226	1153	4.18	46.5	0.480	2.08	227	1158	4.74	56.7	0.480
	1.45												
①	1.45	2.00	226	1153	4.18	46.5	0.480	2.08	229	1170	4.79	57.2	0.480
	0.75												
②	0.75	2.00	226	1153	4.18	46.5	0.480	2.08	233	1192	4.87	58.2	0.480
	0.00												
	0.00	2.00	226	1153	4.18	46.5	0.480	2.08	239	1219	4.97	59.7	0.480
	-0.68												
	-0.68	2.00	226	1153	4.18	46.5	0.480	2.08	239	1216	5.33	59.7	0.480
	-1.40												
③	-1.40	2.00	269	1343	4.73	55.4	0.479	2.08	251	1280	5.22	62.7	0.480
	-2.00												
	-2.00	2.00	298	1463	5.00	61.4	0.478	2.08	258	1314	5.17	64.5	0.480
	-2.51												
	-2.51	2.00	298	1463	5.00	61.4	0.478	2.08	253	1291	5.47	63.2	0.480
	-3.17												
④	-3.17	2.00	298	1463	5.00	61.4	0.478	2.08	253	1291	5.60	56.2	0.480
	-4.07												
⑤	-4.07	2.00	298	1463	5.00	61.4	0.478	2.08	258	1315	5.66	57.3	0.480
	-4.97												
⑥	-4.97	2.00	298	1463	5.00	61.4	0.478	2.08	259	1323	5.77	57.5	0.480
	-5.87												
	-5.87	2.00	298	1463	5.00	61.4	0.478	2.08	258	1318	5.96	56.7	0.480
	-6.78												
	-6.78	2.08	432	1814	3.97	89.0	0.470	2.08	272	1389	5.75	68.0	0.480
	-7.40												
	-7.40	2.08	432	1814	3.97	89.0	0.470	2.08	272	1389	5.75	68.0	0.480
	-8.00												
	-8.00	2.08	596	1821	2.89	122.8	0.440	2.08	271	1383	5.95	67.7	0.480
	-8.70												
	-8.70	2.08	596	1821	2.89	122.8	0.440	2.08	271	1383	5.95	66.0	0.480
	-9.52												
	-9.52	2.32	763	2331	0.64	55.4	0.440	2.32	2134	3325	1.00	485.0	0.150
	-10.40												
	-10.40	2.32	763	2331	0.64	55.4	0.440	2.32	2134	3325	1.00	213.4	0.150
	-12.40												
	-12.40	2.32	763	2331	0.64	55.4	0.440	2.32	2134	3325	1.00	213.4	0.150
	-14.40												
	-14.40	2.32	821	2508	0.53	59.7	0.440	2.32	2134	3325	1.00	174.9	0.150
	-16.84												
	-16.84	2.61	1976	4225	1.00	143.7	0.360						
	-18.67												
	-18.67	2.61	2128	4273	1.00	127.0	0.335						
	-22.02												
	-22.02	2.63	2421	4613	1.00	144.5	0.310						
	-25.37												
	-25.37	2.63	2638	4772	1.00	157.4	0.280						
	-28.72												
	-28.72	2.63	2512	4787	1.00	149.5	0.310						
	-32.08												
	-32.08	2.63	2639	4937	1.00	157.5	0.300						
	-35.43												
	-35.43	2.63	2689	4722	1.00	160.5	0.260						
	-38.78												
	-38.78	2.63	2847	5150	1.00	169.4	0.280						
	-42.14												
	-42.14	2.63	2804	5245	1.00	167.4	0.300						
	-45.49												
	-45.49	2.63	2804	4794	1.00	-	0.240						
	-												

Note: The soil properties of the adjusted layer, shown in the red box, are evaluated from the original properties shown below.

Table 4.3-7 Subsurface Properties for FWSC-CB SSSI Analysis of BE Profile (Continued)

Original data

	EL	Soil						Backfill					
		Unit Weight	Vs	Vp	Damping	Highest Frequency	Poisson's	Unit Weight	Vs	Vp	Damping	Highest Frequency	Poisson's
	[m]	[t/m^3]	[m/sec]	[m/sec]	[%]	[Hz]	ratio	[t/m^3]	[m/sec]	[m/sec]	[%]	[Hz]	ratio
①	1.450	2.00	226	1153	4.18		0.480	2.08	227	1158	4.74		0.480
	1.150												
	1.150	2.00	226	1153	4.18		0.480	2.08	231	1180	4.83		0.480
	0.750												
②	0.750	2.00	226	1153	4.18		0.480	2.08	231	1180	4.83		0.480
	0.230												
	0.230	2.00	226	1153	4.18		0.480	2.08	239	1219	4.97		0.480
	0.000												
③	-1.400	2.00	226	1153	4.18		0.480	2.08	239	1216	5.33		0.480
	-1.600												
	-1.600	2.00	298	1463	5.00		0.478	2.08	258	1314	5.17		0.480
	-2.000												
④	-3.170	2.00	298	1463	5.00		0.478	2.08	253	1291	5.47		0.480
	-3.430												
	-3.430	2.00	298	1463	5.00		0.478	2.08	253	1291	5.65		0.480
	-4.070												
⑤	-4.070	2.00	298	1463	5.00		0.478	2.08	253	1291	5.65		0.480
	-4.340												
	-4.340	2.00	298	1463	5.00		0.478	2.08	260	1325	5.67		0.480
	-4.970												
⑥	-4.970	2.00	298	1463	5.00		0.478	2.08	260	1325	5.67		0.480
	-5.560												
	-5.560	2.00	298	1463	5.00		0.478	2.08	258	1318	5.96		0.480
	-5.870												

Vs and Vp are determined using the equivalent wave travel time procedure.

Example ③: 269=(2.00-1.40)/(0.20/226+0.40/298)

Damping ratio is determined using the thickness weighted average procedure.

Example ③: 4.73=(4.18x(1.60-1.40)+5.00x(2.00-1.60))/(0.20+0.40)

Table 5.2-1 Comparison of CB Slab SDOF Oscillators Maximum Accelerations

Slab SDOF		Vertical Acceleration (g)					
		LB Full Column Profile		UB Full Column Profile		NA3 Enveloping(*)	Standard Design
Elev.	Node No.	SSI	SSSI	SSI	SSSI		
13.80 m	9001	1.01	1.09	1.76	1.76	2.81	2.19
	9002	1.39	1.44	1.44	1.48	2.19	1.34
	9003	0.80	0.78	3.01	2.54	3.01	1.43
9.06 m	9101	1.29	1.39	2.01	2.05	2.85	2.00
	9102	0.83	0.80	1.54	1.39	1.84	1.26
	9103	0.71	0.67	3.08	2.50	3.08	1.43
4.65 m	9201	0.90	0.88	1.13	1.14	1.57	1.30
	9202	0.61	0.58	2.34	1.95	2.34	1.43
-2.00 m	9301	0.55	0.56	1.27	1.13	1.54	1.39

(*) Envelope of results from SSI analyses of CB standalone model for LB, BE, and UB full and partial column profiles

Table 5.5-1 Comparison of Enveloping Maximum Accelerations at CB Floor Mass Locations

Elev. (m)	Node No.	Acceleration (g)								
		SSSI Analyses Envelope			NA3 Enveloping			Standard Design		
		NS	EW	Vert.	NS	EW	Vert.	NS	EW	Vert.
13.80	6	1.23	1.17	0.94	1.83	2.09	1.31	1.26	1.11	1.00
9.06	5	0.82	0.87	0.85	1.41	1.51	1.18	0.88	0.90	0.86
4.65	4	0.66	0.63	0.68	1.07	1.27	0.95	0.86	0.82	0.74
-2.00	3	0.49	0.49	0.60	0.64	0.77	0.62	0.79	0.71	0.56
-7.40	2	0.32	0.37	0.57	0.48	0.43	0.64	0.54	0.54	0.51
-10.40	1	0.32	0.36	0.57	0.48	0.44	0.64	0.54	0.53	0.51

Table 5.5-2 Comparison of Enveloping Maximum CB Member Forces and Moments

Element		SSSI Analyses Envelope					NA3 Enveloping Demands					Standard Design				
Elev. (m)	Node No.	Shear (MN)		Bending (MN-m)		Torsion (MN-m)	Shear (MN)		Bending (MN-m)		Torsion (MN-m)	Shear (MN)		Bending (MN-m)		Torsion (MN-m)
		NS	EW	NS	EW		NS	EW	NS	EW		NS	EW	NS	EW	
13.80	6	31.5	30.3	107	85	88.6	48.0	53.8	135	108	35.0	33.1	29.1	160	124	23.1
	5			230	195				328	290				250	197	
9.06	5	53.8	54.6	310	252	176.6	86.5	92.3	435	374	73.6	53.4	54.8	360	275	44.9
	4			515	465				796	718				573	443	
4.65	4	64.7	76.5	244	144	256.2	114.5	116.9	458	263	63.0	75.6	80.1	723	540	56.9
	3			613	613				1195	969				1136	988	
-2.00	3	40.4	40.7	320	350	130.9	51.4	55.7	652	646	33.0	124.4	99.4	1232	1036	59.9
-7.40	2			450	530				874	924				1570	1525	

Note: The shaded values are exceedance from the SSI models.

Table 5.5-3 Comparison of Total Shear Load Demand on CB Individual Exterior Walls

Element		SSSI Analyses Envelope		NA3 Enveloping Demands		Standard Design	
Elev. (m)	Node No.	Total Shear (MN)		Total Shear (MN)		Total Shear (MN)	
		NS	EW	NS	EW	NS	EW
13.80	6	17.9	15.7	24.7	27.5	17.0	14.9
	5						
9.06	5	30.6	28.3	44.8	47.4	27.6	28.1
	4						
4.65	4	37.8	39.6	58.6	59.5	39.0	41.0
	3						
-2.00	3	23.0	14.8	26.4	19.1	63.5	34.1
-7.40	2						

Table 6.2-1 Comparison of FWSC SDOF Oscillators Maximum Accelerations

SDOF Oscillator			Maximum Acceleration (g)*												
			FWSC-CB SSSI Analysis						FWSC SSI Analysis						
Description	Node No.	Dir.	Input Motion El. 282 ft			Input Motion El. 220 ft			Input Motion El. 282 ft			Input Motion El. 220 ft			Env.	Standard Design
			LB	BE	UB	LB	BE	UB	LB	BE	UB	LB	BE	UB		
FWS Roof	11	Vert.	0.97	1.59	1.83	1.09	3.13	5.67	1.34	1.62	1.58	2.10	3.26	4.22	4.22	3.26
FWS Water Sloshing	60	NS	0.10	0.10	0.10	0.10	0.10	0.10	0.10	0.10	0.10	0.10	0.10	0.10	0.10	0.30
		EW	0.07	0.07	0.07	0.09	0.09	0.09	0.07	0.07	0.07	0.09	0.09	0.09	0.09	0.40
FWS Water Impulsive	30	NS	0.80	0.77	0.74	0.76	0.86	1.08	0.77	0.85	0.72	0.80	0.85	1.02	1.02	1.10
		EW	0.77	0.84	0.72	0.74	0.93	1.07	0.68	0.73	0.64	0.74	0.81	1.08	1.08	1.40

Note: * Results of the SSSI and SSI analyses of the FWSC-CB combined and FWSC standalone models with full stiffness properties and OBE damping values. The shaded values are exceedance from the SSI models.

Table 6.4-1 Comparison of Out-of-Plane Load on FWS Roof

Slab		Flexible Mode (SDOF Oscillator)				Rigid Mode (LMSM)				Eq. Ave. Acc. (g)		
Elev. (m)	Location	Weight (kN)	Mass Node	Acceleration (g)		Mass Node	Weight (kN)	Acceleration (g)		NA3 Site-Specific		Stand. Design
				SSSI	SSI			SSSI	SSI	SSSI	SSI	
19.70	FWS Roof	1339	11	3.98	3.36	10	2480	1.40	1.43	2.30	2.11	**1.74**

Note: * Results of the SSSI and SSI analyses of the FWSC-CB combined and FWSC standalone models with full stiffness properties and SSE damping values. The shaded values are exceedance from the SSI models.

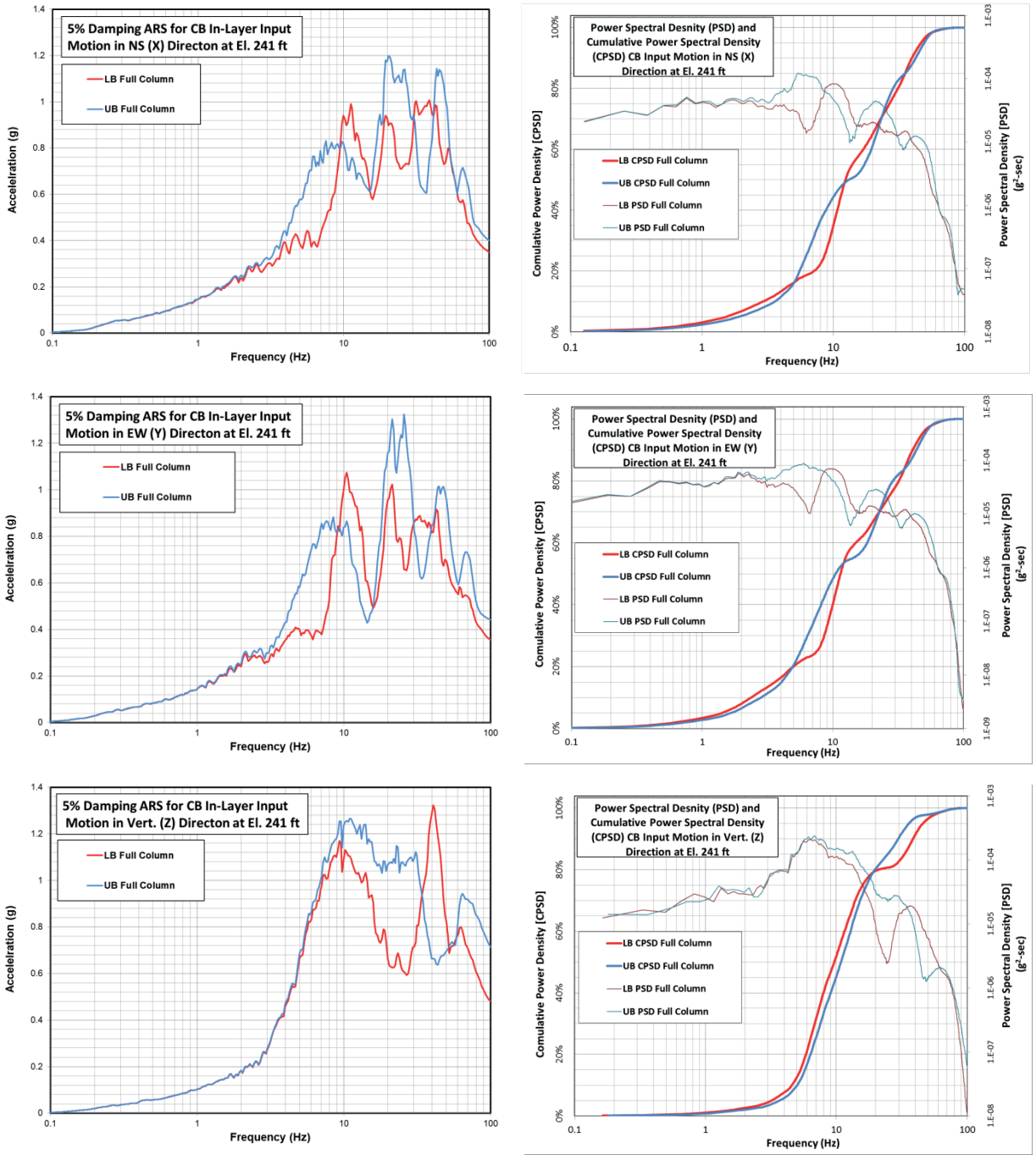

Figure 3.2-1 5% Damped ARS, PSD, and CPSD of Input Acceleration Time Histories for CB-FWSC SSSI Analyses

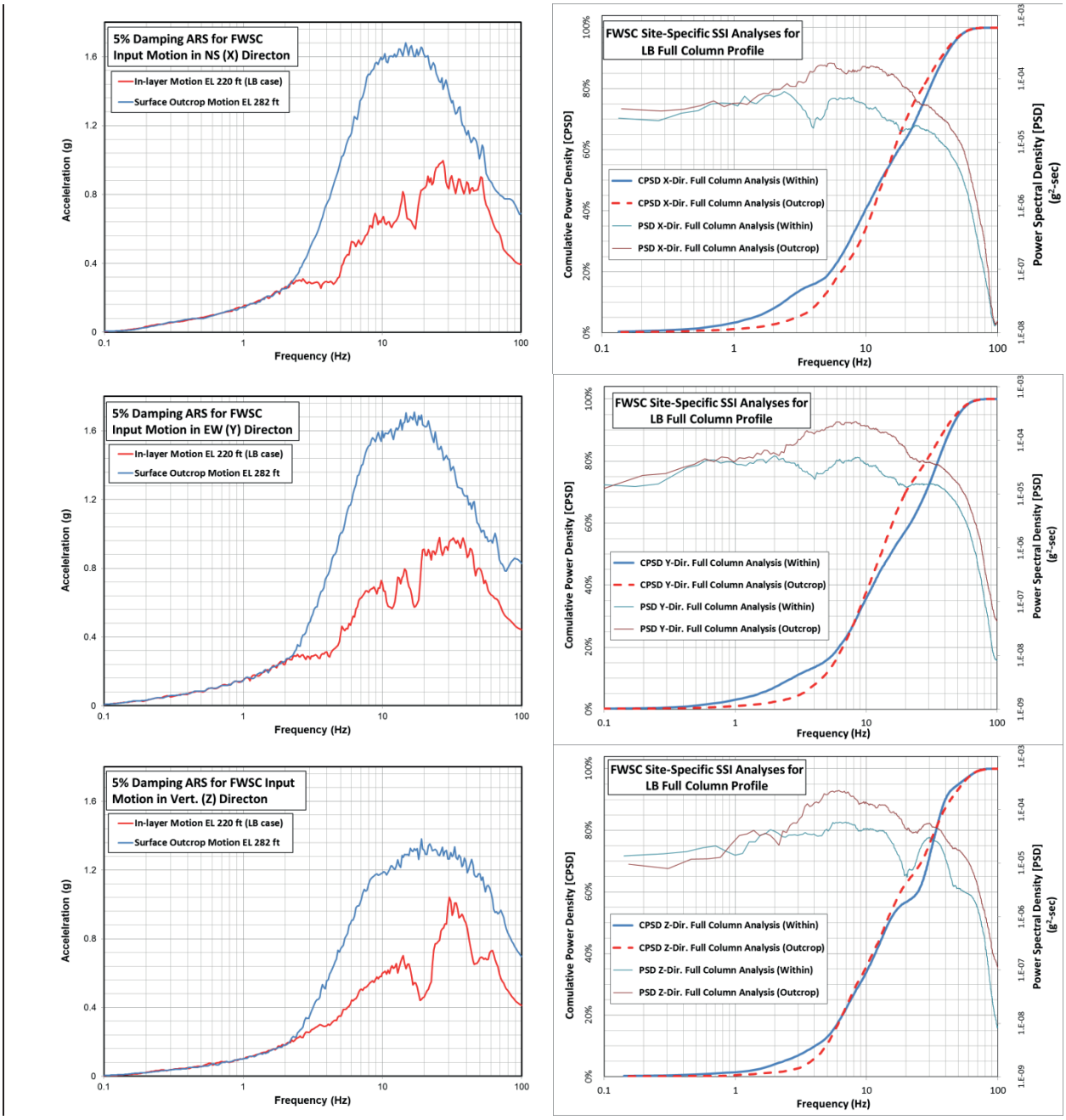

Figure 3.2-2 5% Damped ARS, PSD, and CPSD of Input Acceleration Time Histories for FWSC-CB Analyses of LB Subgrade Profile

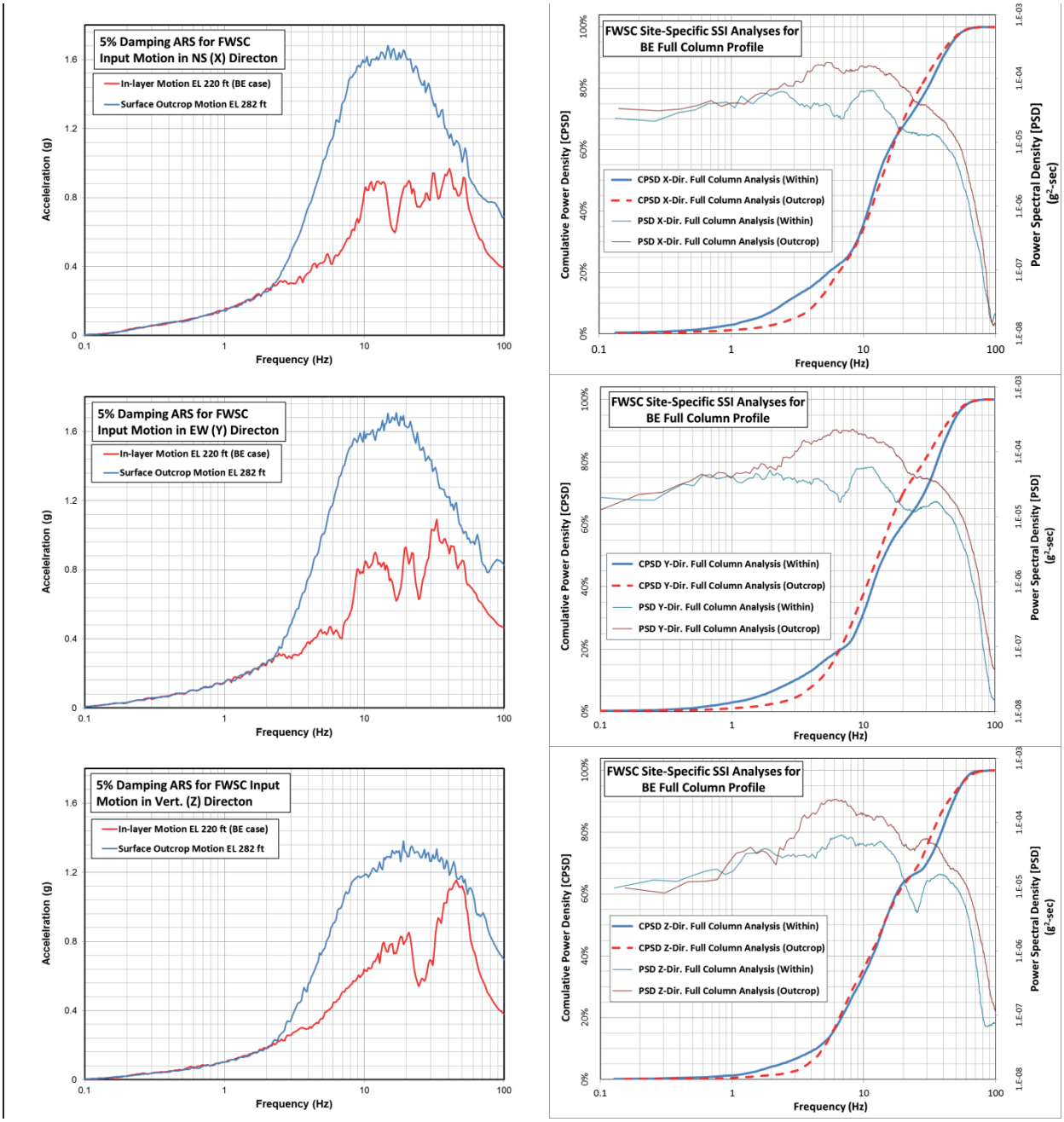

Figure 3.2-3 5% Damped ARS, PSD, and CPSD of Input Acceleration Time Histories for FWSC-CB Analyses of BE Subgrade Profile

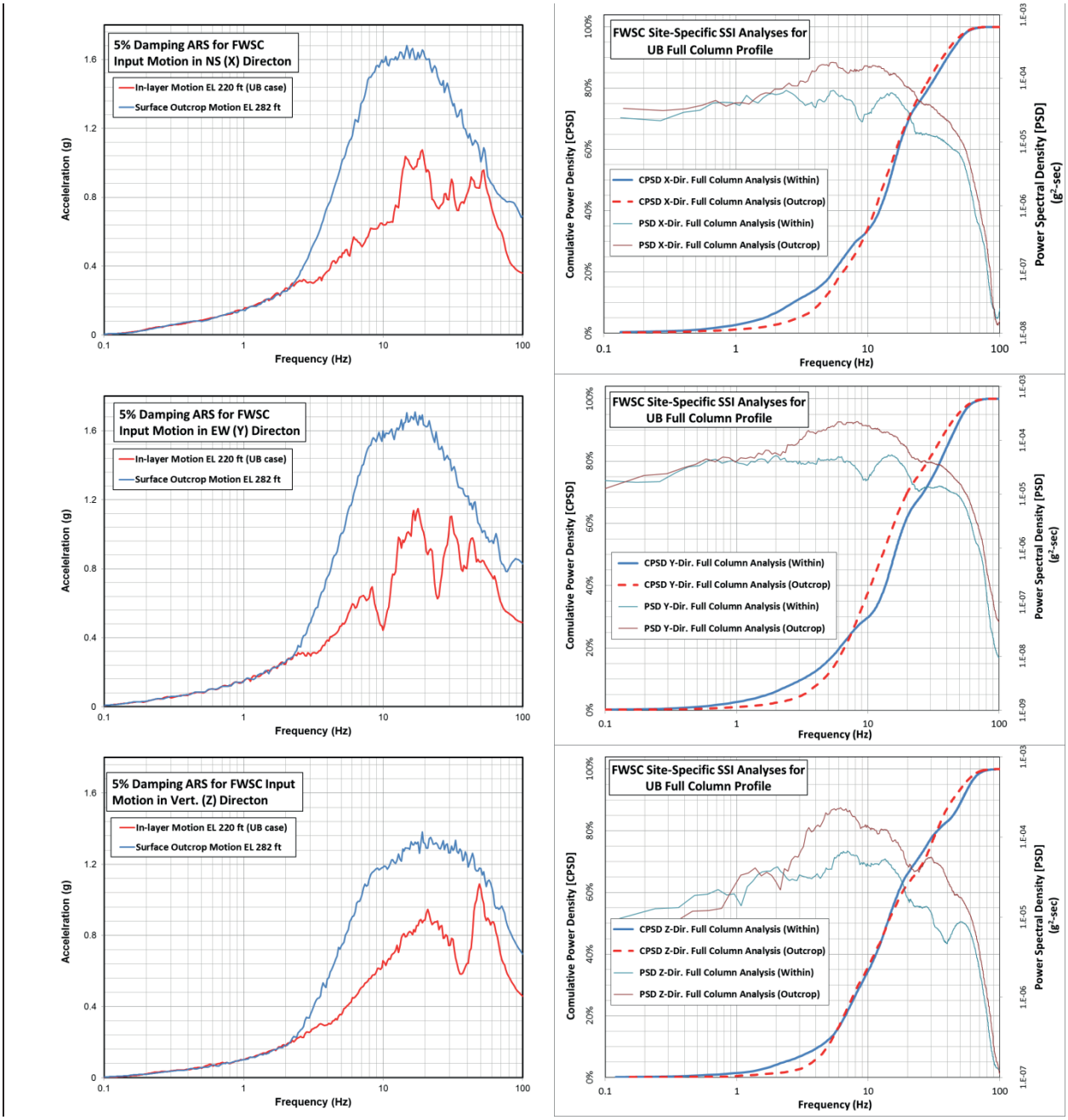

Figure 3.2-4 5% Damped ARS, PSD, and CPSD of Input Acceleration Time Histories for FWSC-CB Analyses of UB Subgrade Profile

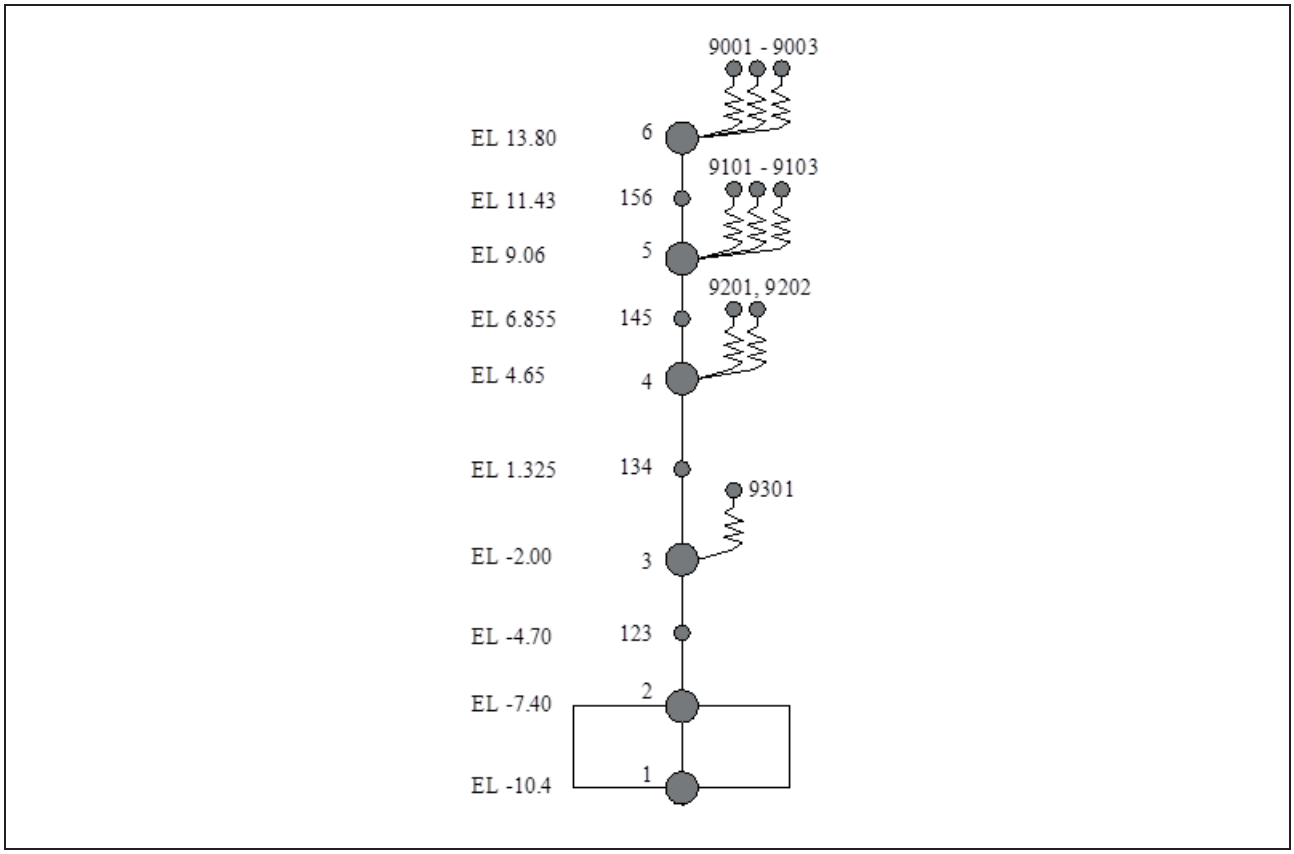

Figure 4.3-1 CB Lumped Mass Stick Model

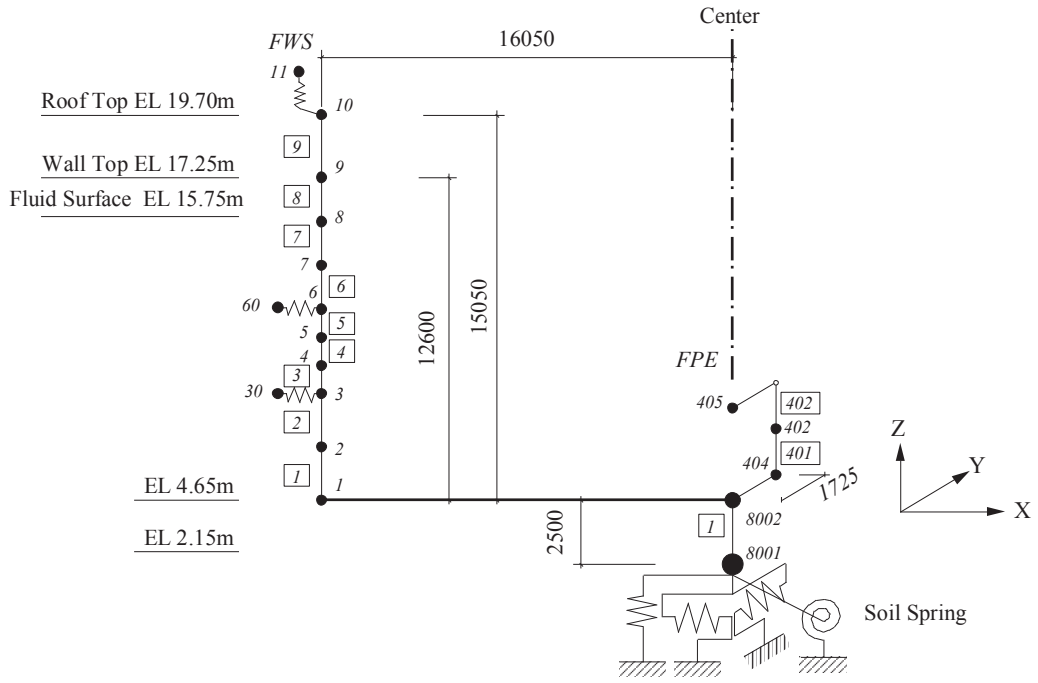

Mass at Node 30 represents the impulsive mode.
Mass at Node 60 represents the fundamental sloshing (convective) mode.
The model is assumed to be symmetric about YZ-plane including the center line.

Figure 4.3-2 FWSC Lumped Mass Stick Model

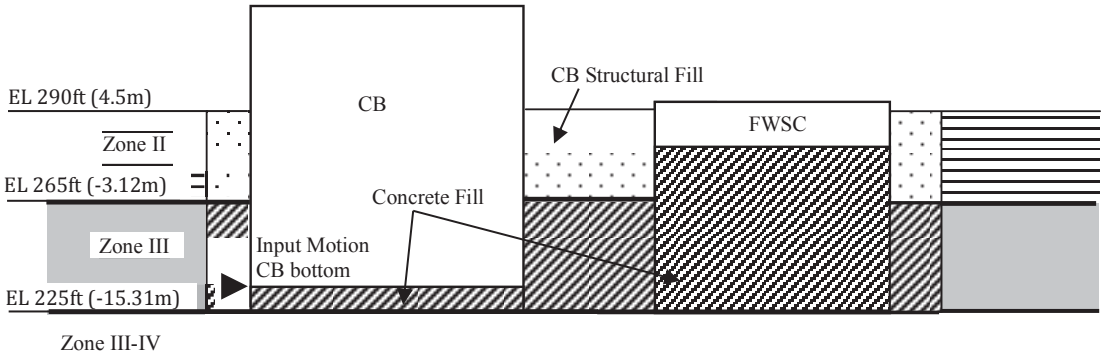

Figure 4.3-3 Conceptual Representation of CB-FWSC SSSI Combined Model

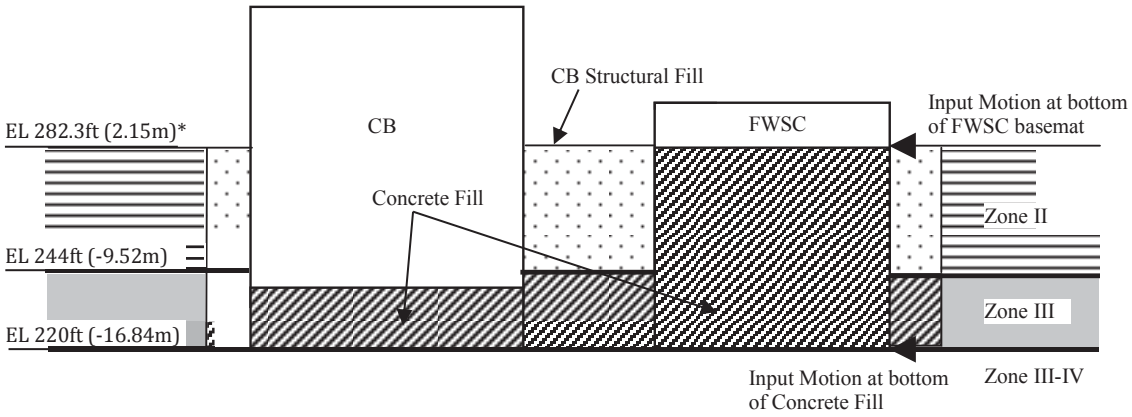

* The elevation of the basemat bottom 282 ft is modified to be consistent with the elevation 2.15 m in DCD as shown in DCD Figure 3A.7-15 (Reference 2-h).

Figure 4.3-4 Conceptual Representation of FWSC-CB SSSI Combined Model

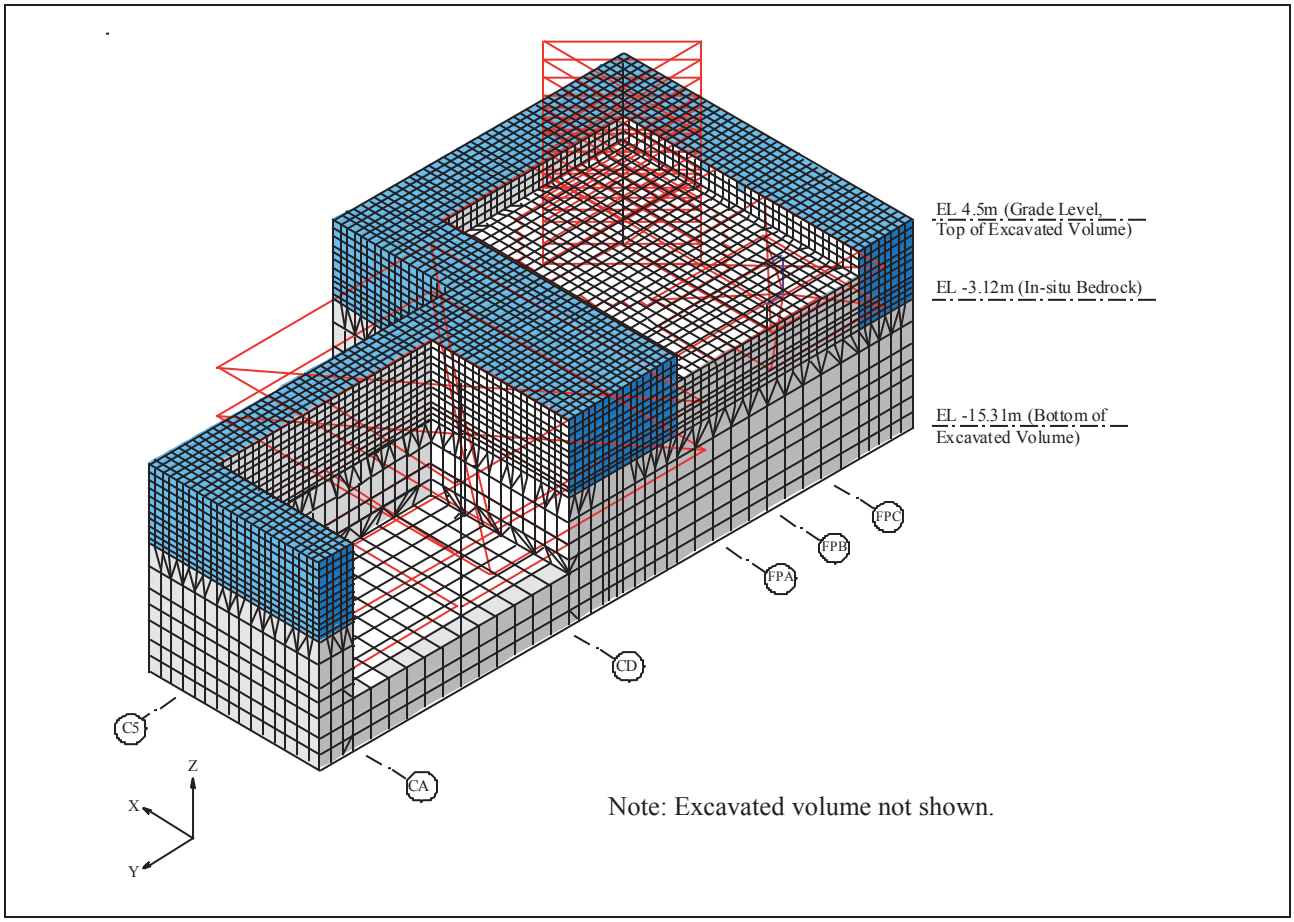

Figure 4.3-5 Overview of CB-FWSC SSSI Combined Model

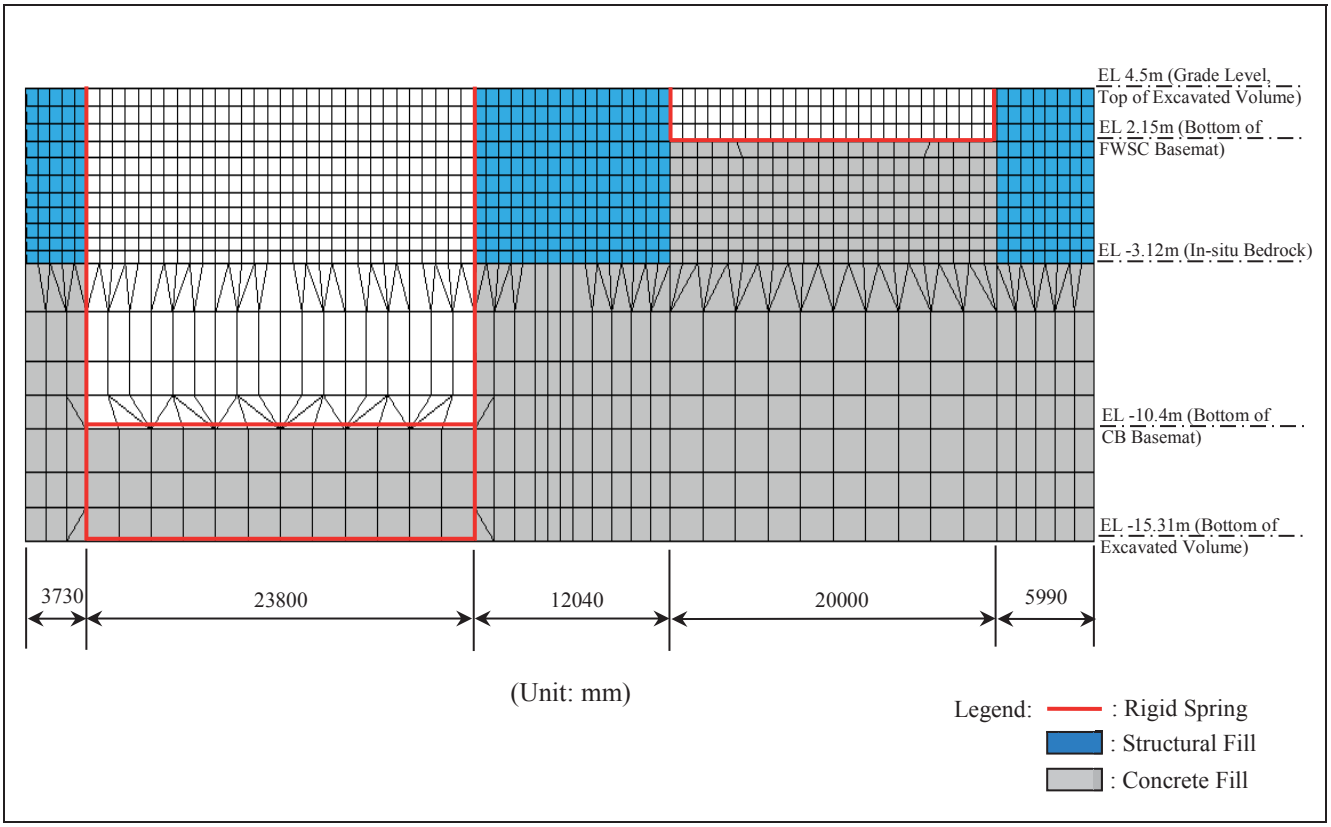

Figure 4.3-6 Plate Elements for CB and FWSC Exterior Walls in CB-FWSC SSSI Combined Model

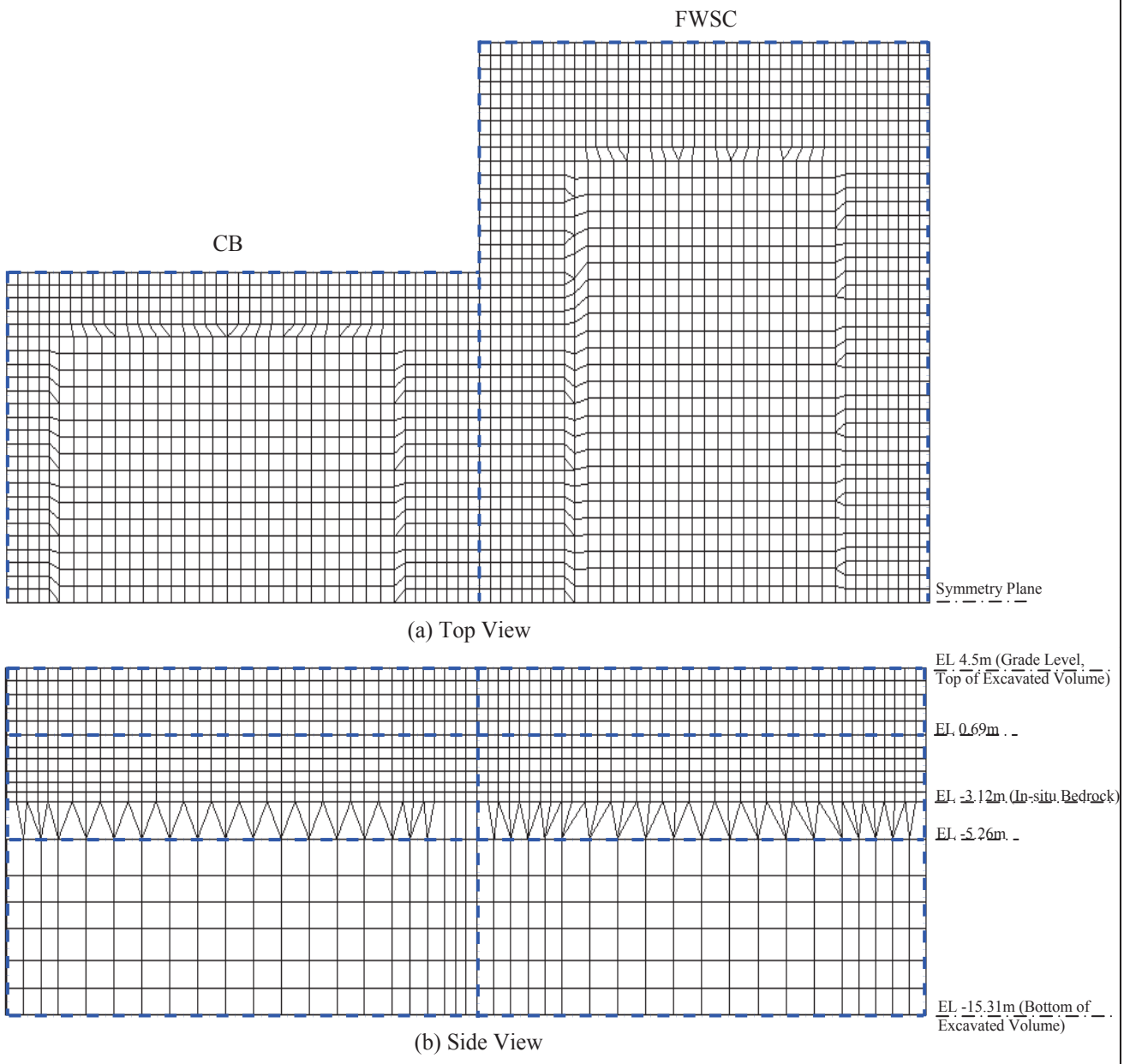

Note: Vertical and horizontal plane of interaction nodes are shown in blue lines.

Figure 4.3-7 Excavated Volume of CB-FWSC SSSI Combined Model

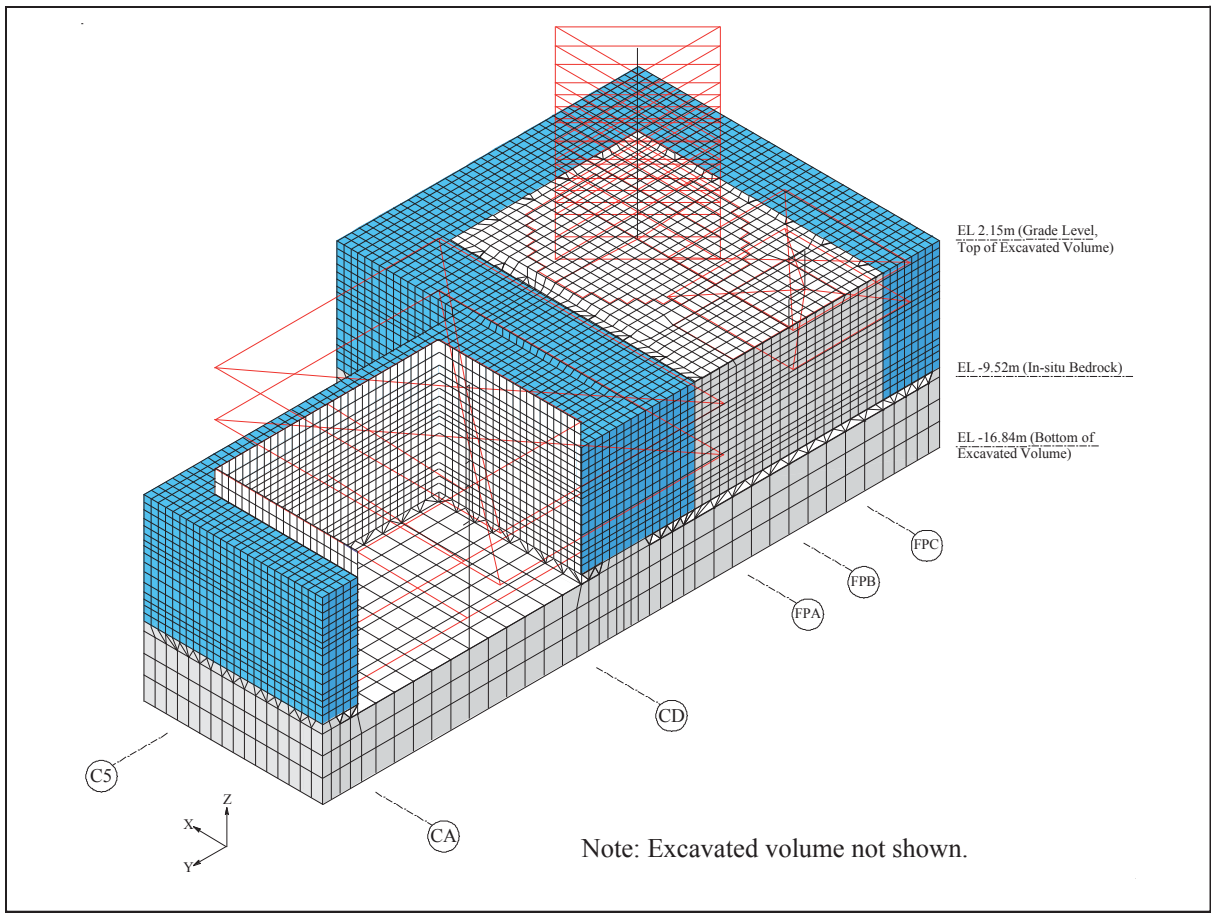

Figure 4.3-8 Overview of FWSC-CB SSSI Combined Model

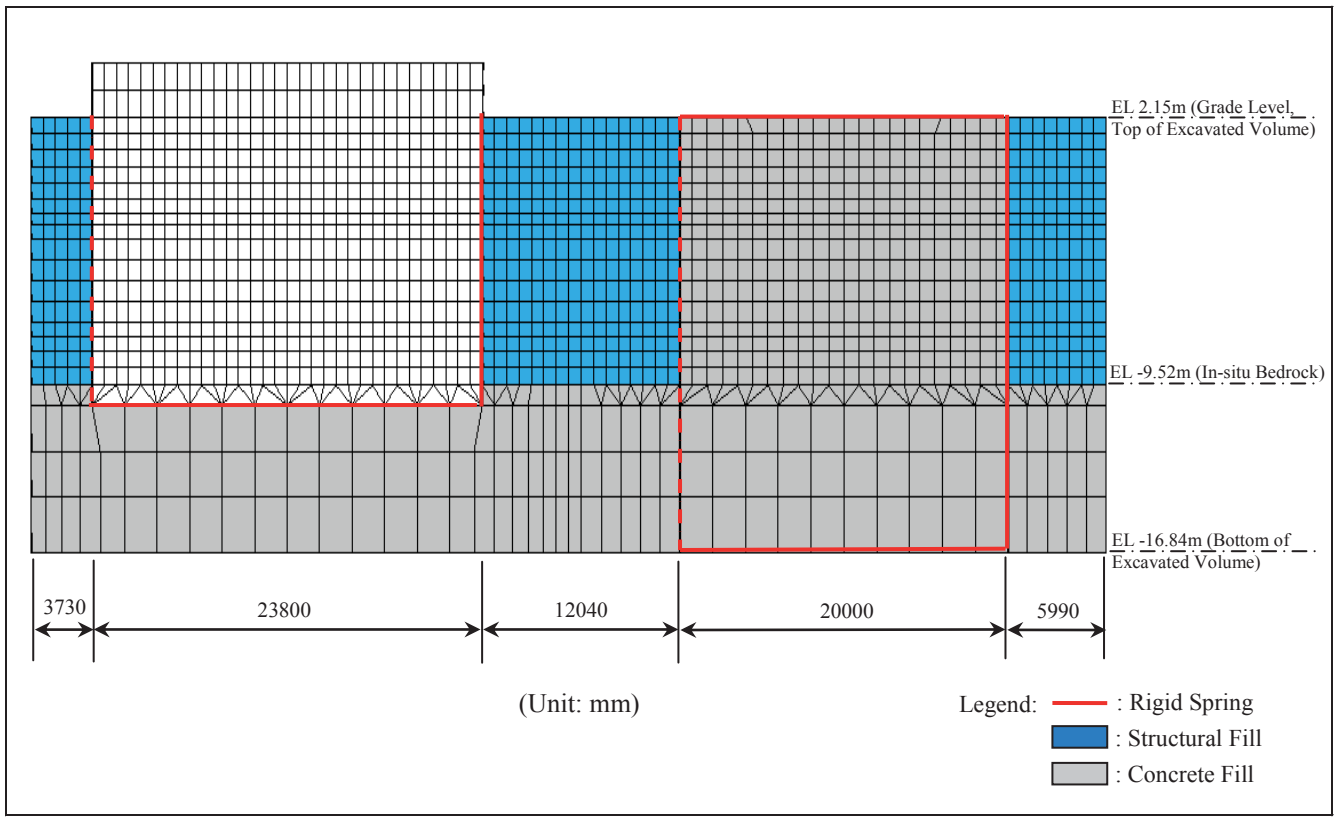

Figure 4.3-9 Plate Elements for CB Exterior Walls in FWSC-CB SSSI Combined Model

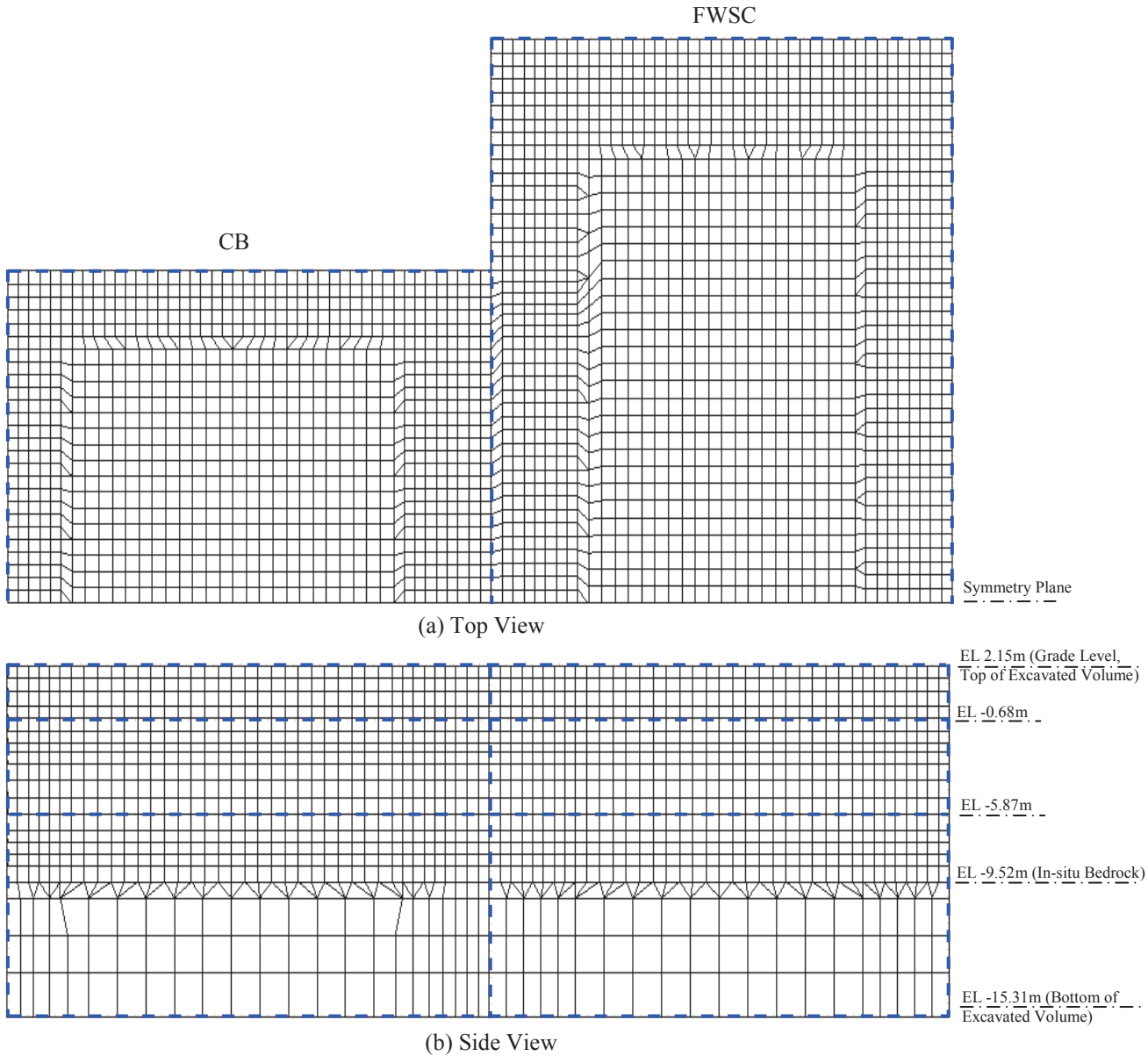

Note: Vertical and horizontal plane of interaction nodes are shown in blue lines.

Figure 4.3-10 Excavated Volume of FWSC-CB SSSI Combined Model

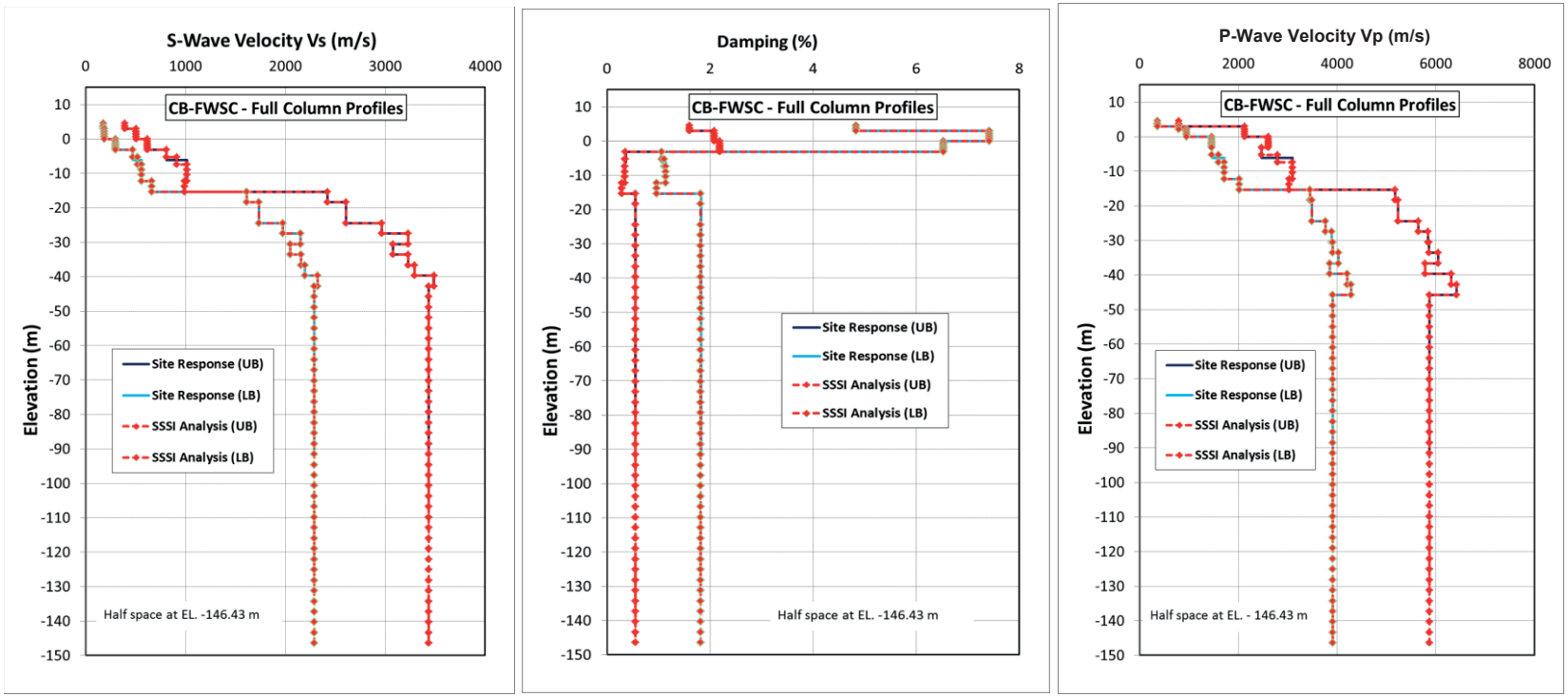

Figure 4.3-11 CB-FWSC Combined Model Input Subgrade Profiles

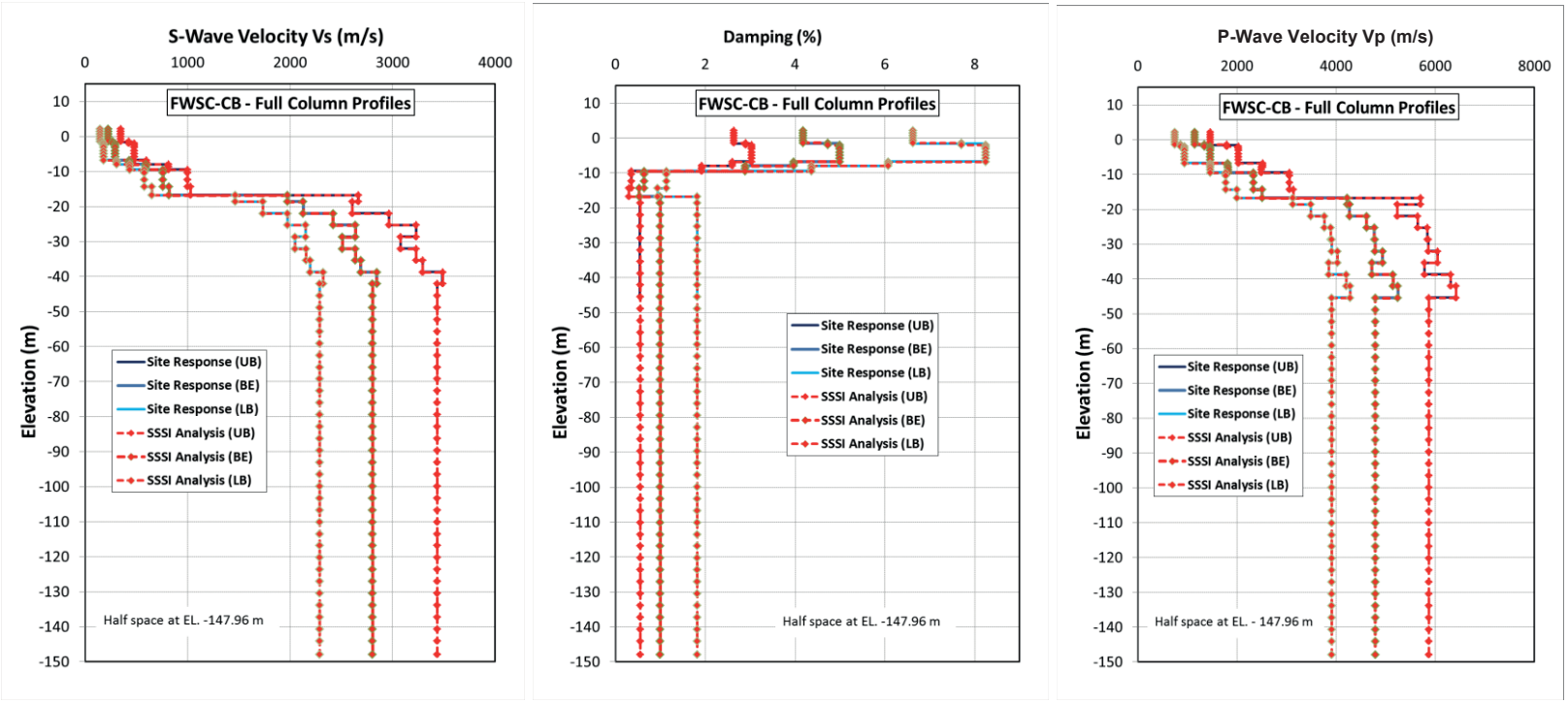

Figure 4.3-12 FWSC-CB Combined Model Input Subgrade Profiles

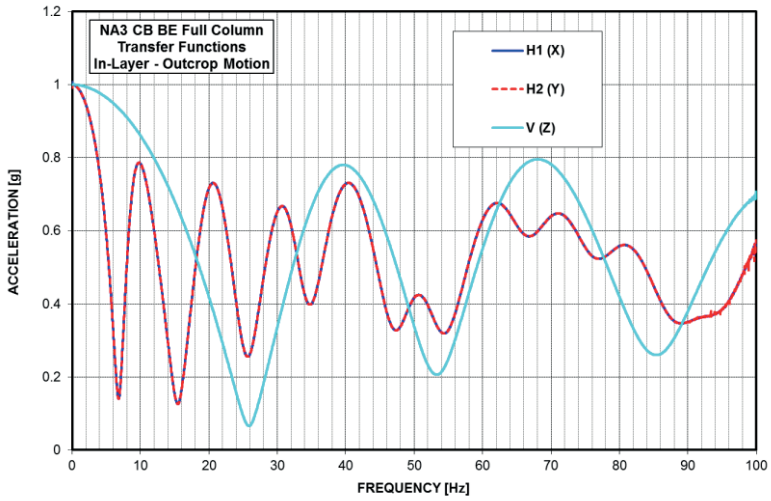

(a) LB Full Column Profile

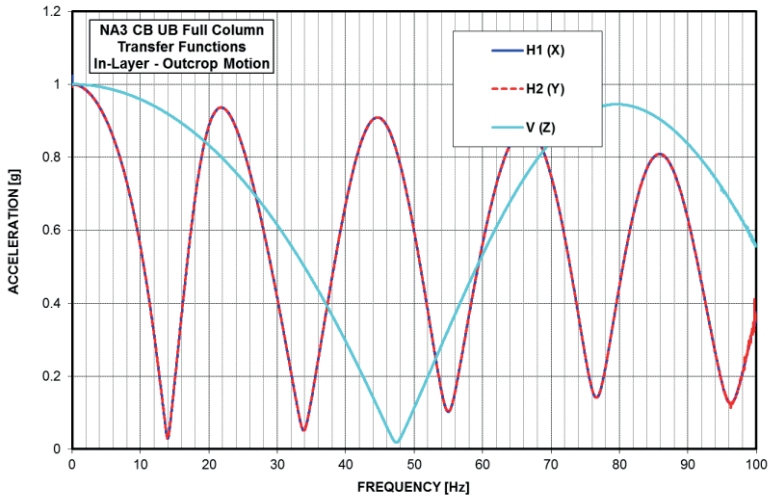

(b) UB Full Column Profile

Figure 5.1-1 Transfer Functions for Transformation of CB Full Column In-Layer Motion into Outcrop Motion

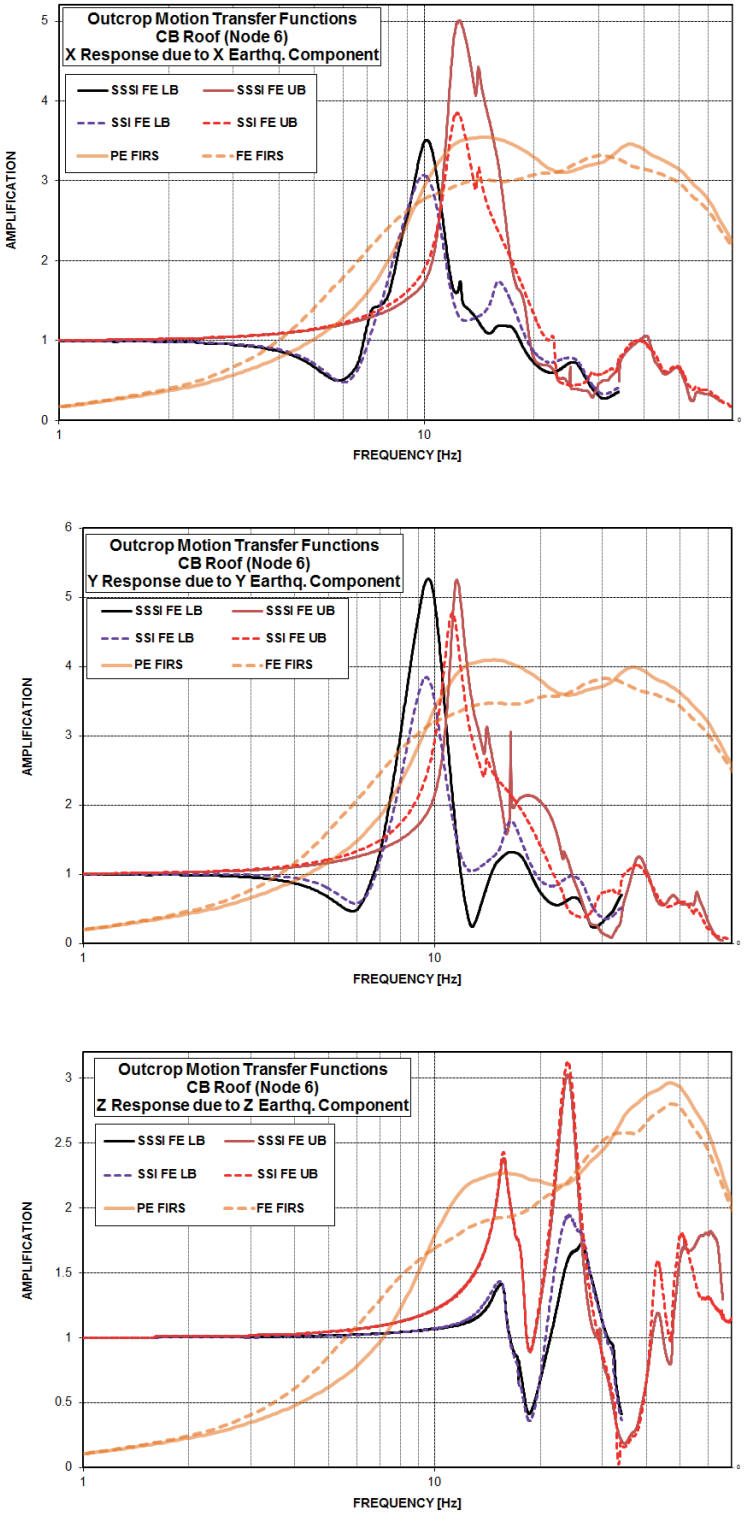

Figure 5.1-2 Comparison of Outcrop Transfer Functions for Response of CB Top

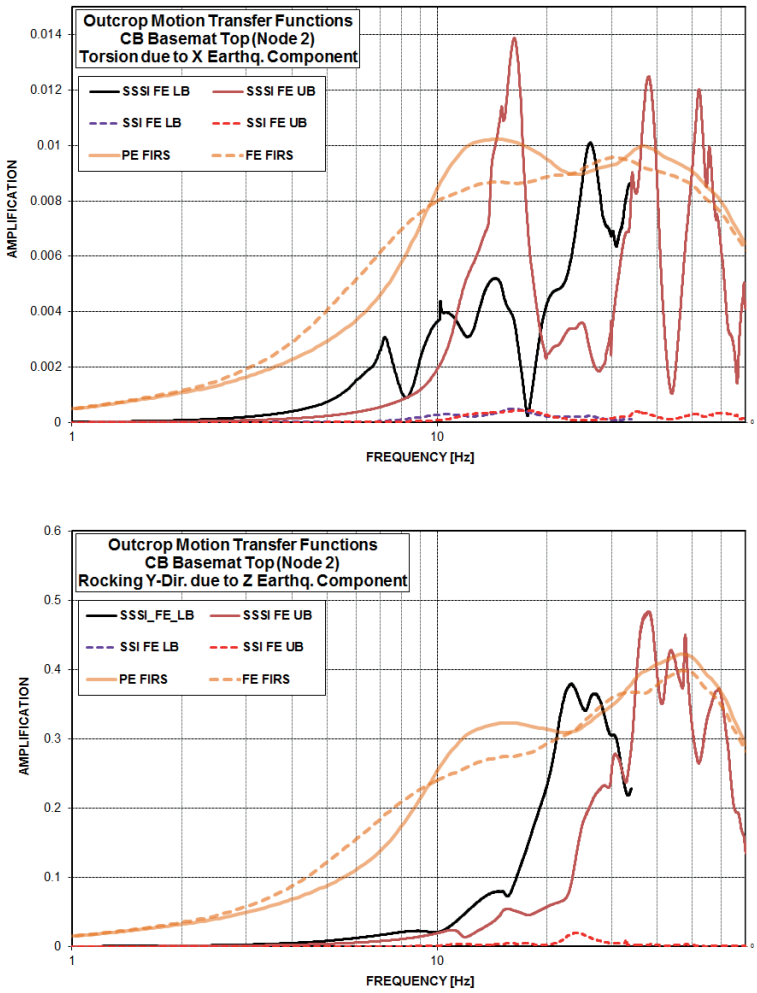

Figure 5.1-3 Comparison of Outcrop Transfer Functions for Rotation of CB Basemat

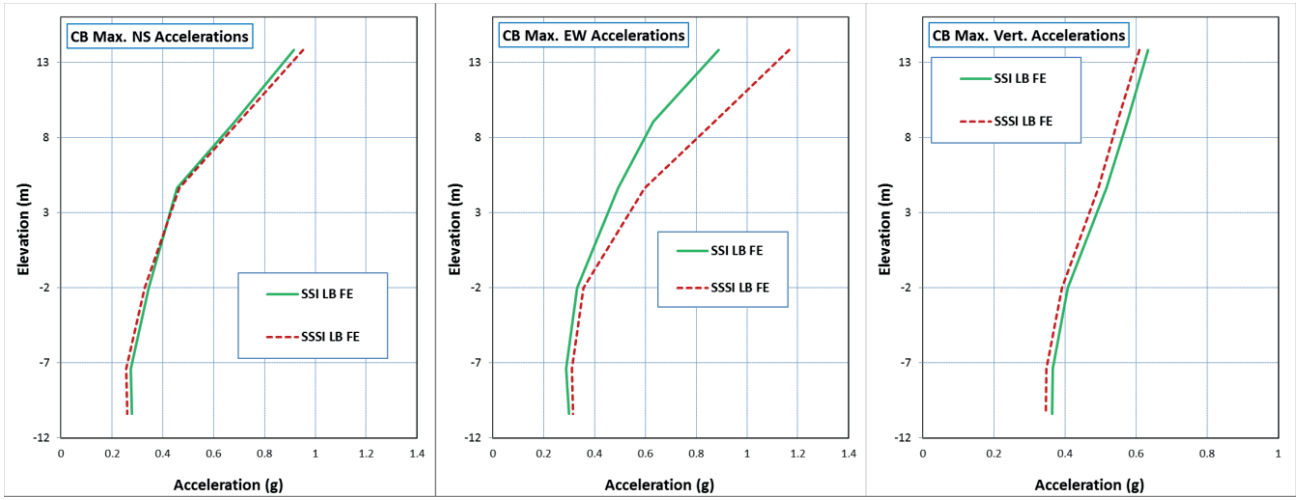

(a) LB Full Column Profile

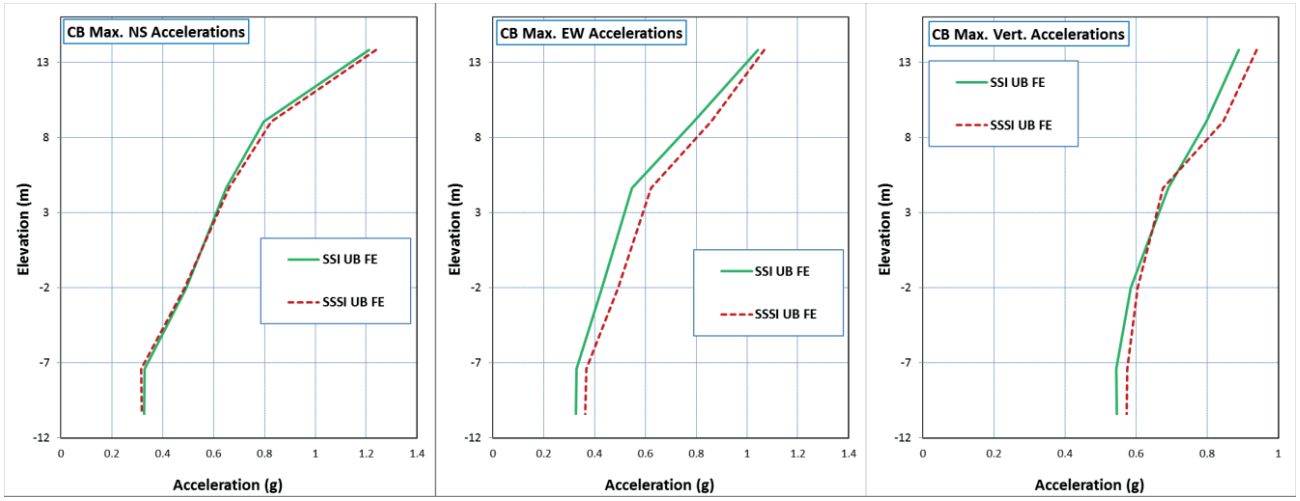

(b) UB Full Column Profile

Figure 5.2-1 Comparison of CB Maximum Accelerations

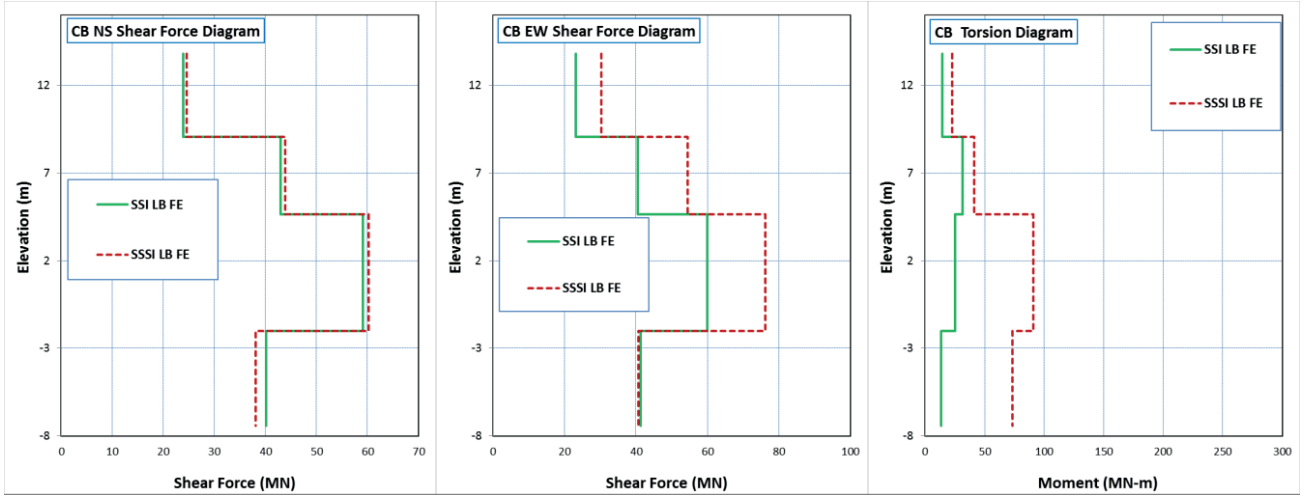

(a) LB Full Column Profile

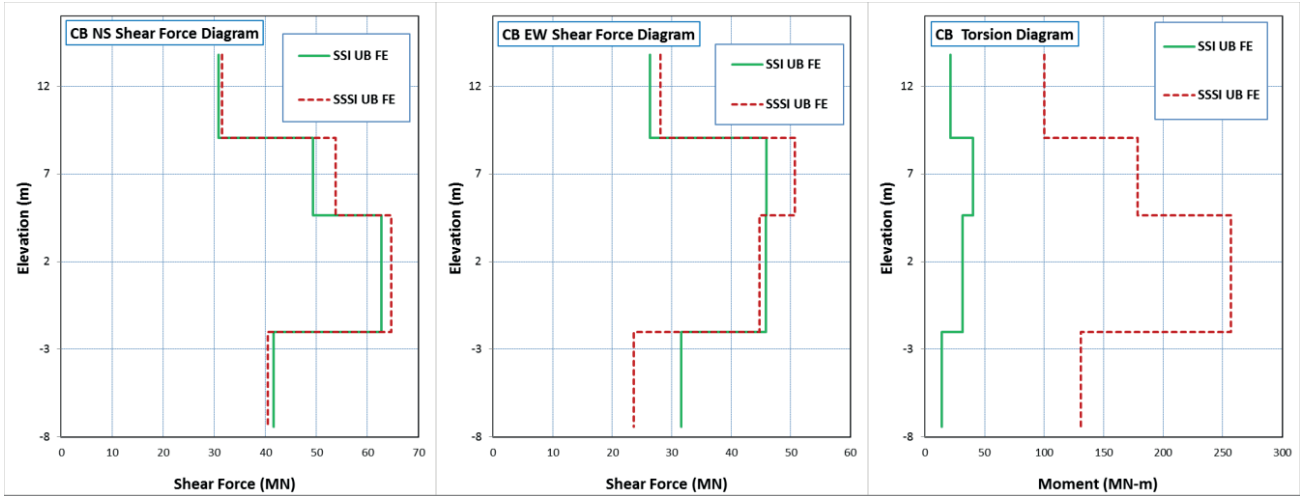

(b) UB Full Column Profile

Figure 5.2-2 Comparison of CB Maximum Shear Forces and Torsion

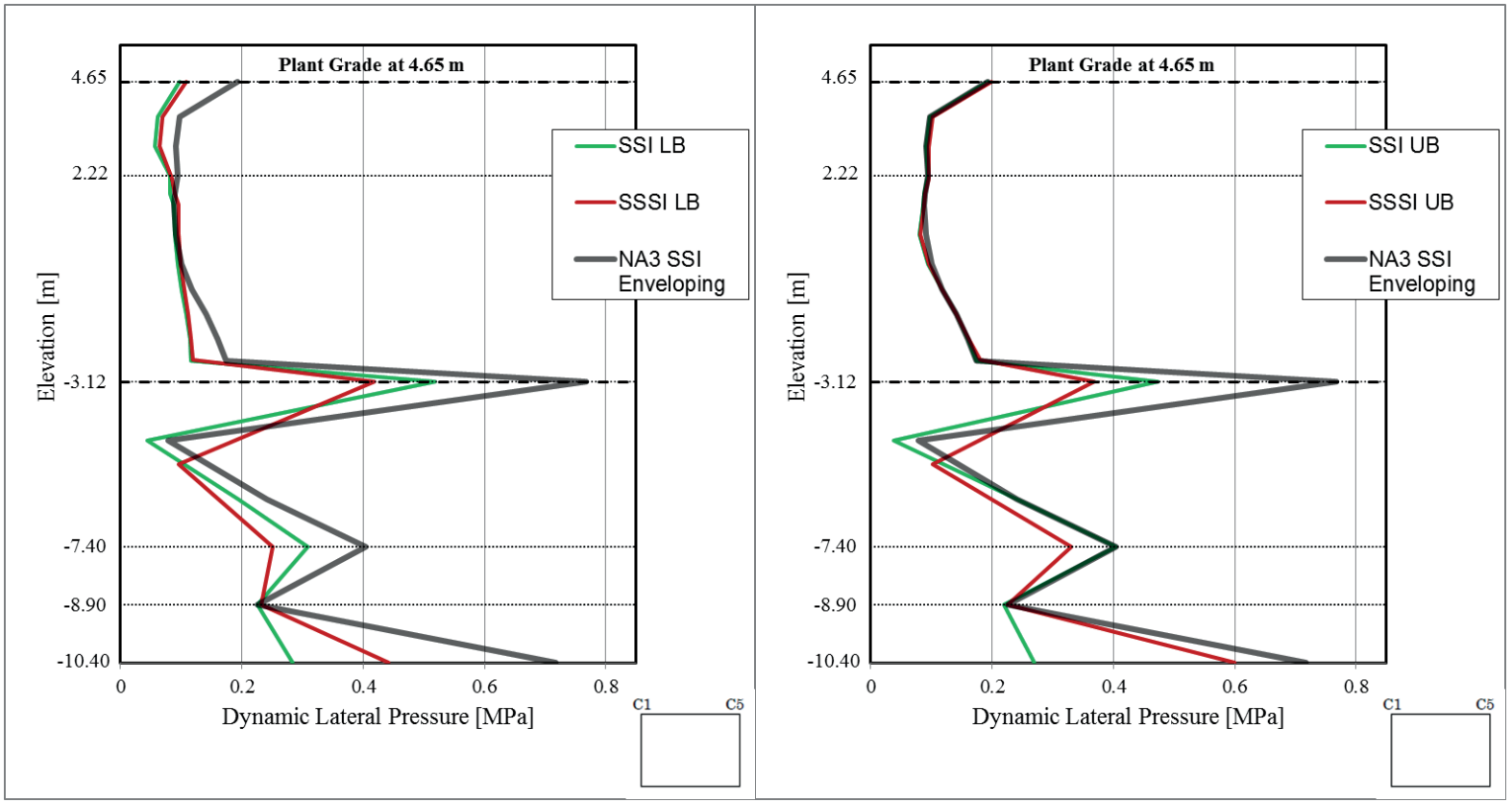

(a) LB Full Column Profiles **(b) UB Full Column Profiles**

Figure 5.3-1 Comparison of Dynamic Lateral Pressures CB Below-Grade Walls at Column Line C1 and C5

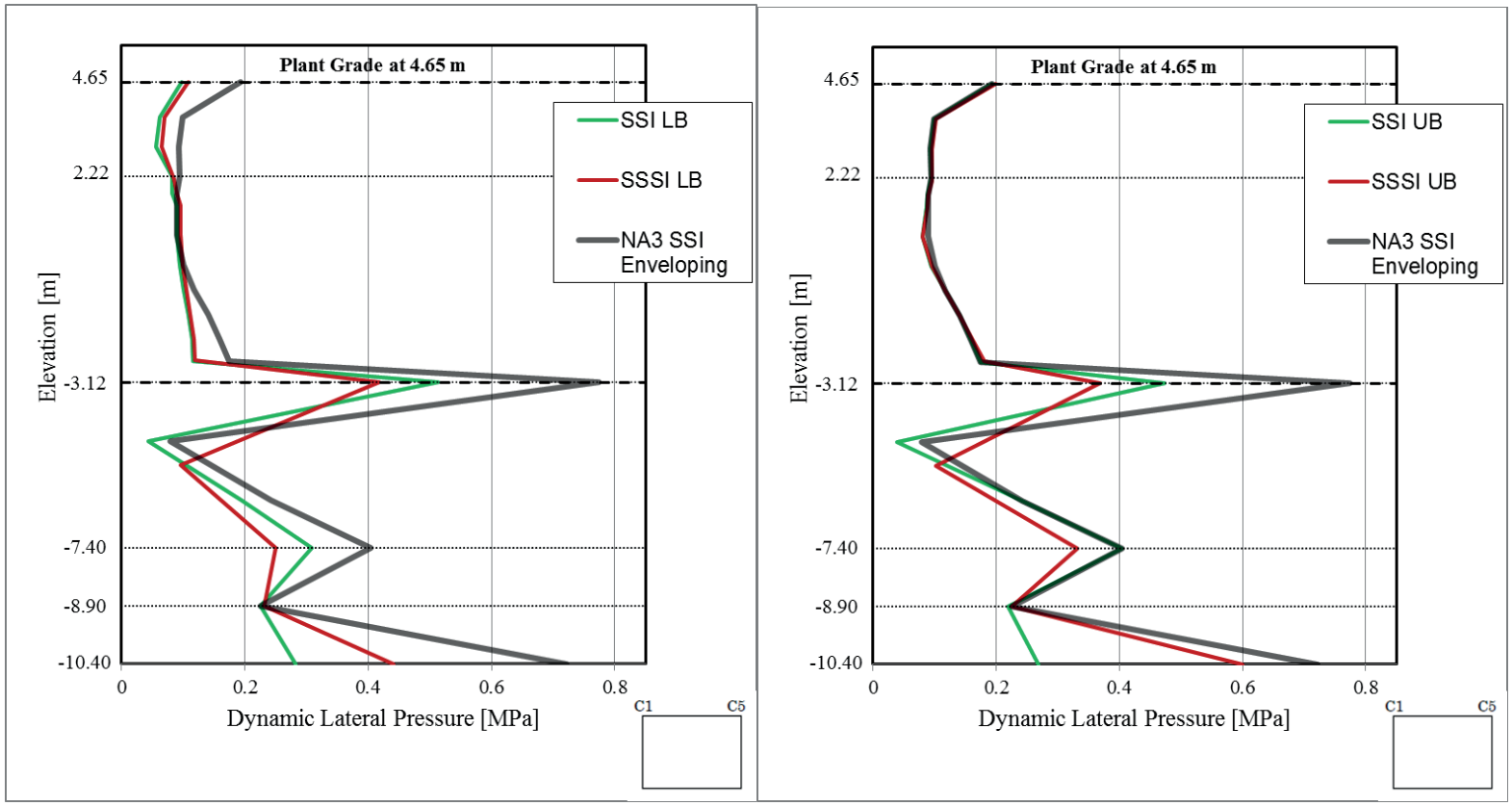

(a) LB Full Column Profiles **(b) UB Full Column Profiles**

Figure 5.3-2 Comparison of Dynamic Lateral Pressures CB Below-Grade Walls at Column Line C5

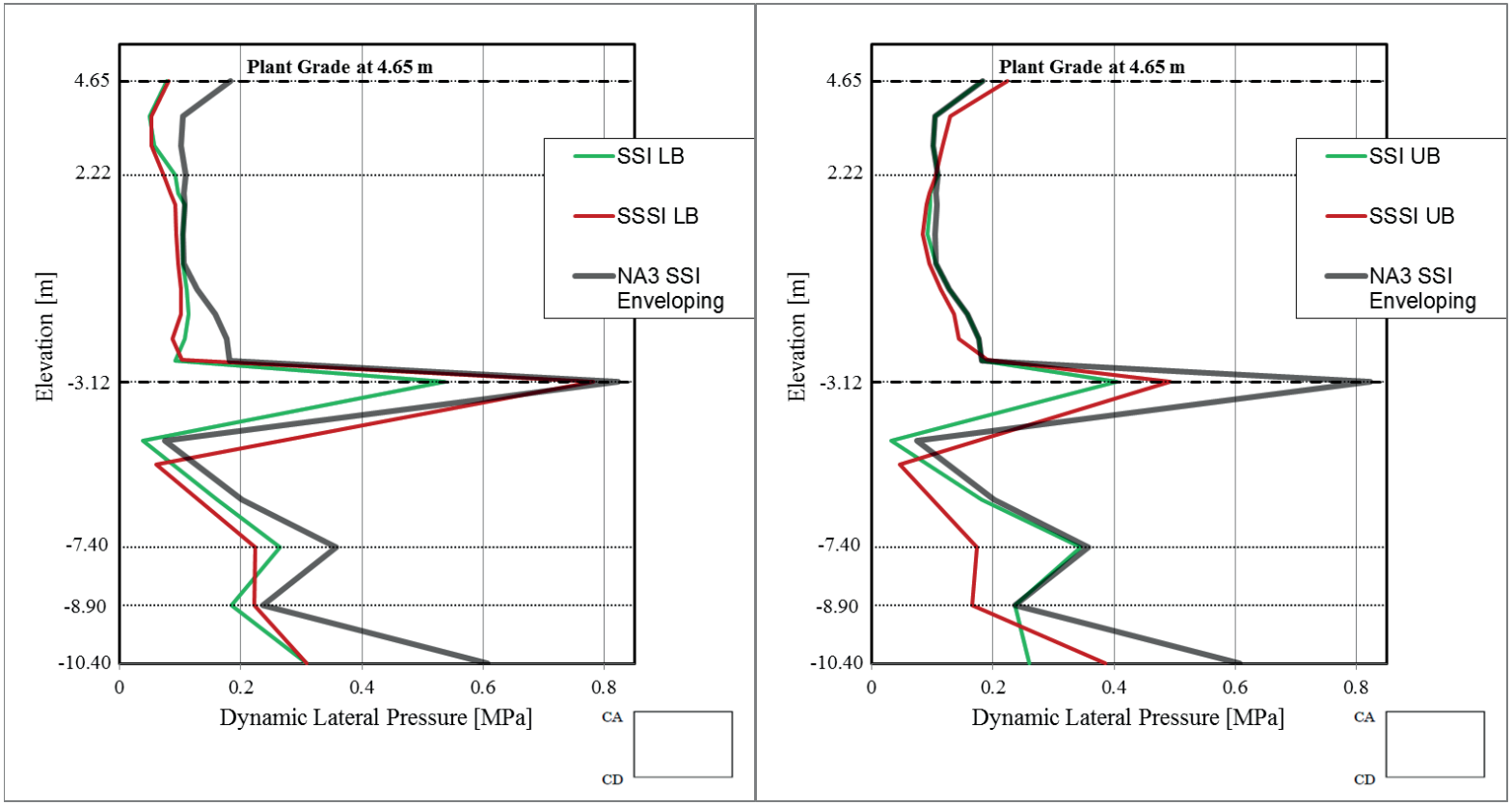

(a) LB Full Column Profiles **(b) UB Full Column Profiles**

Figure 5.3-3 Comparison of Dynamic Lateral Pressures CB Below-Grade Walls at Column Line CA

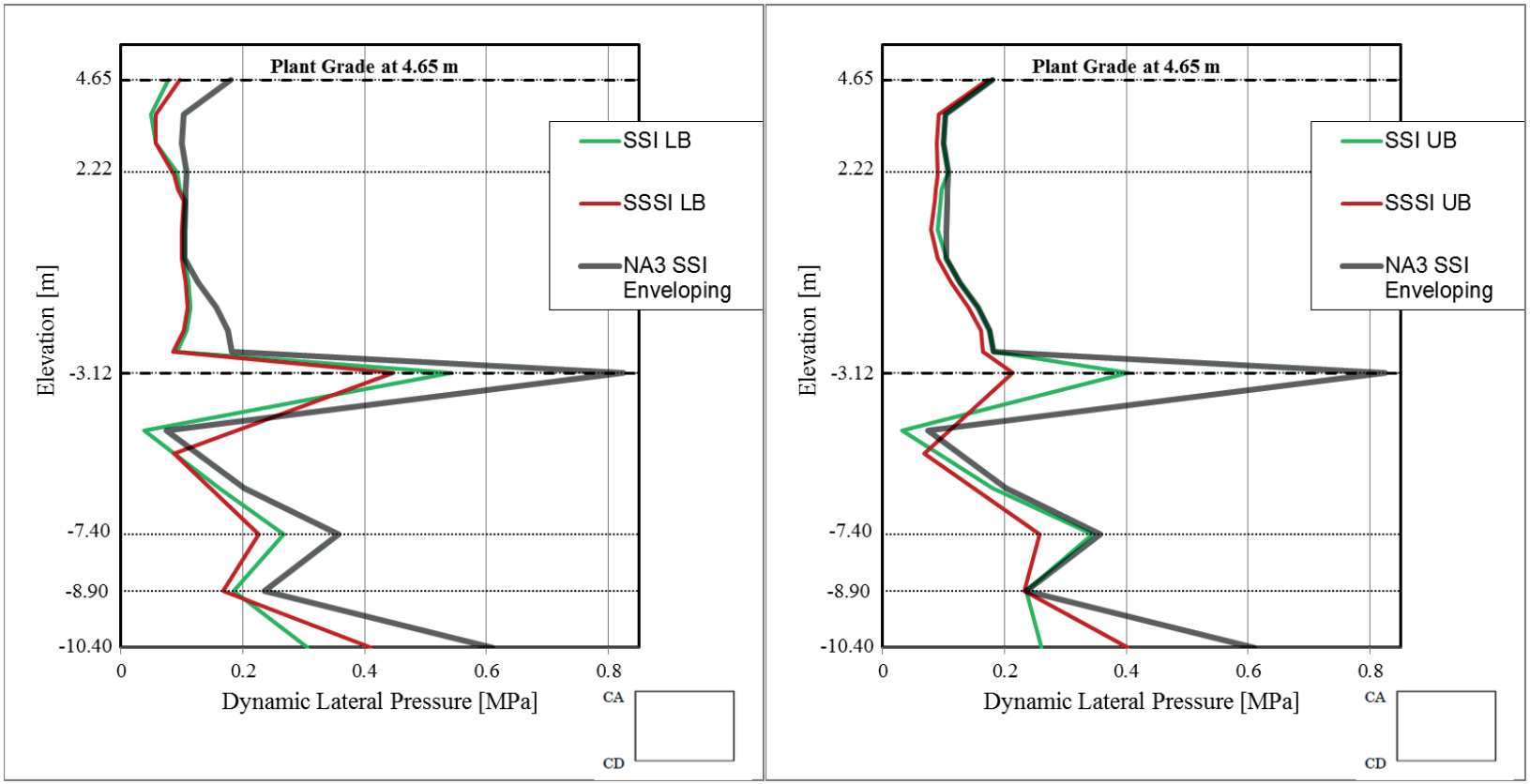

(a) LB Full Column Profiles **(b) UB Full Column Profiles**

Figure 5.3-4 Comparison of Dynamic Lateral Pressures CB Below-Grade Walls at Column Line CD

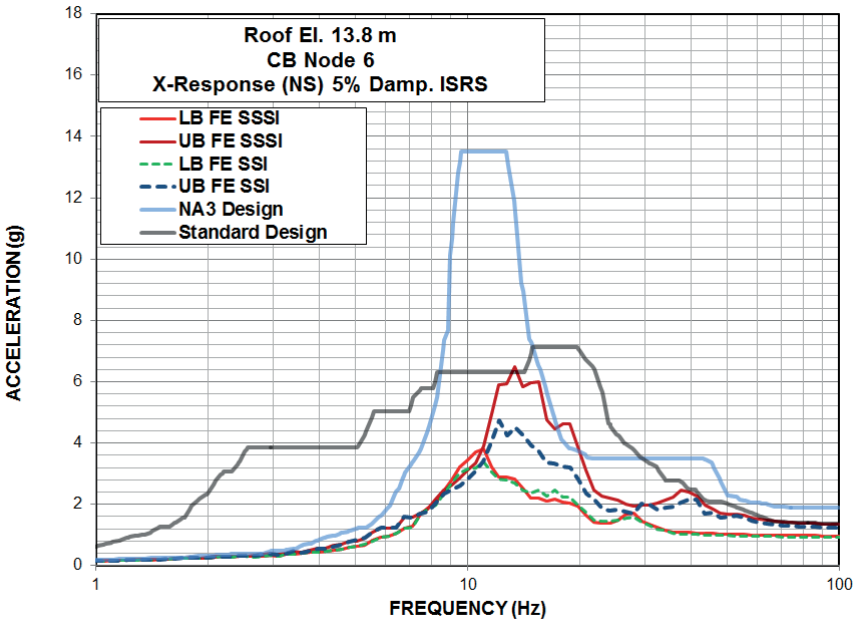

(a) CB Roof at Elevation 13.8 m

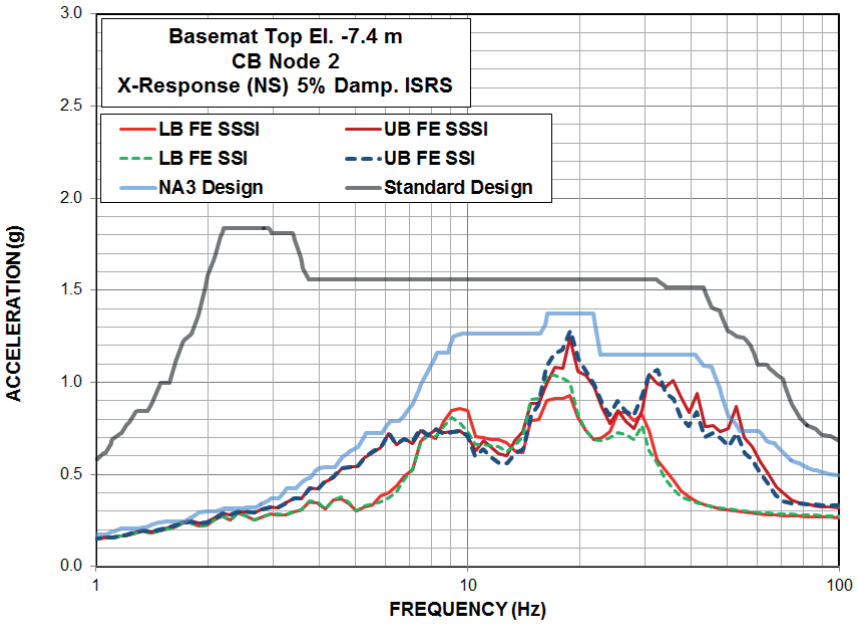

(b) Top of CB Basemat at Elevation - 7.4 m

Figure 5.4-1 Comparison of ISRS for CB Response in NS (X) Direction

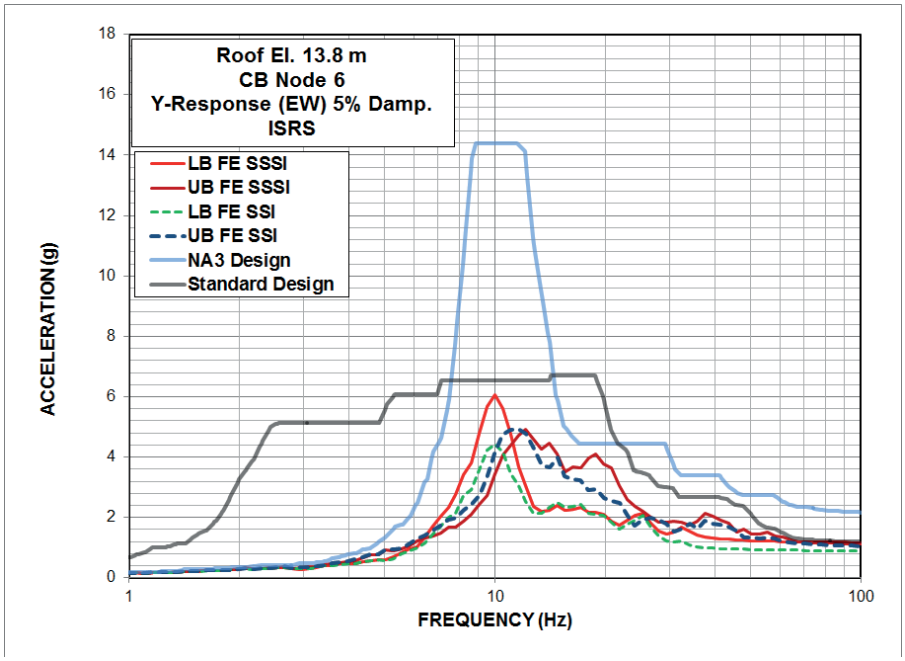

(a) CB Roof at Elevation 13.8 m

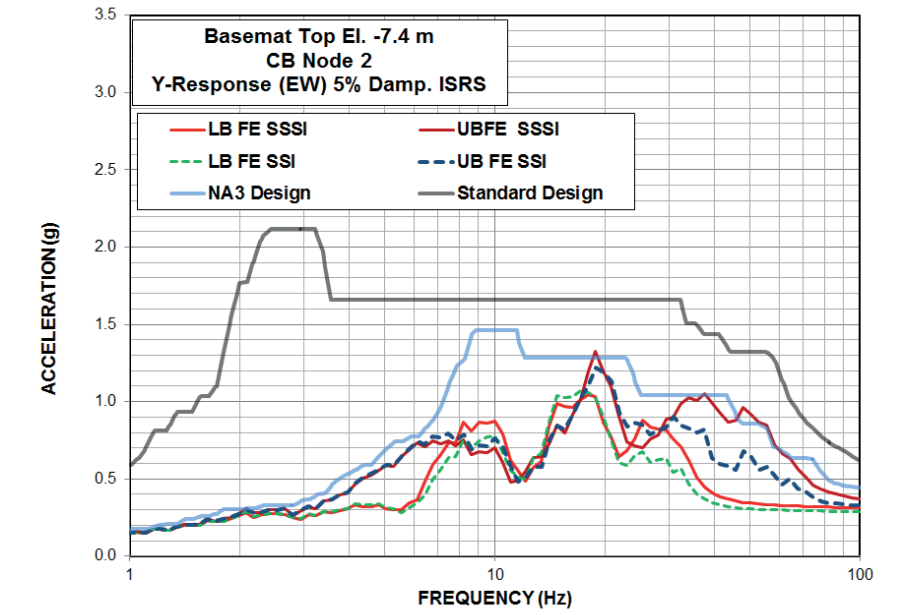

(b) Top of CB Basemat at Elevation - 7.4 m

Figure 5.4-2 Comparison of ISRS for CB Response in EW (Y) Direction

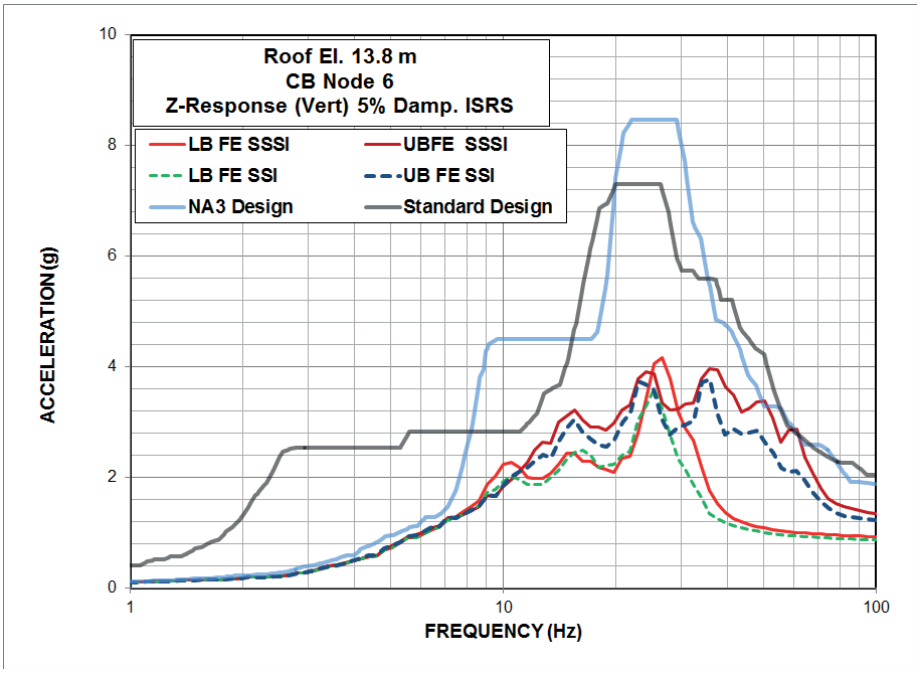

(a) CB Roof at Elevation 13.8 m

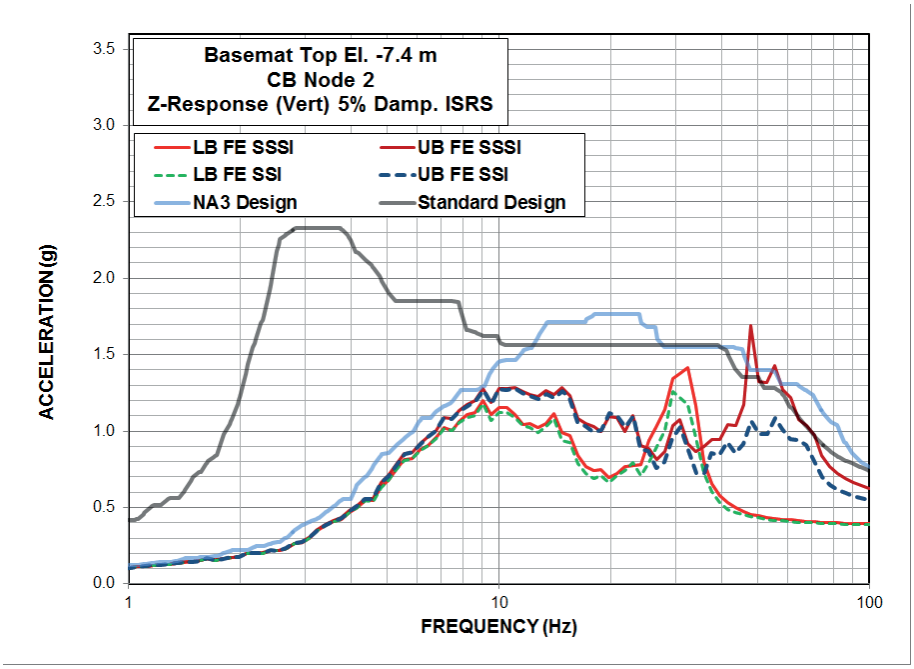

(b) Top of CB Basemat at Elevation - 7.4 m

Figure 5.4-3 Comparison of ISRS for CB Response in Vertical (Z) Direction

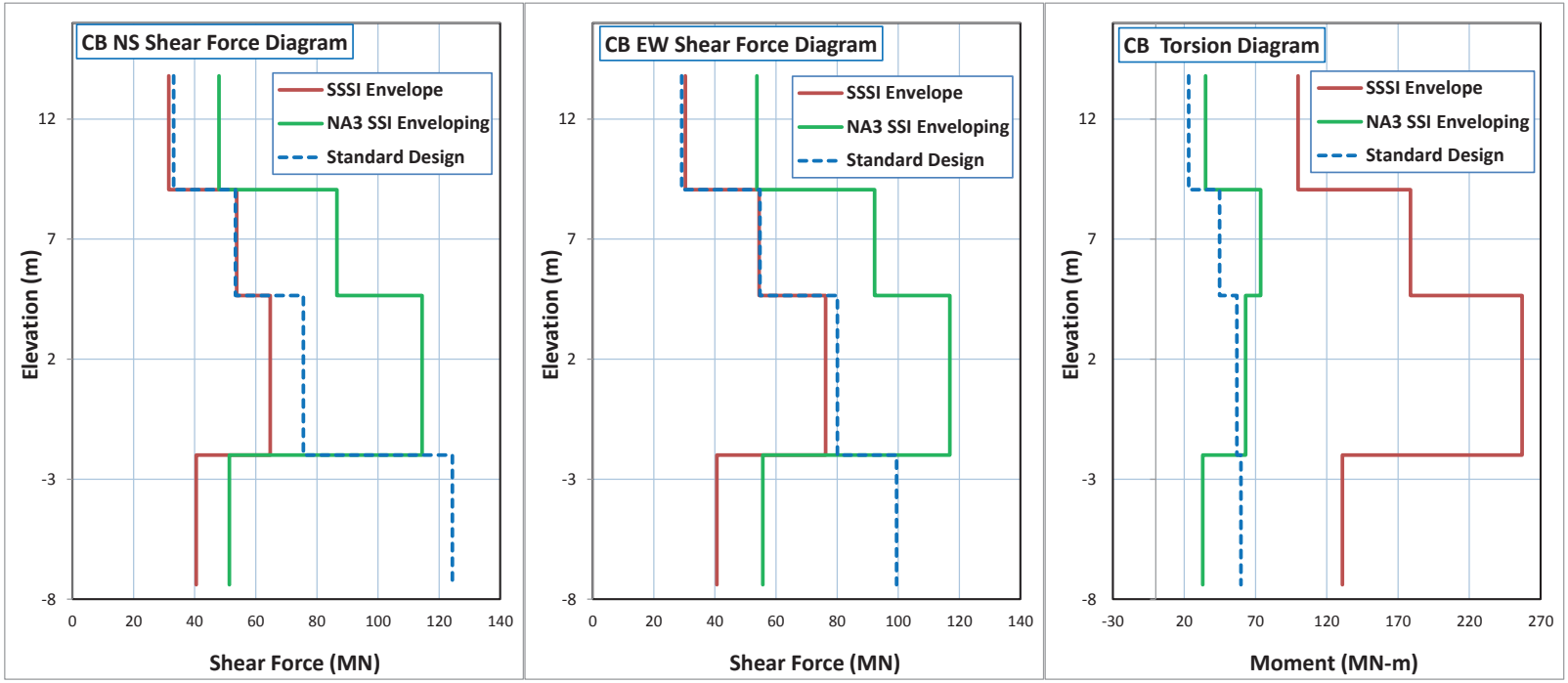

Figure 5.5-1 Comparison of Horizontal Seismic Load Demands on CB Structure

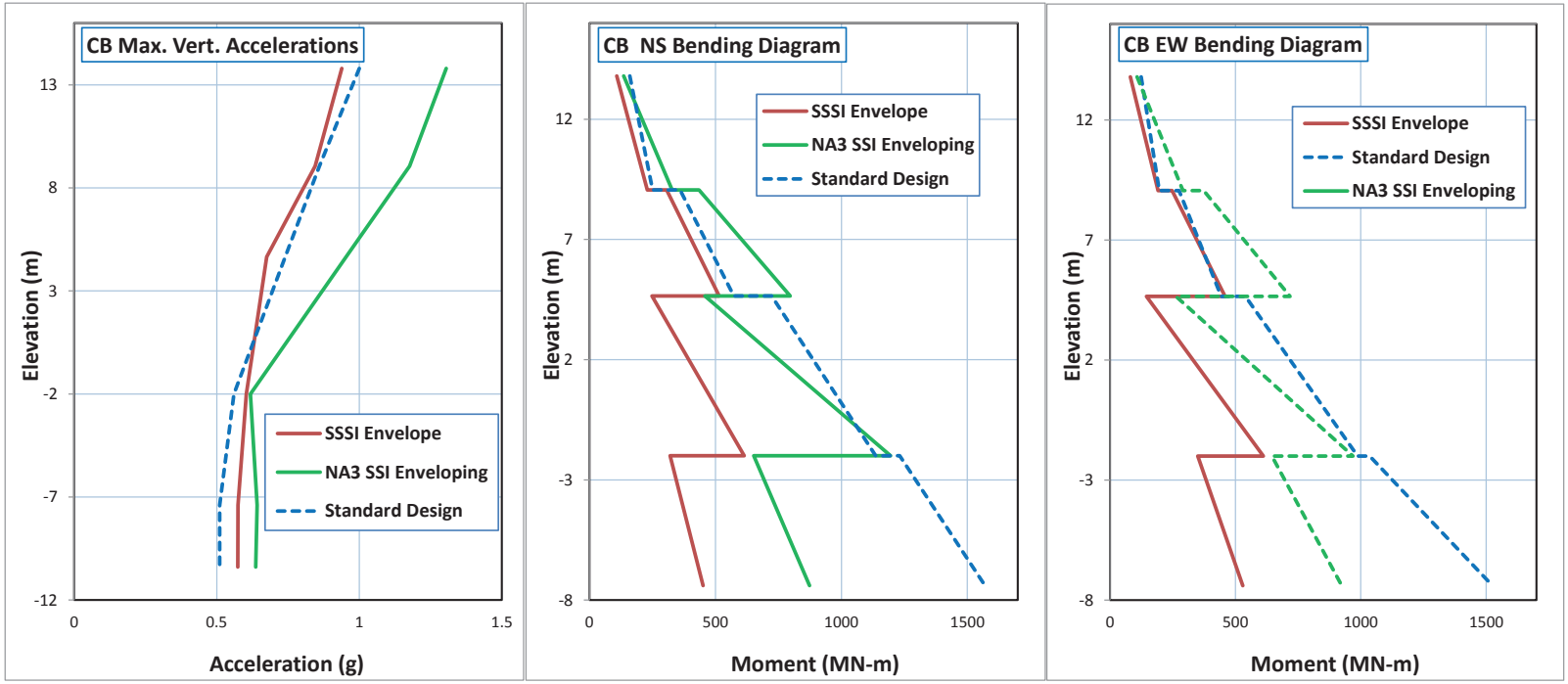

Figure 5.5-2 Comparison of Vertical Seismic Load Demands on CB Structure

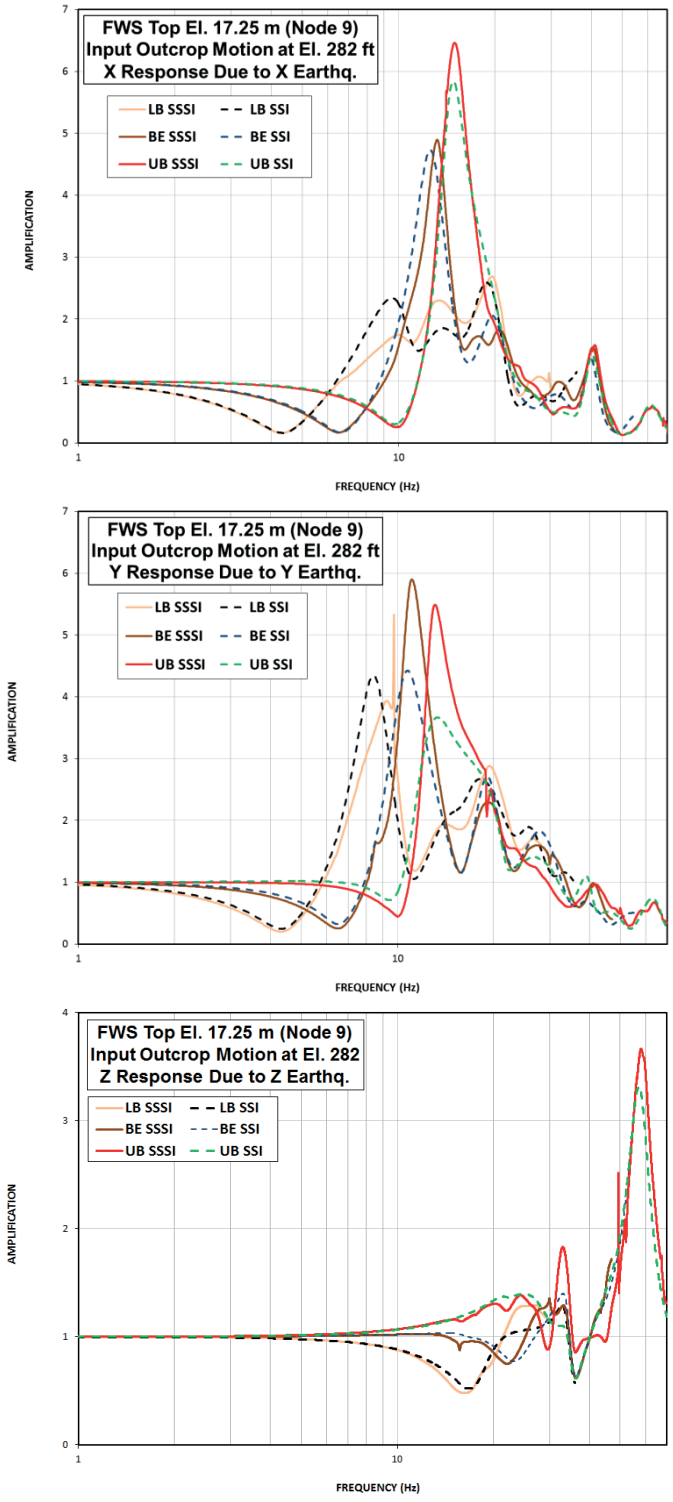

Figure 6.1-1 Comparison of Outcrop Transfer Functions for FWS Co-Directional Response

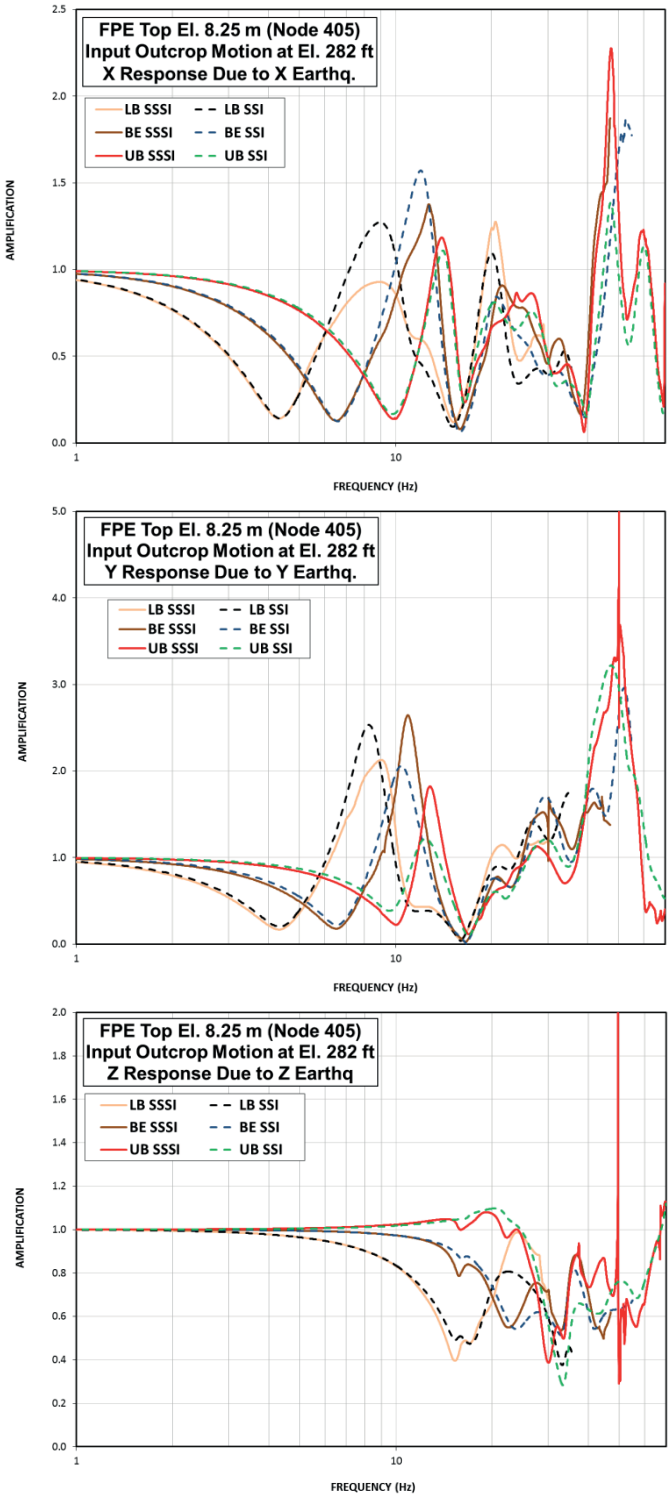

Figure 6.1-2 Comparison of Outcrop Transfer Functions for FPE Co-Directional Response

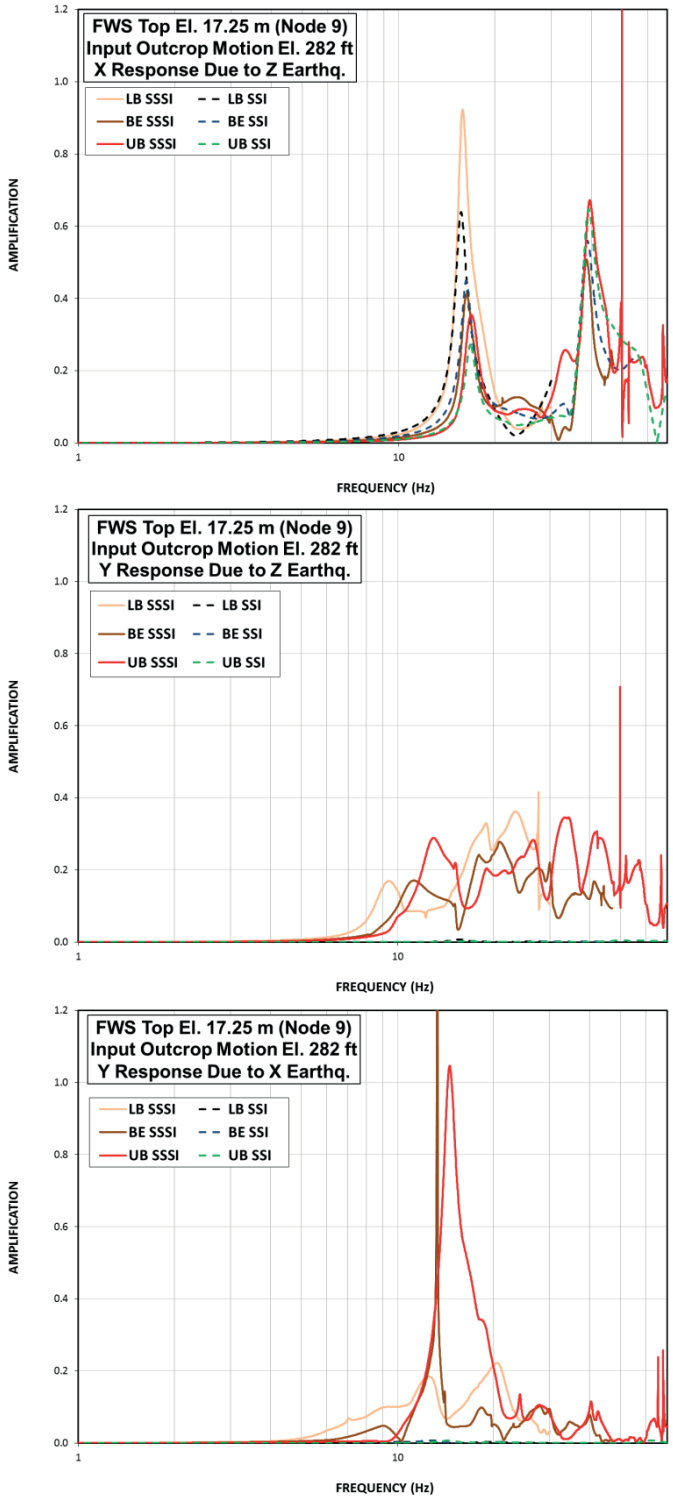

Figure 6.1-3 Comparison of Outcrop Transfer Functions for FWS Cross-Directional Response

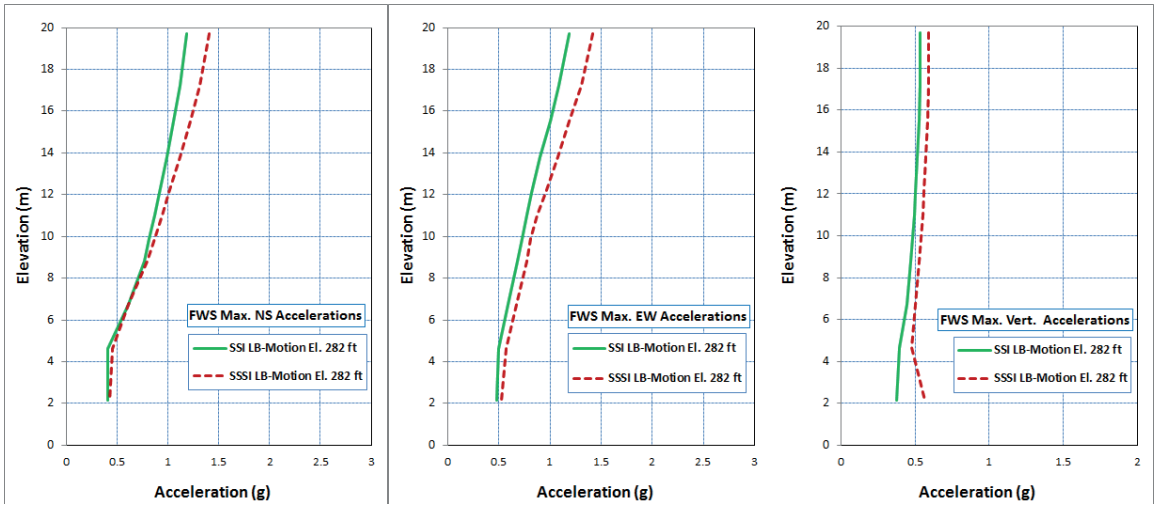

(a) Motion at El. 282 ft

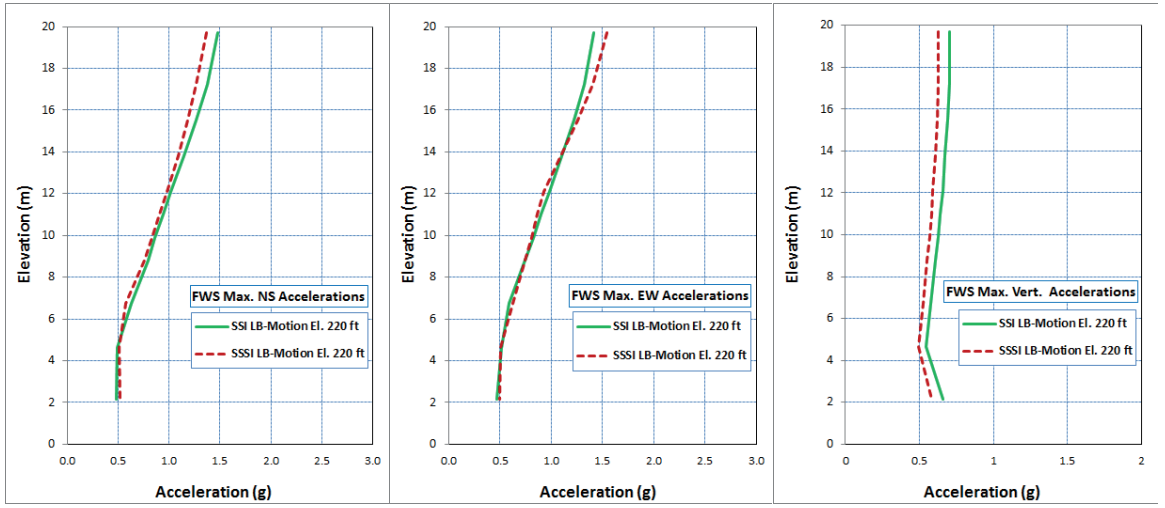

(b) Motion at El. 220 ft

Figure 6.2-1 Comparison of FWS Maximum Accelerations (LB Analysis Cases FC1 and FC4)

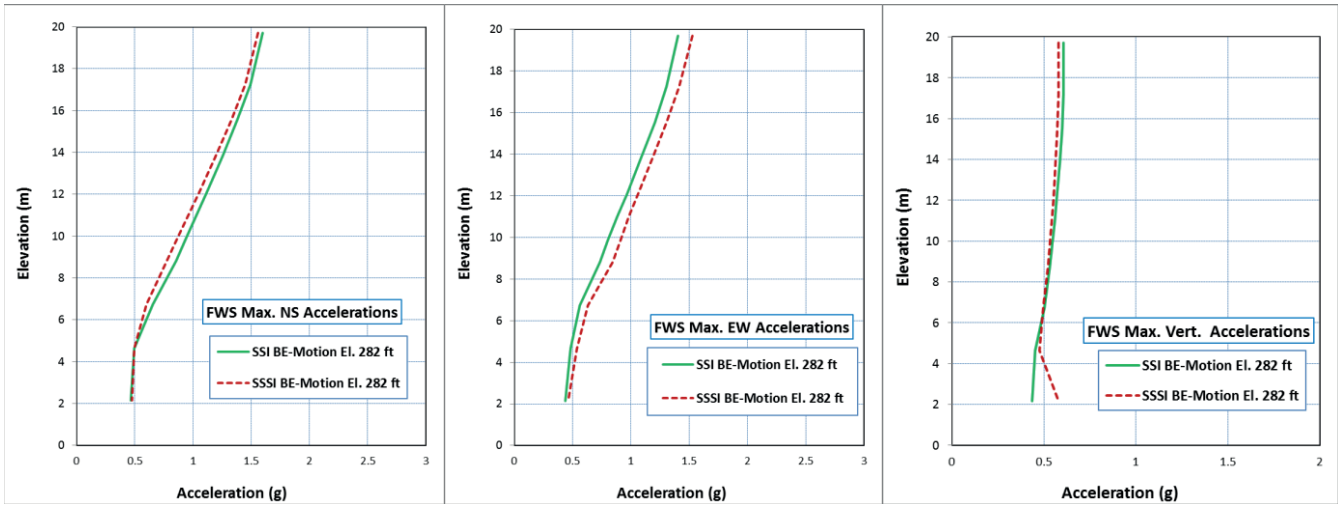

(a) Motion at El. 282 ft

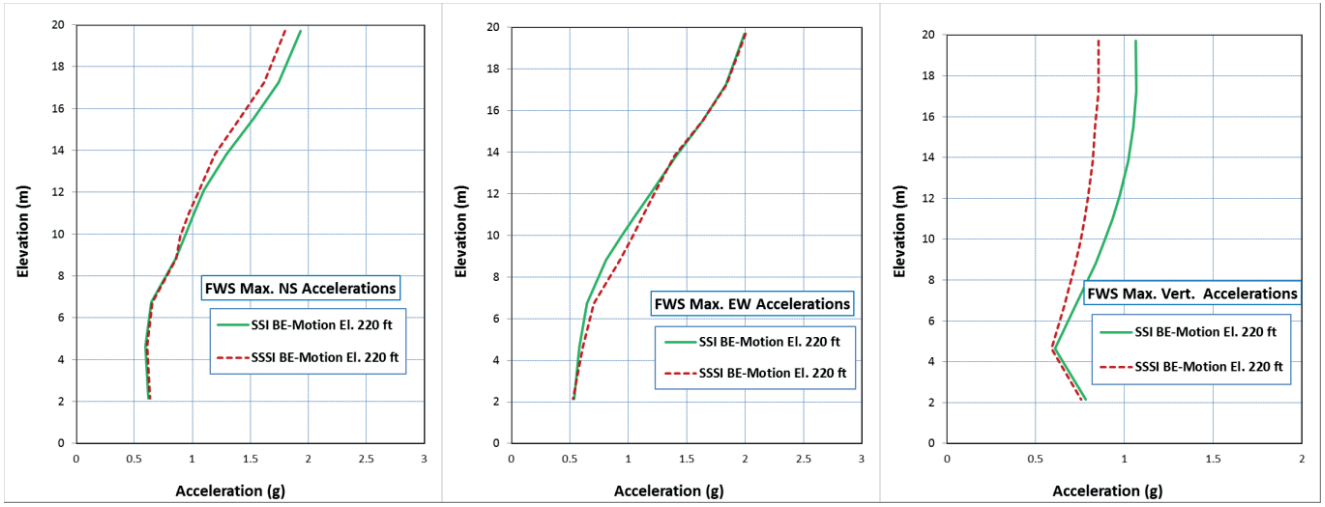

(b) Motion at El. 220 ft

Figure 6.2-2 Comparison of FWS Maximum Accelerations (BE Analysis Cases FC2 and FC5)

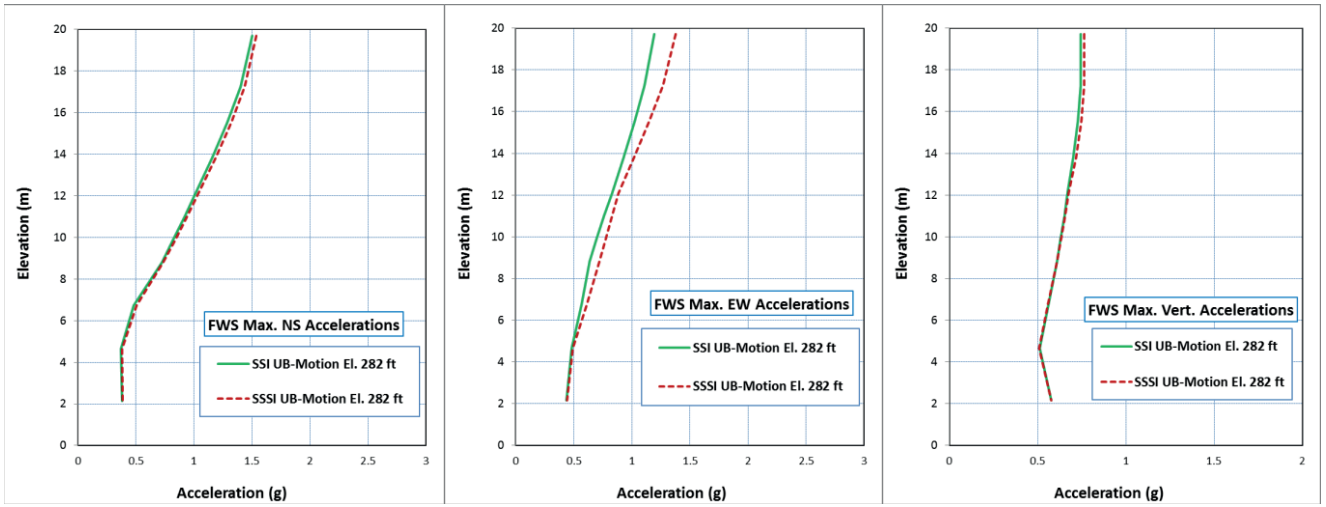

(a) Motion at El. 282 ft

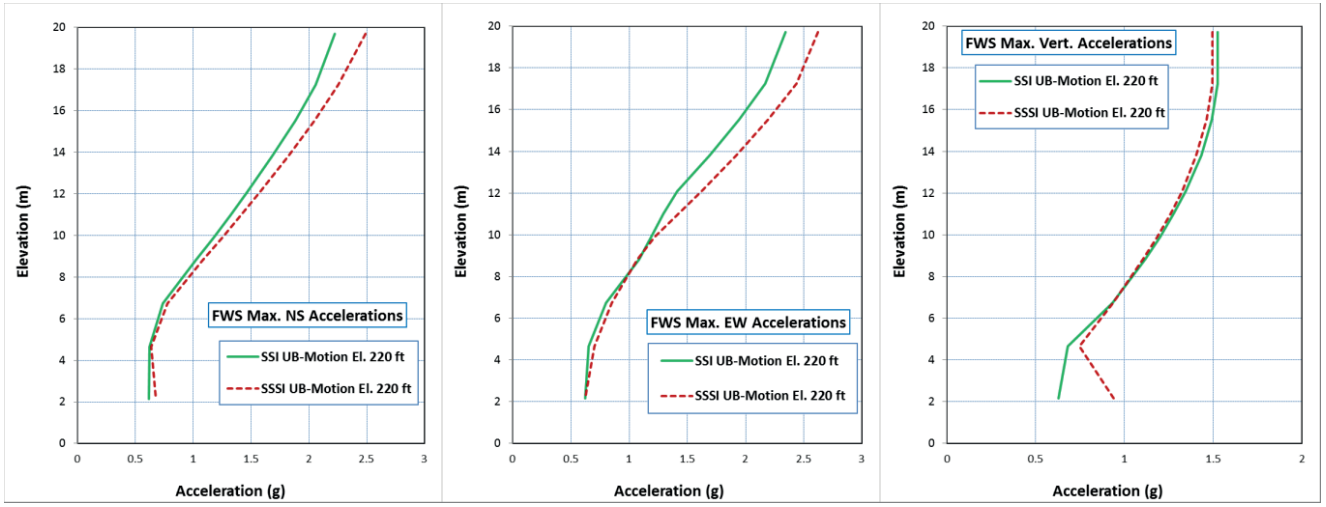

(b) Motion at El. 220 ft

Figure 6.2-3 Comparison of FWS Maximum Accelerations (UB Analysis Cases FC3 and FC6)

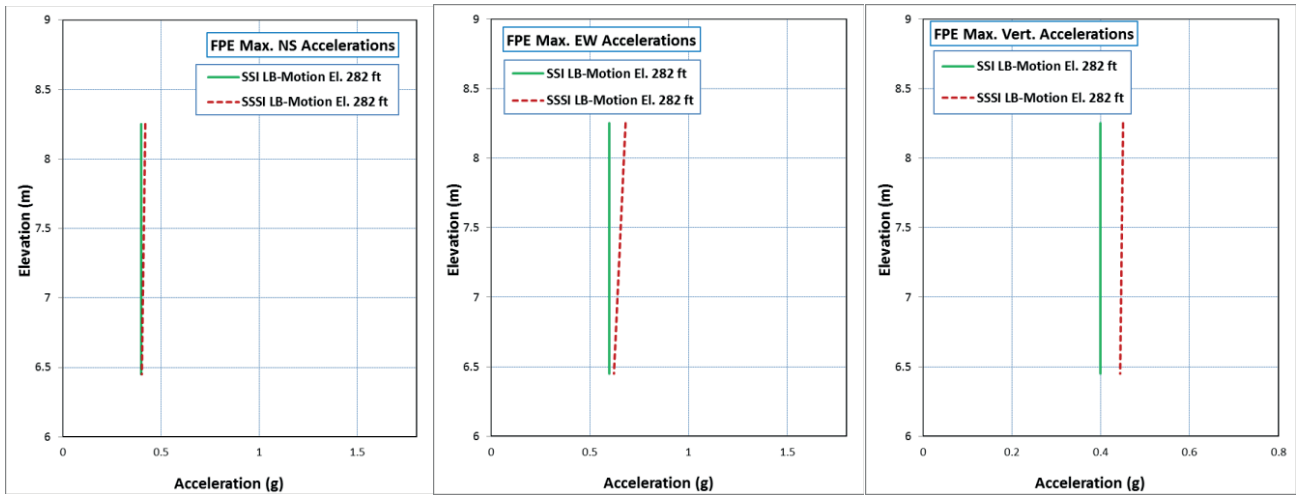

(a) Motion at El. 282 ft

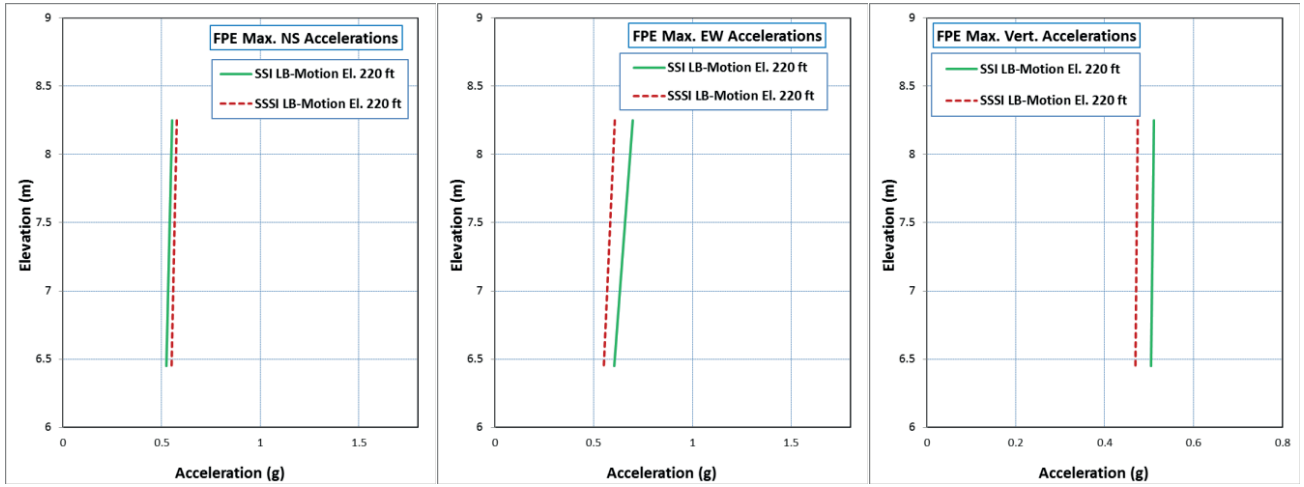

(b) Motion at El. 220 ft

Figure 6.2-4 Comparison of FPE Maximum Accelerations (LB Cases FC1 and FC4)

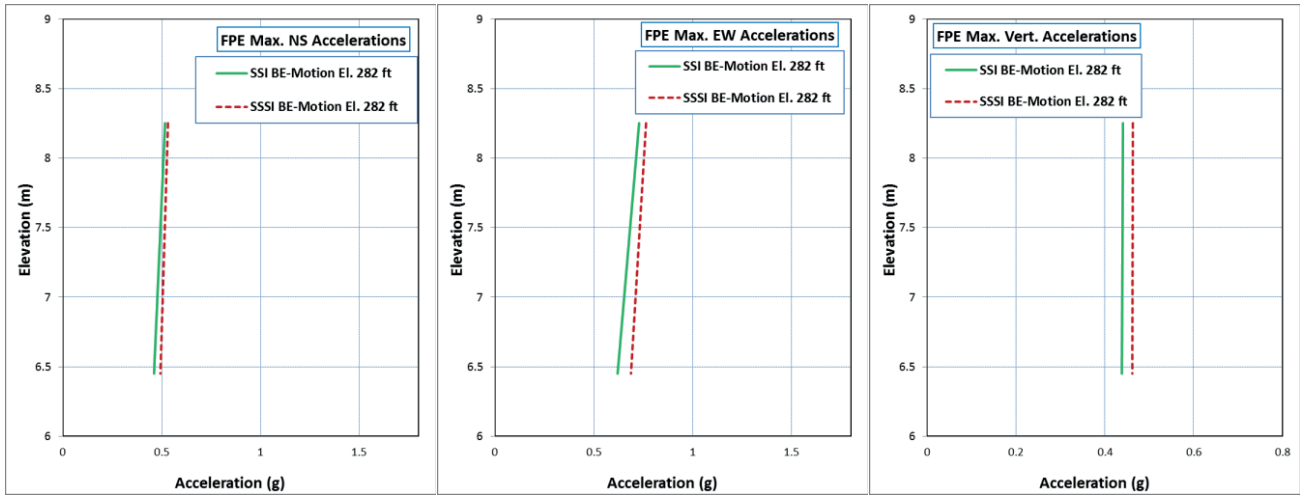

(a) Motion at El. 282 ft

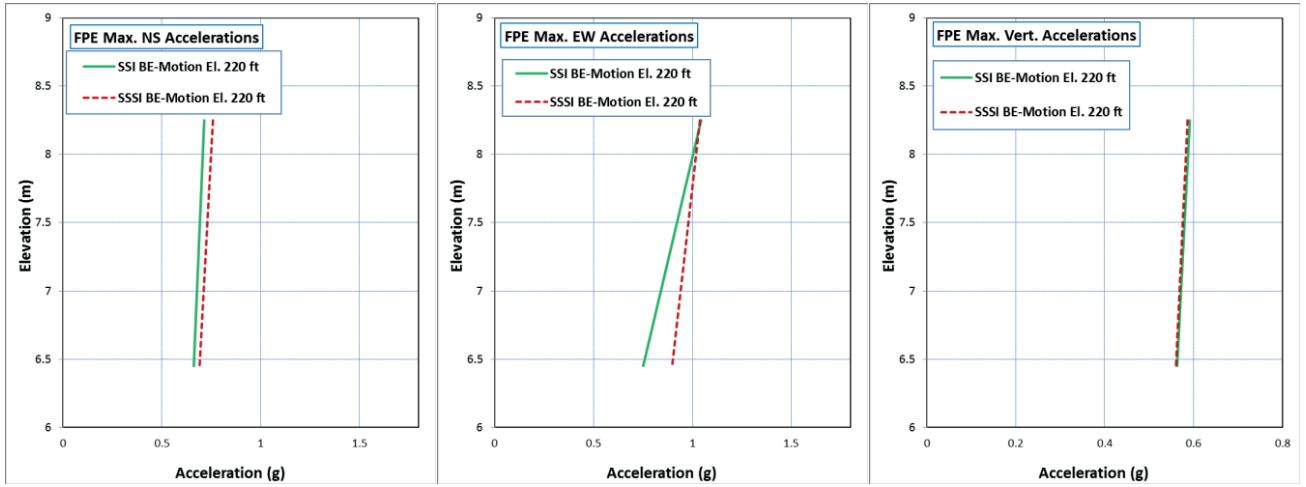

(b) Motion at El. 220 ft

Figure 6.2-5 Comparison of FPE Maximum Accelerations (BE Analysis Cases FC2 and FC5)

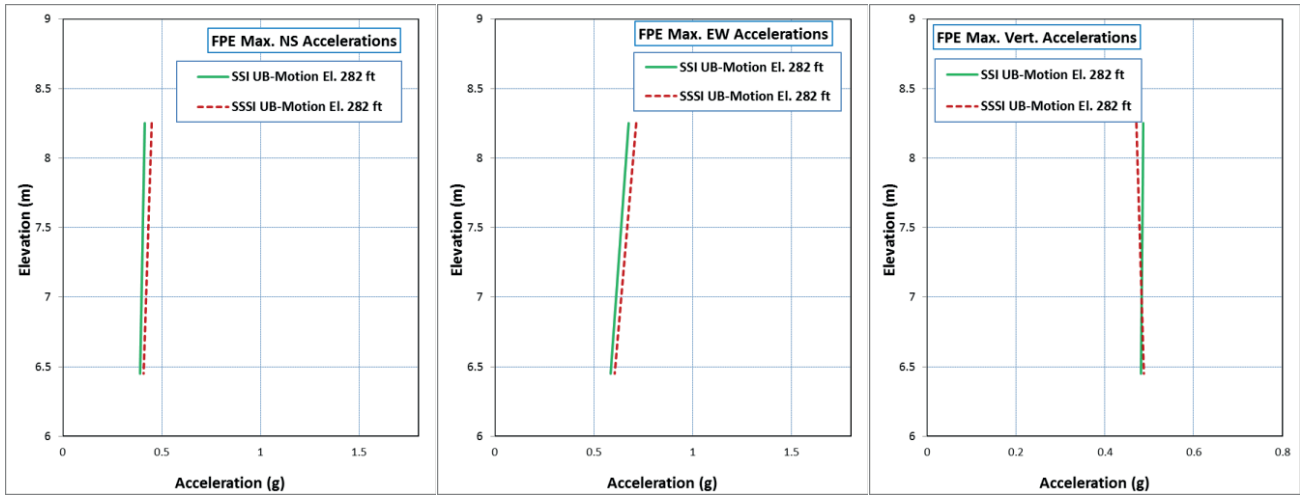

(a) Motion at El. 282 ft

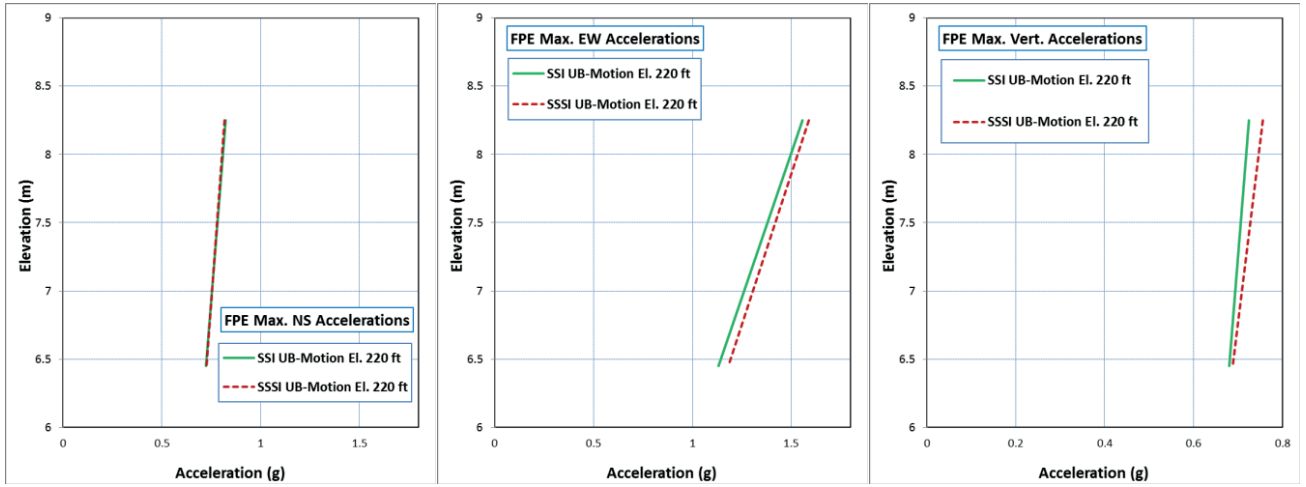

(b) Motion at El. 220 ft

Figure 6.2-6 Comparison of FPE Maximum Accelerations (UB Analysis Cases FC3 and FC6)

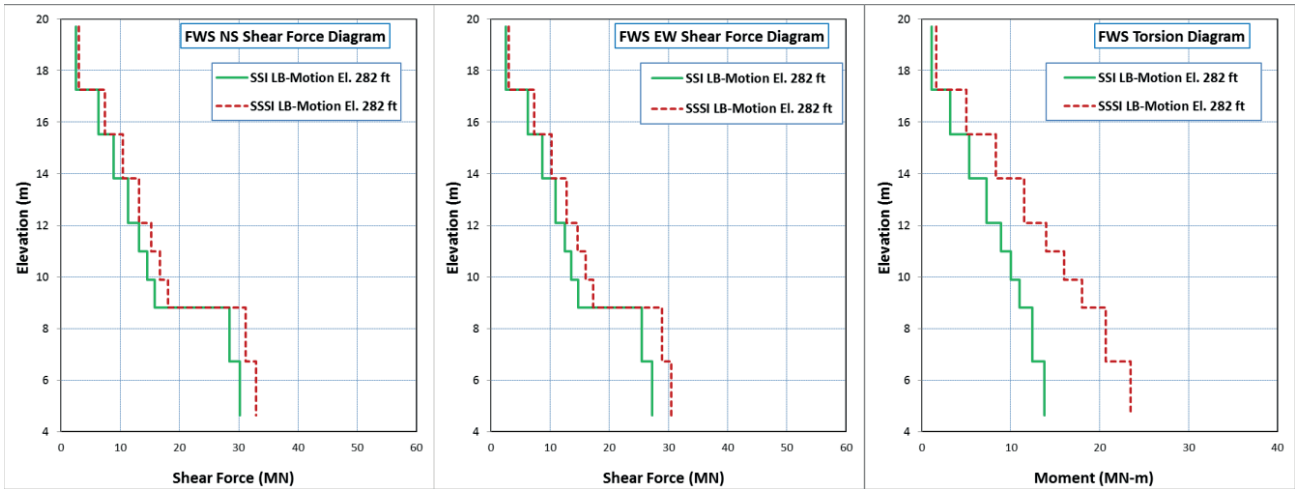

(a) Motion at El. 282 ft

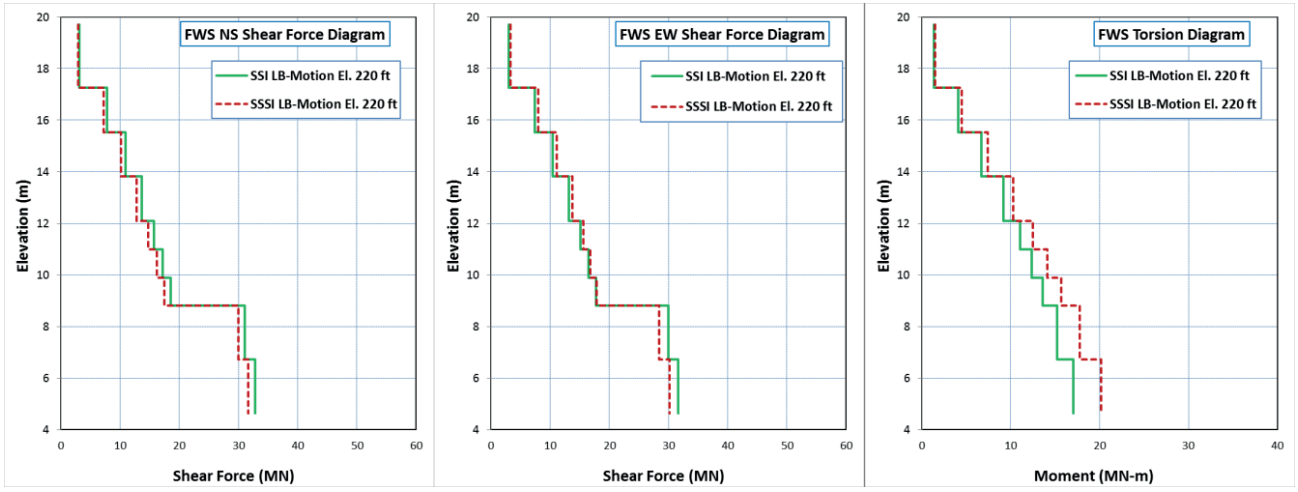

(b) Motion at El. 220 ft

Figure 6.2-7 Comparison of FWS Maximum Shears and Torsion (LB Analysis Cases FC1 and FC4)

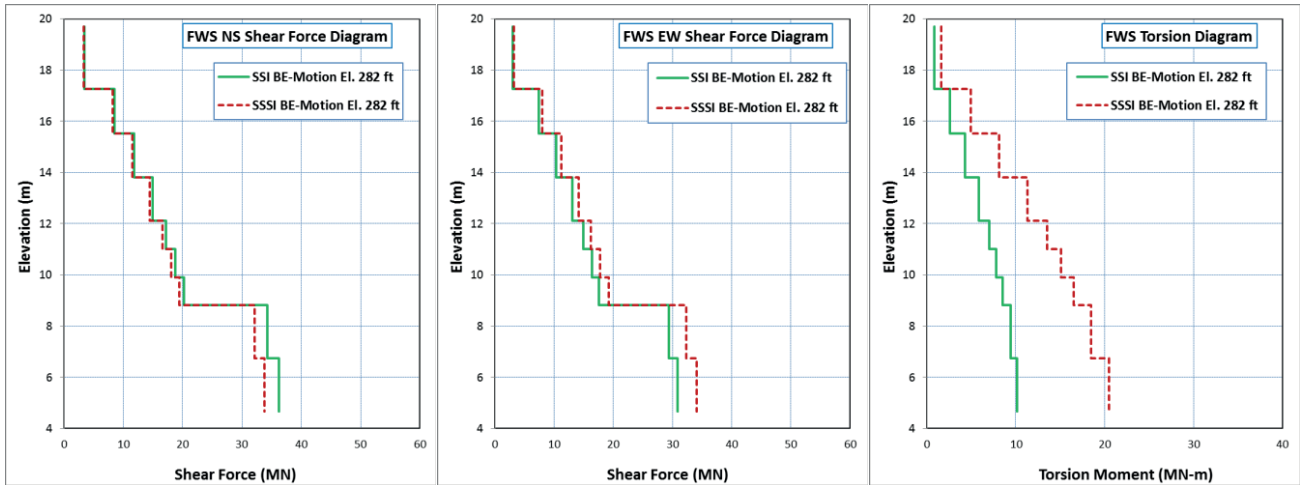

(a) Motion at El. 282 ft

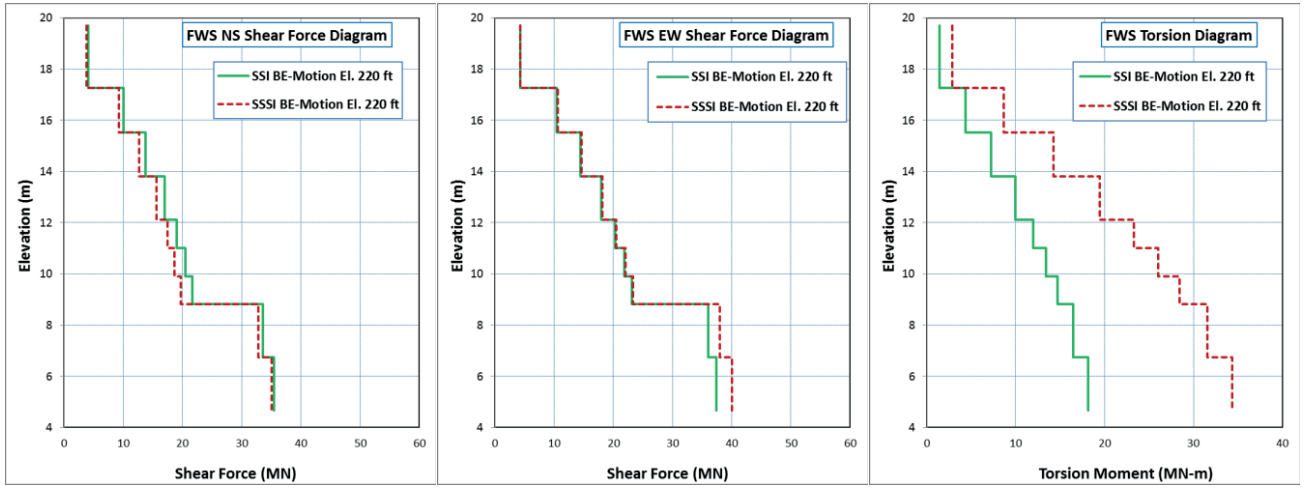

(b) Motion at El. 220 ft

Figure 6.2-8 Comparison of FWS Maximum Shears and Torsion (BE Analysis Cases FC2 and FC5)

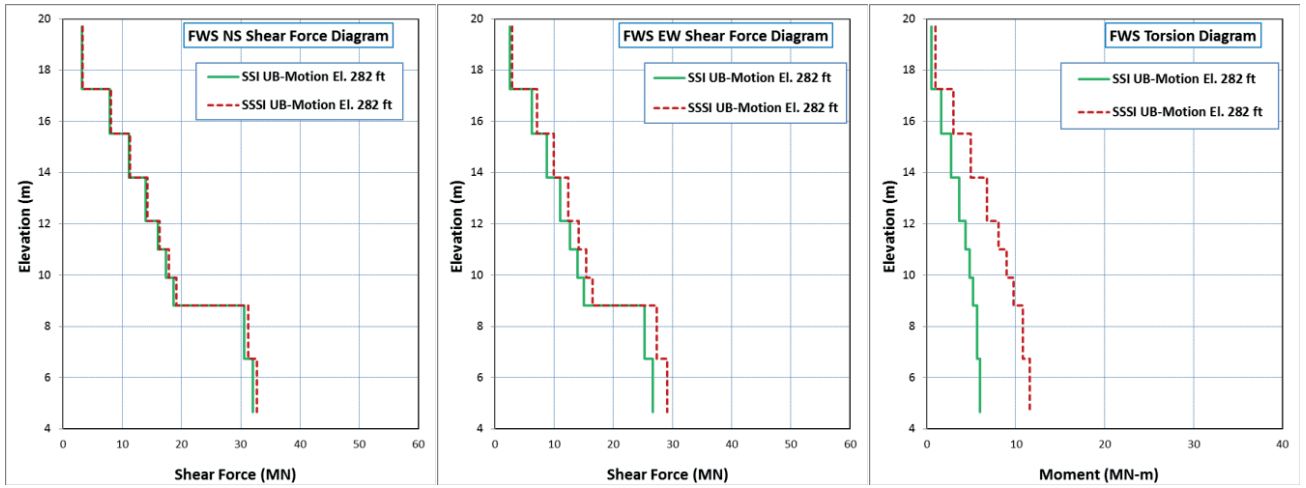

(a) Motion at El. 282 ft

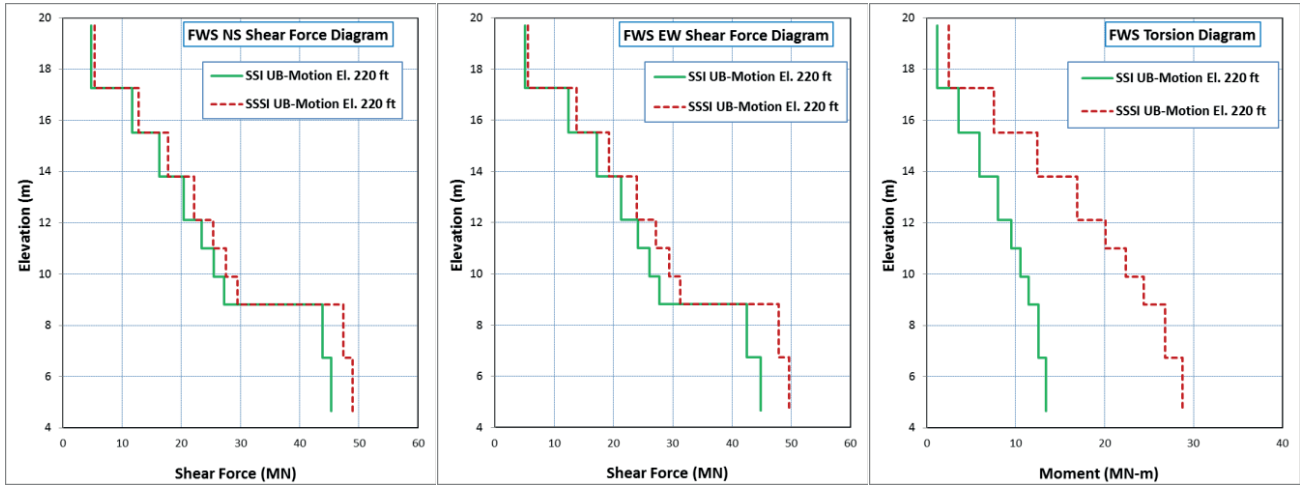

(b) Motion at El. 220 ft

Figure 6.2-9 Comparison of FWS Maximum Shears and Torsion (UB Analysis Cases FC3 and FC6)

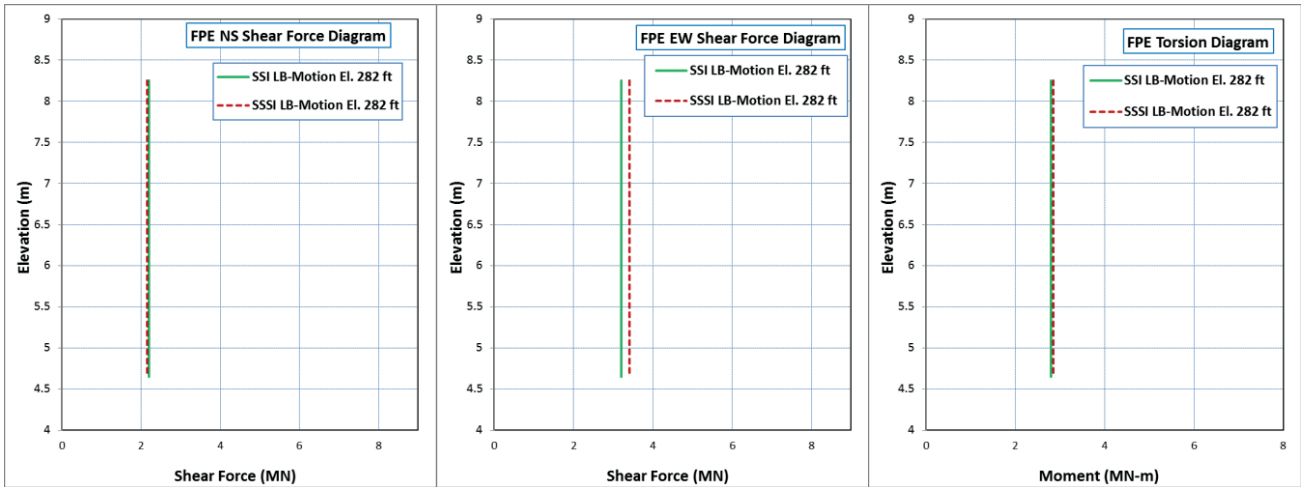

(a) Motion at El. 282 ft

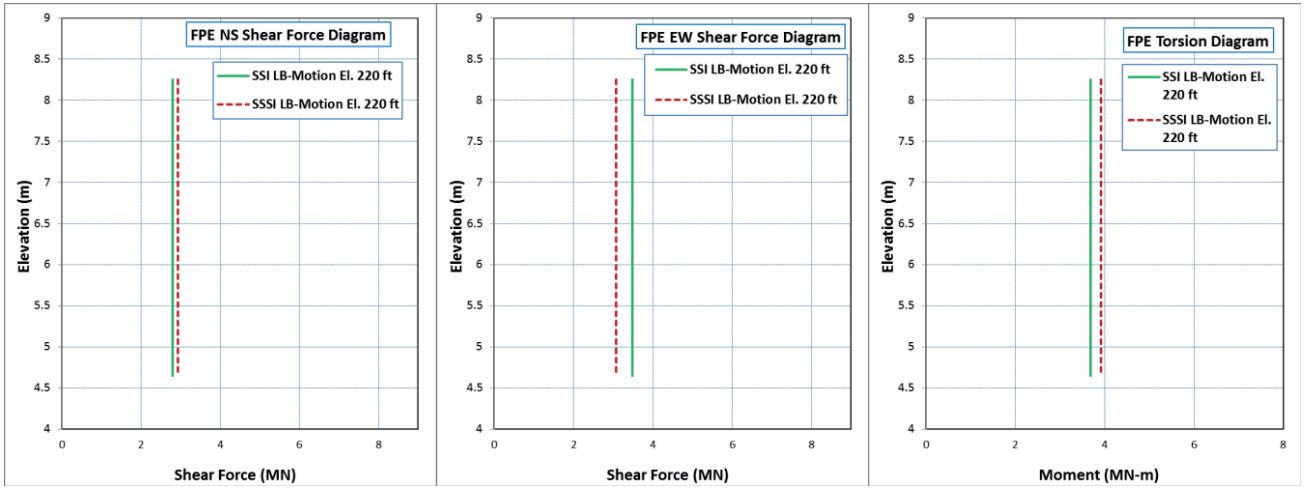

(b) Motion at El. 220 ft

Figure 6.2-10 Comparison of FPE Maximum Shears and Torsion (LB Analysis Cases FC1 and FC4)

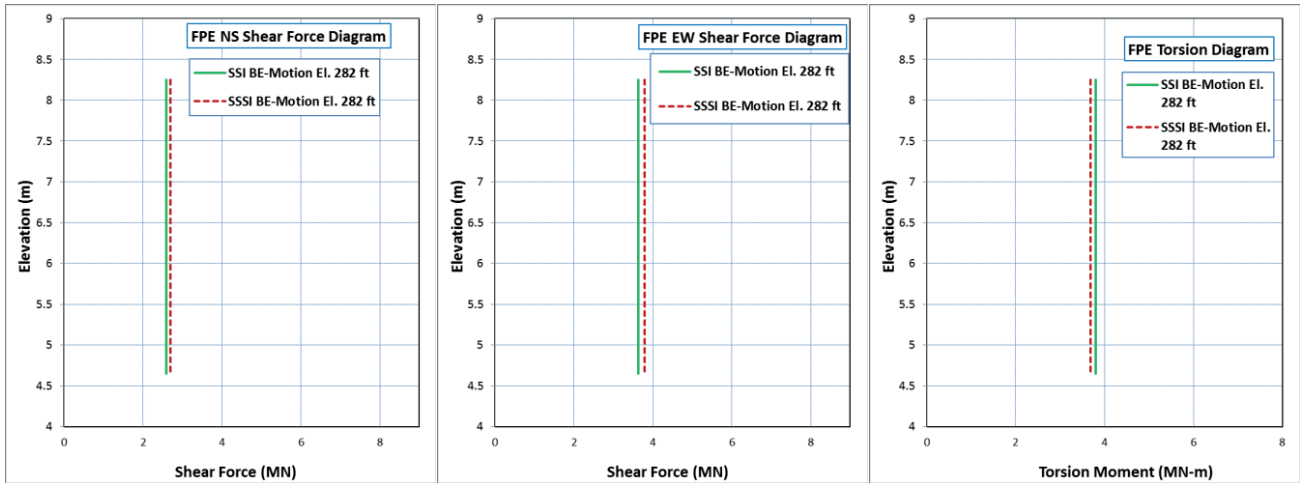

(a) Motion at El. 282 ft

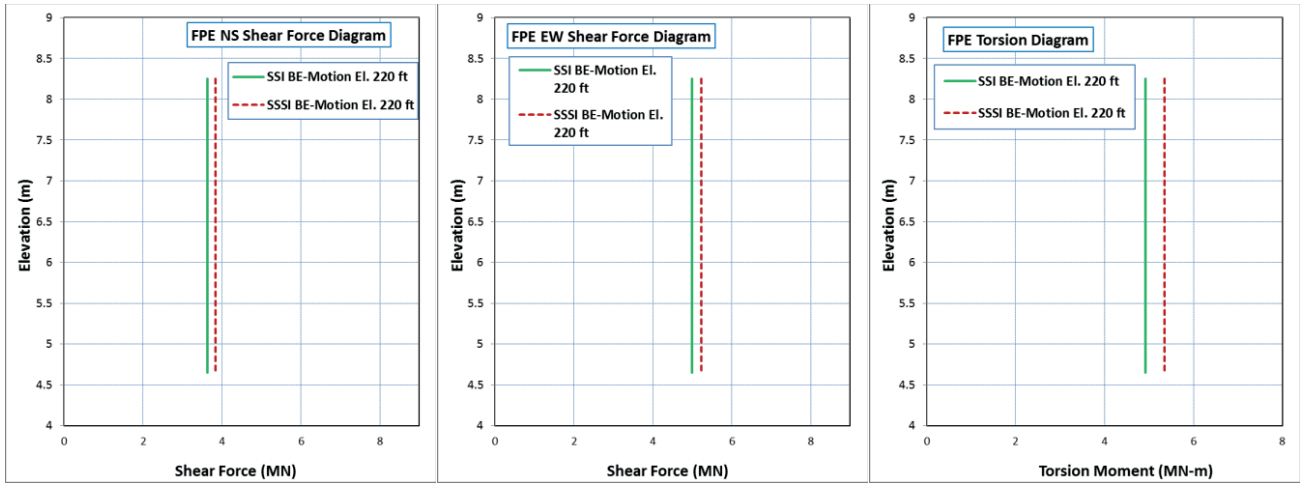

(b) Motion at El. 220 ft

Figure 6.2-11 Comparison of FPE Maximum Shears and Torsion (BE Analysis Cases FC2 and FC5)

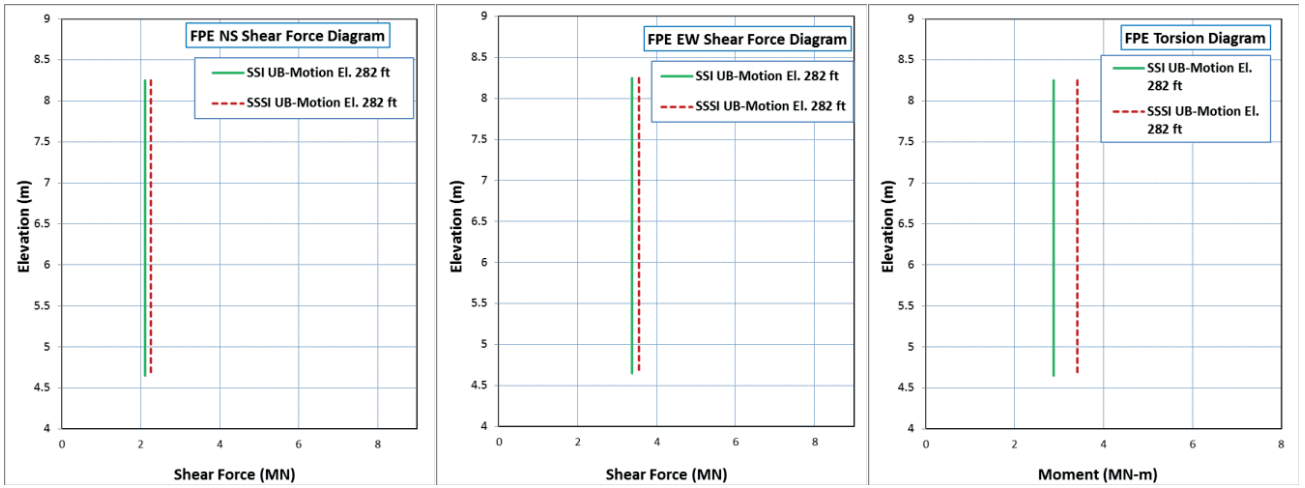

(a) Motion at El. 282 ft

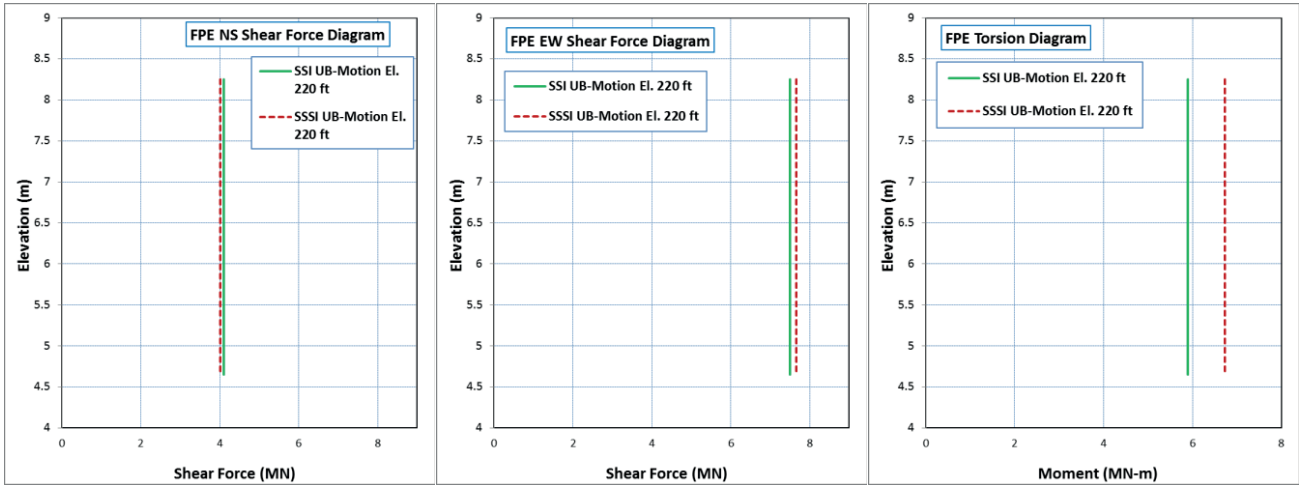

(b) Motion at El. 220 ft

Figure 6.2-12 Comparison of FPE Maximum Shears and Torsion (UB Analysis Cases FC3 and FC6)

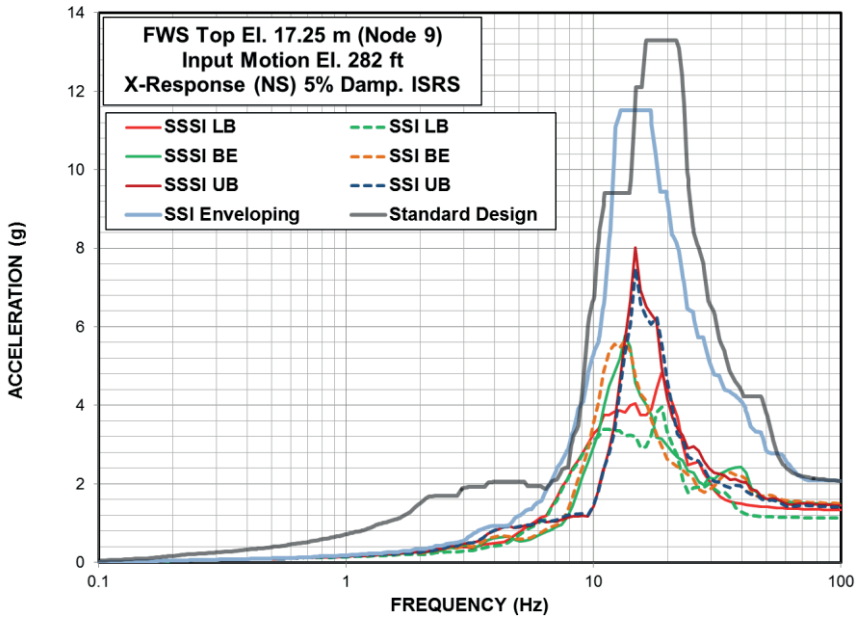

(a) Input Motion at El. 282 ft

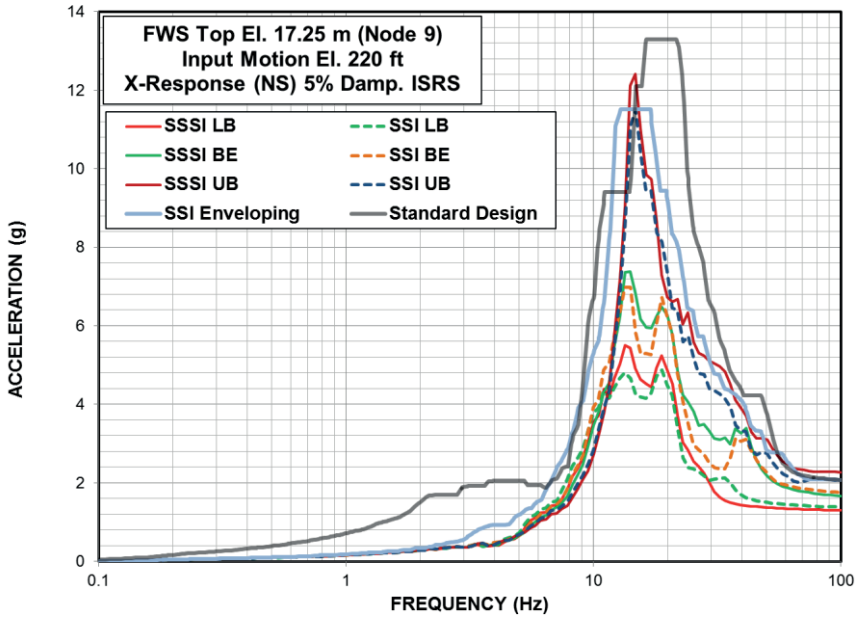

(b) Input Motion at El. 220 ft

Figure 6.3-1 Comparison of ISRS for Response of FWS Roof in NS (X) Direction

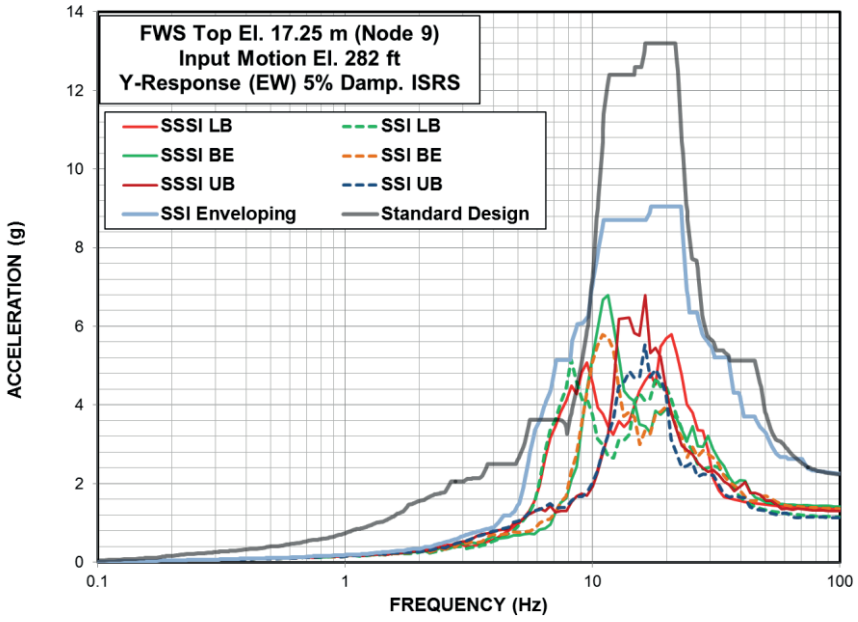

(a) Input Motion at El. 282 ft

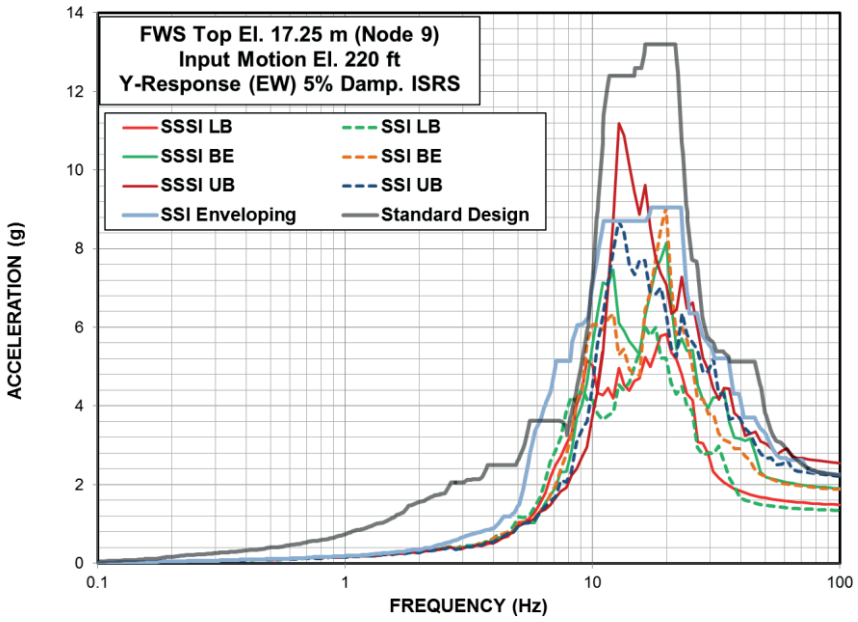

(b) Input Motion at El. 220 ft

Figure 6.3-2 Comparison of ISRS for Response of FWS Roof in EW (Y) Direction

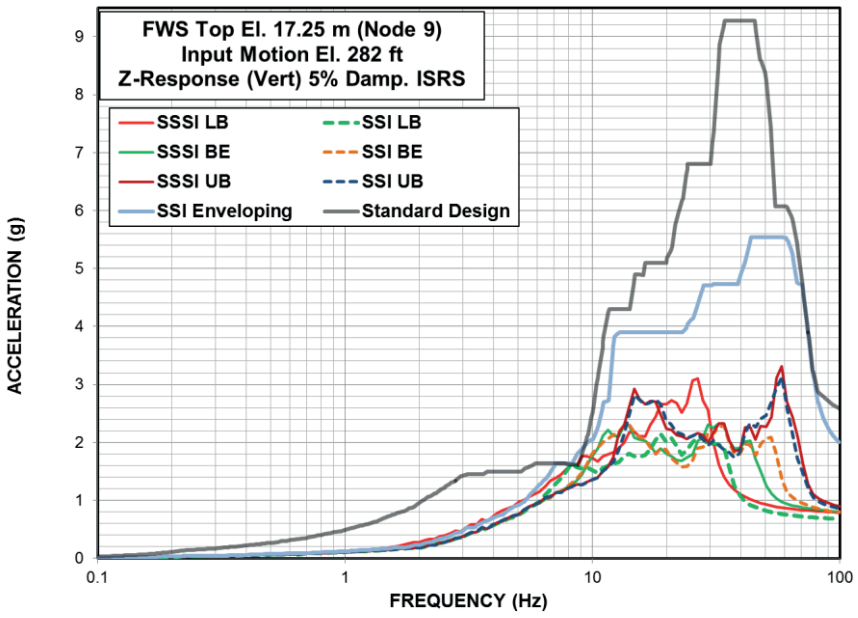

(a) Input Motion at El. 282 ft

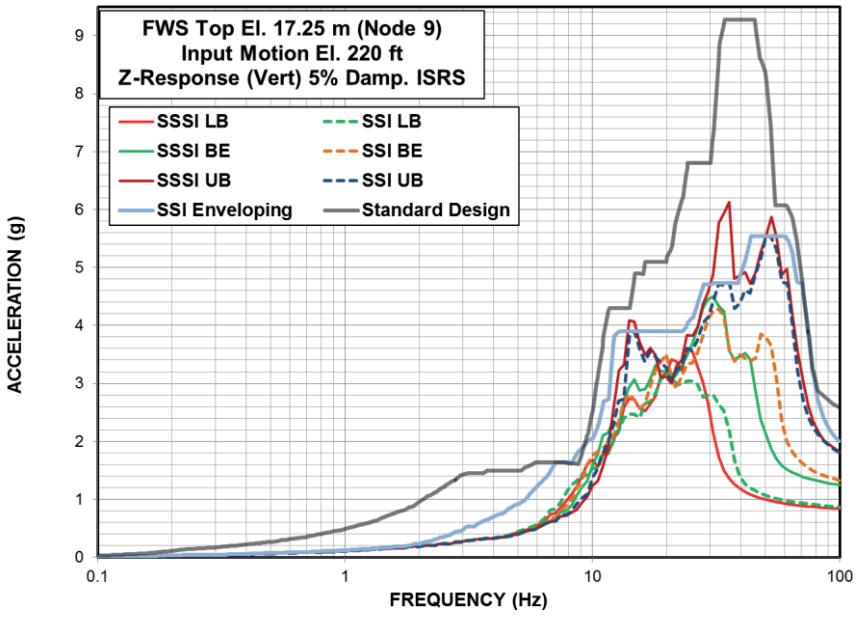

(b) Input Motion at El. 220 ft

Figure 6.3-3 Comparison of ISRS for Response of FWS Roof in Vertical (Z) Direction

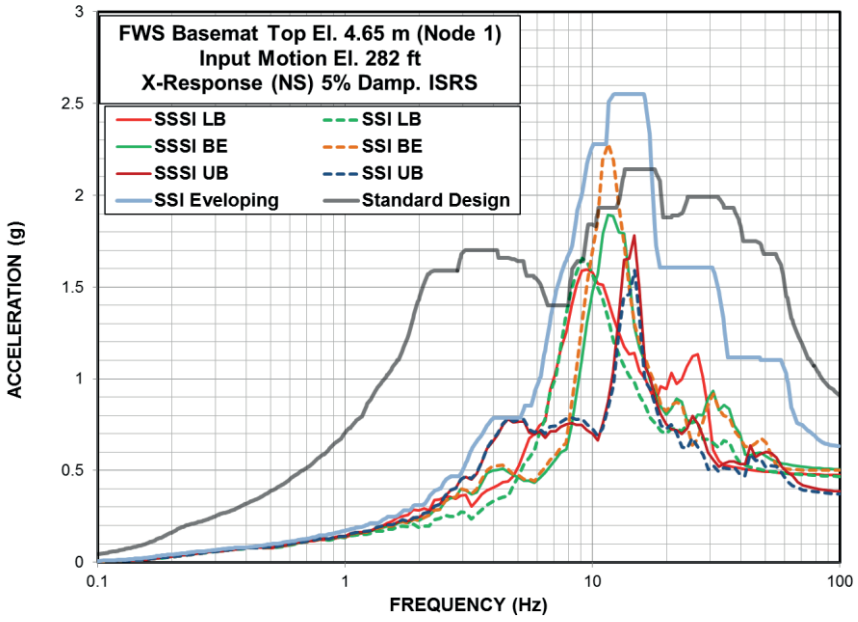

(a) Input Motion at El. 282 ft

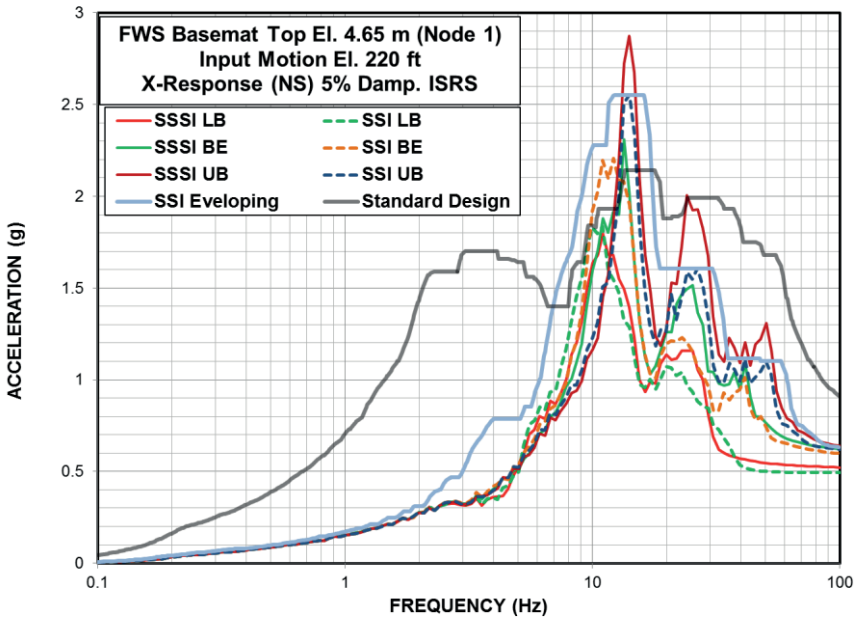

(b) Input Motion at El. 220 ft

Figure 6.3-4 Comparison of ISRS for Response of FWS Basemat in NS (X) Direction

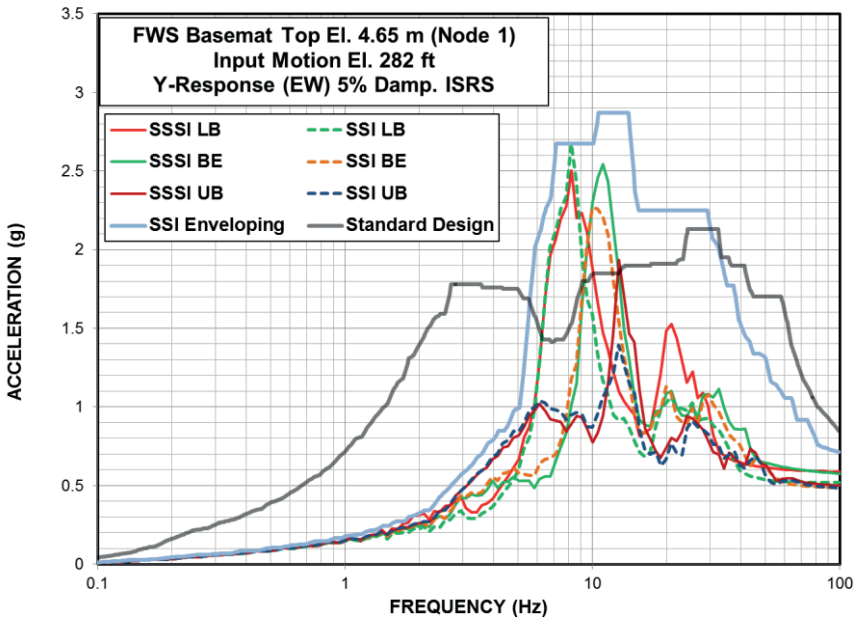

(a) Input Motion at El. 282 ft

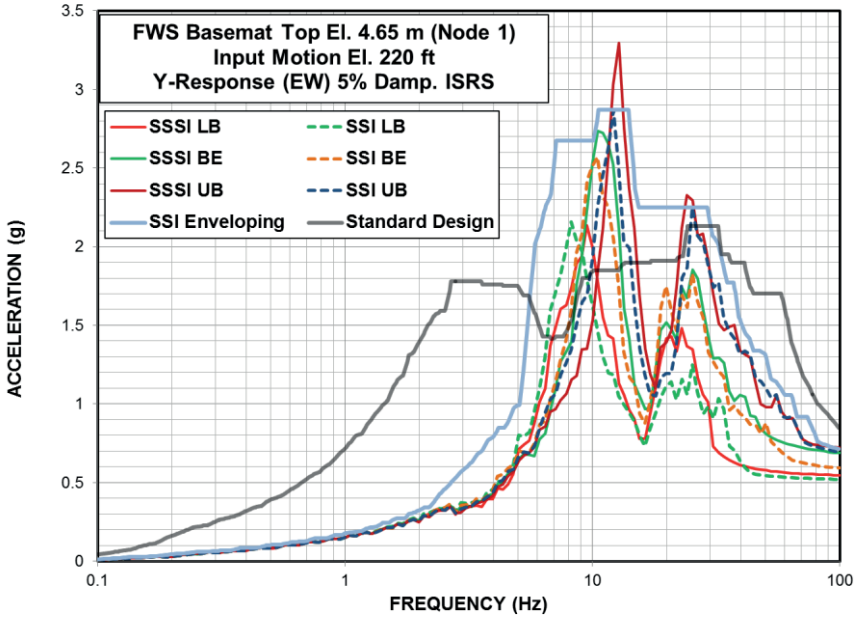

(b) Input Motion at El. 220 ft

Figure 6.3-5 Comparison of ISRS for Response of FWS Basemat in EW (Y) Direction

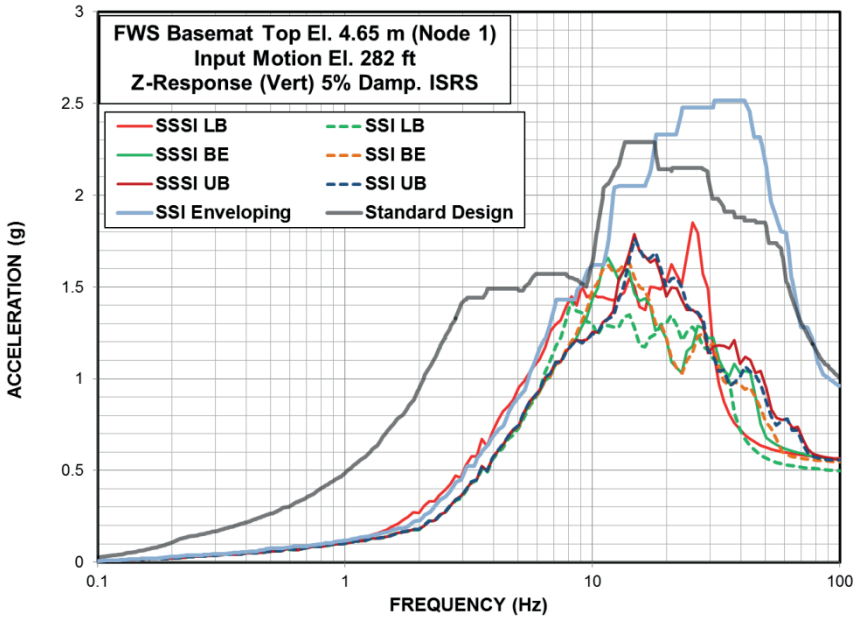

(a) Input Motion at El. 282 ft

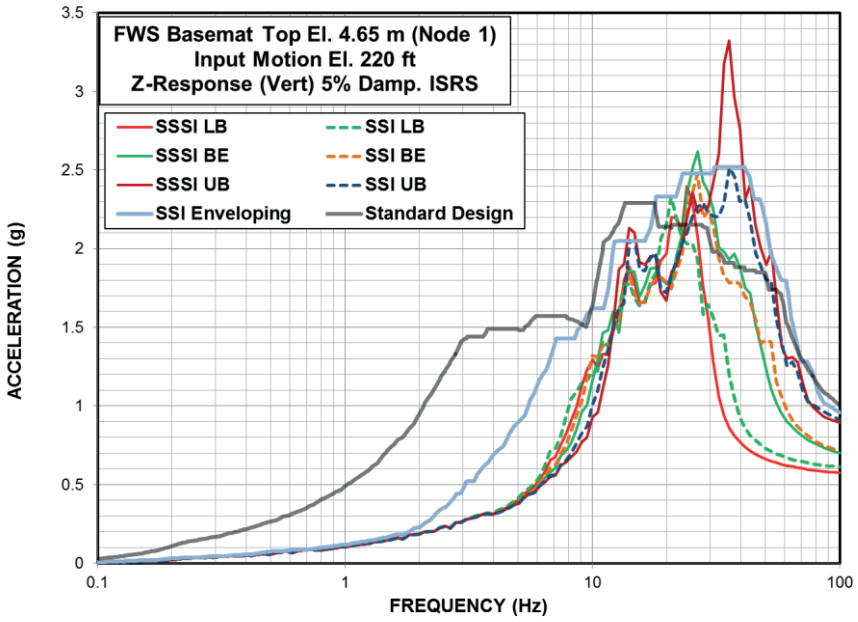

(b) Input Motion at El. 220 ft

Figure 6.3-6 Comparison of ISRS for Response of FWS Basemat in Vertical (Z) Direction

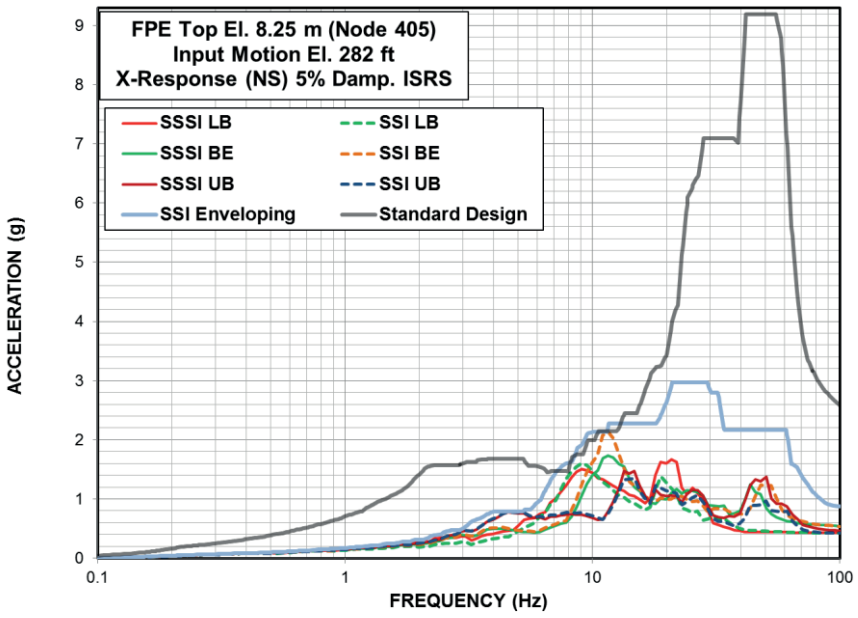

(a) Input Motion at El. 282 ft

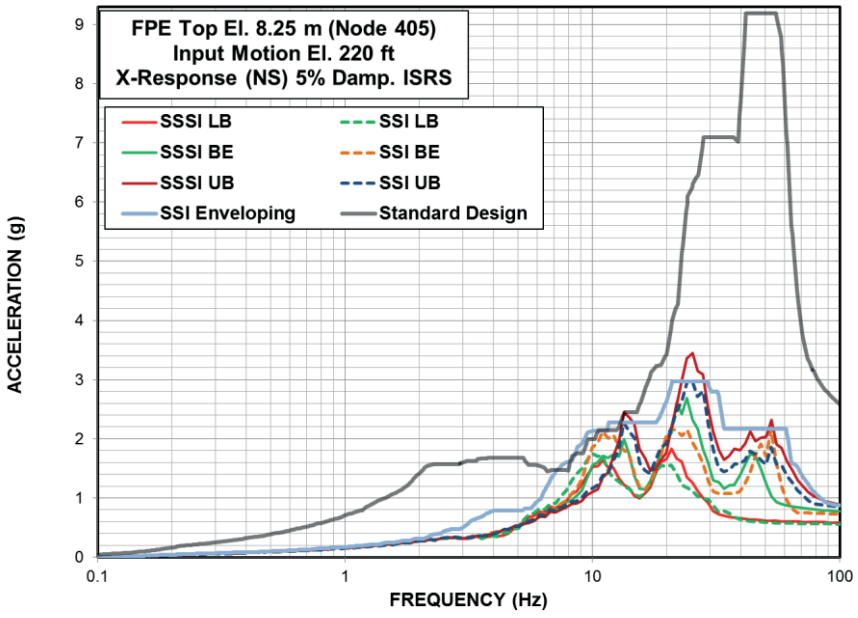

(b) Input Motion at El. 220 ft

Figure 6.3-7 Comparison of ISRS for Response of FPE Roof in NS (X) Direction

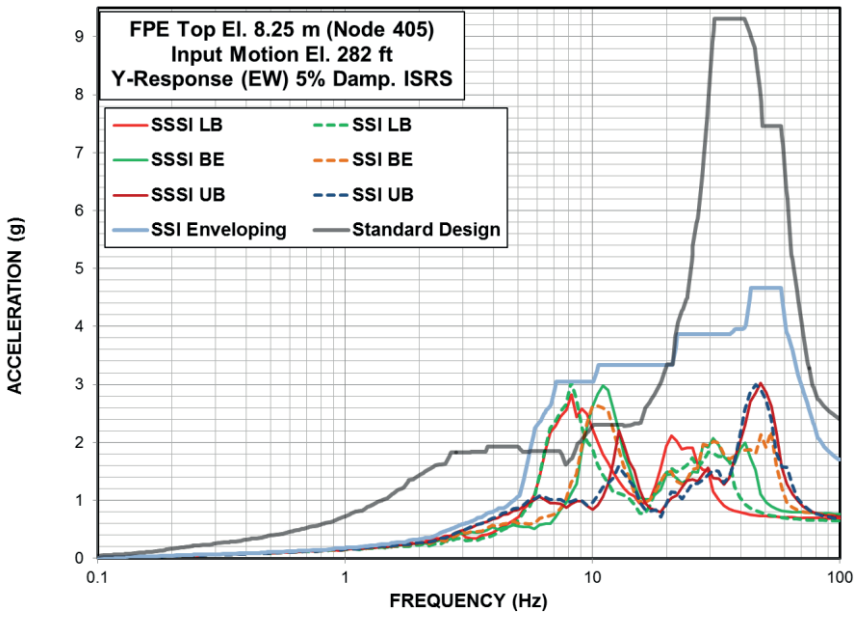

(a) Input Motion at El. 282 ft

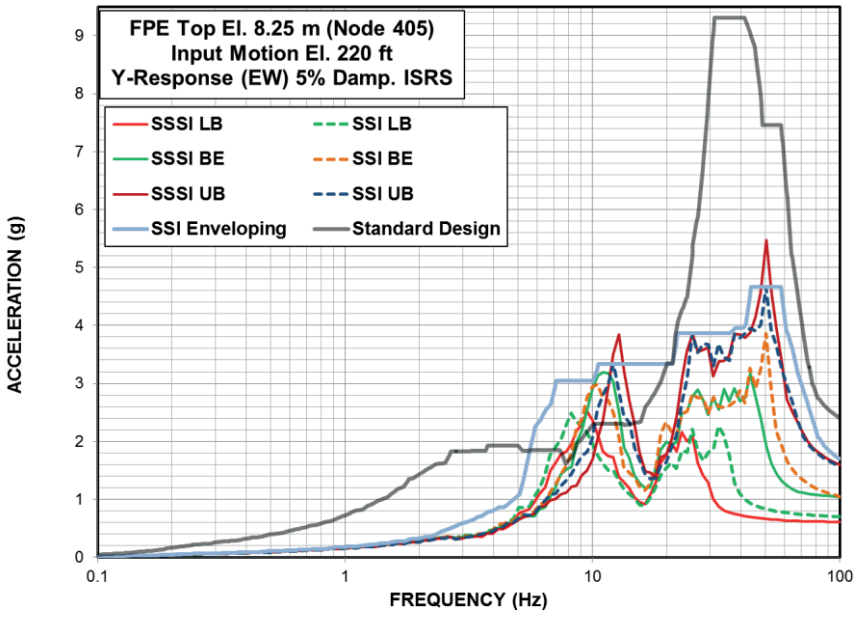

(b) Input Motion at El. 220 ft

Figure 6.3-8 Comparison of ISRS for Response of FPE Roof in EW (Y) Direction

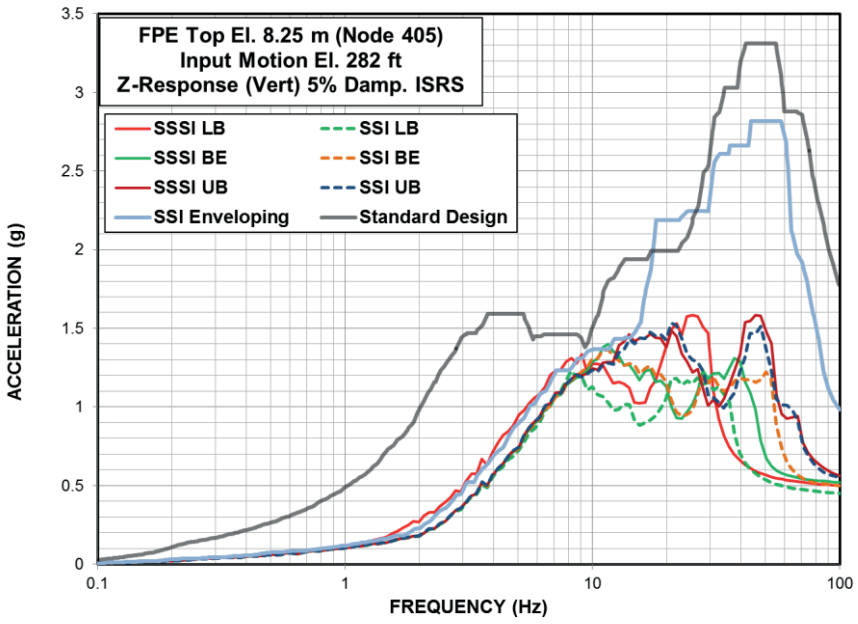

(a) Input Motion at El. 282 ft

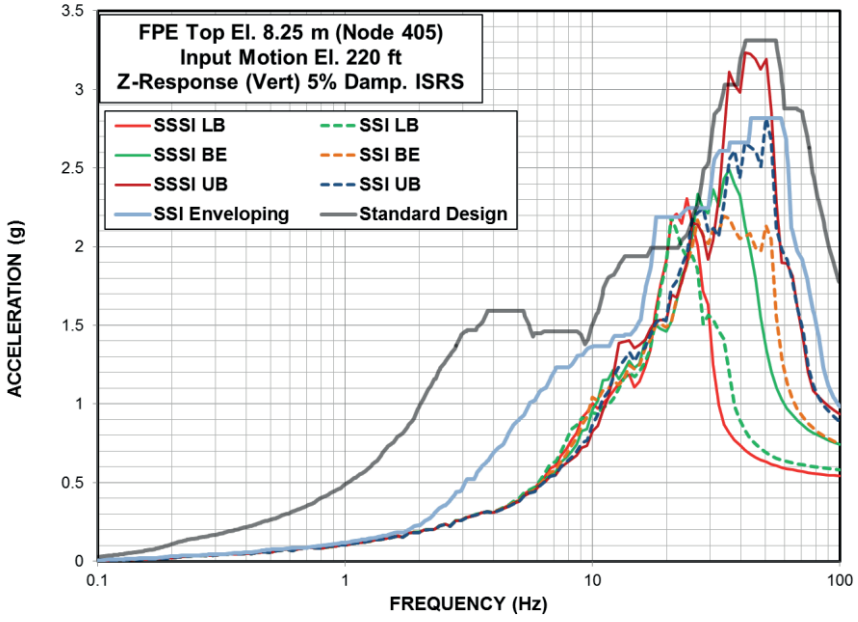

(b) Input Motion at El. 220 ft

Figure 6.3-9 Comparison of ISRS for Response of FPE Roof in Vertical (Z) Direction

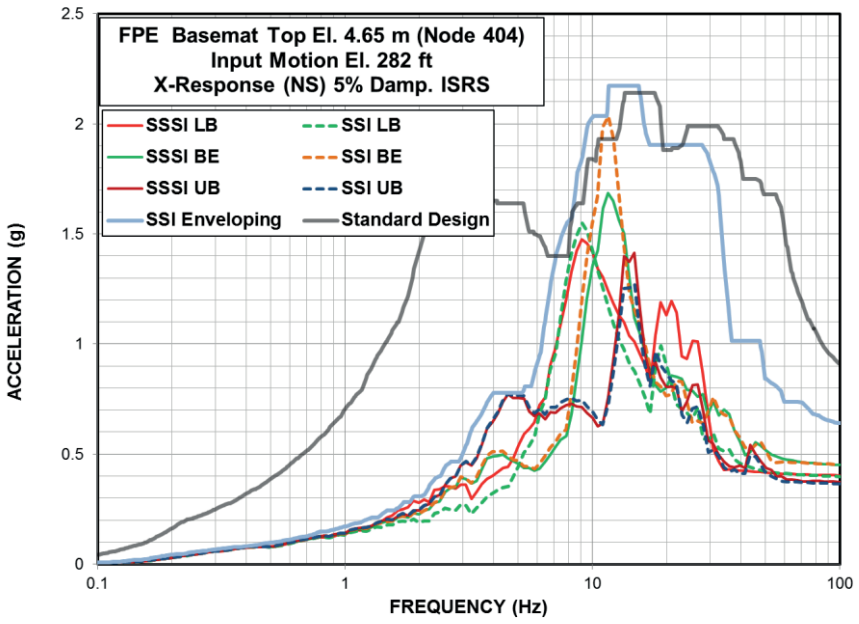

(a) Input Motion at El. 282 ft

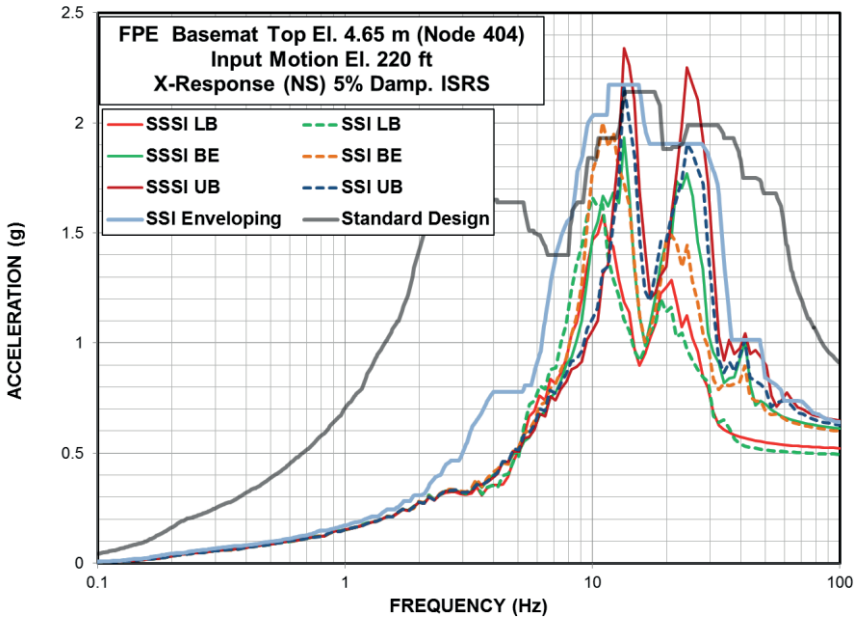

(b) Input Motion at El. 220 ft

Figure 6.3-10 Comparison of ISRS for Response of FPE Basemat in NS (X) Direction

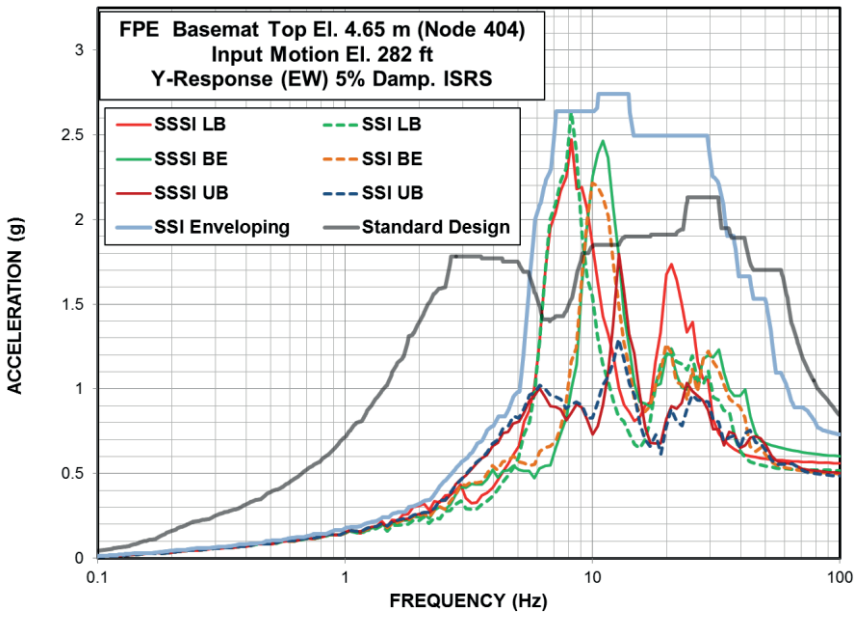

(a) Input Motion at El. 282 ft

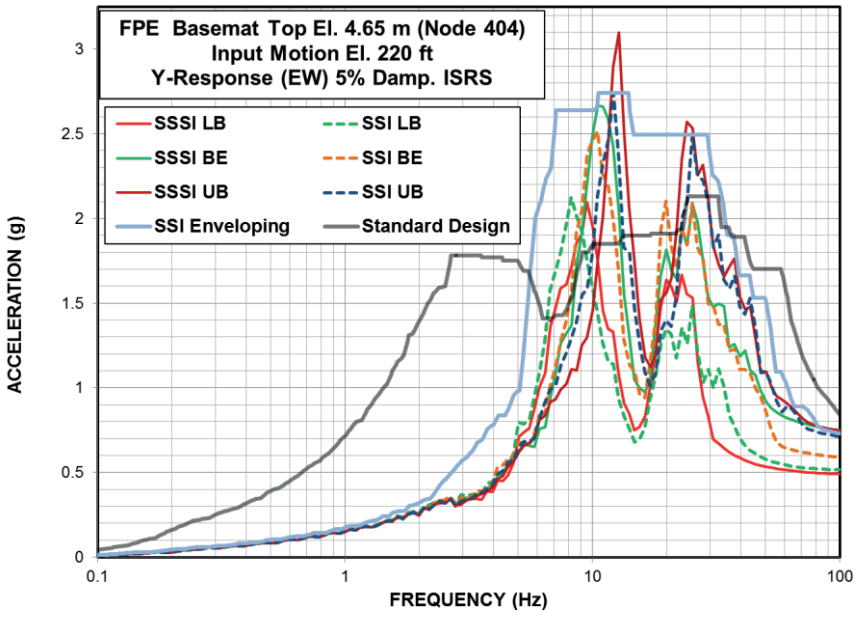

(b) Input Motion at El. 220 ft

Figure 6.3-11 Comparison of ISRS for Response of FPE Basemat in EW (Y) Direction

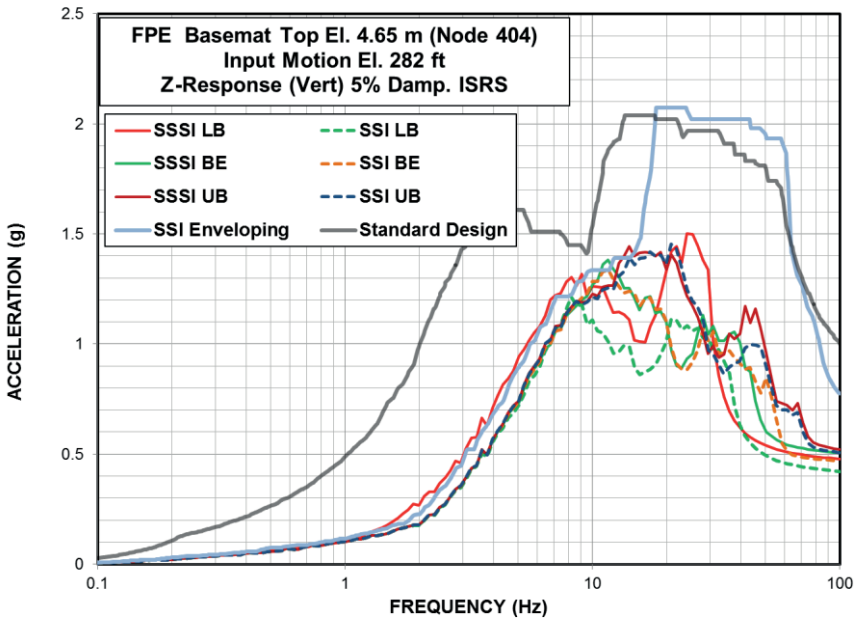

(a) Input Motion at El. 282 ft

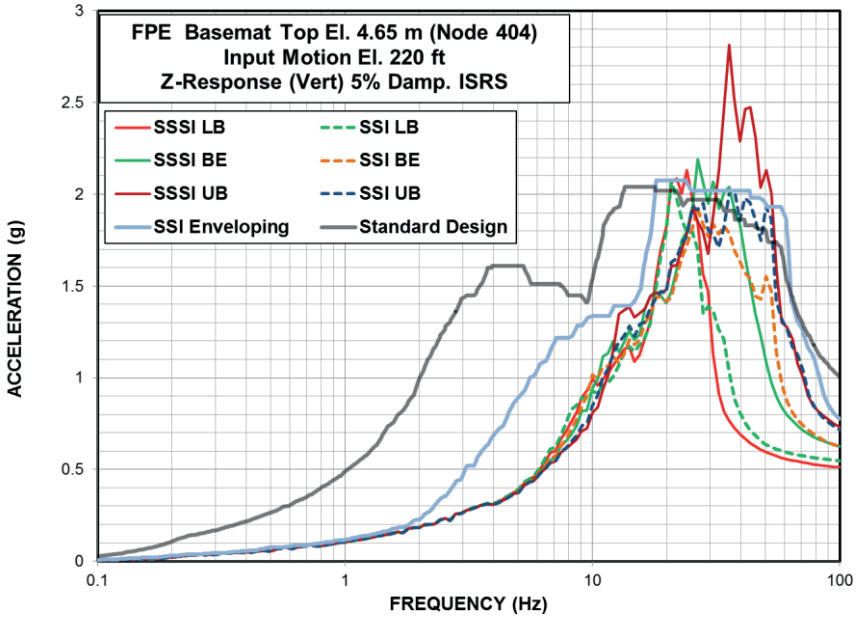

(b) Input Motion at El. 220 ft

Figure 6.3-12 Comparison of ISRS for Response of FPE Basemat in Vertical (Z) Direction

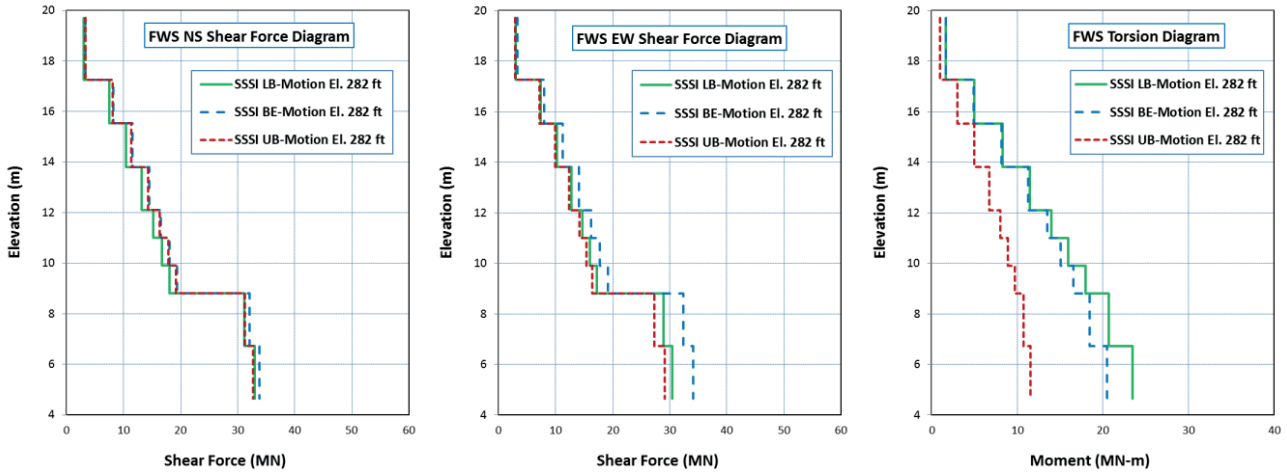

(a) Motion at El. 282 ft

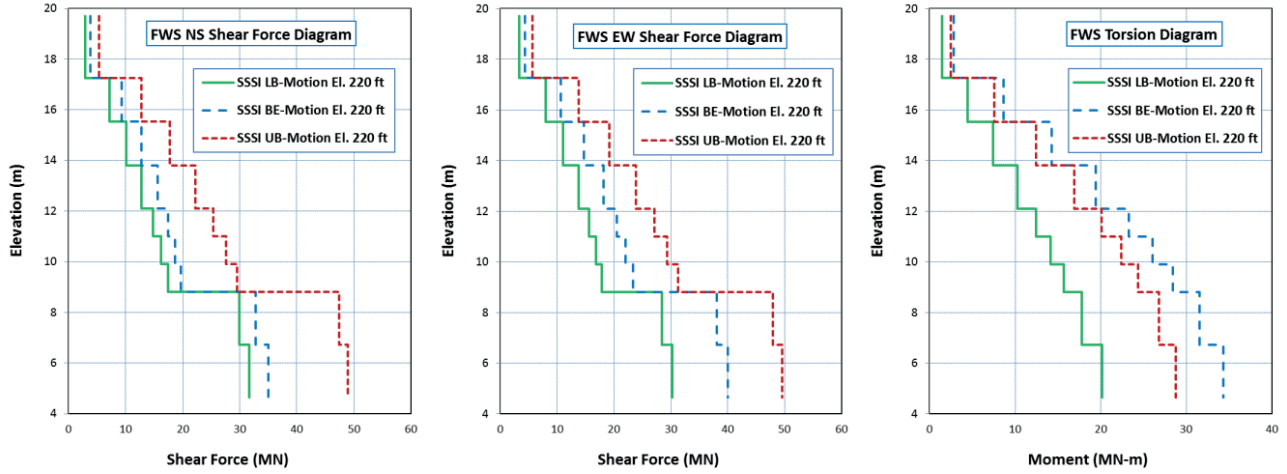

(b) Motion at El. 220 ft

Figure 6.4-1 FWS Horizontal Load Diagrams - SSSI Analysis of FWSC-CB Model with OBE Damping

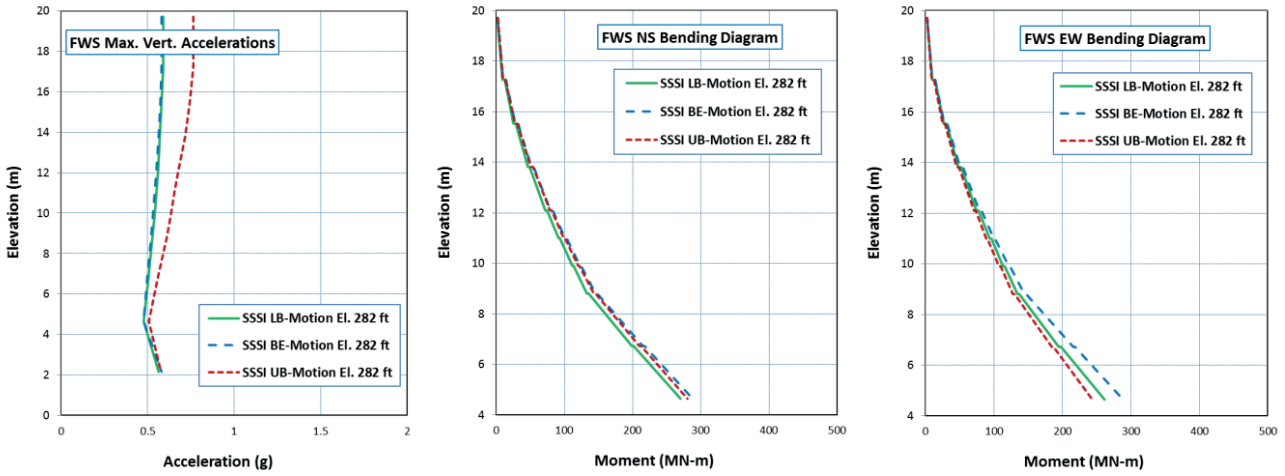

(a) Motion at El. 282 ft

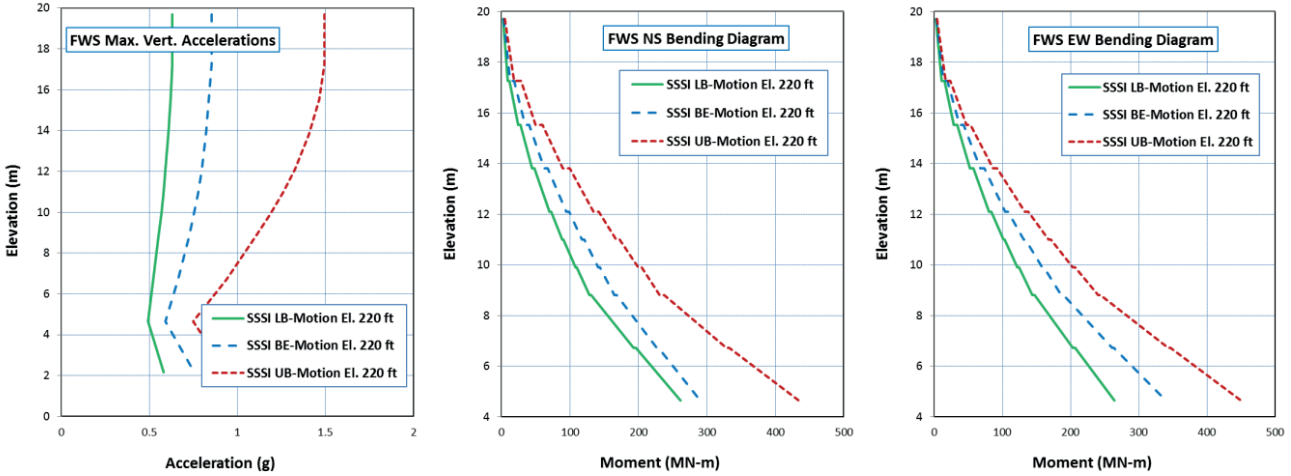

(b) Motion at El. 220 ft

Figure 6.4-2 FWS Vertical Load Diagrams - SSSI Analysis of FWSC-CB Model with OBE Damping

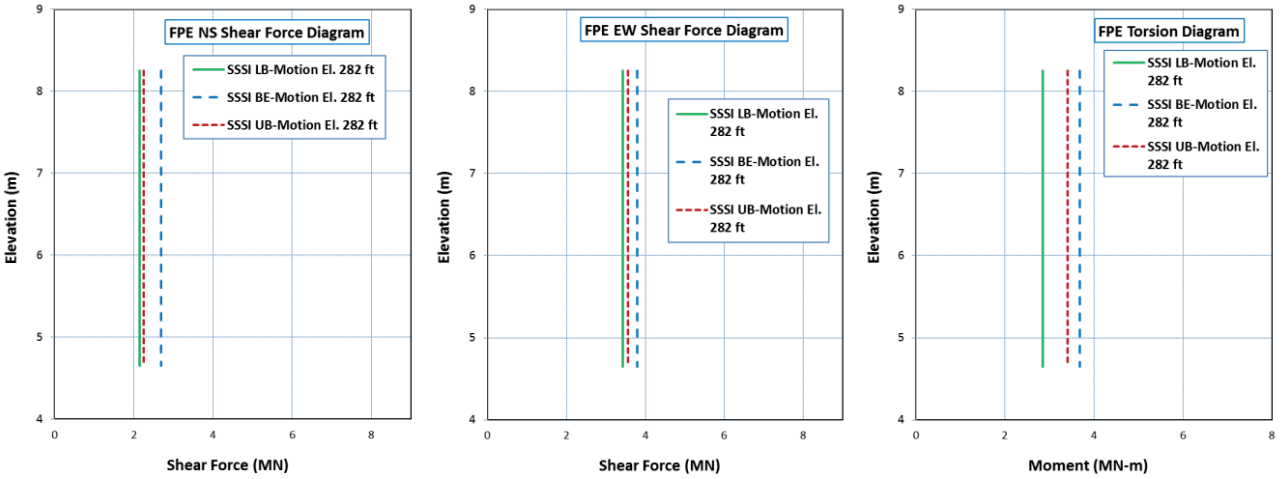

(a) Motion at El. 282 ft

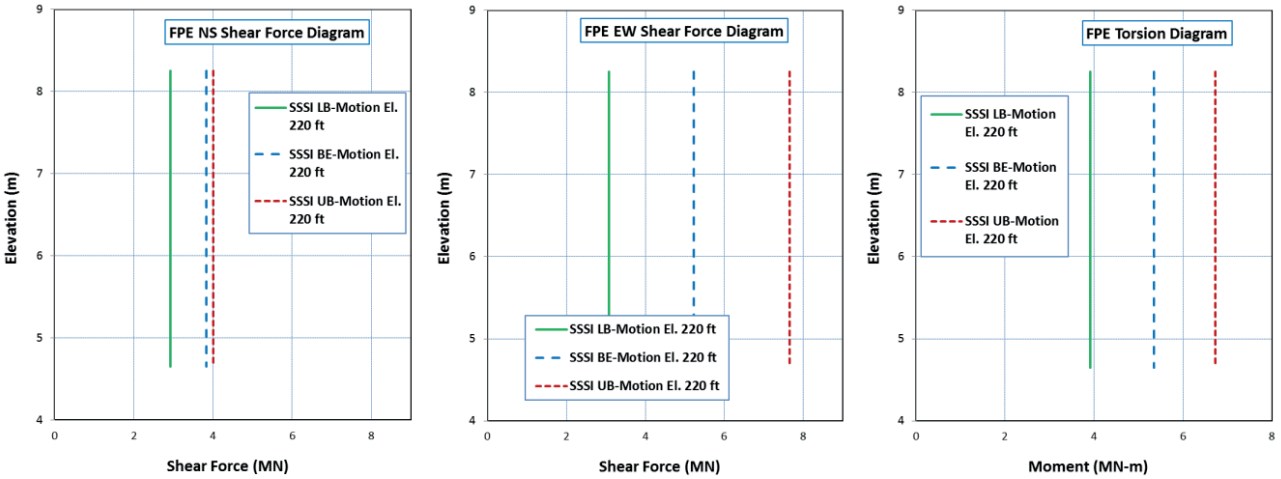

(b) Motion at El. 220 ft

Figure 6.4-3 FPE Horizontal Load Diagrams - SSSI Analysis of FWSC-CB Model with OBE Damping

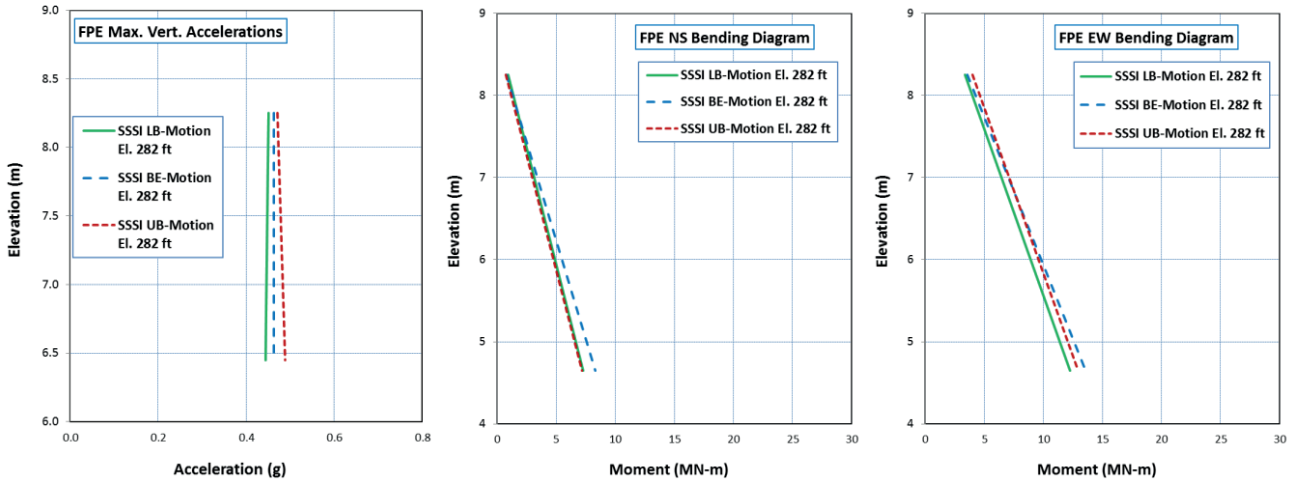

(a) Motion at El. 282 ft

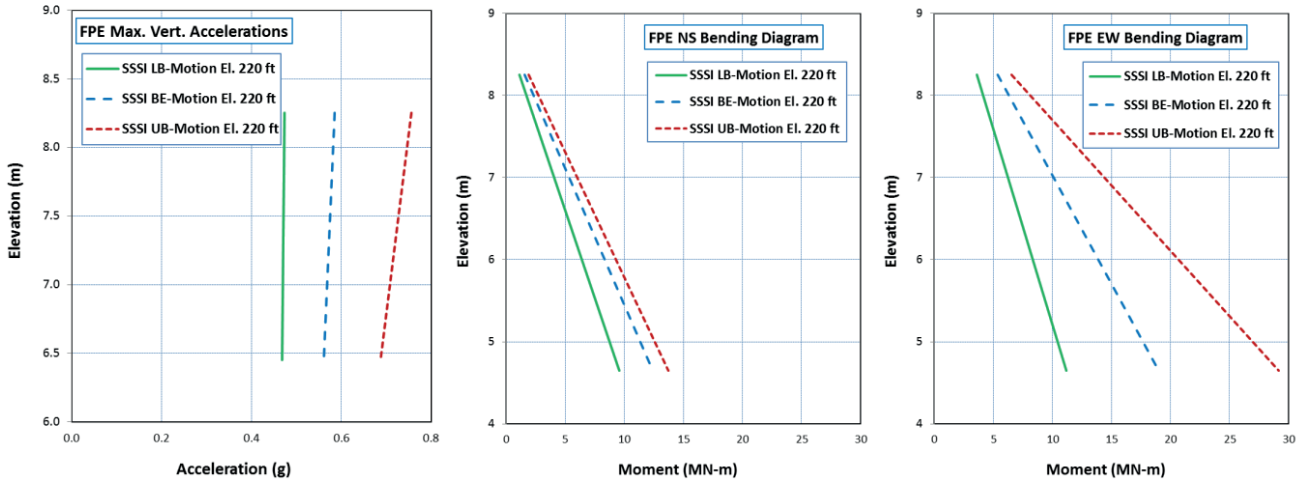

(b) Motion at El. 220 ft

Figure 6.4-4 FPE Vertical Load Diagrams - SSSI Analysis of FWSC-CB Model with OBE Damping

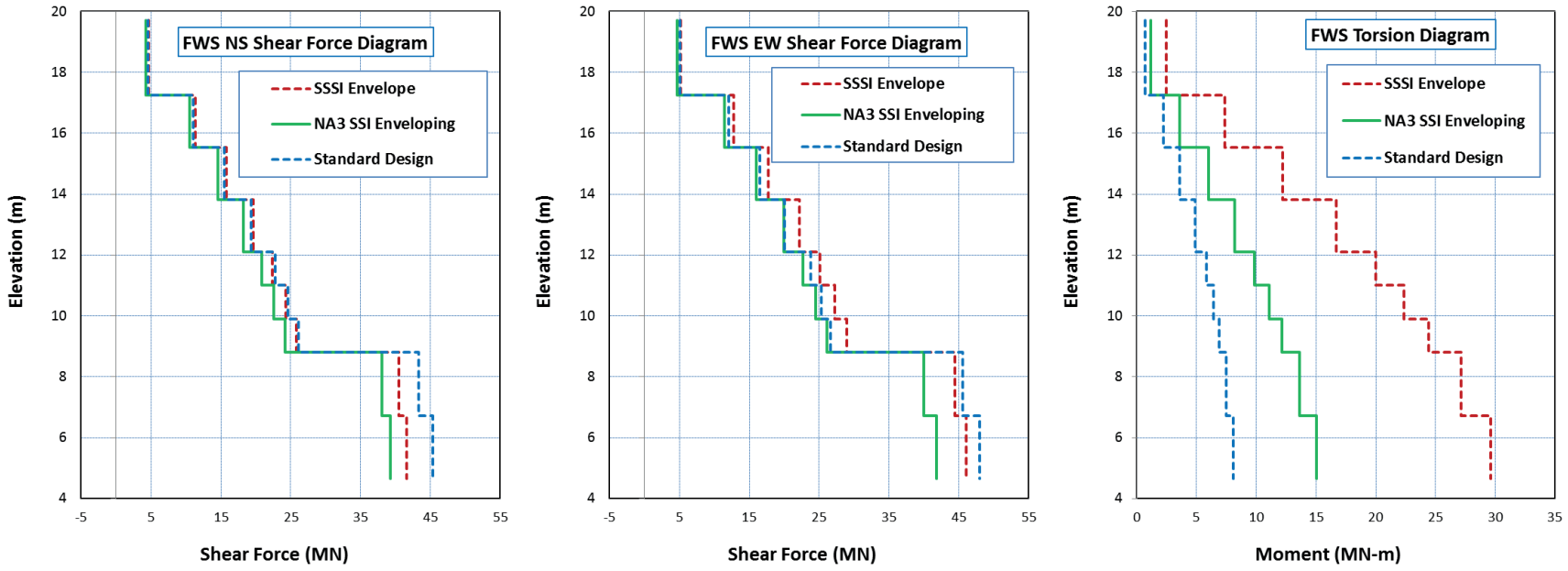

Figure 6.4-5 Comparison of Horizontal Seismic Load Demands on FWS Structure

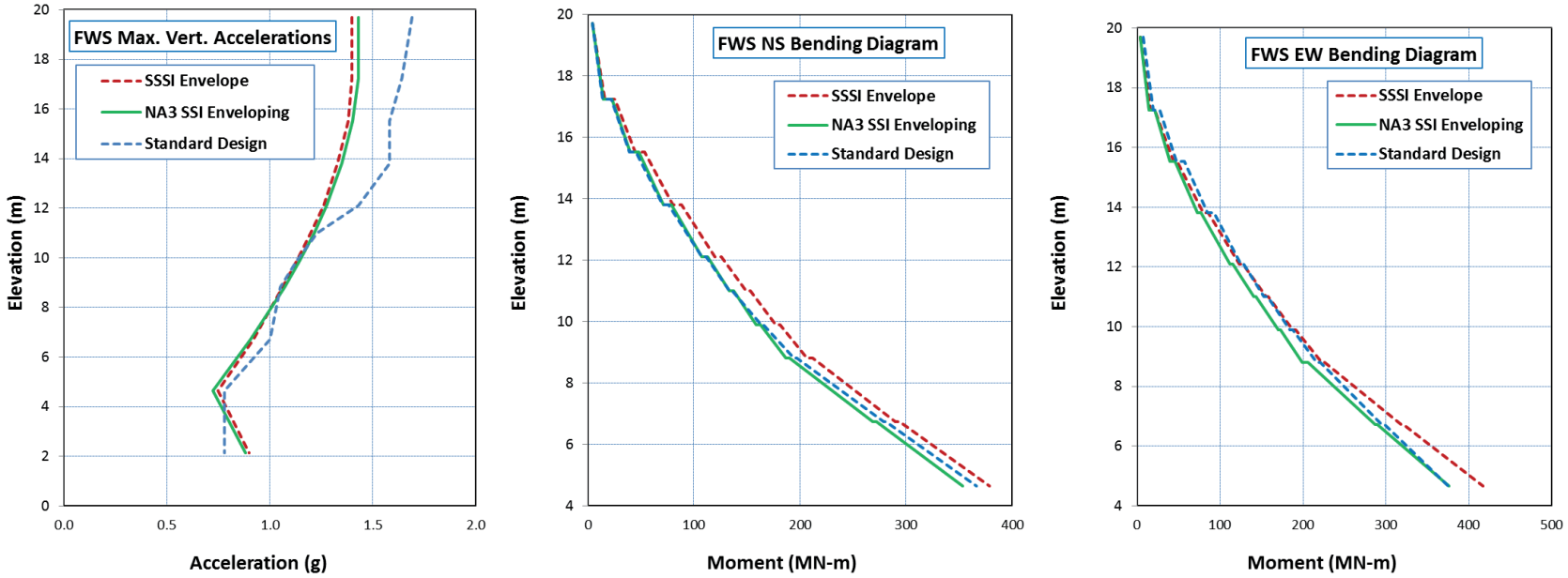

Figure 6.4-6 Comparison of Vertical Seismic Load Demands on FWS Structure

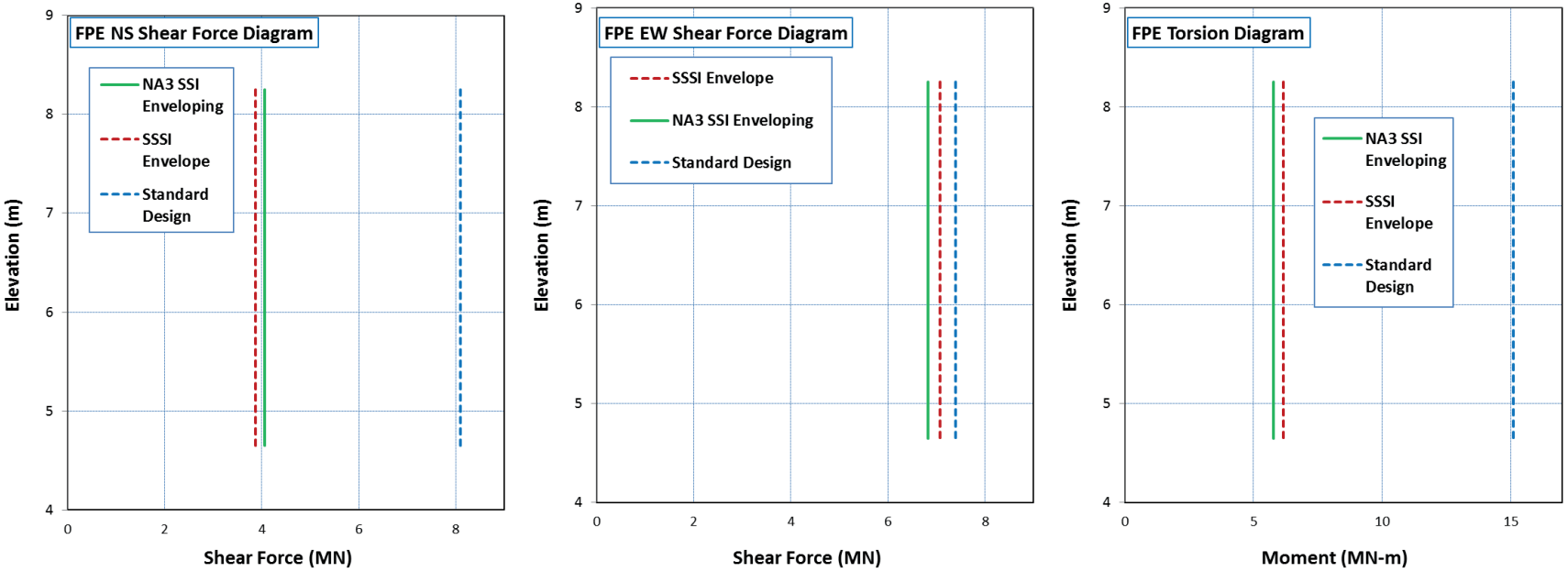

Figure 6.4-7 Comparison of Horizontal Seismic Load Demands on FPE Structure

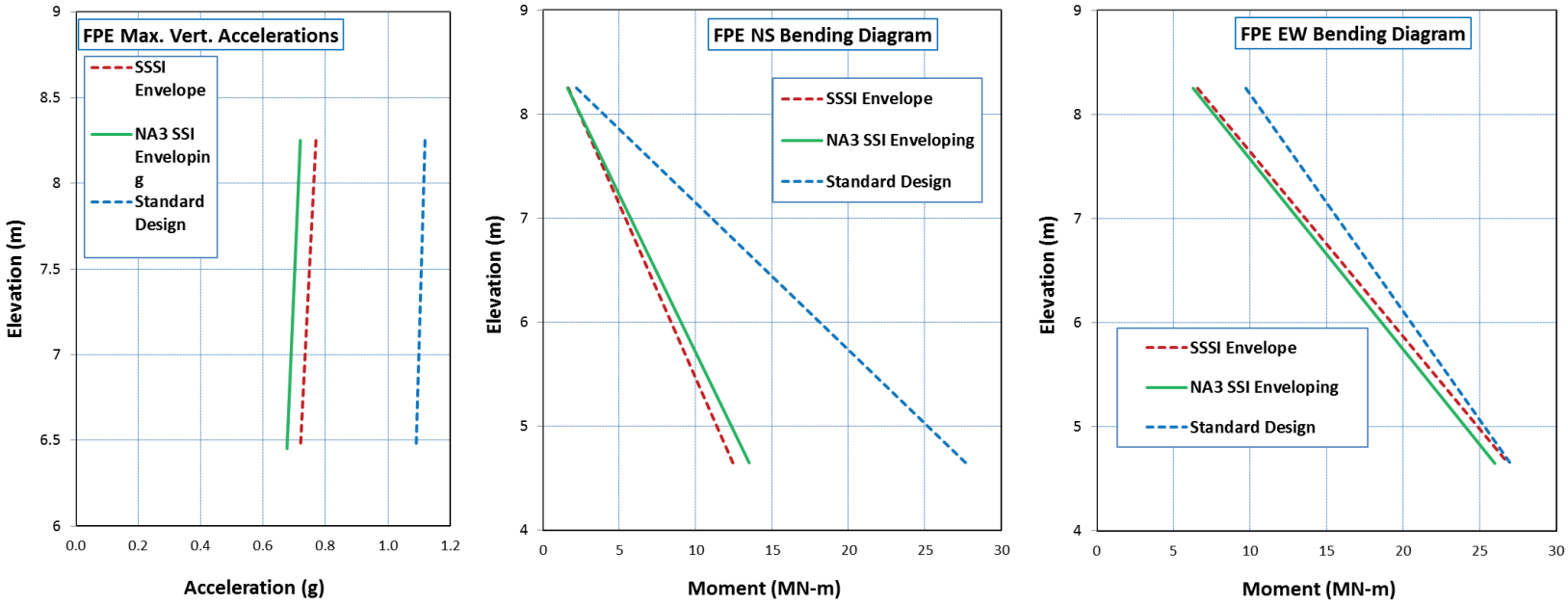

Figure 6.4-8 Comparison of Vertical Seismic Load Demands on FPE Structure

APPENDIX A
RESULTS FOR MAXIMUM SEISMIC FORCES AND ACCELERATIONS

TABLE OF CONTENTS

LIST OF TABLES

A.1 MAXIMUM STRUCTURAL FORCE AND MOMENT DEMANDS (OBE DAMPING)

A.2 MAXIMUM STRUCTURAL FORCE AND MOMENT DEMANDS (SSE DAMPING)

A.3 MAXIMUM ACCELERATIONS (OBE DAMPING)

A.4 MAXIMUM ACCELERATIONS (SSE DAMPING)

Table A.1-1 FWS Maximum Structural Force and Moment Demands – Input Motion at 282 ft. (Model with OBE Damping)

Elev. (m)	Element No.	Node No.	LB Full Column Profile					BE Full Column Profile					UB Full Column Profile				
			Shear (MN)		Bending (MN-m)		Torsion (MN-m)	Shear (MN)		Bending (MN-m)		Torsion (MN-m)	Shear (MN)		Bending (MN-m)		Torsion (MN-m)
			NS	EW	NS	EW		NS	EW	NS	EW		NS	EW	NS	EW	
19.70	9	10	3.0	3.0	2	2	1.6	3.3	3.3	2	2	1.6	3.3	2.9	2	2	1.0
		9			9	9				10	10				10	9	
17.25	8	9	7.5	7.4	12	14	5.0	8.2	8.0	14	14	4.9	8.1	7.1	13	13	3.0
		8			25	26				28	27				27	25	
15.53	7	8	10.4	10.2	28	31	8.3	11.5	11.2	32	32	8.1	11.3	9.9	31	29	5.0
		7			46	48				51	51				50	46	
13.81	6	7	13.2	12.8	49	53	11.5	14.4	14.1	55	54	11.3	14.2	12.4	54	49	6.7
		6			72	74				80	79				78	71	
12.10	5	6	15.2	14.7	74	78	14.0	16.6	16.2	82	82	13.5	16.3	14.2	81	73	8.0
		5			91	94				101	100				99	89	
11.00	4	5	16.7	16.0	93	96	16.0	18.1	17.8	103	102	15.1	17.8	15.4	101	91	8.9
		4			111	113				123	121				120	107	
9.90	3	4	18.1	17.3	113	116	18.0	19.4	19.2	124	124	16.5	19.1	16.5	122	110	9.7
		3			133	134				146	144				143	127	
8.81	2	3	31.1	28.9	135	137	20.7	32.1	32.4	148	147	18.5	31.2	27.3	145	130	10.8
		2			199	195				215	216				210	185	
6.73	1	2	33.0	30.5	202	198	23.5	33.8	34.1	218	218	20.5	32.7	29.1	213	187	11.6
4.65		8002			270	262				288	289				281	244	

Table A.1-2 FPE Maximum Structural Force and Moment Demands – Input Motion at 282 ft. (Model with OBE Damping)

Elev. (m)	Element No.	Node No.	LB Full Column Profile					BE Full Column Profile					UB Full Column Profile				
			Shear (MN)		Bending (MN-m)		Torsion (MN-m)	Shear (MN)		Bending (MN-m)		Torsion (MN-m)	Shear (MN)		Bending (MN-m)		Torsion (MN-m)
			NS	EW	NS	EW		NS	EW	NS	EW		NS	EW	NS	EW	
8.25	405	402	2.1	3.4	1	3	2.9	2.7	3.8	1	4	3.7	2.3	3.6	1	4	3.4
4.65	404	401			7	12				8	14				7	13	

Table A.1-3 FWS Maximum Structural Force and Moment Demands – Input Motion at 220 ft. (Model with OBE Damping)

Elev. (m)	Element No.	Node No.	LB Full Column Profile					BE Full Column Profile					UB Full Column Profile				
			Shear (MN)		Bending (MN-m)		Torsion (MN-m)	Shear (MN)		Bending (MN-m)		Torsion (MN-m)	Shear (MN)		Bending (MN-m)		Torsion (MN-m)
			NS	EW	NS	EW		NS	EW	NS	EW		NS	EW	NS	EW	
19.70	9	10	2.9	3.3	2	2	1.5	3.8	4.3	3	3	2.8	5.3	5.6	5	4	2.5
		9			9	10				12	13				18	17	
17.25	8	9	7.2	8.0	12	15	4.5	9.3	10.6	18	19	8.6	12.7	13.8	28	23	7.5
		8			24	29				34	37				50	47	
15.53	7	8	10.1	11.1	27	33	7.4	12.7	14.7	40	43	14.2	17.8	19.2	60	53	12.4
		7			45	52				62	68				90	86	
13.81	6	7	12.8	13.7	48	57	10.3	15.6	18.1	68	73	19.4	22.2	23.9	99	92	16.9
		6			70	80				94	104				135	133	
12.10	5	6	14.8	15.6	72	84	12.5	17.5	20.5	99	108	23.3	25.4	27.1	142	138	20.1
		5			88	101				118	131				168	168	
11.00	4	5	16.2	16.8	90	104	14.1	18.7	22.0	121	134	26.0	27.6	29.4	173	171	22.4
		4			108	122				141	158				200	203	
9.90	3	4	17.5	17.9	110	124	15.7	19.7	23.3	144	161	28.5	29.5	31.2	205	206	24.4
		3			129	144				165	186				232	240	
8.81	2	3	30.0	28.4	131	147	17.8	32.8	38.0	169	190	31.6	47.4	47.9	238	244	26.8
		2			193	203				227	261				329	343	
6.73	1	2	31.7	30.2	196	206	20.2	35.0	40.0	230	264	34.4	48.9	49.6	333	347	28.8
4.65		8002			262	264				290	340				434	450	

Table A.1-4 FPE Maximum Structural Force and Moment Demands – Input Motion at 220 ft. (Model with OBE Damping)

Elev. (m)	Element No.	Node No.	LB Full Column Profile					BE Full Column Profile					UB Full Column Profile				
			Shear (MN)		Bending (MN-m)		Torsion (MN-m)	Shear (MN)		Bending (MN-m)		Torsion (MN-m)	Shear (MN)		Bending (MN-m)		Torsion (MN-m)
			NS	EW	NS	EW		NS	EW	NS	EW		NS	EW	NS	EW	
8.25	405	402	2.9	3.1	1	4	3.9	3.8	5.2	2	5	5.3	4.0	7.7	2	7	6.7
4.65	404	401			10	11				12	19				14	29	

Table A.2-1 FWS Maximum Structural Force and Moment Demands – Input Motion at 220 ft. (Model with SSE Damping)

Elev. (m)	Element No.	Node No.	LB Full Column Profile					BE Full Column Profile					UB Full Column Profile				
			Shear (MN)		Bending (MN-m)		Torsion (MN-m)	Shear (MN)		Bending (MN-m)		Torsion (MN-m)	Shear (MN)		Bending (MN-m)		Torsion (MN-m)
			NS	EW	NS	EW		NS	EW	NS	EW		NS	EW	NS	EW	
19.70	9	10	2.8	3.1	2	2	1.3	3.5	4.1	3	3	2.4	4.7	5.2	5	3	2.1
		9			8	10				11	12				16	15	
17.25	8	9	6.8	7.6	11	14	4.0	8.5	9.9	16	18	7.4	11.4	12.8	25	21	6.3
		8			23	27				31	35				44	43	
15.53	7	8	9.6	10.5	26	32	6.7	11.6	13.8	36	40	12.2	15.8	17.8	54	48	10.5
		7			42	50				56	63				80	80	
13.81	6	7	12.1	13.0	45	54	9.3	14.4	17.0	60	68	16.7	19.7	22.1	88	85	14.2
		6			66	76				85	97				120	123	
12.10	5	6	14.0	14.8	68	79	11.2	16.2	19.3	89	101	20.0	22.4	25.1	126	127	16.9
		5			84	96				106	123				149	155	
11.00	4	5	15.4	15.9	85	98	12.7	17.4	20.8	109	125	22.3	24.3	27.2	153	158	18.9
		4			102	115				128	148				178	188	
9.90	3	4	16.6	16.9	104	118	14.1	18.5	22.0	130	151	24.4	25.8	29.0	182	191	20.5
		3			122	136				150	175				207	222	
8.81	2	3	28.6	27.5	124	139	16.1	30.8	36.3	153	178	27.1	40.5	44.5	212	226	22.6
		2			183	192				210	246				290	318	
6.73	1	2	30.2	29.2	186	196	18.3	32.2	38.2	213	248	29.6	41.6	46.1	294	321	24.3
4.65		8002			249	251				272	323				379	417	

Table A.2-2 FPE Maximum Structural Force and Moment Demands – Input Motion at 220 ft. (Model with SSE Damping)

Elev. (m)	Element No.	Node No.	LB Full Column Profile					BE Full Column Profile					UB Full Column Profile				
			Shear (MN)		Bending (MN-m)		Torsion (MN-m)	Shear (MN)		Bending (MN-m)		Torsion (MN-m)	Shear (MN)		Bending (MN-m)		Torsion (MN-m)
			NS	EW	NS	EW		NS	EW	NS	EW		NS	EW	NS	EW	
8.25	405	402	2.9	3.0	1	4	3.9	3.8	5.4	1	5	5.3	3.9	7.1	2	7	6.2
4.65	404	401			9	11				12	18				12	27	

Table A.3-1 FWS Maximum Accelerations – Input Motion at 282 ft. (Model with OBE Damping)

Elev. (m)	Node No.	LB Full Column Profile			BE Full Column Profile			UB Full Column Profile		
		NS (g)	EW (g)	Vert. (g)	NS (g)	EW (g)	Vert. (g)	NS (g)	EW (g)	Vert. (g)
19.70	10	1.40	1.42	0.59	1.56	1.53	0.58	1.54	1.38	0.76
17.25	9	1.31	1.30	0.59	1.45	1.41	0.58	1.44	1.27	0.76
15.53	8	1.22	1.19	0.58	1.33	1.31	0.57	1.32	1.15	0.75
13.81	7	1.12	1.08	0.57	1.20	1.19	0.56	1.19	1.02	0.72
12.10	6	1.01	0.96	0.56	1.05	1.06	0.55	1.04	0.88	0.68
11.00	5	0.94	0.88	0.55	0.96	0.98	0.54	0.94	0.83	0.65
9.90	4	0.87	0.81	0.54	0.87	0.91	0.53	0.84	0.78	0.63
8.81	3	0.80	0.77	0.53	0.77	0.84	0.52	0.74	0.72	0.61
6.73	2	0.62	0.67	0.50	0.60	0.63	0.50	0.50	0.61	0.56
4.65	8002	0.45	0.57	0.48	0.50	0.54	0.48	0.38	0.49	0.51
2.15	8001	0.43	0.53	0.56	0.48	0.46	0.58	0.38	0.44	0.58

Table A.3-2 FPE Maximum Accelerations – Input Motion at 282 ft. (Model with OBE Damping)

Elev. (m)	Node No.	LB Full Column Profile			BE Full Column Profile			UB Full Column Profile		
		NS (g)	EW (g)	Vert. (g)	NS (g)	EW (g)	Vert. (g)	NS (g)	EW (g)	Vert. (g)
8.25	405	0.42	0.68	0.45	0.53	0.76	0.46	0.45	0.72	0.47
6.45	402	0.40	0.62	0.44	0.49	0.69	0.46	0.41	0.61	0.49

Table A.3-3 Vertical SDOF Maximum Accelerations – Input Motion at 282 ft. (Model with OBE Damping)

Elev. (m)	Node No.	LB Full Column Profile (g)	BE Full Column Profile (g)	UB Full Column Profile (g)
19.70	11	0.97	1.59	1.83

Table A.3-4 Horizontal FWS Tank Hydrodynamic SDOF Maximum Accelerations – Input Motion at 282 ft. (Model with OBE Damping)

Elev. (m)	Node No.	Dir.	LB Full Column Profile (g)	BE Full Column Profile (g)	UB Full Column Profile (g)
12.10	60	X	0.10	0.10	0.10
		Y	0.07	0.07	0.07
8.81	30	X	0.80	0.77	0.74
		Y	0.77	0.84	0.72

Table A.3-5 FWS Maximum Accelerations – Input Motion at 220 ft. (Model with OBE Damping)

Elev. (m)	Node No.	LB Full Column Profile			BE Full Column Profile			UB Full Column Profile		
		NS (g)	EW (g)	Vert. (g)	NS (g)	EW (g)	Vert. (g)	NS (g)	EW (g)	Vert. (g)
19.70	10	1.37	1.54	0.63	1.80	2.00	0.86	2.49	2.62	1.49
17.25	9	1.27	1.40	0.63	1.62	1.84	0.85	2.26	2.43	1.50
15.53	8	1.18	1.26	0.62	1.41	1.64	0.84	2.05	2.20	1.46
13.81	7	1.09	1.09	0.61	1.20	1.39	0.82	1.82	1.92	1.41
12.10	6	0.98	0.92	0.59	1.06	1.23	0.80	1.58	1.62	1.33
11.00	5	0.91	0.87	0.58	0.97	1.13	0.78	1.42	1.42	1.26
9.90	4	0.83	0.80	0.57	0.89	1.03	0.75	1.25	1.22	1.19
8.81	3	0.76	0.74	0.55	0.86	0.93	0.72	1.08	1.07	1.10
6.73	2	0.57	0.62	0.52	0.66	0.70	0.66	0.78	0.85	0.94
4.65	8002	0.51	0.51	0.49	0.61	0.61	0.59	0.64	0.70	0.75
2.15	8001	0.52	0.49	0.58	0.63	0.53	0.76	0.68	0.62	0.94

Table A.3-6 FPE Maximum Accelerations – Input Motion at 220 ft. (Model with OBE Damping)

Elev. (m)	Node No.	LB Full Column Profile			BE Full Column Profile			UB Full Column Profile		
		NS (g)	EW (g)	Vert. (g)	NS (g)	EW (g)	Vert. (g)	NS (g)	EW (g)	Vert. (g)
8.25	405	0.58	0.61	0.47	0.76	1.04	0.59	0.82	1.59	0.76
6.45	402	0.55	0.55	0.47	0.69	0.90	0.56	0.73	1.18	0.69

Table A.3-7 Vertical SDOF Maximum Accelerations – Input Motion at 220 ft. (Model with OBE Damping)

Elev. (m)	Node No.	LB Full Column Profile (g)	BE Full Column Profile (g)	UB Full Column Profile (g)
19.70	11	1.09	3.13	5.67

Table A.3-8 Horizontal FWS Tank Hydrodynamic SDOF Maximum Accelerations – Input Motion at 220 ft. (Model with OBE Damping)

Elev. (m)	Node No.	Dir.	LB Full Column Profile (g)	BE Full Column Profile (g)	UB Full Column Profile (g)
12.10	60	X	0.10	0.10	0.10
		Y	0.09	0.09	0.09
8.81	30	X	0.76	0.86	1.08
		Y	0.74	0.93	1.07

Table A.4-1 FWS Maximum Accelerations – Input Motion at 220 ft. (Model with SSE Damping)

Elev. (m)	Node No.	LB Full Column Profile			BE Full Column Profile			UB Full Column Profile		
		NS (g)	EW (g)	Vert. (g)	NS (g)	EW (g)	Vert. (g)	NS (g)	EW (g)	Vert. (g)
19.70	10	1.30	1.46	0.62	1.63	1.89	0.84	2.21	2.42	1.40
17.25	9	1.21	1.33	0.62	1.48	1.73	0.84	2.00	2.26	1.40
15.53	8	1.13	1.19	0.61	1.31	1.54	0.83	1.80	2.04	1.38
13.81	7	1.03	1.03	0.60	1.12	1.33	0.82	1.58	1.78	1.33
12.10	6	0.93	0.89	0.59	0.99	1.15	0.80	1.35	1.50	1.26
11.00	5	0.87	0.84	0.57	0.92	1.06	0.77	1.20	1.32	1.20
9.90	4	0.80	0.78	0.56	0.84	0.96	0.75	1.05	1.13	1.13
8.81	3	0.73	0.72	0.55	0.79	0.88	0.72	0.94	1.00	1.06
6.73	2	0.57	0.61	0.52	0.61	0.68	0.66	0.70	0.81	0.92
4.65	8002	0.51	0.50	0.49	0.61	0.58	0.59	0.63	0.66	0.75
2.15	8001	0.51	0.48	0.57	0.63	0.52	0.75	0.66	0.58	0.90

Table A.4-2 FPE Maximum Accelerations – Input Motion at 220 ft. (Model with SSE Damping)

Elev. (m)	Node No.	LB Full Column Profile			BE Full Column Profile			UB Full Column Profile		
		NS (g)	EW (g)	Vert. (g)	NS (g)	EW (g)	Vert. (g)	NS (g)	EW (g)	Vert. (g)
8.25	405	0.57	0.59	0.48	0.75	0.98	0.59	0.77	1.46	0.77
6.45	402	0.55	0.53	0.46	0.68	0.85	0.56	0.70	1.10	0.72

Table A.4-3 Vertical SDOF Maximum Accelerations – Input Motion at 220 ft. (Model with SSE Damping)

Elev. (m)	Node No.	LB Full Column Profile (g)	BE Full Column Profile (g)	UB Full Column Profile (g)
19.70	11	1.07	2.48	3.98

Table A.4-4 Horizontal FWS Tank Hydrodynamic SDOF Maximum Accelerations – Input Motion at 220 ft. (Model with SSE Damping)

Elev. (m)	Node No.	Dir.	LB Full Column Profile (g)	BE Full Column Profile (g)	UB Full Column Profile (g)
12.10	60	X	0.10	0.10	0.10
		Y	0.09	0.09	0.09
8.81	30	X	0.73	0.79	0.94
		Y	0.72	0.88	1.00

APPENDIX B
PLOTS OF AMPLITUDES OF ACCELERATION TRANSFER FUNCTIONS FROM SSSI ANALYSES OF CB-FWSC COMBINED MODEL

LIST OF FIGURES

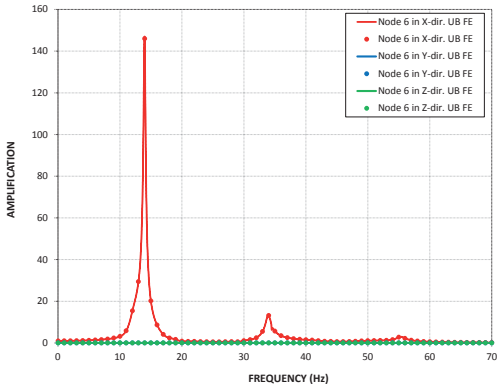

(a)X-Direction Input

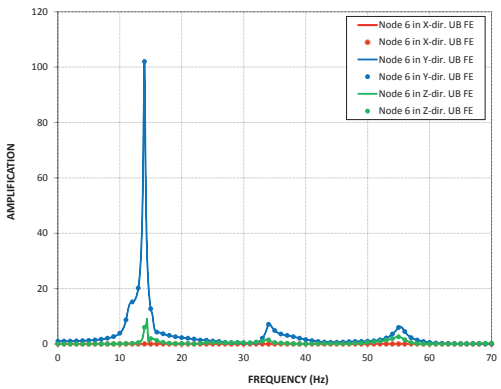

(b) Y-Direction Input

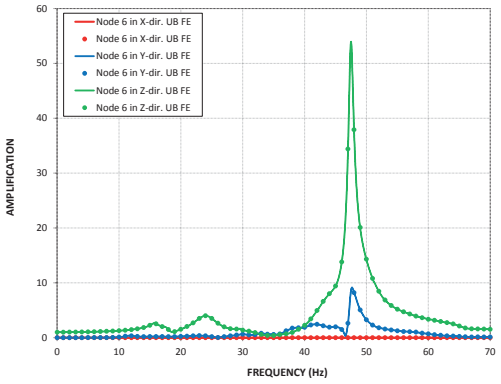

(c) Z-Direction Input

Figure B-1a Transfer Functions of CB Top Response from Analysis of UB Full Column Profile (Model with OBE Damping)

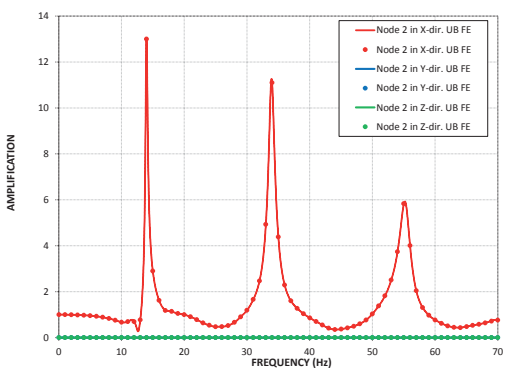

(a)X-Direction Input

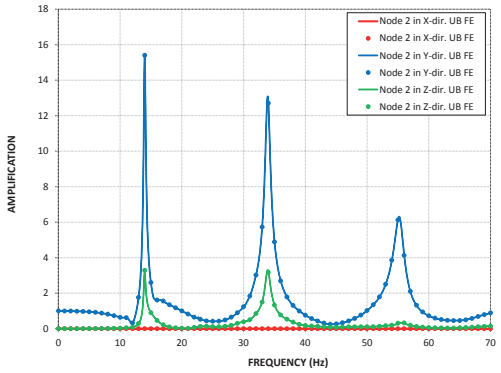

(b) Y-Direction Input

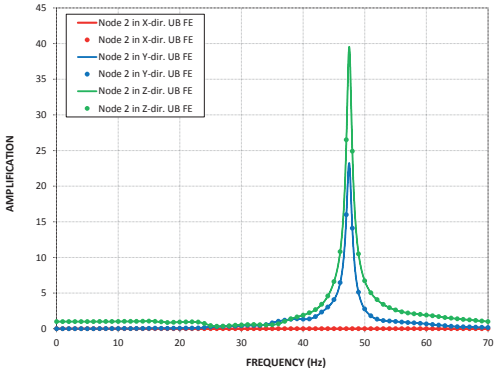

(c) Z-Direction Input

Figure B-1b Transfer Functions of CB Basemat Response from Analysis of UB Full Column Profile (Model with OBE Damping)

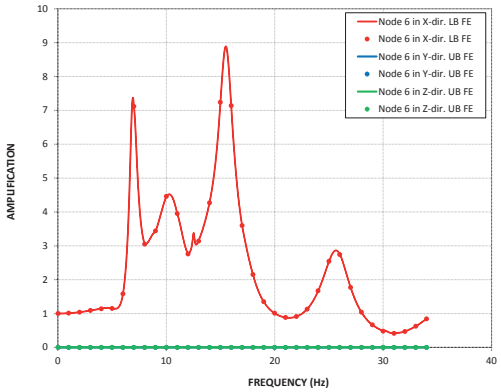

(a)X-Direction Input

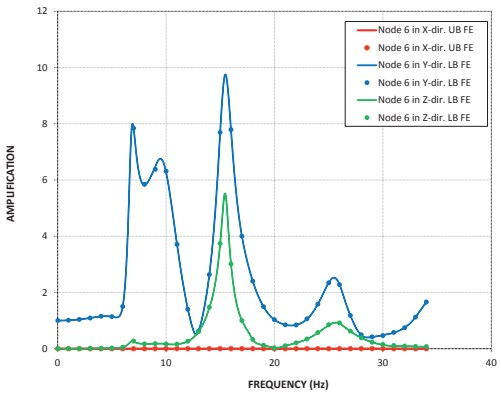

(b) Y-Direction Input

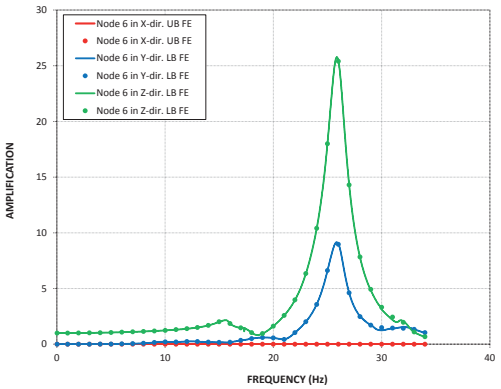

(c) Z-Direction Input

Figure B-1c Transfer Functions of CB Top Response from Analysis of LB Full Column Profile (Model with OBE Damping)

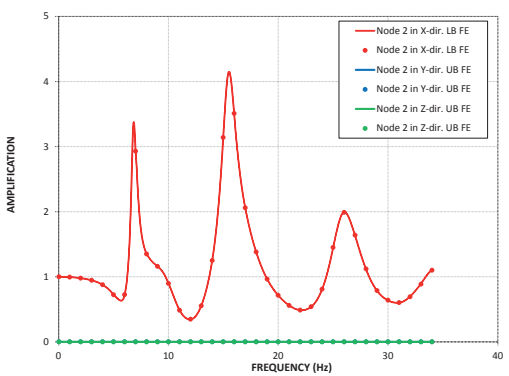

(a)X-Direction Input

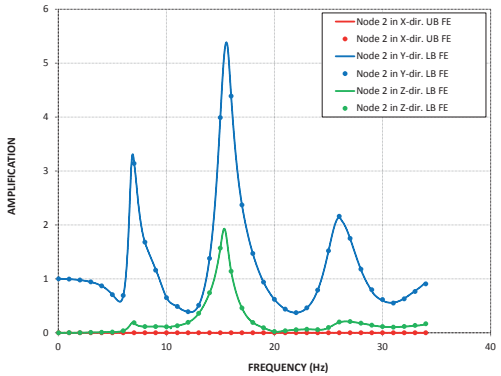

(b) Y-Direction Input

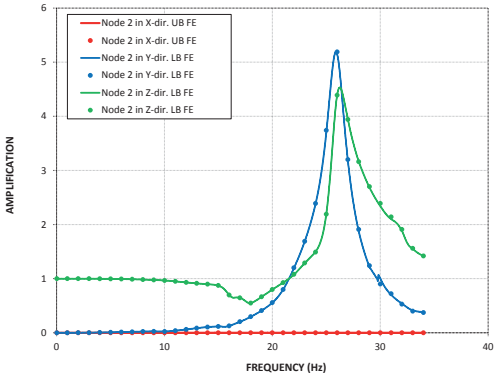

(c) Z-Direction Input

Figure B-1d Transfer Functions of CB Basemat Response from Analysis of LB Full Column Profile (Model with OBE Damping)

APPENDIX C
PLOTS OF AMPLITUDES OF ACCELERATION TRANSFER FUNCTIONS FROM SSSI ANALYSES OF FWSC-CB COMBINED MODEL

LIST OF FIGURES

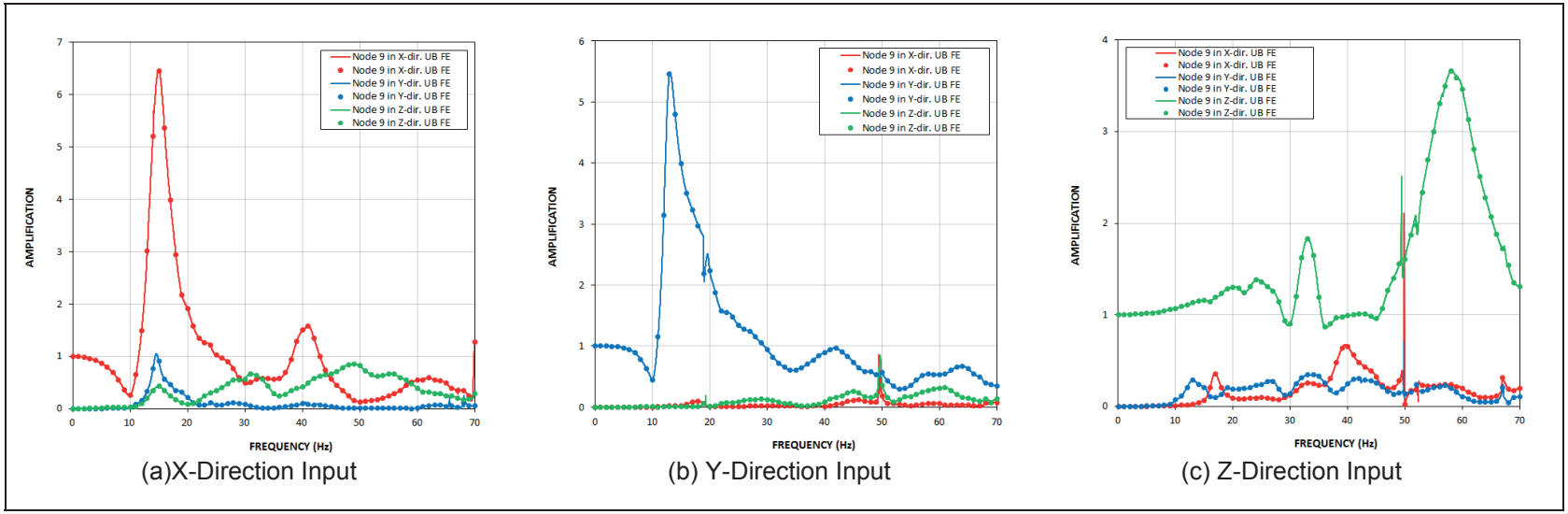

Figure C-1a Transfer Functions of FWS Wall Top Response from Analysis of UB Full Column Profile – Input Motion at 282 ft. (Model with OBE Damping)

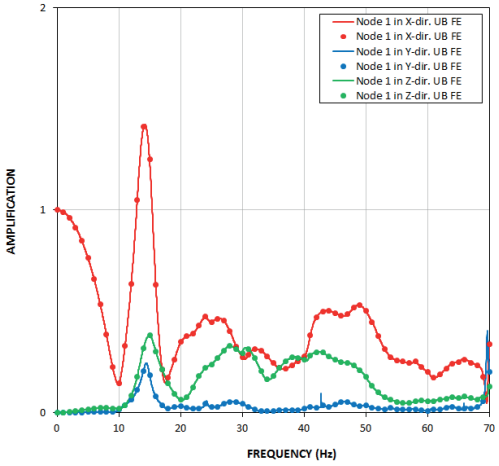

(a)X-Direction Input

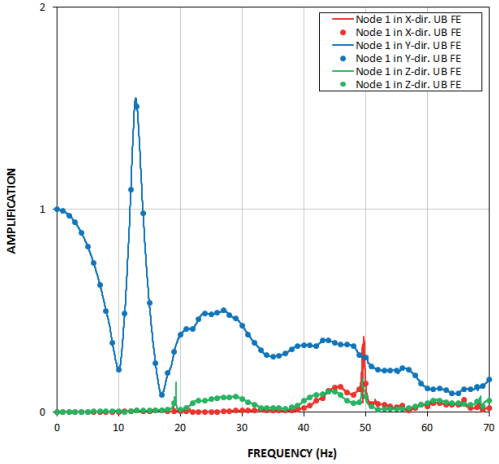

(b) Y-Direction Input

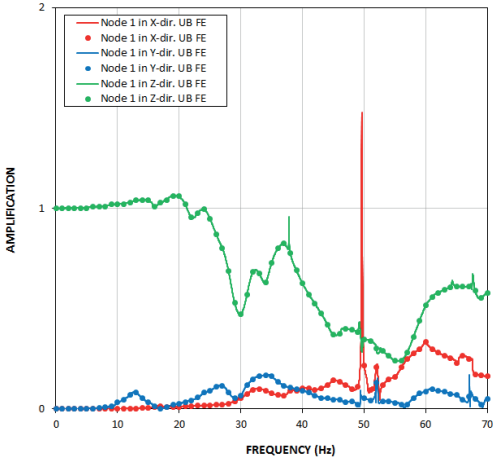

(c) Z-Direction Input

Figure C-1b Transfer Functions of FWS Base Response from Analysis of UB Full Column Profile – Input Motion at 282 ft. (Model with OBE Damping)

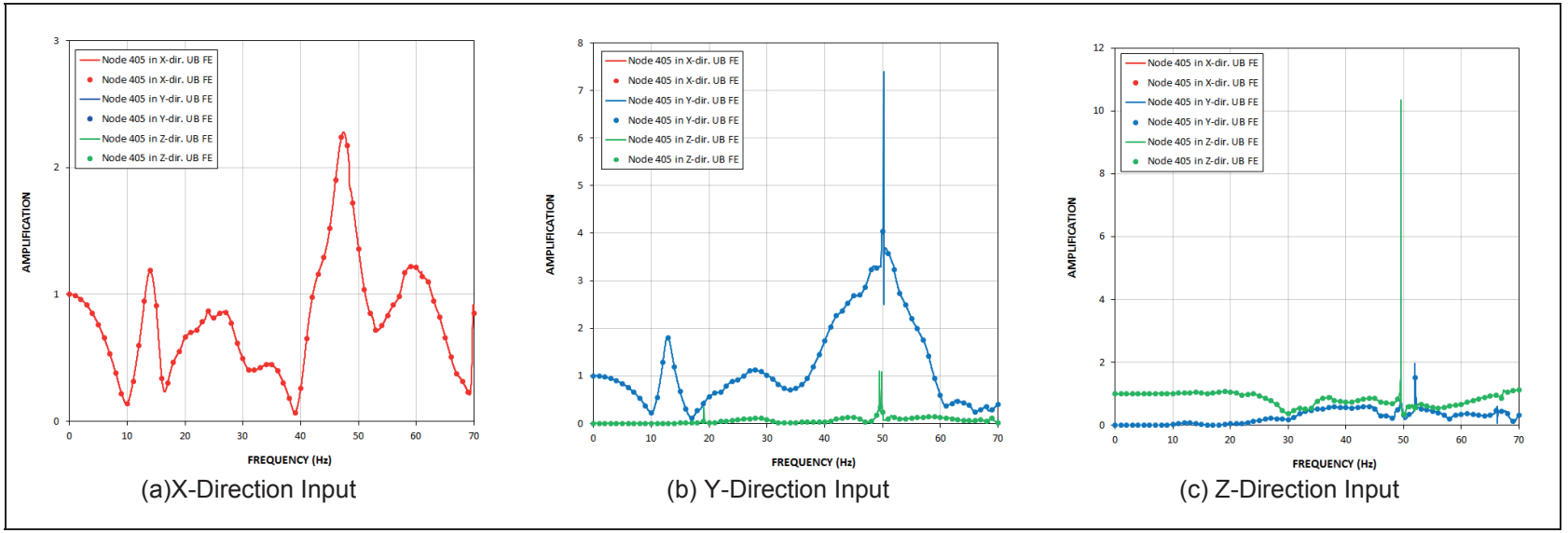

Figure C-1c Transfer Functions of FPE Top Response from Analysis of UB Full Column Profile – Input Motion at 282 ft. (Model with OBE Damping)

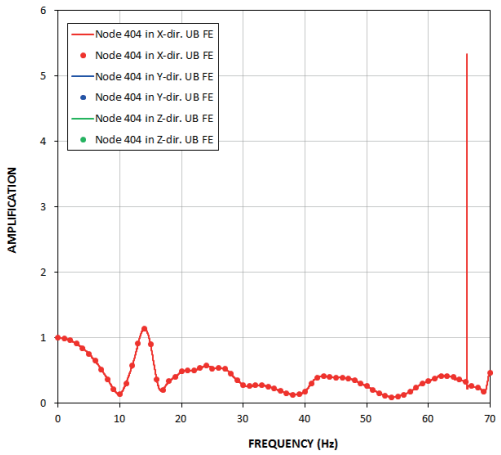

(a)X-Direction Input

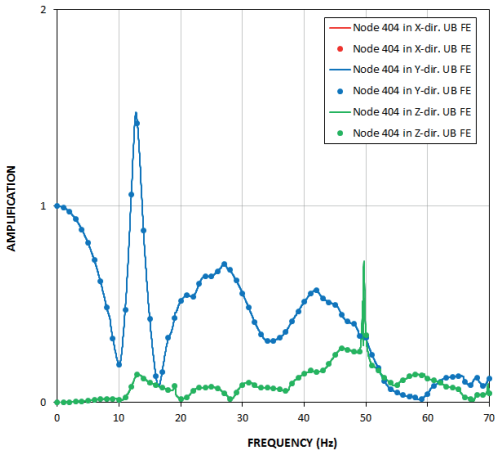

(b) Y-Direction Input

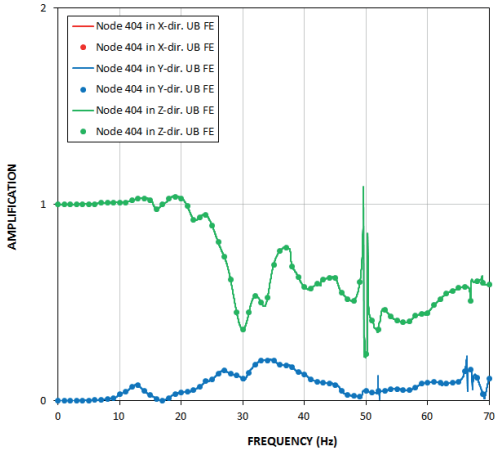

(c) Z-Direction Input

Figure C-1d Transfer Functions of FPE Base Response from Analysis of UB Full Column Profile – Input Motion at 282 ft. (Model with OBE Damping)

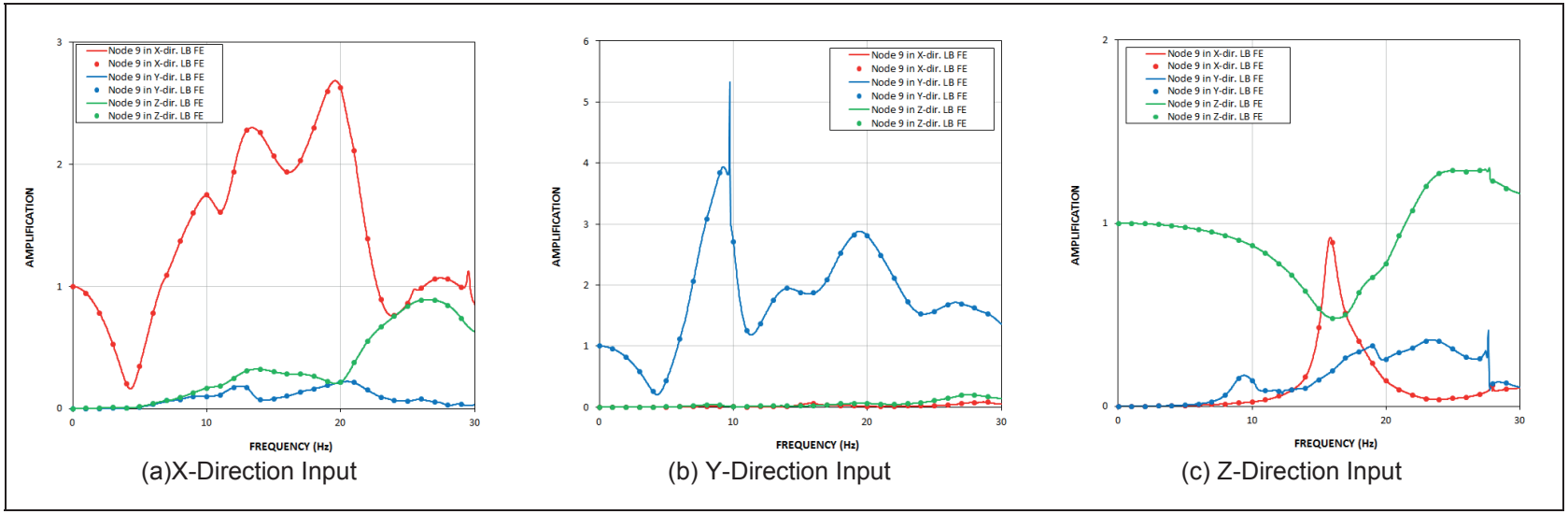

Figure C-2a Transfer Functions of FWS Wall Top Response from Analysis of LB Full Column Profile – Input Motion at 282 ft. (Model with OBE Damping)

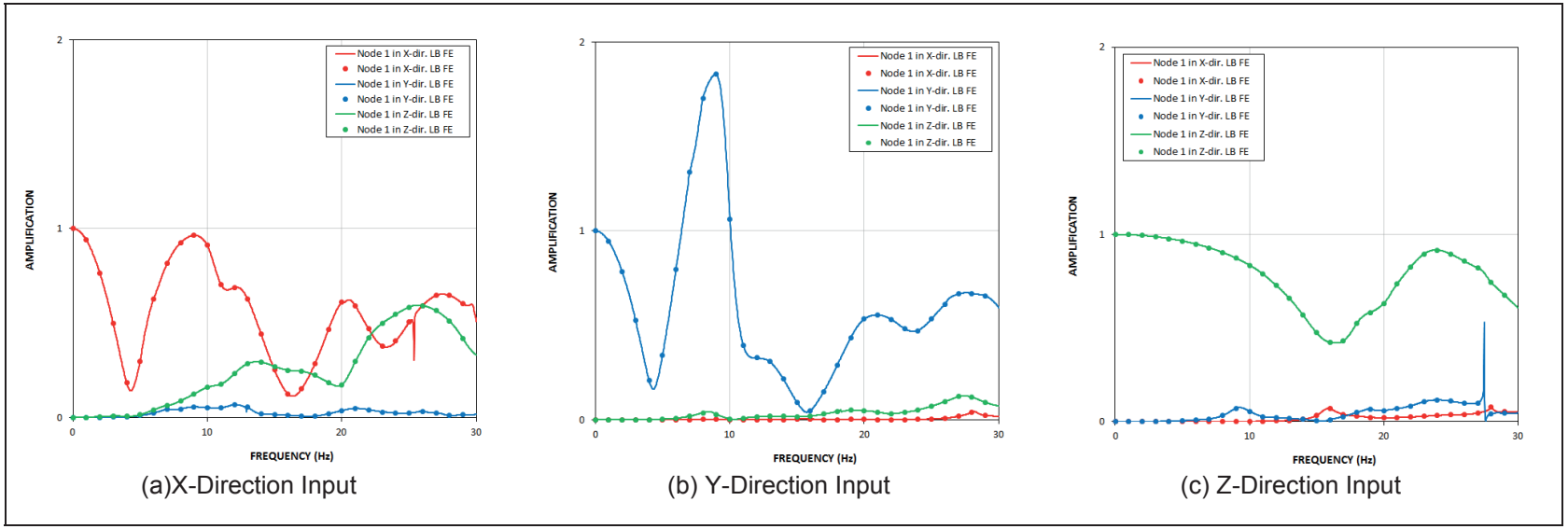

(a)X-Direction Input (b) Y-Direction Input (c) Z-Direction Input

Figure C-2b Transfer Functions of FWS Base Response from Analysis of LB Full Column Profile – Input Motion at 282 ft. (Model with OBE Damping)

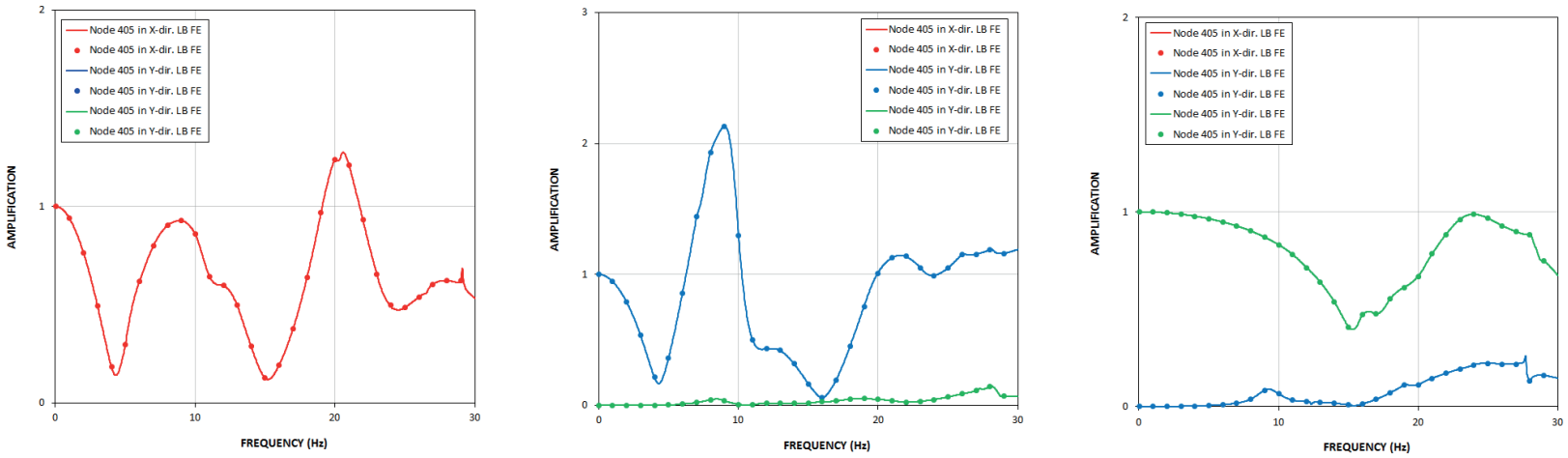

Figure C-2c Transfer Functions of FPE Top Response from Analysis of LB Full Column Profile – Input Motion at 282 ft. (Model with OBE Damping)

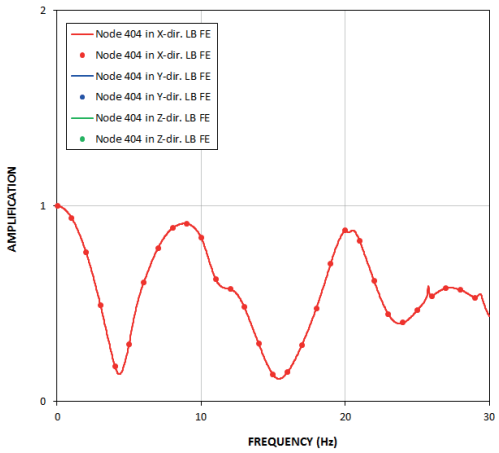

(a)X-Direction Input

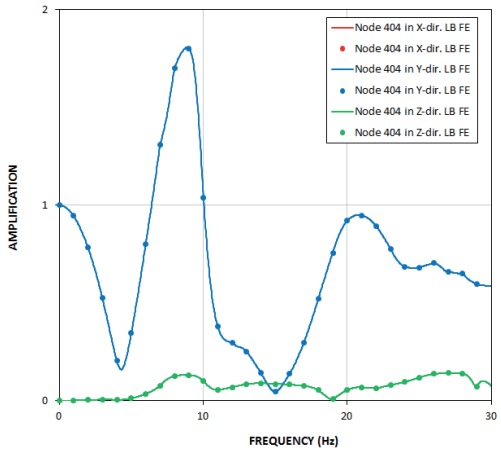

(b) Y-Direction Input

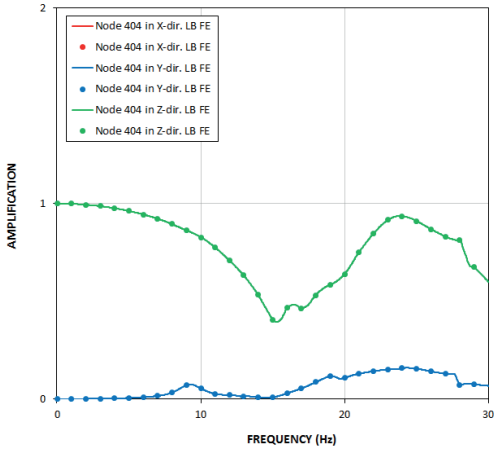

(c) Z-Direction Input

Figure C-2d Transfer Functions of FPE Base Response from Analysis of LB Full Column Profile – Input Motion at 282 ft. (Model with OBE Damping)

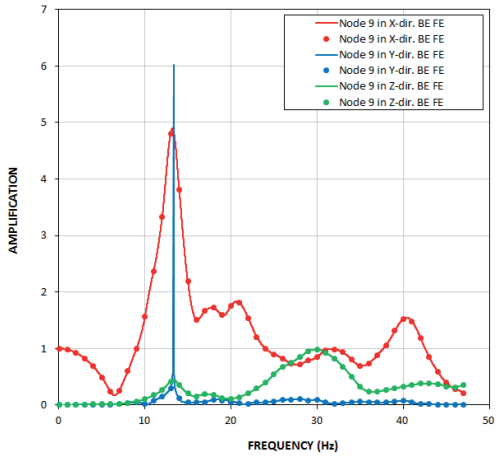

(a)X-Direction Input

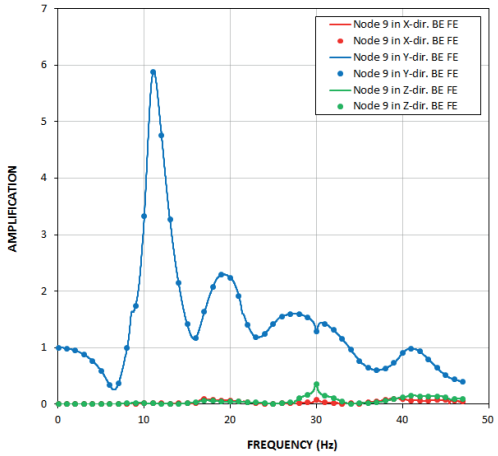

(b) Y-Direction Input

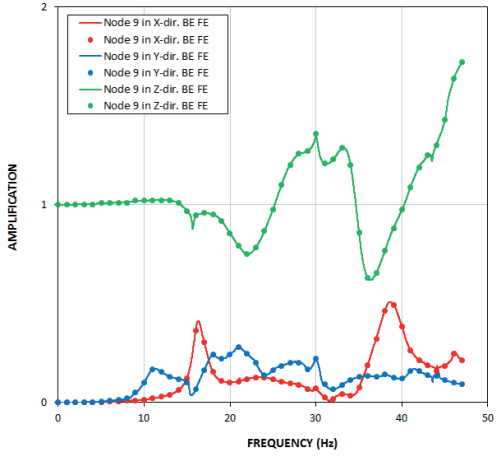

(c) Z-Direction Input

Figure C-3a Transfer Functions of FWS Wall Top Response from Analysis of BE Full Column Profile – Input Motion at 282 ft. (Model with OBE Damping)

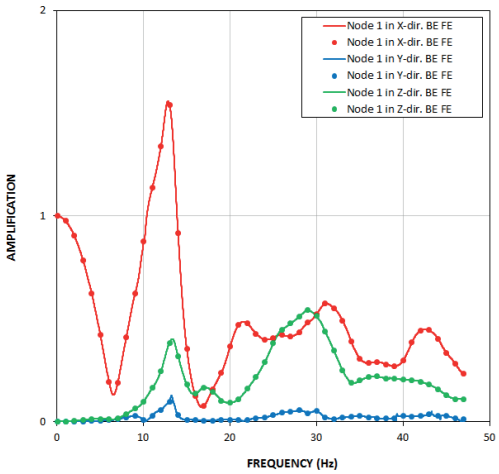

(a)X-Direction Input

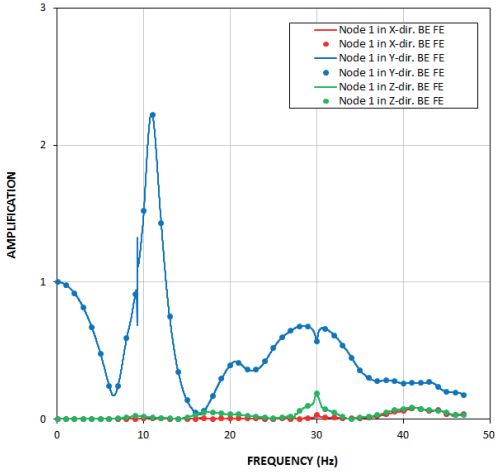

(b) Y-Direction Input

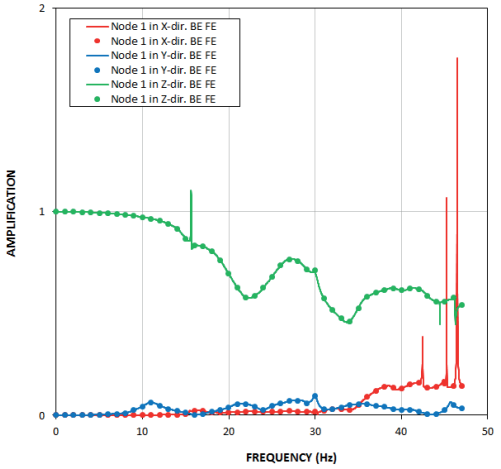

(c) Z-Direction Input

Figure C-3b Transfer Functions of FWS Base Response from Analysis of BE Full Column Profile – Input Motion at 282 ft. (Model with OBE Damping)

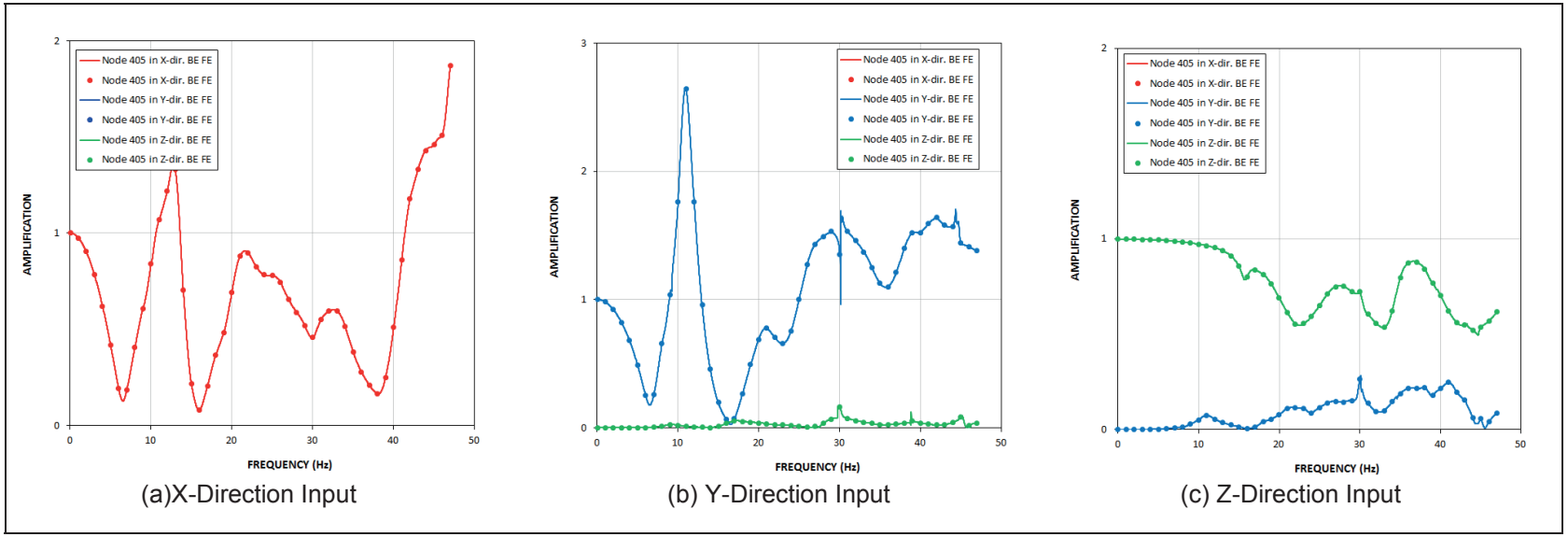

Figure C-3c Transfer Functions of FPE Top Response from Analysis of BE Full Column Profile – Input Motion at 282 ft. (Model with OBE Damping)

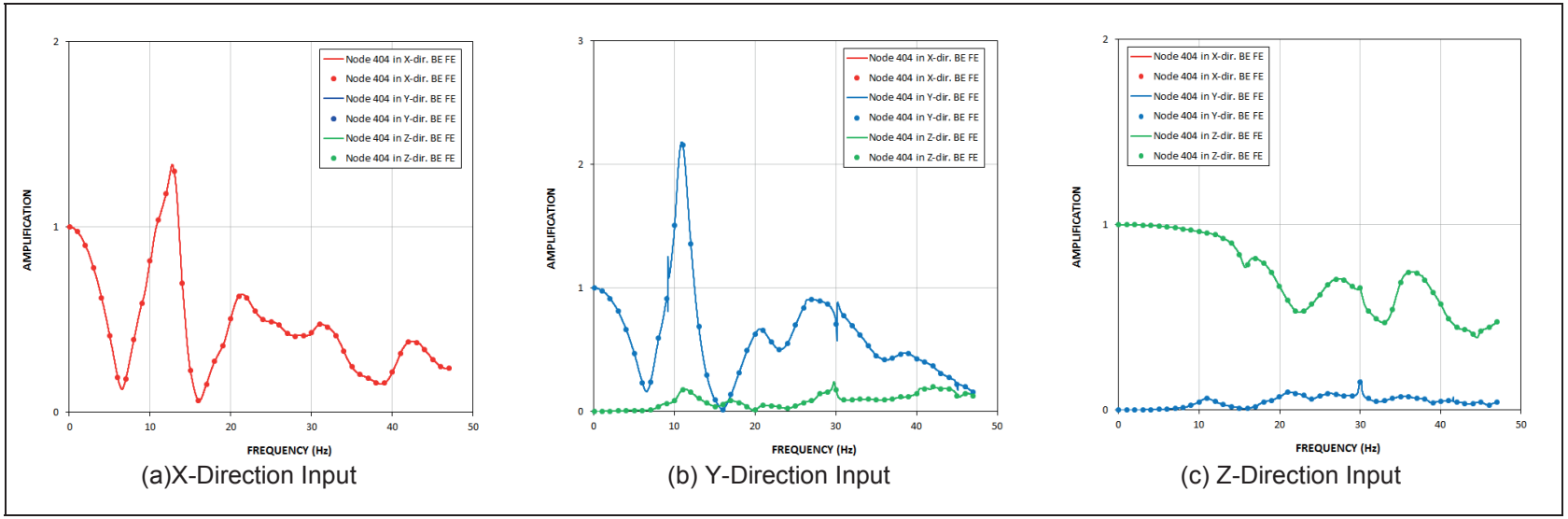

Figure C-3d Transfer Functions of FPE Base Response from Analysis of BE Full Column Profile – Input Motion at 282 ft. (Model with OBE Damping)

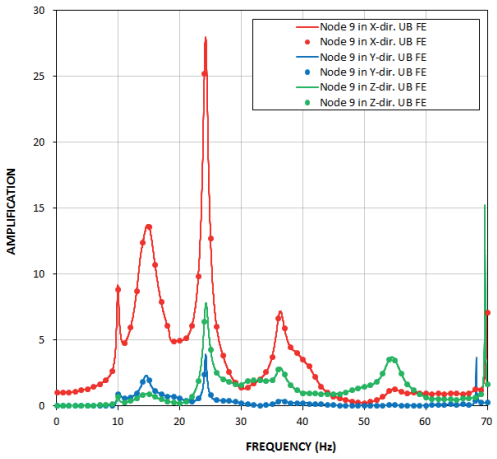

(a)X-Direction Input

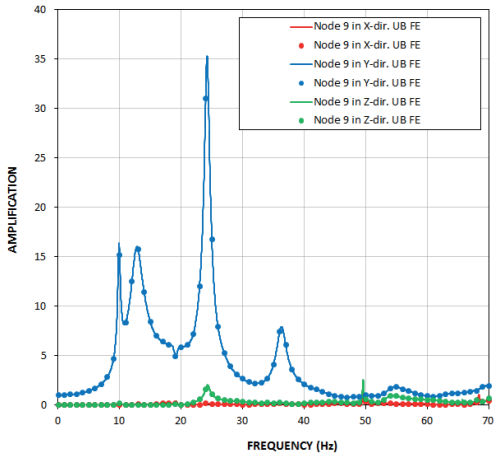

(b) Y-Direction Input

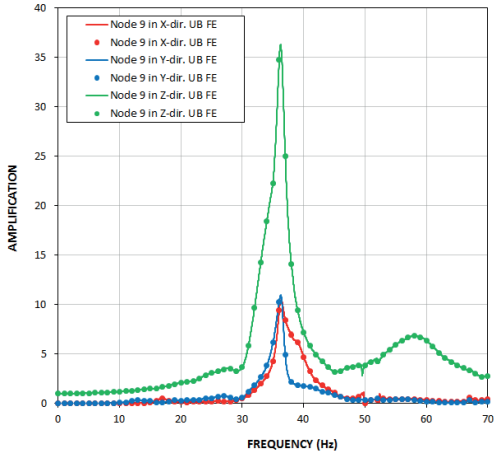

(c) Z-Direction Input

Figure C-4a Transfer Functions of FWS Wall Top Response from Analysis of UB Full Column Profile – Input Motion at 220 ft. (Model with OBE Damping)

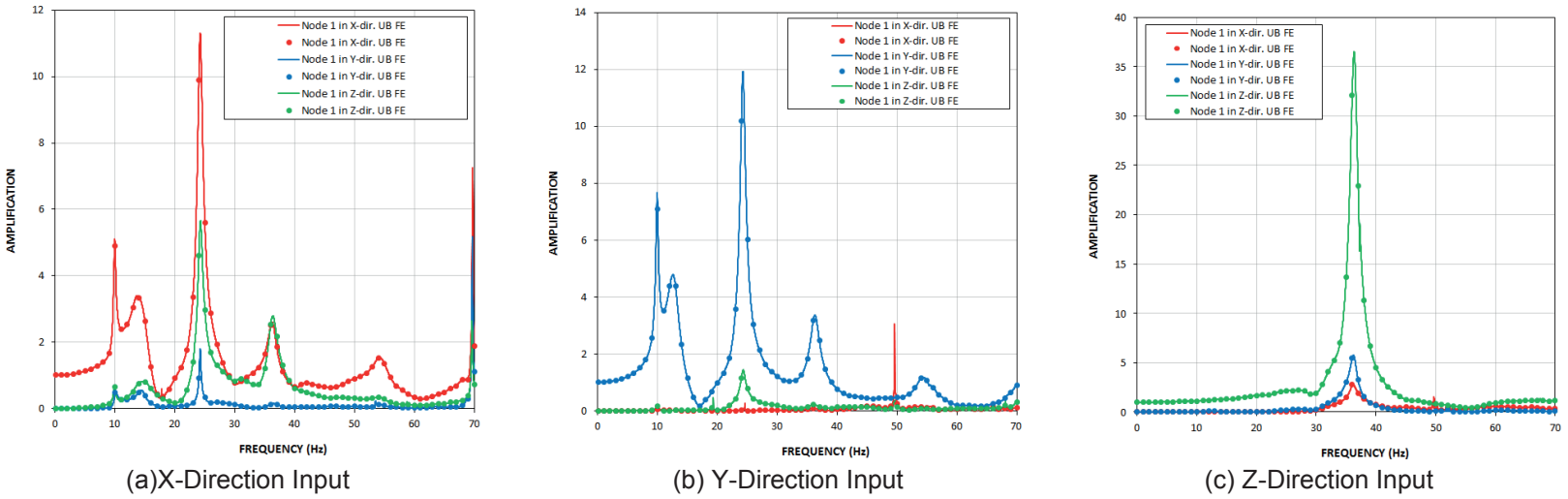

(a)X-Direction Input (b) Y-Direction Input (c) Z-Direction Input

Figure C-4b Transfer Functions of FWS Base Response from Analysis of UB Full Column Profile – Input Motion at 220 ft. (Model with OBE Damping)

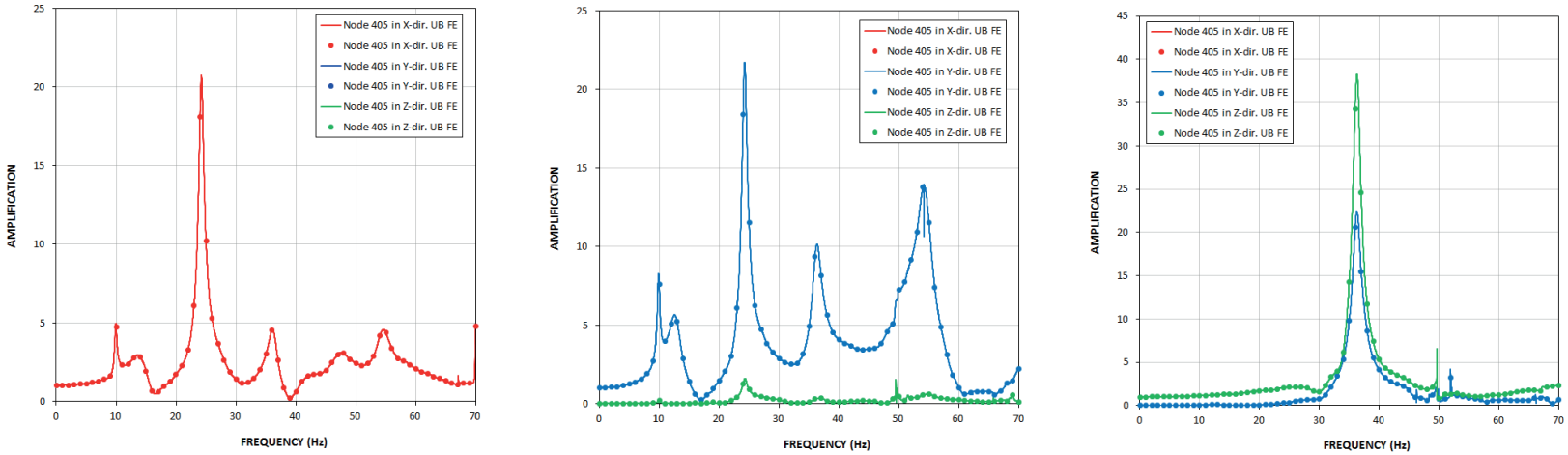

(a)X-Direction Input (b) Y-Direction Input (c) Z-Direction Input

Figure C-4c Transfer Functions of FPE Top Response from Analysis of UB Full Column Profile – Input Motion at 220 ft. (Model with OBE Damping)

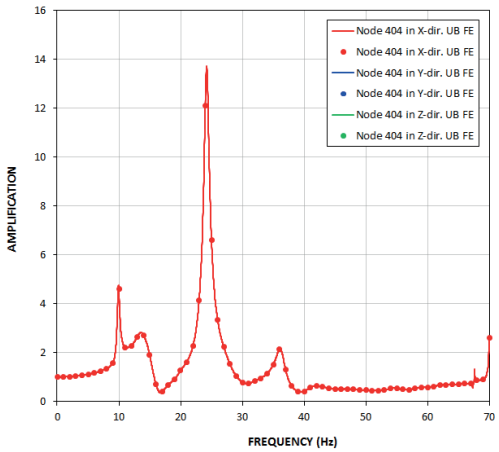

(a)X-Direction Input

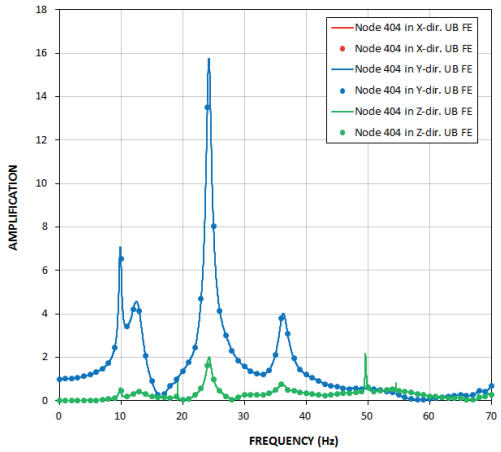

(b) Y-Direction Input

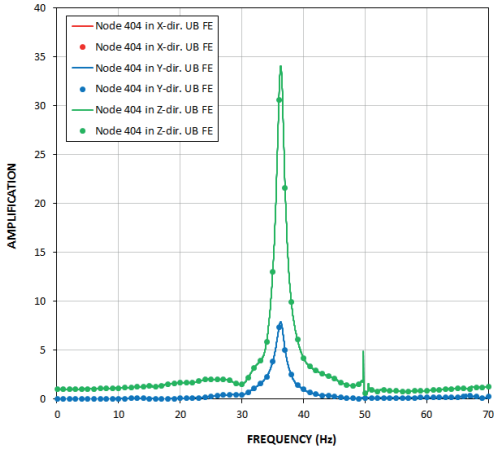

(c) Z-Direction Input

Figure C-4d Transfer Functions of FPE Base Response from Analysis of UB Full Column Profile – Input Motion at 220 ft. (Model with OBE Damping)

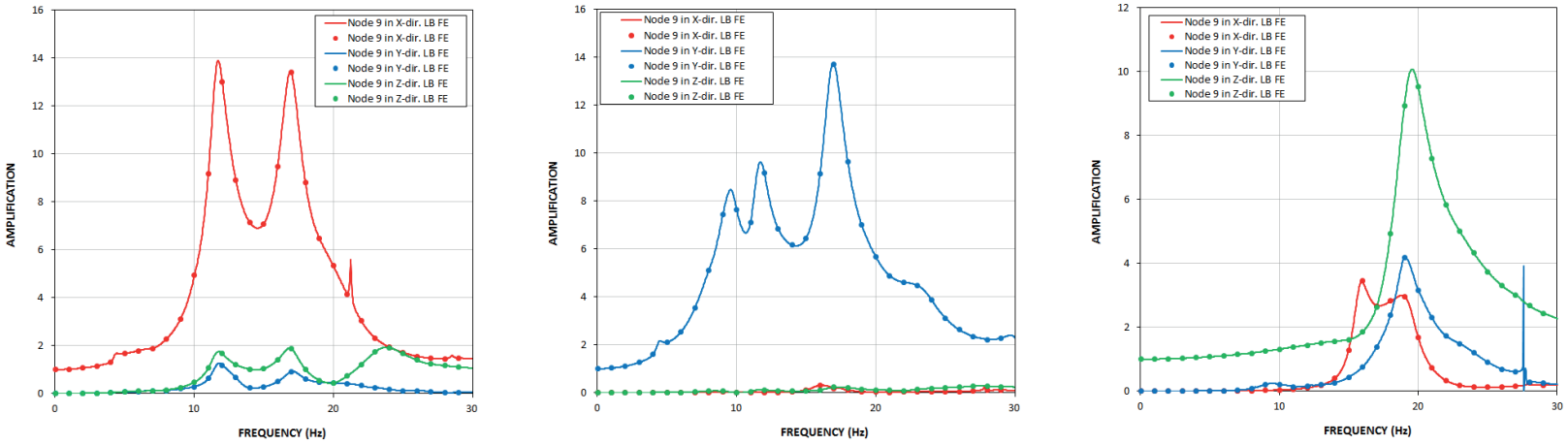

(a)X-Direction Input (b) Y-Direction Input (c) Z-Direction Input

Figure C-5a Transfer Functions of FWS Wall Top Response from Analysis of LB Full Column Profile – Input Motion at 220 ft. (Model with OBE Damping)

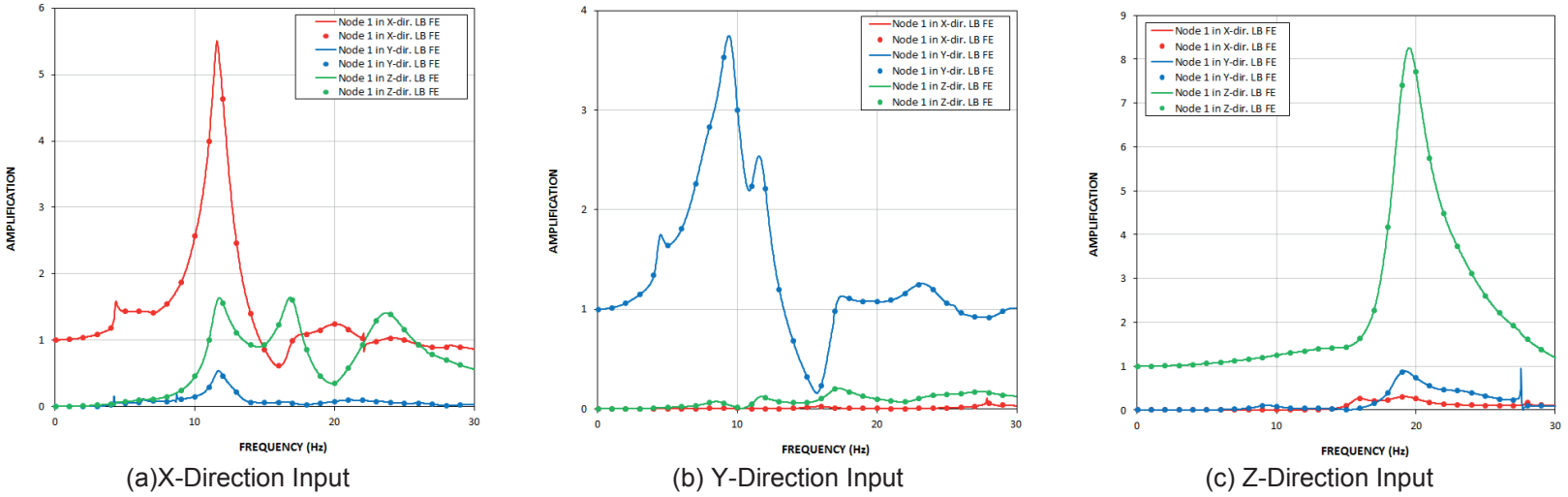

Figure C-5b Transfer Functions of FWS Base Response from Analysis of LB Full Column Profile – Input Motion at 220 ft. (Model with OBE Damping)

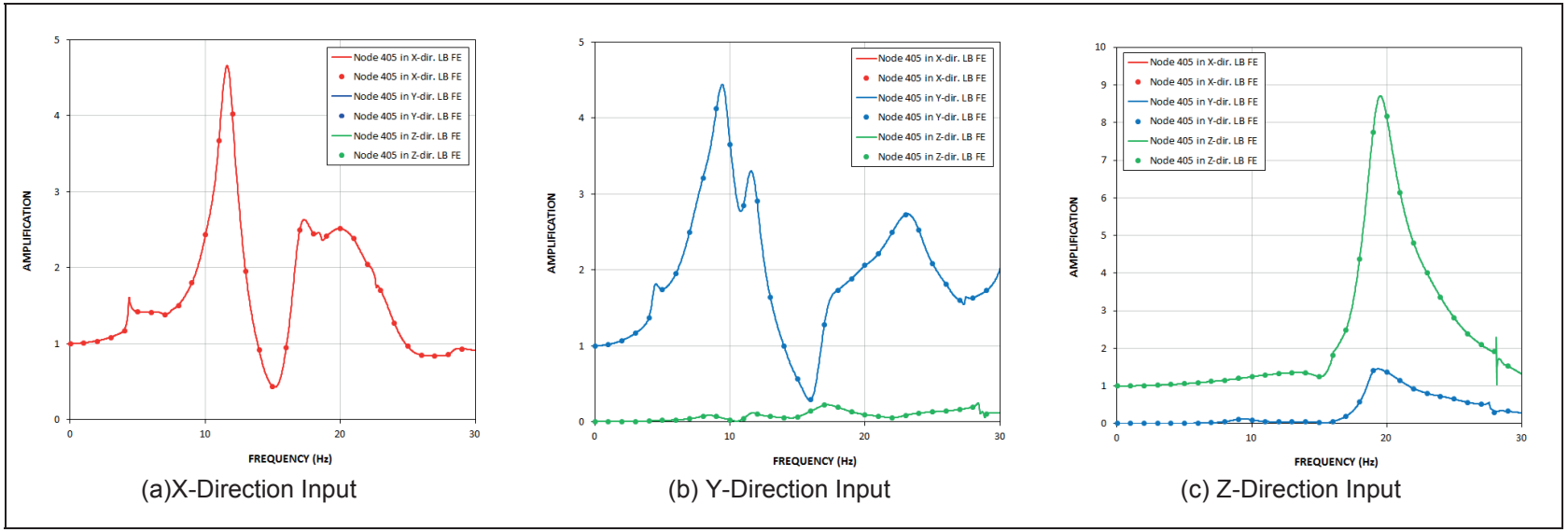

(a)X-Direction Input (b) Y-Direction Input (c) Z-Direction Input

Figure C-5c Transfer Functions of FPE Top Response from Analysis of LB Full Column Profile – Input Motion at 220 ft. (Model with OBE Damping)

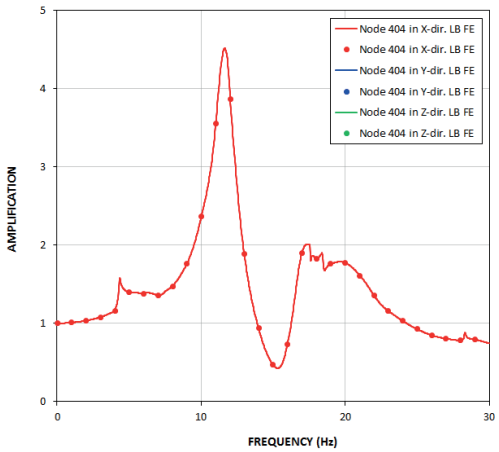

(a)X-Direction Input

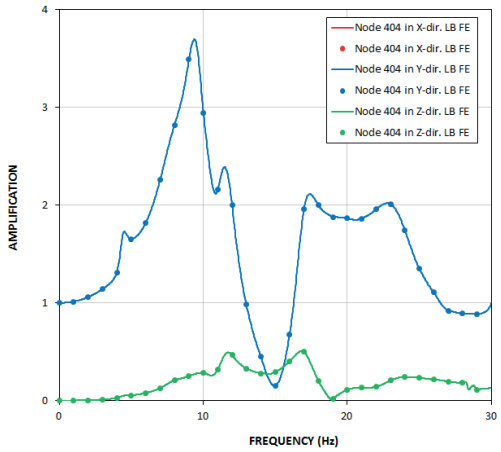

(b) Y-Direction Input

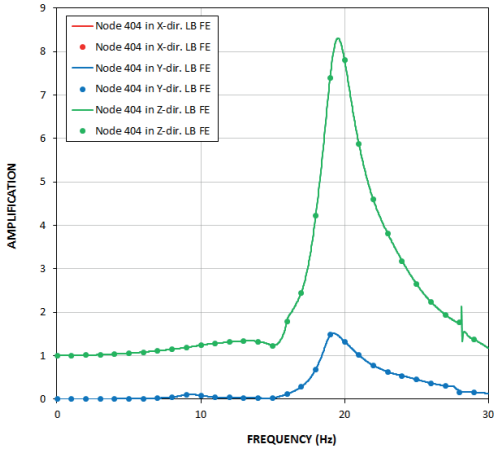

(c) Z-Direction Input

Figure C-5d Transfer Functions of FPE Base Response from Analysis of LB Full Column Profile – Input Motion at 220 ft. (Model with OBE Damping)

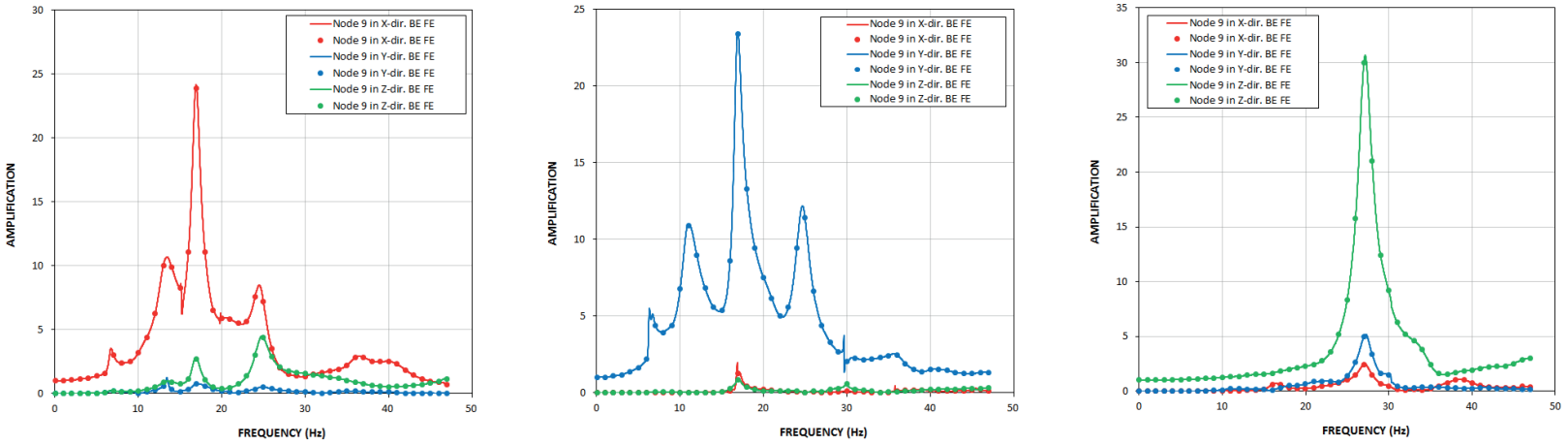

(a)X-Direction Input (b) Y-Direction Input (c) Z-Direction Input

Figure C-6a Transfer Functions of FWS Wall Top Response from Analysis of BE Full Column Profile – Input Motion at 220 ft. (Model with OBE Damping)

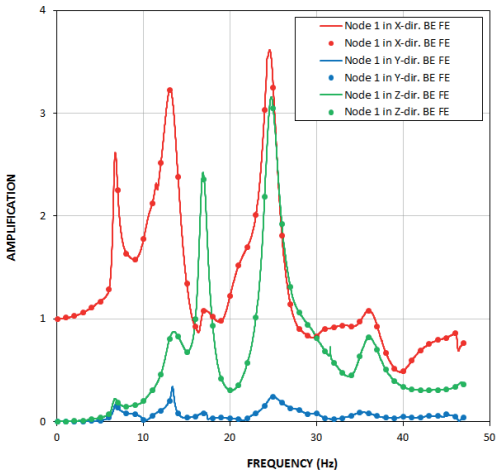

(a)X-Direction Input

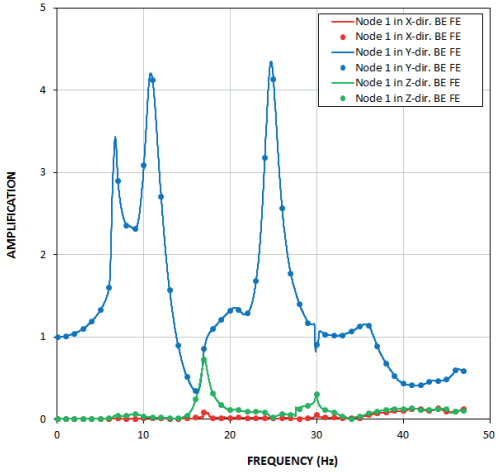

(b) Y-Direction Input

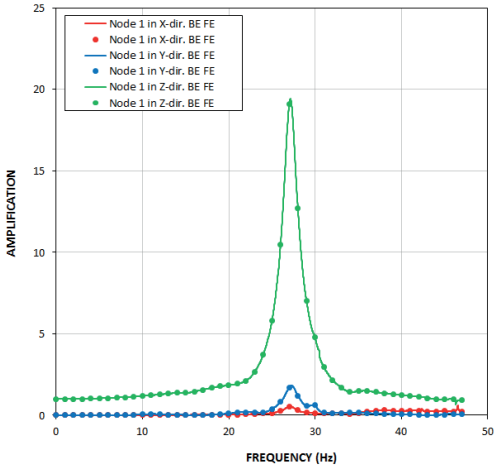

(c) Z-Direction Input

Figure C-6b Transfer Functions of FWS Base Response from Analysis of BE Full Column Profile – Input Motion at 220 ft. (Model with OBE Damping)

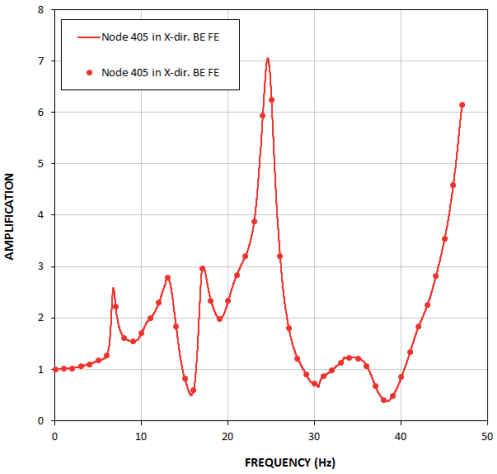

(a)X-Direction Input

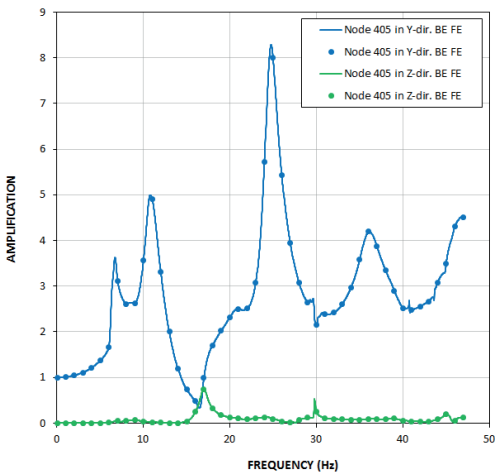

(b) Y-Direction Input

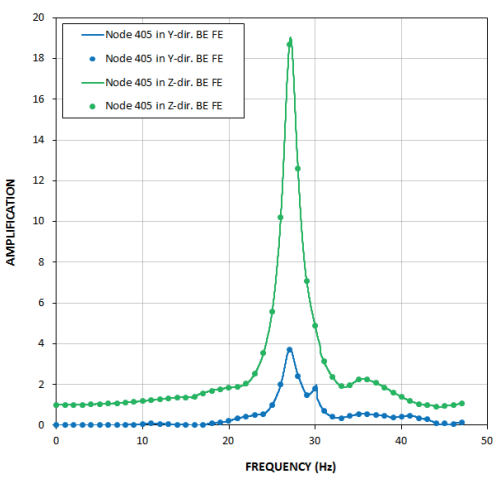

(c) Z-Direction Input

Figure C-6c Transfer Functions of FPE Top Response from Analysis of BE Full Column Profile – Input Motion at 220 ft. (Model with OBE Damping)

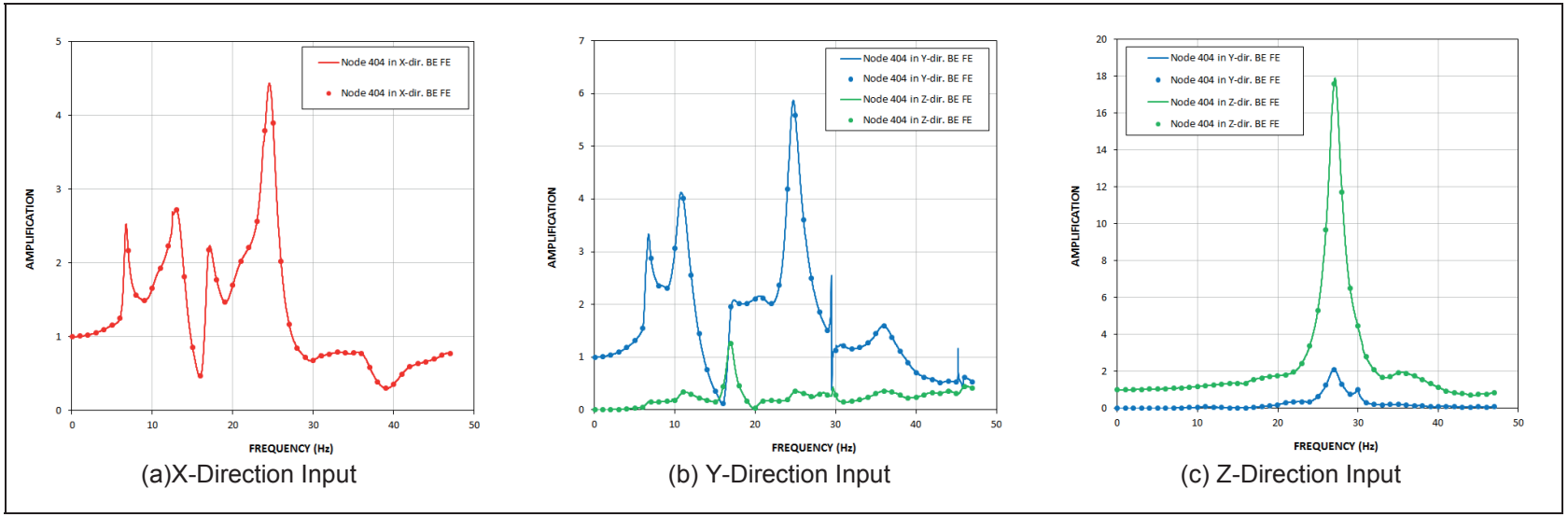

Figure C-6d Transfer Functions of FPE Base Response from Analysis of BE Full Column Profile – Input Motion at 220 ft. (Model with OBE Damping)

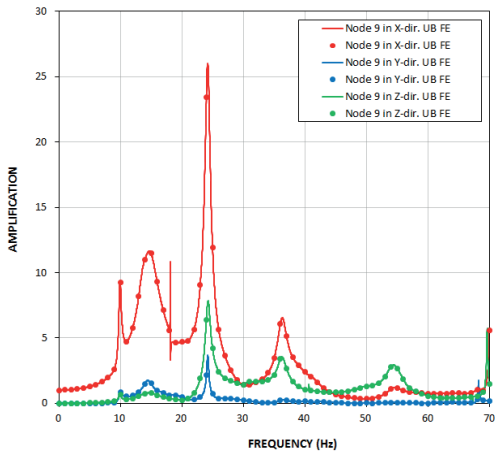

(a)X-Direction Input

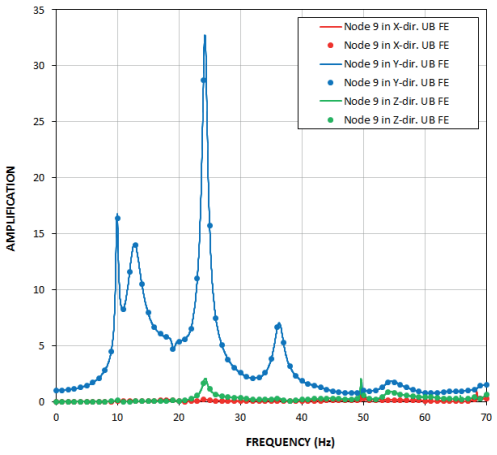

(b) Y-Direction Input

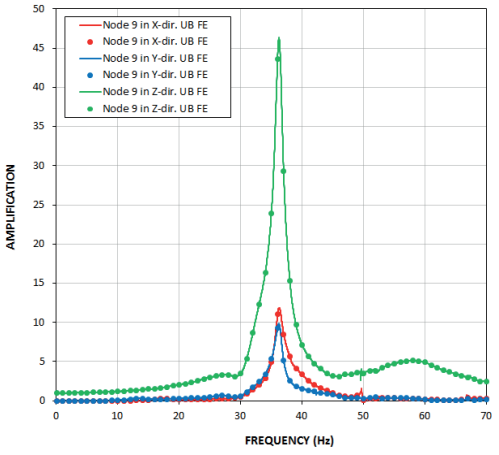

(c) Z-Direction Input

Figure C-7a Transfer Functions of FWS Wall Top Response from Analysis of UB Full Column Profile – Input Motion at 220 ft. (Model with SSE Damping)

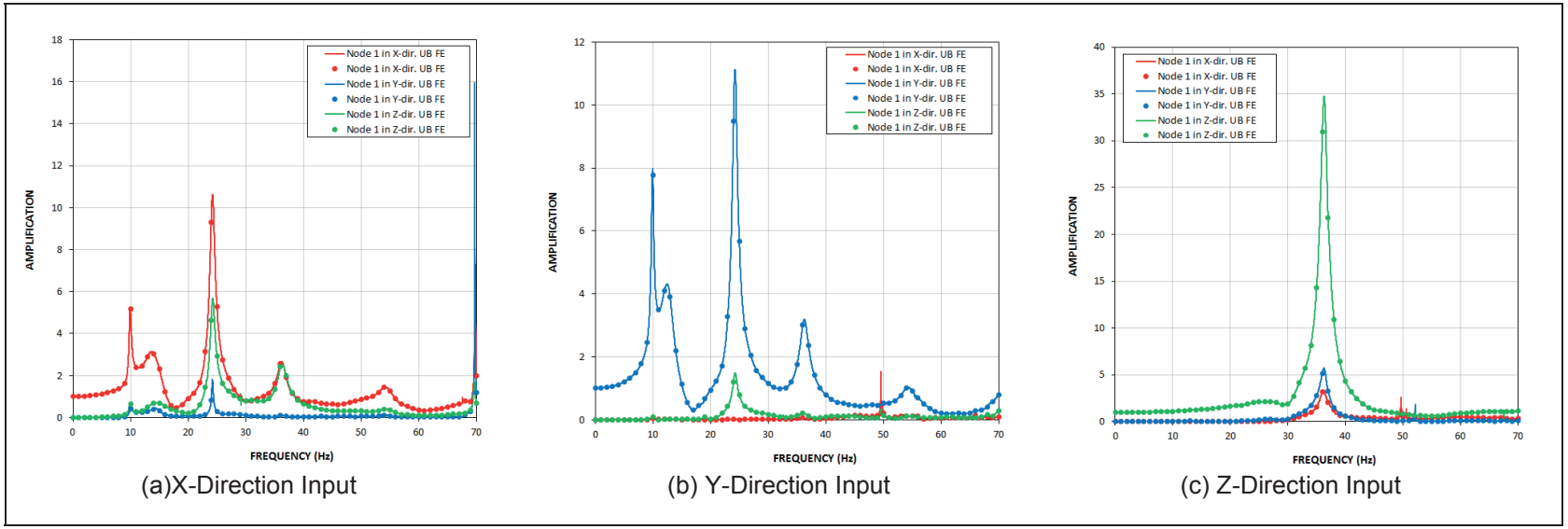

(a)X-Direction Input (b) Y-Direction Input (c) Z-Direction Input

Figure C-7b Transfer Functions of FWS Base Response from Analysis of UB Full Column Profile – Input Motion at 220 ft. (Model with SSE Damping)

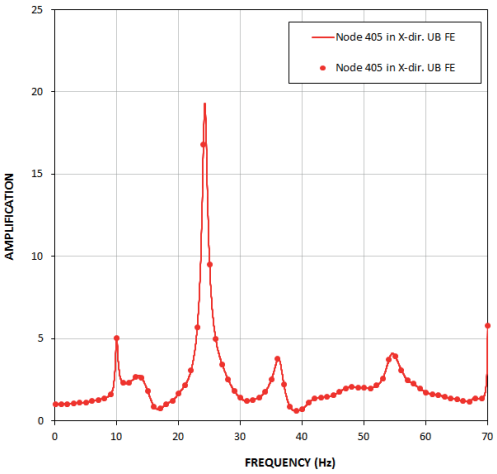

(a)X-Direction Input

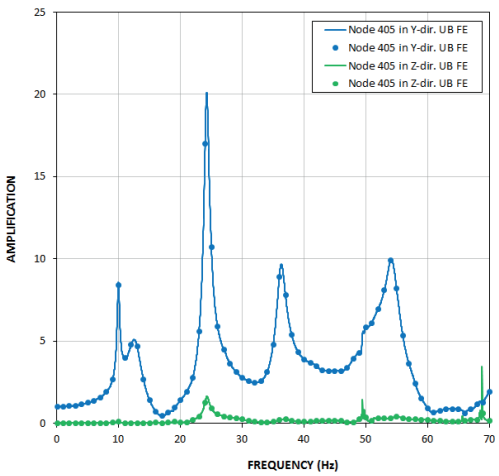

(b) Y-Direction Input

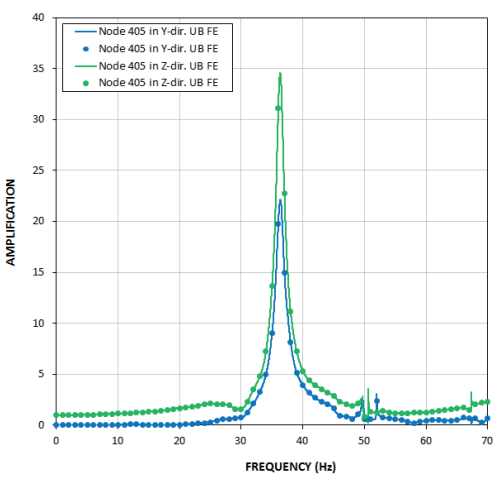

(c) Z-Direction Input

Figure C-7c Transfer Functions of FPE Top Response from Analysis of UB Full Column Profile – Input Motion at 220 ft. (Model with SSE Damping)

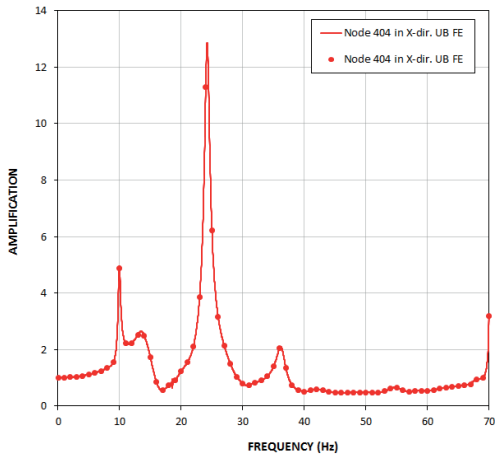

(a)X-Direction Input

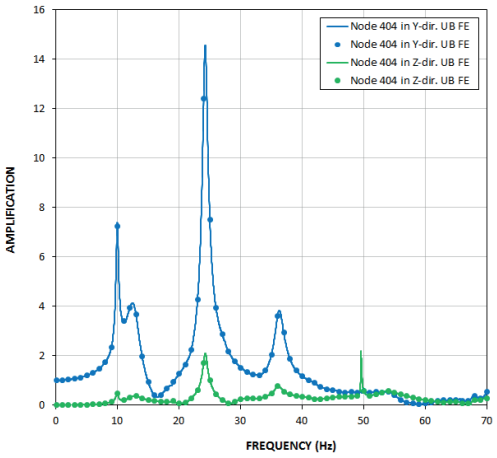

(b) Y-Direction Input

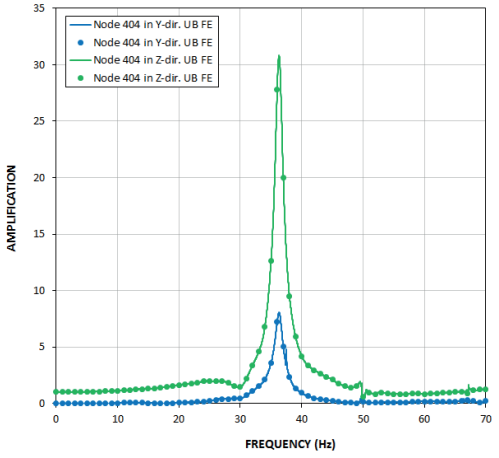

(c) Z-Direction Input

Figure C-7d Transfer Functions of FPE Base Response from Analysis of UB Full Column Profile – Input Motion at 220 ft. (Model with SSE Damping)

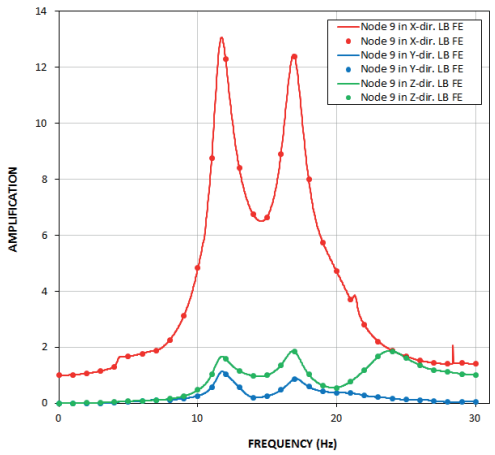

(a)X-Direction Input

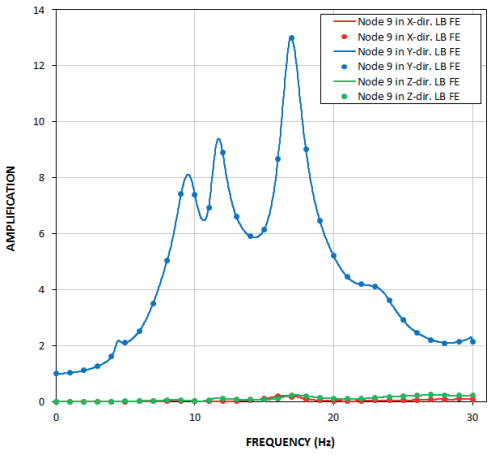

(b) Y-Direction Input

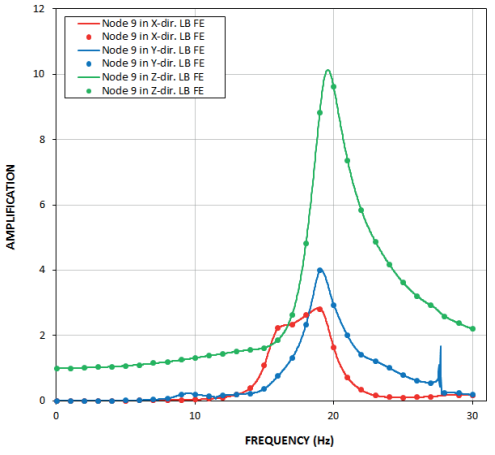

(c) Z-Direction Input

Figure C-8a Transfer Functions of FWS Wall Top Response from Analysis of LB Full Column Profile – Input Motion at 220 ft. (Model with SSE Damping)

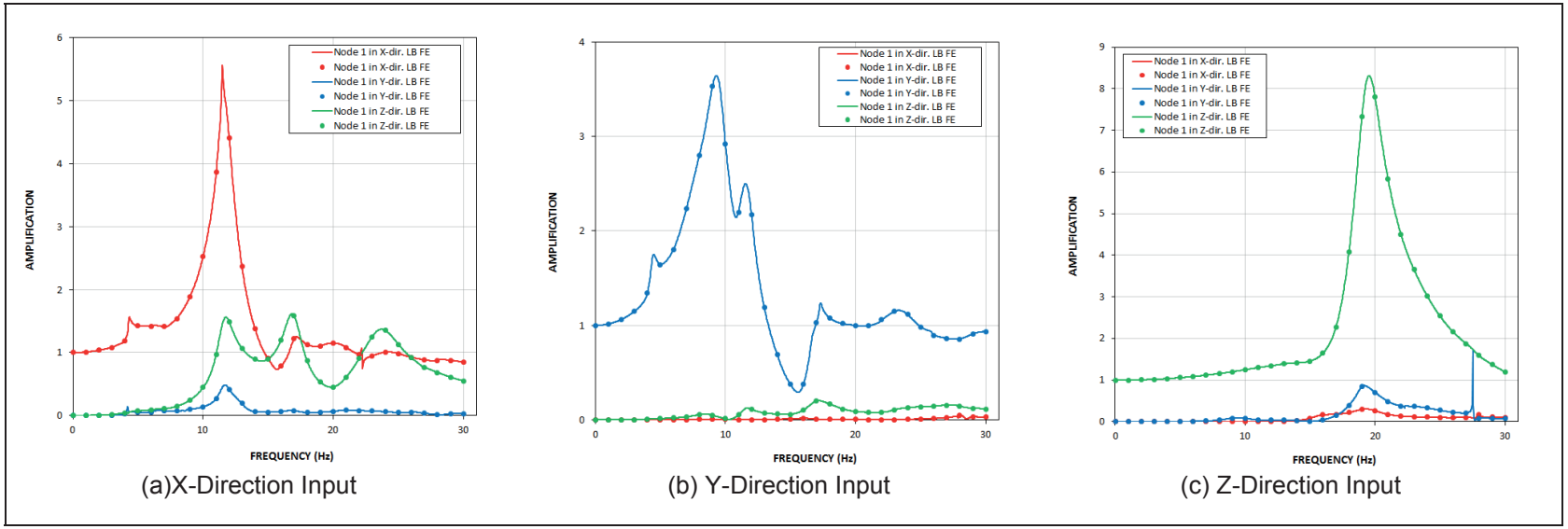

Figure C-8b Transfer Functions of FWS Base Response from Analysis of LB Full Column Profile – Input Motion at 220 ft. (Model with SSE Damping)

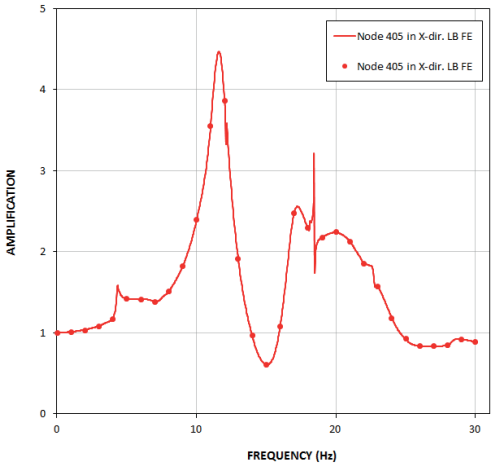

(a)X-Direction Input

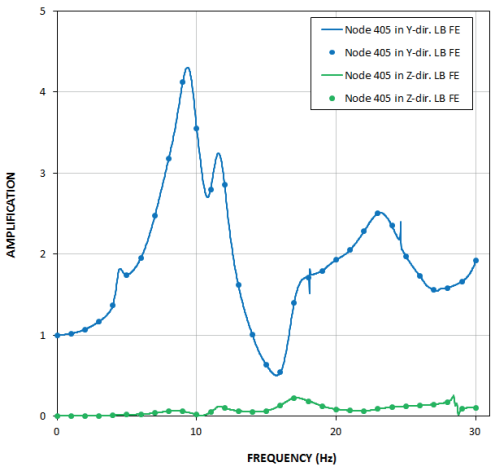

(b) Y-Direction Input

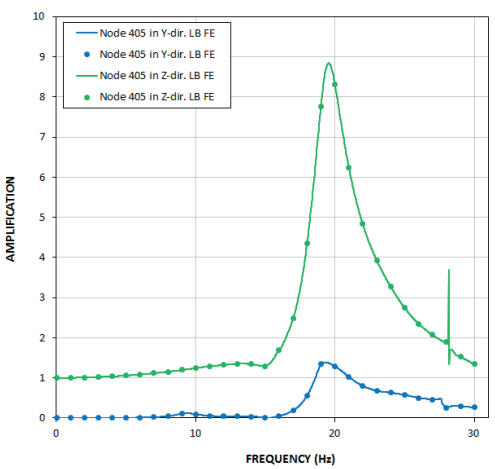

(c) Z-Direction Input

Figure C-8c Transfer Functions of FPE Top Response from Analysis of LB Full Column Profile – Input Motion at 220 ft. (Model with SSE Damping)

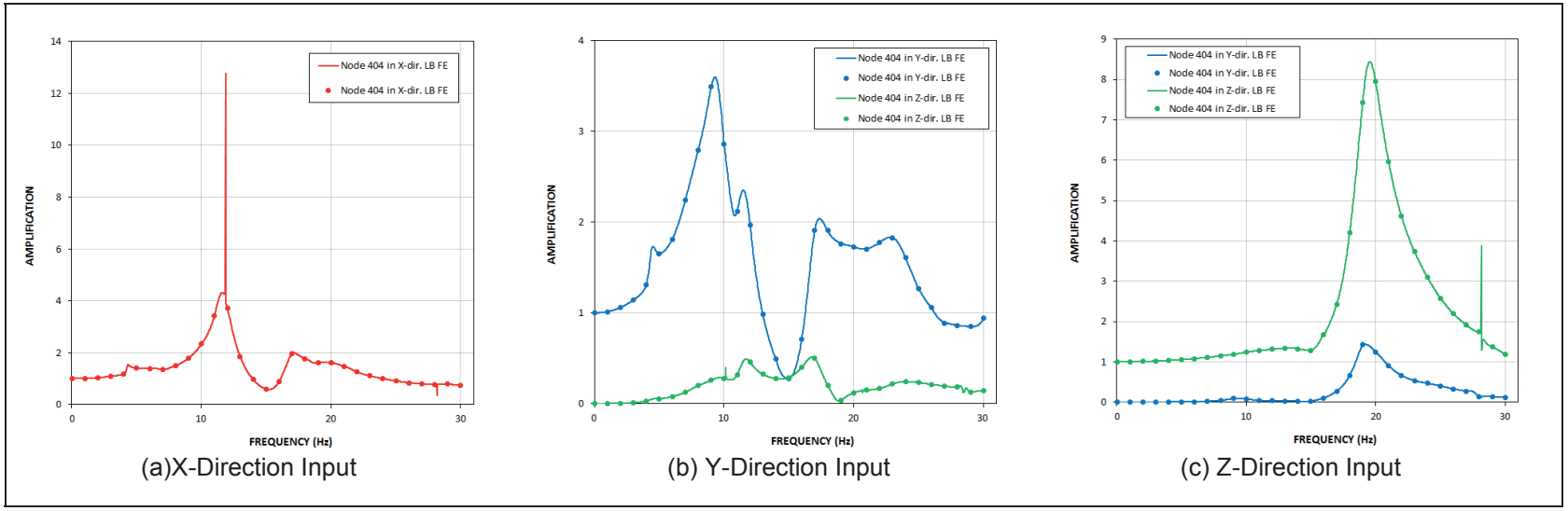

(a)X-Direction Input (b) Y-Direction Input (c) Z-Direction Input

Figure C-8d Transfer Functions of FPE Base Response from Analysis of LB Full Column Profile – Input Motion at 220 ft. (Model with SSE Damping)

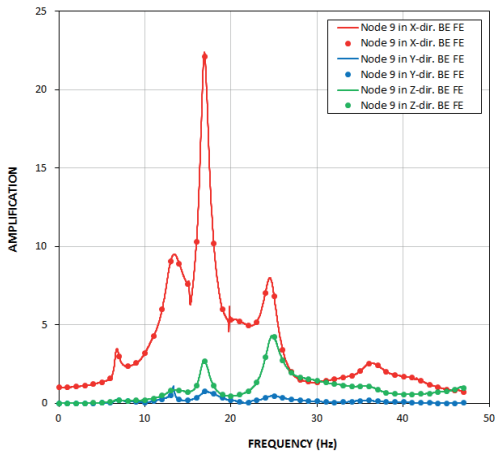

(a)X-Direction Input

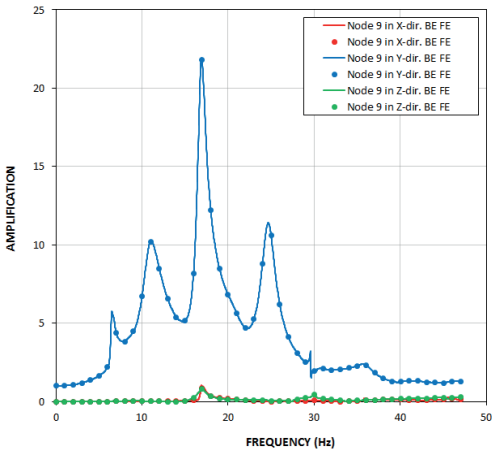

(b) Y-Direction Input

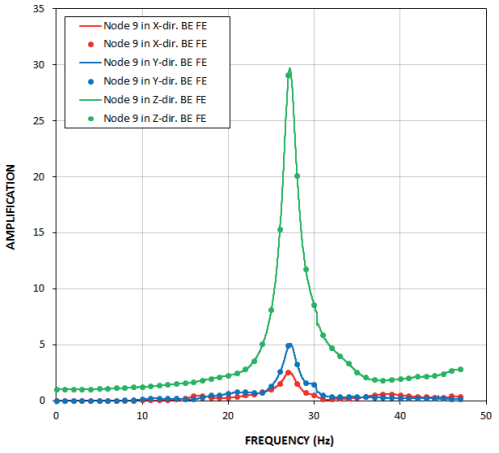

(c) Z-Direction Input

Figure C-9a Transfer Functions of FWS Wall Top Response from Analysis of BE Full Column Profile – Input Motion at 220 ft. (Model with SSE Damping)

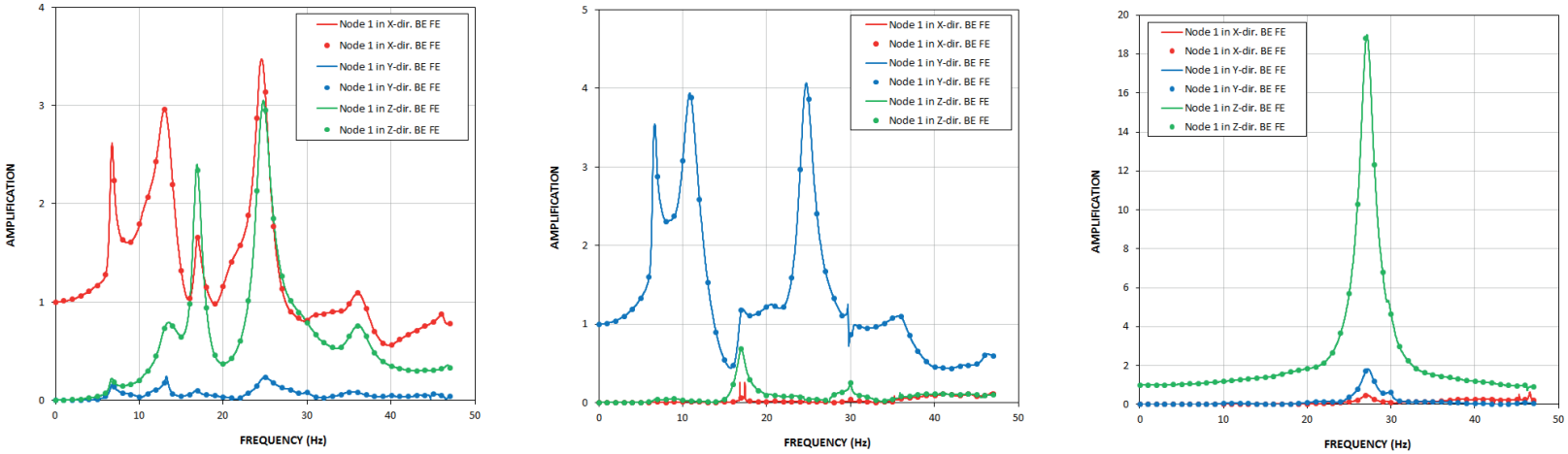

(a)X-Direction Input (b) Y-Direction Input (c) Z-Direction Input

Figure C-9b Transfer Functions of FWS Base Response from Analysis of BE Full Column Profile – Input Motion at 220 ft. (Model with SSE Damping)

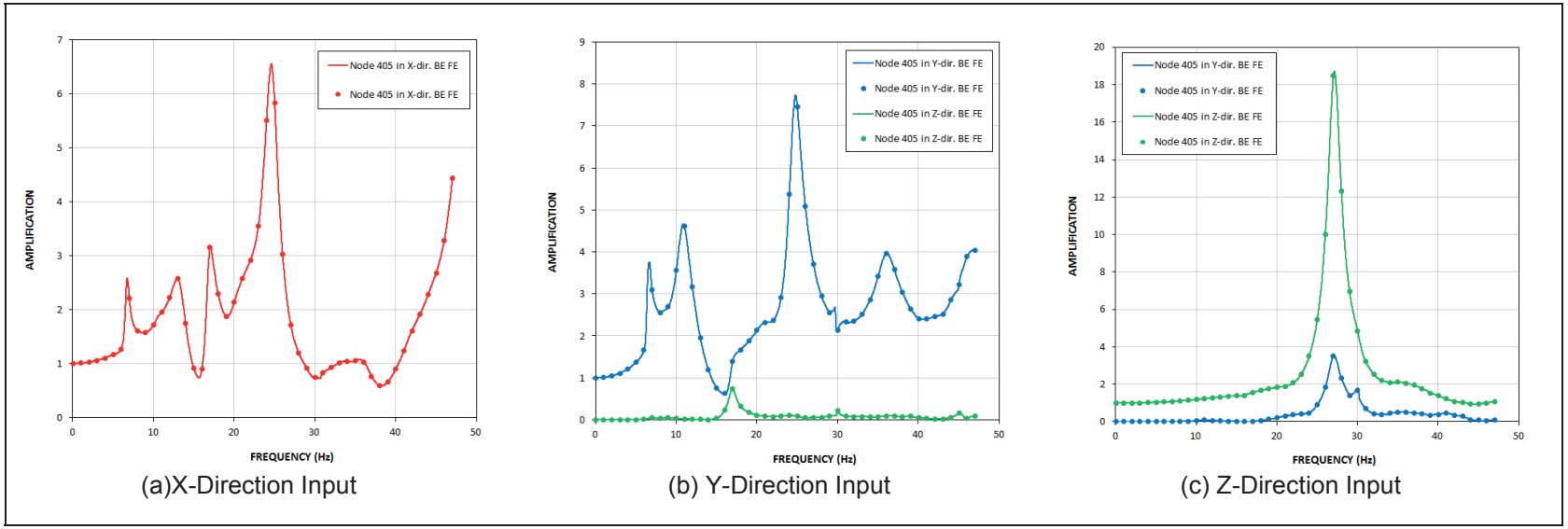

(a)X-Direction Input (b) Y-Direction Input (c) Z-Direction Input

Figure C-9c Transfer Functions of FPE Top Response from Analysis of BE Full Column Profile – Input Motion at 220 ft. (Model with SSE Damping)

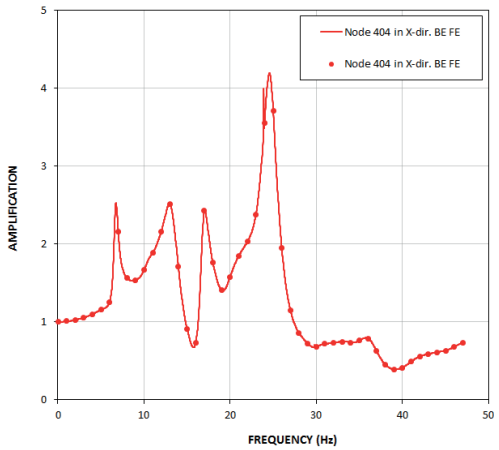

(a)X-Direction Input

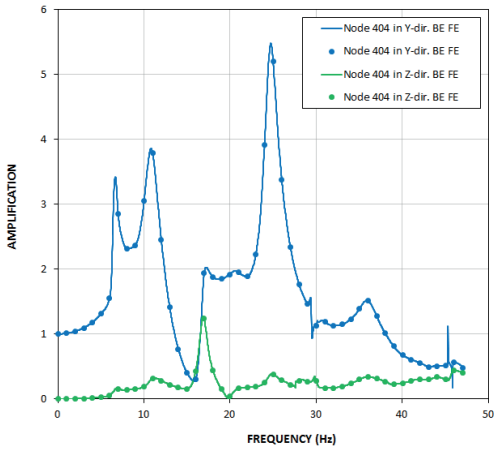

(b) Y-Direction Input

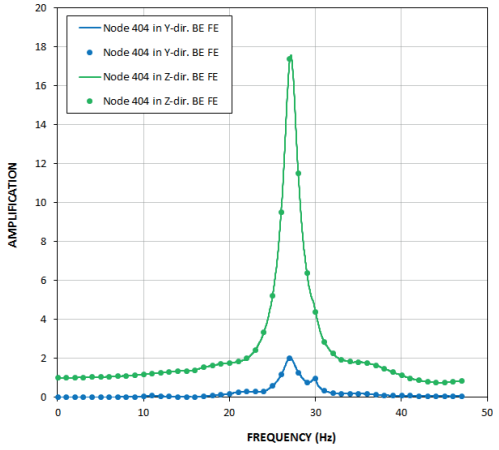

(c) Z-Direction Input

Figure C-9d Transfer Functions of FPE Base Response from Analysis of BE Full Column Profile – Input Motion at 220 ft. (Model with SSE Damping)